12-2016

Design and Synthesis of Lipid Probes Used for Membrane Derivatization and Fusion

Stuart Allen Whitehead
University of Tennessee, Knoxville, swhiteh3@vols.utk.edu

To the Graduate Council:

I am submitting herewith a dissertation written by Stuart Allen Whitehead entitled "Design and Synthesis of Lipid Probes Used for Membrane Derivatization and Fusion." I have examined the final electronic copy of this dissertation for form and content and recommend that it be accepted in partial fulfillment of the requirements for the degree of Doctor of Philosophy, with a major in Chemistry.

Michael D. Best, Major Professor

We have read this dissertation and recommend its acceptance:

John E. Bartmess, Brian Long, Todd B. Reynolds

Accepted for the Council:

Carolyn R. Hodges

Vice Provost and Dean of the Graduate School

(Original signatures are on file with official student records.)

Design and Synthesis of Lipid Probes Used for Membrane Derivatization and Fusion

A Dissertation Presented for the
Doctor of Philosophy
Degree
The University of Tennessee, Knoxville

Stuart Allen Whitehead
December 2016

DEDICATION

“If you wish to make an apple pie from scratch, you must first invent the universe.” – Carl Sagan, *Cosmos*

For Grandpa Marek and Grandpa Whitehead, who loved golf, family and golf a second time

ACKNOWLEDGEMENTS

I'm proud of the relationships that I've built and made here in Knoxville. Graduate school has been a humbling experience to say the least, and I wish I could list and thank every individual I've met for guiding me through this uneasy time of my life. I will do my best in attempting to complement each major figure (or figures) that I've had the pleasure of connecting with over the course of this wild ride.

Like any fledgling scientist, I kept trying the same thing over and over again, resistant to try new things. Consequently, I made mistakes, but later on I really buckled down and said to myself, "if I'm going to fail at this, at least I'll go down with a fight and giving everything I've got". You know, the same quote muttered in a million underdog sports movies. I went back to square one and made sure I didn't leave any stone unturned. I could sense I was getting better at my craft, and I knew it wasn't because I got lucky. When I set out to synthesize one complex molecule, I made three. I later found success in putting one of those lipids to the test, which put a cap on the hardest I've ever worked in a four-month stretch. I experienced 4 ½ years of failure to finally experience ½ year of success. That's a lesson I'll never forget.

Now, I'd like to thank my principal advisor, Dr. Michael D. Best, for sticking with me through the tough times and continuing to provide valuable insight into my methods and techniques throughout my time here when it seemed like there was

nothing else to do. You kept assuring me that things can come together quickly, and after the year I just experienced, there is no doubt about that.

To my committee members: Dr. Bartmess, Dr. Long, and Dr. Reynolds. Dr. Bartmess, I had the pleasure of taking notes for your classes, and I will always admire how you kept class amusing. “Story time” is an undeniable feature and should be part of the curriculum for every professor. Dr. Long, I always appreciated the close proximity of your office to our lab, and more importantly that the door was often open. It made it quite easy to ask for advice and general trash-talk. Dr. Reynolds, you are a fantastic professor to have on a committee. You balance out the synthesis side of my project by bringing a necessary and brilliant knowledge to the biology side. I will always be grateful towards that.

Drs. Baker, Campagna, and Foister, thank you for your contributions in helping me learn how to pursue my dream and for having a depth of knowledge in chemistry that I can aspire to.

To the Best lab members, past and present, thank you for your support. I’d like to elaborate on that, but it’s too hard to reflect on everything we’ve been together.

To my fellow colleagues who began their studies in Fall 2011, we vetted, laughed, cried, and socialized with one another too many times to keep track of. I’ve enjoyed every minute of it. Brian, thank you for your mutual interest in Boston sports and I’m glad we got to share those exciting (and depressing) moments together.

To my graduated colleagues from outside the Fall 2011 and Best lab vortex, Drs. Andrew and Kimberly Goodwin, Dr. Brianna Hughes, Camille Kite-Bussen, Dr. Stefanie Bragg, Dr. Samuel Rosalina, Dr. Eric Barrowclough, Drs. Chris and Allyn Milojevich, Dr. Chad Lacroix, and Dr. Adam Lamb, if I have the character that all of you have, then I think I'll be alright.

Alia, Nick, Amelia, and Ben, thank you for your loving and caring support through the highs and lows of my time here at UT. There's still time for me to be the crazy uncle who lives in the basement, but I'm not ready to be that, yet, because you are all inspiring to the nth degree and allowing me to strive for something bigger.

Mom and Dad, thanks for your perpetual guidance throughout this whole journey. The 6 am wake-up calls to hockey practice, being in the stands at little league, the pep-talks when I needed them, everything. I couldn't have accomplished this much without both of you there by my side.

Finally, to my fiancée, Marissa. I am a better student because of you. I'm a better person because of you. Thank you for your encouraging words and belief in me when I didn't have much to say for myself. You are also responsible for introducing me to a whole other group of people that puts into perspective how isolating life sometimes can get in the lab, and for developing new relationships outside of my comfort zone. I'm excited to begin the next chapter of my life with you, and carry that flame on throughout the rest of our lives.

ABSTRACT

Lipids control a variety of complex biological processes. Bulk lipids such as phosphatidylcholine (PC), phosphatidylserine (PS), and phosphatidylethanolamine (PE) represent the major components of cellular membranes. In addition, unilamellar vesicles composed of lipids (liposomes) are valuable for delivery applications since they can encapsulate and transport drugs and other agents. In order to maximize delivery efficiency and target specific membranes, the ability to trigger and control vesicle-vesicle fusion is desirable. Such approaches generally seek to mimic the membrane fusion machinery present in nature while imparting specificity in the membranes that undergo fusion. The goal of this work is selective drug delivery to diseased cells. We have explored the copper-free click reaction as a bioorthogonal means to drive fusion between membranes containing cyclooctyne-tagged and azido-tagged lipids.

We synthesized three novel lipids containing either the cyclooctyne or azide functional group at the headgroup. In chapter one, we describe the synthesis of Oxy-dibenzocyclooctyne (ODIBO) lipids **1** and **15** and azido-lipid **18**, which contain reactive partners for copper-free click chemistry. In these compounds, the phosphate headgroup typically seen in phospholipids is substituted for a triazole ring. In chapter two, we describe the analysis of these compounds for membrane derivatization and fusion. We first set out to confirm the successful derivatization of liposomes containing ODIBO lipids **1** and **15** using a Förster resonance energy transfer (FRET) assay. Next, we investigated membrane fusion by mixing

complementary reactive liposomes including ODIBO **1** and azido-lipids, which was again studied through FRET. We studied the effects of liposome composition on fusion, including the PC / PE ratio and the structures of the cyclooctyne-lipids (**1-4**) and azido-lipids (**5**, **36**). Through these studies, we identified that ODIBO-lipid **1** and azido-lipid **5** yielded the greatest amount of fusion when incorporated into opposing liposomes containing a 45% / 45% PC/PE ratio. We also attempted to facilitate fusion by the addition of oppositely charged lipids and cholesterol into liposomes, although we were unsuccessful in seeing anything meaningful. This provides, to our knowledge, the first example of exploiting copper-free click chemistry to drive membrane fusion.

TABLE OF CONTENTS

LIST OF FIGURES

LIST OF ABBREVIATIONS

ADIBO	Aza-dibenzocyclooctyne
Boc	*tert*-Butoxycarbonyl
Boc_2O	Di-*tert*-butyl Dicarbonate
CuAAC	Copper Catalyzed Azide-alkyne Click
DAG	Diacylglyerol
DCC	*N,N*'-Dicyclohexylcarbodiimide
DCM	Dichloromethane
DIBAL-H	Diisobutylaluminum Hydride
DIEA	Diisopropylethylamine
DLS	Dynamic Light Scattering
DMAP	4-Dimethylaminopyridine
DMF	*N,N*-Dimethylformamide
DOTAP	1,2-Dioleoyl-3-trimethylammonium-propane
EDC·HCl	*N*-(3-Dimethylaminopropyl)-*N'*-ethyldicarbodiimide Hydrochloride
EtOAc	Ethyl Acetate
EtOH	Ethanol
FRET	Förster Resonance Energy Transfer
h	Hour(s)
KHPTA	Potassium Phosphotungstic Acid

LPC	Lyso-phosphotidylcholine
MeOH	Methanol
min	Minute(s)
NBD	7-Nitrobenz-2-oxa-l,3-diazol- 4-yl
NBD-PE	*N*-(7-Nitrobenz-2-Oxa-1,3-Diazol-4-yl)-1,2-dihexadecanoyl-sn-glycero-3-phosphoethanolamine
NMM	*N*-Methylmorpholine
NMR	Nuclear Magnetic Resonance
ODIBO	Oxy-dibenzocyclooctyne
ODIBO-TEG-COOH	1-((2-(tert-Butyl)-11,12-didehydro-6H-dibenzo[b,f]oxocin-8-yl)oxy)-13-oxo-3,6,9-trioxa-12-azahexadecan-16-oic Acid
PA	Phosphatidic Acid
PC	Phosphatidylcholine
PE	Phosphatidylethanolamine
PEG	Polyethylene glycol
PI	Phosphatidylinositol
PIP_n	Phosphatidylinositol-(number)-phosphates
PG	Phosphatidylglycerol
PS	Phosphatidylserine
R_f	Retention Factor
Rhd	Rhodamine B

Rhd-PE	1,2-Dioleoyl-sn-glycero-3-phosphoethanolamine-*N*-(lissamine rhodamine B sulfonyl)
SNARE	Soluble *N*-ethylmaleimide Attachement Receptor
SPAAC	Strain Promoted Azide-alkyne Click
STEM	Scanning Transmission Electron Microscopy
t-BuOH	tert-Butyl Alcohol
TEAI	Tetraethylammonium Iodide
TEG	Tetraethylene Glycol
TFA	Trifluoroacetic Acid
THF	Tetrahydrofuran
THPTA	Tris(3-hydroxypropyltriazolylmethyl)amine
TLC	Thin Layer Chromatography

Chapter 1: Roles and Properties of Lipids and Membranes

Lipids are critical to maintaining and controlling key cellular processes. They are responsible for attracting proteins and other biomolecules that regulate biological functions in and out of the cell. The most fundamental role of cellular lipids is based upon their spontaneous self-assembly into membrane bilayers driven by molecular attractions.[1] This is such that the charged/polar headgroups of lipids will interact favorably with hydrophilic entities at the aqueous interfaces surrounding the membrane, and hydrophobic lipid chains will aggregate inside the membrane core.[2] As a result of this assembly, membranes act as barriers that separate not only the outside and inside of cells (via the plasma membrane), but also surround the different organelles that exist inside the cell. Lipids thus intrinsically control the flow of molecules and ions into cells and their trafficking between various intracellular compartments.[3-5] While these processes are often driven by proteins such as through ion channels and processes including endocytosis,[6-8] lipids are also capable of translocating molecules, particularly through membrane fusion. Therefore, it is important to understand and mimic the roles of lipids in these processes to control the delivery of molecules such as drugs.

1.1 Bulk lipids vs. signaling lipids

We can divide lipids into two sub-classes: the bulk lipids and the signaling lipids. Bulk lipids (Figure 1.1), such as phosphatidylcholine (PC), phosphatidylserine (PS), and phosphatidylethanolamine (PE), make up the majority of the cell membrane and define its shape, and are not typically involved in controlling

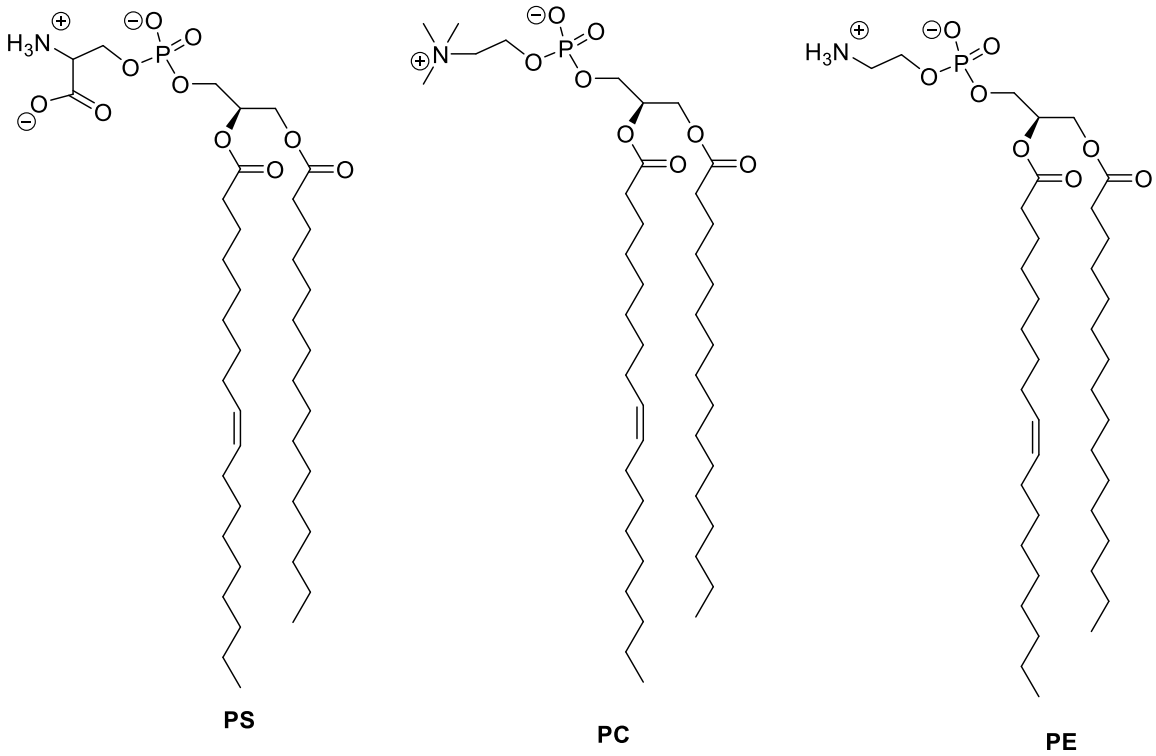

Figure 1.1 Structures of bulk phospholipids: phosphotidylcholine (PC), phosphotidylserine (PS), and phosphotidylethanolamine (PE)

biological processes.[9] Bulk lipids are present in much larger abundance in cellular membranes and thus have greater control over the passage of molecules into and out of cells and organelles.[10-11] PC is the most abundant lipid present in eukaryotic membranes (~45-55%), followed by PE (~15-25%) and PS (~5-15%).[12] Signaling lipids (Figure 1.2), such as diacyglycerol (DAG), phosphatidylglycerol (PG), phosphatidic acid (PA) and the phosphoinositides (PIP_nS) regulate biological processes through a range of activities including the binding and activation of proteins, which attract proteins to membrane surfaces and regulate their function. PS can also be classified as an important signaling lipid due to its negatively-charged headgroup. PA and PIP_n reside in eukaryotic membranes at 1-2% and 0.5-1%, respectively, of all lipids.[11] Their localization is tightly controlled, presenting opportunities to target specific membranes and cell types.

1.2. Lipid geometries and effects on self-assembled structures

Lipids can be divided into separate categories based on their shapes. The geometries of lipids dictate key membrane properties including the structures formed during self-assembly based on the relative surface areas of the head group and hydrophobic tail regions. These aspects are important to consider when designing membrane systems for targeted delivery and fusion. The most abundant membrane lipid, PC, is considered to adopt a cylindrical shape between both polar and non-polar regions of its structure. This geometry has the appropriate curvature for forming membrane bilayer assemblies such as liposomes.

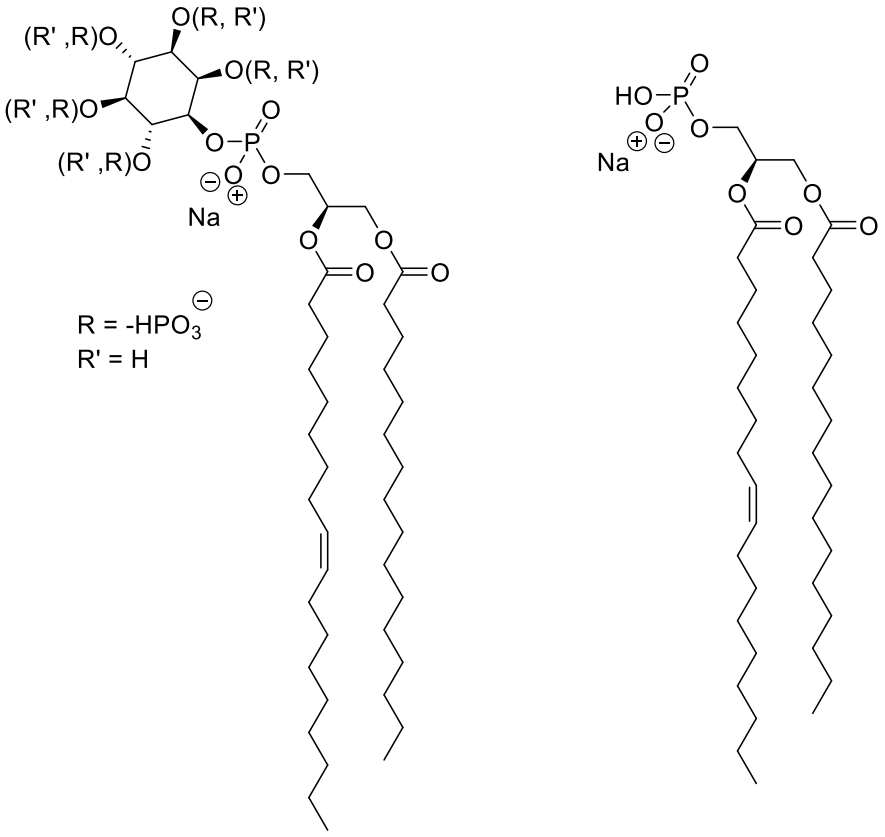

Phosphatidyl(1'-myoinositol) phosphate (PIP_n)

Phosphatidic Acid (PA)

Figure 1.2 Structures of signaling phospholipids: phosphatidyl(1'-myoinositol) phosphate (PIP_n) and phosphatidic acid (PA)

Changing the structure by either increasing or decreasing the size of one of these two regions can alter the shape of the lipid assembly that is formed.[13] For example, increasing the polar head group region with respect to the tail region, as is the case with lyso-phosphatidylcholine (lyso PC) (Figure 1.3), will produce greater positive membrane curvature, and facilitate the formation of micelles, spherical assemblies in which the hydrophobic tails fill the core. When the opposite is done, such as in the case of PE, the shape can resemble that of a cone, which introduces negative curvature into the membrane. In other words, a layer of lipids in this shape has a tendency to fold inward, and head groups face toward the center of the membrane. Incorporating lipids with a tendency to form this shape is commonly beneficial for instigating membrane fusion between membranes because the negative curvature results in destabilization of the membrane.[13-14]

1.3. Derivatizing membrane surfaces towards targeted drug delivery

Membrane bilayers can be labeled with groups such as peptides, antibodies, and reactive groups through the use of functionalized lipids. This can be pursued to targeting groups that guide the liposomes to specific cells or to trigger release of contents. Lipids can be synthesized in order to improve biocompatibility for targeted drug delivery, thus facilitating labeling events to that lipid.[15]

Functionalized lipids and other synthetic molecules can be incorporated into membrane bilayers as a means to promote more compatible labeling and improve drug targeting practices.[16-20] These fabrication methods include tethering long lipid

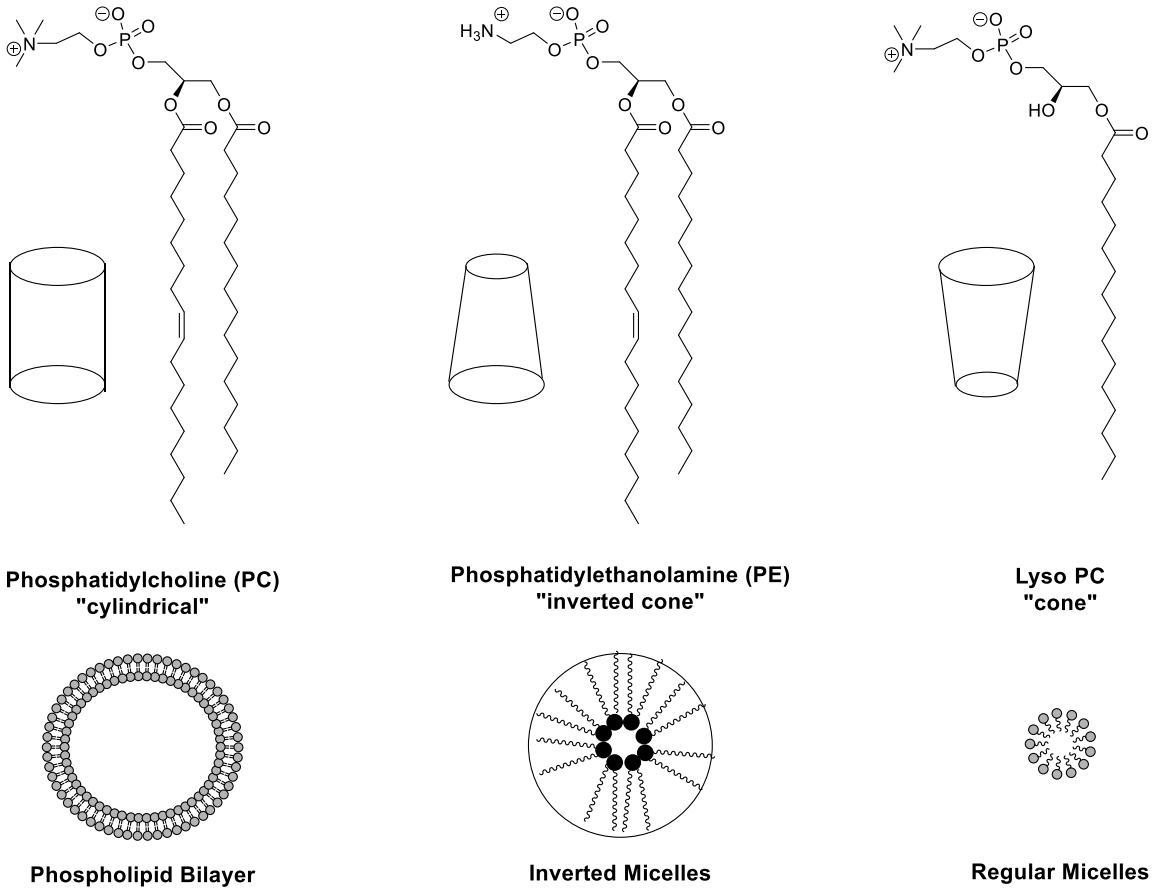

Figure 1.3 Shape of various phospholipids as they relate to the preferred assembly properties. Phosphatidylcholine (PC) bears a 'cylindrical' shape; phosphatidylethanolamine (PE) bears an 'inverted cone'; lyso-phosphatidyl choline (lyso PC, LPC) forms a regular micelle shape i.e. "cone"

chains through liposome immobilization,[21-22] assembly of polymers onto phospholipid vesicles,[23-25] and coating membranes with metal oxides.[26-29]

This process is rather tough to localize due to the complex nature of biological systems and degradation of liposomes once in the bloodstream. It is beneficial to understand the role of lipids so functionalized membranes can be delivered unencumbered. Therefore, it is pivotal that the proper chemistry is chosen on the membrane surface, or the functional group may be compromised and unable to react under biological conditions. It is thus beneficial to choose a delivery vehicle that proceeds in a biological setting unperturbed and enables the drug to be delivered efficiently.

Regular (lipid) and polymeric micelles, single layer membranes with a hydrophobic core, have shown potential as drug carriers in vivo because of their ability to solubilize water-soluble and water-insoluble drugs[30-34] and their low cytotoxicity.[35-38] Both forms of micelles are susceptible to target moieties on the hydrophilic leaflet, thus enhancing delivery systems and bioavailability,[17] but the advantage of polymer-coated micelles over lipid micelles is that the increased molecular weight in their hydrophilic region can raise the critical micelle concentration (CMC) and provide thermodynamic stability in aqueous media.

In 2006, Gao and coworkers reported on the use of multifunctional micelles as carriers to deliver drugs and magnetic resonance imaging (MRI) imaging agents to cancer cells.[39] A chemotherapeutic agent, doxorubicin, was encapsulated into the hydrophobic core of the micelle, and then released by a pH-dependent

mechanism. Cancer cells were targeted by a cyclic amino acid complex (cRGD) ligand coated as a surfactant onto the micelles. The drug could be selectively delivered to the cell, and a contrast in MRI capability was seen specifically from the cRGD-coated micelles and not the cRGD free micelles. In addition to pH-dependent targeted release from micelles,[40-46] there has also been recent work on thermal,[47-48] PEG,[49-52] and polypeptide[51, 53] dependent mechanisms for targeted drug delivery.

Our goal is to achieve targeted drug delivery by selectively directing liposomes to certain functional groups along the surface of cancer cells, or through active delivery capabilities. This requires the use of a targeting group on the surface of the delivery vesicle that drives selective localization to cells based on a partner functionality present on the cell surface, much like the example reported by Gao and coworkers. [39, 54] Consequently, targeting molecules such as antibodies, peptides, and small nucleic acid molecules have gained traction as receptor-binding entities due to their strong adherence to targeted cellular surfaces.[55-59] Antibodies and antibody fragments offer the highest binding affinities and selectivities for the target of interest because of the presence of two epitome-binding sites on the molecule,[60-61] but likely suffer from the large antibody size, which could inhibit delivery efficiency.[62-63] Thus, it is desirable to pursue alternate strategies that incorporate selective tags onto the surfaces of the liposomes and cells.

1.4 Bioorthogonal Reactions

Bioorthogonal reactions on the interface of membranes are heavily used in facilitating drug and gene delivery systems.[64-66] The hallmarks of bioorthogonal chemistry is the use of tags that selectively react with one another within complex systems and do not engage in non-specific reactions with biomolecules. Examples such as the thiol-ene “click” reaction, normal Diels-Alder, and aldehyde-amine (oxime) linkage have been reported as suitable reactions for protein,[67-73] oligonucleotide,[74-75] and glycan modification.[76] However, the functional groups involved in these reactions (thiols, alkenes, ketones, etc.) have either a vast presence or are sensitive in/to intracellular environments, thus diminishing selectivity in this setting.[77-78]

Therefore, the most prevalent biorthogonal reactions in the literature have been the Staudinger ligation, copper-catalyzed click, and copper-free click reactions (Figure 1.4). The common link between these three reactions is the presence of an azide reactive group. Azides offer unique character to biological systems because they lie dormant, but show selective reactivity towards alkynes and phosphines. These functional groups are not present in biological systems, so the aforementioned ‘click’ reactions and Staudinger ligation benefit from being bioorthogonal. There has been extensive research on the mechanism for the Staudinger ligation,[79,80,81,82,83,84] specifically to optimize the phosphine groups used in the reaction.[85] It has been suggested the Staudinger ligation is most reactive when a 6-membered transition state is in place between an azaylide and

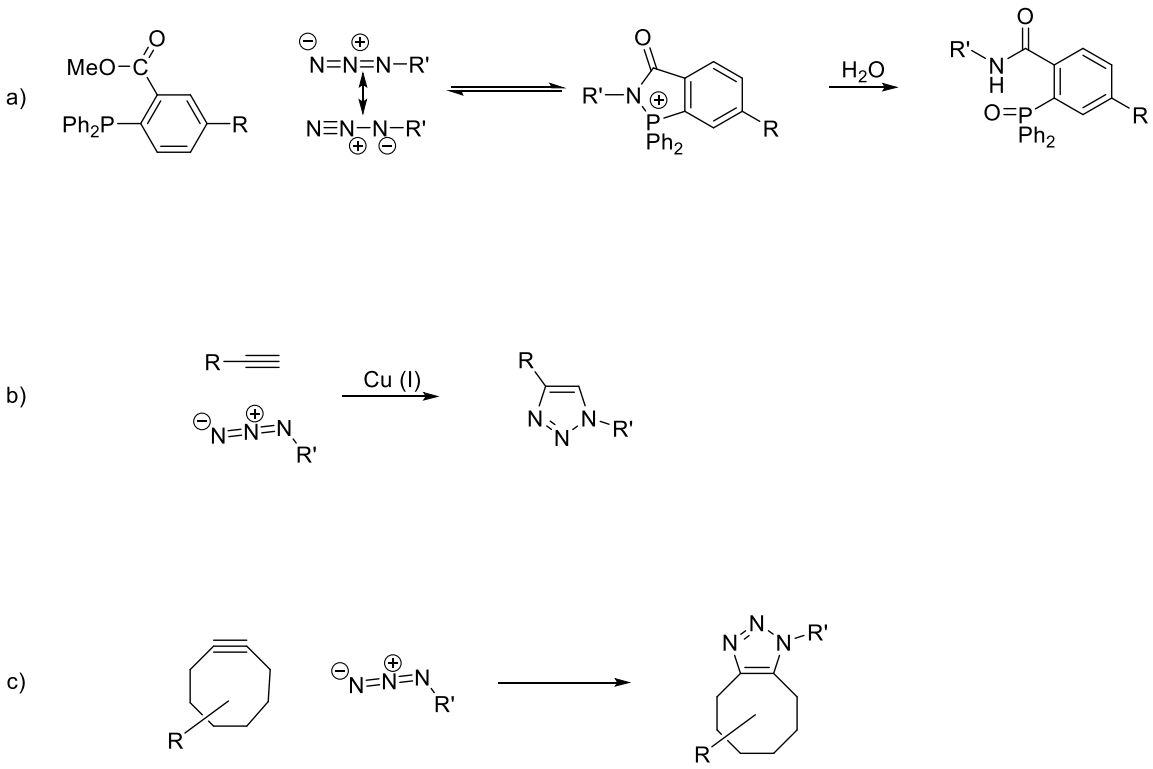

Figure 1.4 List of Bioorthogonal Reactions a) Mechanistic approach for Staudinger Reduction b) copper-catalyzed click reaction c) copper-free click reaction

ester/thioester. The reaction can be tuned to initiate certain reaction rates based on the substitution patterns around each component involved in the reaction. For example, placing electron-donating groups around the phosphine and electron-withdrawing groups around the azide increases the rate of reactivity. The drawback of the Staudinger ligation is the arduous synthesis required to access the phosphine-lipid analogue on the surface, as well as the reagent being unstable and prone to phosphine oxidation.

The most commonly implemented reaction for functionalizing membranes has been the copper-catalyzed “click” reaction (CuAAC). This reaction is tolerant of many functional groups found in biomolecules, and can be performed in aqueous solution. It was simulanteously discovered by Meldal *et. al* in Denmark and Fokin and Sharpless in the U.S.[86-87] The normal azide-alkyne cycloaddition reaction, reported by Huisgen over the course of investigating various 1,3-dipolar cycloadditions,[88] is a highly exothermic reaction, however the reaction suffers from a high activation barrier and requires extreme temperatures to achieve the proper regiochemistry. The introduction of the copper catalyst increased the rate of reactivity by a factor of 10^7 relative to the uncatalyzed reaction, and thus the reaction proceeds at or near room temperature and is regiospecific, generating the 1,4-disubstituted triazole product.[89] The introduction of the copper-catalyzed click reaction (CuAAC) has led to many applications of its use in organic synthesis, small molecule labeling, and surface chemistry.[90-94]

1.5. Copper-free click chemistry

The copper-catalyzed click reaction is limited for certain applications by the requirement for the copper catalyst, which can be a detrimental additive into a biological system. This catalyst could lead to membrane degradation, toxicity, and metal-catalyzed side reactions, thus making it undesirable particularly for live-cell environments. Given the facile reactivity between an alkyne and azide, there has been a desire to find ways to eliminate the copper catalyst but retain the two moieties in a reaction together. Bertozzi and coworkers reported the first cyclooctyne moiety used for this purpose in literature, which circumvents the need for copper since the strained cyclooctyne ring does not require a catalyst to react.[95]

The presence of a copper catalyst for the original click reaction enables better overlap between the frontier molecular orbitals (MO's) of the azide and alkyne. When there is no copper catalyst present, the difference in energy between the lowest unoccupied molecular orbital (LUMO) of the azide and the highest occupied molecular orbital (HOMO) of the alkyne is far apart, thus leading to a slow rate of reactivity. When the copper is introduced, the gap between the HOMO and LUMO of each respective moiety is narrowed, thus lowering the activation energy of the reaction.

The interaction between the HOMO and LUMO of the azide and alkyne, respectively, in the copper-catalyzed click reaction can be used to trace the kinetics of the copper-free click reaction. As the name suggests, the copper-free click reaction operates in the absence of a copper catalyst. This is due to the

make-up of the alkyne moiety, which is incorporated into strain cyclic systems in these reagents. This phenomenon promotes ring strain due to the bending of the normally 180^0 linear *sp*-hybridized orbitals. With each additional degree of bending, the energies associated with the MOs for the alkyne are altered, and this theory has led to further understanding on the topic.

Houk and coworkers have studied the transition state of the 1,3-dipolar cycloaddition and how the stabilizing interactions overshadow the destabilizing interactions.[96] They were able to calculate the angles between atoms within the intermediates, and describe them as distortion angles. These angles remained largely unchanged for the azides throughout the reaction, but understanding the bond angles of the alkyne moiety led to a breakthrough in understanding the role of this reagent. This study provides a model for the distortion/interaction analysis for the cycloaddition reactions, and insight into the origin of the “strain promoted” click reaction between the cycloalkyne and azide.

The transition state for the cyclooctyne was measured to be 1.6 kcal/mol, which is 4.5 kcal/mol less than what was observed for the azide. This is due in large part to the decreased distortion energy for the cycloalkyne, and the 4.5 kcal/mol corresponds to the distortion energy for the linear alkyne. It is shown that the cycloalkyne, due to the bond angles being distorted from 180^0, has a higher starting energy than acetylene, so it requires less activation energy to reach its preferred transition state. This results in a greater rate enhancement, which can be attributed to the lower distortion energies for the ‘strain-promoted’ cycloaddition

reaction. Faster reaction kinetics can be achieved through charge-transfer methods. Bertozzi and coworkers reported the use of a difluoromethylene unit adjacent to the alkyne.[97] The added fluorines in this compound raised the HOMO significantly, which enhanced the reactivity towards azide. In turn, this lowers the activation energy on account of greater interaction between the frontier MOs. In review, the 1,3-dipole cycloaddition between a cyclooctyne and azide can be achieved through changes in distortion energies and better interaction between the frontier molecular orbitals of each respective moiety.

The goal of these enhancements is to improve its stability and efficacy when introduced to complex biological systems. For example, the azadibenzocyclooctyne (ADIBO) moiety has been abundantly used in literature due to its ease of synthetic preparation and favorable kinetic properties.[98-100] In 2012, McNitt and Popik reported the oxa-dibenzocyclooctyne (ODIBO) moiety as a tool for metal-free ligations.[101] This particular cycloalkyne was prepared through a cyclopropenone intermediate, which was subjected to light to produce the final product in quantitative yield. ODIBO displayed faster reaction kinetics than the ADIBO moiety (2.5:1 in MeOH), and produced rate constants 14-20 times faster in aqueous solutions than organic solvents. This enhanced reactivity in aqueous solutions makes the ODIBO moiety highly effective for biological applications.

1.6 Förster Resonance Energy Transfer (FRET)

FRET is a phenomenon associated with fluorescence spectroscopy that is most commonly used to detect changes in the distance between various biomolecules.

This is done by using two fluorophores, one that acts as a donor and the other acting as an acceptor. The key to these fluorophore pairs is that the emission wavelength of the donor must overlap with the excitation wavelength of the acceptor, which enables energy transfer between the two when they are in proximity. FRET is extremely sensitive to the slightest change in distance, since energy transfer has an inverse sixth order energy dependence on the radius between the dyes. Excitation of the donor in the absence of acceptor will lead to donor emission. However, when the donor and acceptor are sufficiently close, excitation of the donor can lead to energy transfer to the acceptor through based on long-range dipole-dipole interactions, after which the acceptor will instead emit. FRET changes can be observed through either changes in donor emission, acceptor emission or the ratio between the two.[102]

A popular FRET pair is the donor tag 7-nitrobenz-2-oxa-l,3-diazol- 4-yl (NBD) (λ_{ex} = 450 nm, λ_{em} = 520 nm) and acceptor tag rhodamine B (λ_{ex} = 540 nm, λ_{em} = 580 nm). This pair has been extensively used to track membrane fusion, small molecule recognition, and protein interactions.[103-105] Thus, we selected this pair for the membrane derivatization and fusion studies described in later chapter. In Figure 1.5, the concept of FRET is outlined in the context of two complementary liposomes carrying an NBD-tagged lipid and Rhd-tagged lipid, respectively. Before mixing, the FRET signal is deactivated due to the lack of proximity between the donor and acceptor lipids, resulting in only donor (NBD) emission. When the two liposomes are mixed and fusion occurs, the proximity

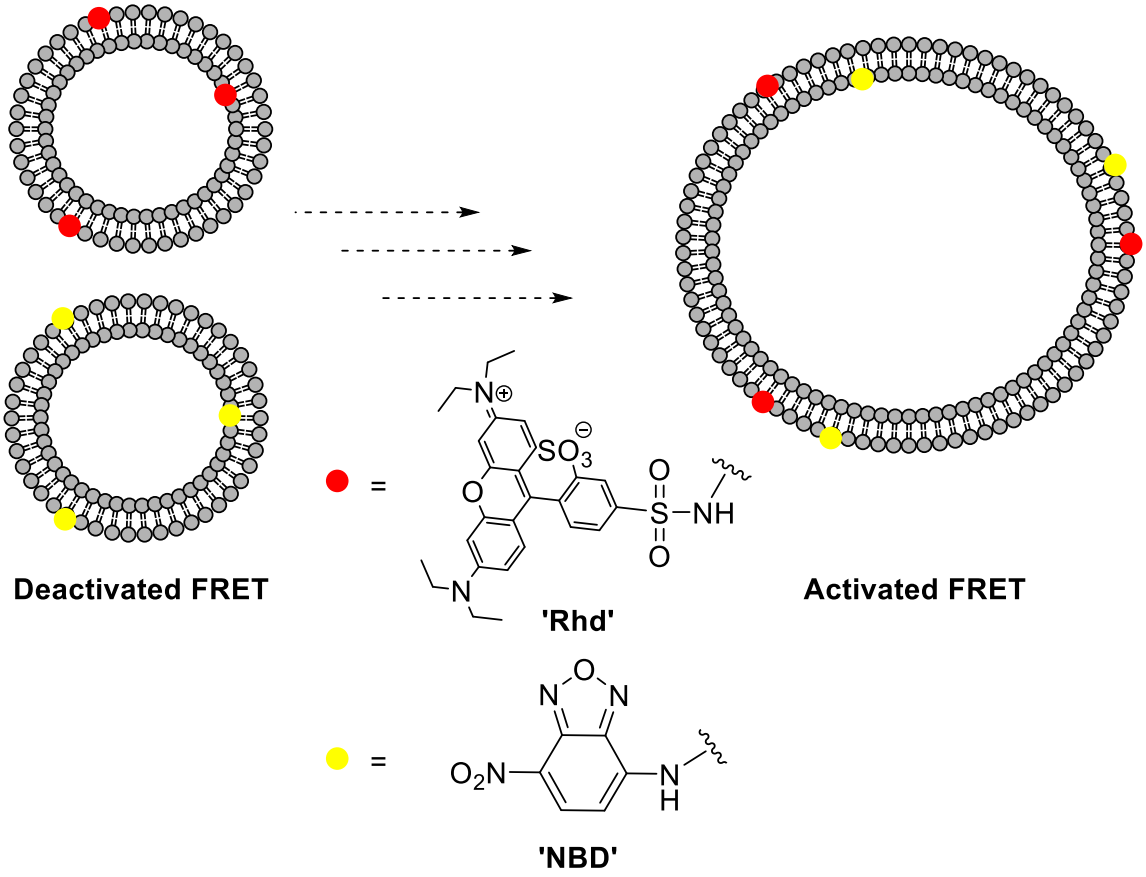

Figure 1.5 Cartoon depicting Förster resonance energy transfer (FRET) taking place upon fusion between NBD-tagged liposomes (yellow) and Rhd-tagged liposomes (red). The FRET signal is initially quenched, but fusion causes the FRET-tagged lipids to be mized within the same membrane; causing FRET to be activated.

of the donor tag and acceptor tag is close enough to facilitate a transfer in energy, and thus activate the emission signal of the acceptor (Rhd).

1.7. Click chemistry for the derivatization of membrane surfaces

Due to the beneficial properties of click reactions, particularly their bioorthogonal nature and fast kinetics, these reactions have been explored for derivatizing membrane surfaces. In 2006, Schuber and coworkers[106] labeled small unilamellar vesicles (liposomes) with monoglycosylated sugars by clicking together an alkyne-tagged lipid with an azido-tagged mannose moiety. This reaction was confirmed by incubating these liposomes with concanavalin A, a lectin that non-covalently interacts with mannose, and observing the increase in turbidity of the solution due to the specific recognition of the mannose analogs on the liposome surface by the concanavalin A that resulted in aggregation. Concurrently, Kros and coworkers[107] used a FRET assay to successfully derivatize liposome surfaces by CuAAC. They used alkynyl-tagged lipids within liposomes containing the fluorescent lipid Rhd-PE to react with an azido-tagged NBD-lysine analogue. When a successful click reaction was achieved, the close proximity of the NBD and rhodamine moieties activated the FRET signal. This opposed the observation seen for liposomes lacking an alkyne moiety, since the lack of a click reaction did not drive proximity between the two fluorescent labels. Since then, multiple studies have been reported employing the CuAAC on membrane surfaces (Figure 1.6) as a means for targeting carbohydrates and proteins, promoting complex biological functions, and constructing bolaamphiphiles[108-110] and biopolymers.[111-113]

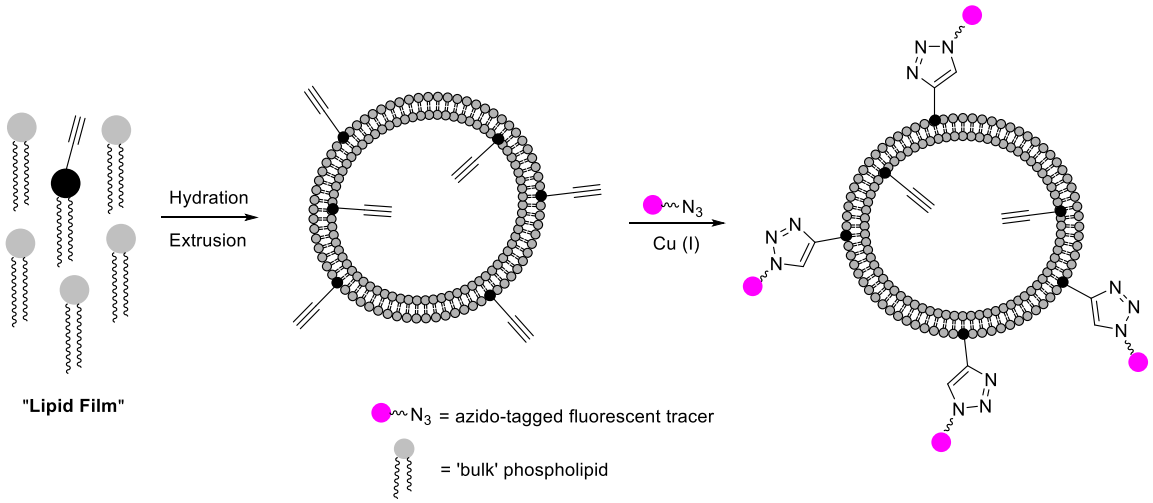

Figure 1.6 Step-by-step process for general derivatization of membranes. First, lipid components are hydrated to generate heterogeneous unilamellar vesicles; extrusion produces homogeneous unilamellar vesicles. Fluorescent tracer with a clickable tag can be introduced to the liposome solution to confirm membrane derivatization

Despite the previous examples showing membrane functionalization through the copper-catalyzed click reaction, a drawback of this approach is that the copper catalyst is known to promote membrane decomposition.[114-115] As a result, the copper-free click reaction has been explored as an alternative for membrane modification. In 2012, Bostic and coworkers reported the first known use of functionalizing membranes via copper-free click chemistry. This study used azido-tagged lipids as an anchor onto liposomes, and these functionalized liposomes were incubated with a cyclooctyne-tagged biotin analogue. A successful reaction between the azide and cyclooctyne resulted in the liposomes being coated onto a streptavidin coated microplate.[116] In 2015, Martin and coworkers[117] also employed the copper-free click reaction to functionalize membranes, but instead the role of which reactive partner was labeled onto the liposome was reversed. These two studies show that either azides or cyclooctynes can be linked to lipid analogues, incorporated into liposomes, and modified by this reaction. Continuous enhancements have been made to the cyclooctyne moiety in order to improve its reactivity, stability, and ease of synthesis.

1.8 Membrane fusion in biological systems

Cell-cell and cell-liposome fusion are critical processes that define physiological and pathophysiological events. In natural systems, these processes can be mediated by soluble attachment protein receptors (SNARE)", along the cell surface. These receptors, in combination with other regulatory proteins, interact with membranes to form a four-helix SNARE assembly (Figure 1.7). This process

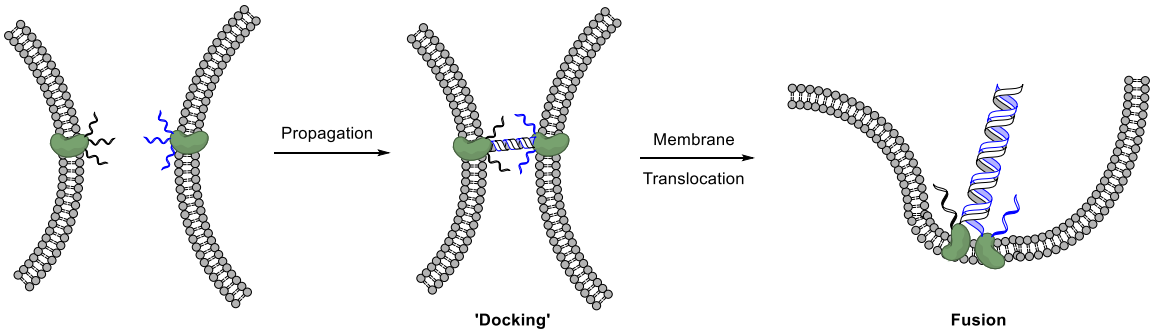

Figure 1.7 Representation of cell-cell fusion directed by SNARE Proteins. 'Docking' brings complementary cells closer together, and fusion is triggered by proximity

has numerous advantages in biological systems, including drug and gene delivery, because it can potentially be exploited and mimicked via chemical means, and research has been done to elucidate the SNARE complex.[118-121] SNAREs are responsible for driving opposing membranes to close proximity, holding them in close contact, and bending the membranes to create an unstable bilayer. That last point is critical in facilitating fusion because 'docking' (Figure 1.7) only connects the outer leaflets of opposing membranes, whereas the inner leaflets remain intact, yielding a state referred to as 'hemifusion'. Next, these proteins regulate the destabilized bi-layer and generate fusion pores inside the plasma membrane, completing the event.

Liposomes can be engineered to artificially mimic this process of SNARE-mediated fusion.[122] To do so, functionalized lipids bearing partner reactive or binding groups are commonly introduced into opposing liposomes. These complementary functionalities cause the liposomes to interact, which can be exploited to drive fusion. The lipid composition of liposomes (i.e. PC/PE/PS)

composition in the membrane can be manipulated to facilitate membrane fusion. In this case, non-bilayer lipids such as PE or other additives may be necessary to promote fusion due to the negative curvature it imparts in the membrane, which mimics the destabilizing effect of the inner leaflet seen in the SNARE system. PS has been reported to have inhibitory effects on the rate of fusion due to the negatively charged headgroup at physiological pH, which could cause electrostatic repulsion with opposing membranes.[123] However, metal-complex systems have been performed to induce aggregation of PS-labeled liposomes through the use of multivalent cations.[124]

In 2014, Lentz and coworkers studied the effects of Ca^{2+} addition to liposomes containing PS.[123] This report shed some intriguing insight into the mechanism for metal-based fusion applications. Upon introducing the Ca^{2+} adduct to the vesicle solution, the divalent ion binds to two negatively-charged PS lipids from opposing membranes, which brings them into proximity. Polyethylene glycol (PEG) was added to initiate dehydration[125] in between the vesicle bilayers. This is done to push the hydrophobic tail region out of the plasma membrane and generate fusion pores thereby leading to fusion.

DNA- and polypeptide-mediated systems are often used to mimic the SNARE motif as well. In 2008, Hook and coworkers incorporated cholesterol-modified DNA constructs into liposomes to facilitate fusion.[126] Cholesterol was incorporated into liposome mixtures as an anchor for single or double stranded DNA chains, which triggered fusion with liposomes containing complementary DNA strands.

The formation of the helical shape made from the binding of complementary DNA strands was meant to mimic the action seen from SNARE proteins, which commences protein binding at the N-terminus and works its way to transmembrane proteins in a 'zipper-like' fashion. It was also found that the DNA linker length has a profound effect on the rate of fusion. As the DNA chain length increases, the binding strands are separated further from the membrane bilayer, and thus the fusion rate is diminished on account of failing to overcome van der Waals forces.

Boxer and coworkers built on this strategy and incorporated DNA strands onto phospholipid anchors in the membrane.[127-128] Like the work seen with the cholesterol-anchored DNA strands, it was discovered that fusion was optimal when the DNA strands were connected between the 3' and 5' ends of each strand. The resulting complex forms a similar parallel orientation to the SNARE complex, which is the preferred conformation for inducing membrane fusion. DNA linker length also played a role in controlling fusion rate, and a greater linker length led to decreased fusogenic activity.

1.9 Chemical triggering of membrane fusion

Although these strategies have been successfully implemented using unilamellar vesicles *in vitro*, these systems could potentially fail in vivo due to the challenges of enforcing strong liposome binding in biological systems and the inability to selectively introduce the partner reactive handle onto particular cell types. Many of the drawbacks that hinder membrane derivatization studies from *in vivo* are also problematic for triggered membrane fusion studies.[129]

However, one strategy that shows significant promise in circumventing these pitfalls is a biorthogonal strategy. In 2012, Zumbuehl and coworkers[130] reported the use of a copper-catalyzed 'click' reaction (CuAAC) to stimulate fusion between liposomes (Figure 1.8). Here, liposomes containing an azido-lipid were mixed with those bearing an alkynyl-lipid to trigger a click reaction and drive fusion. In this system oppositely charged lipids were incorporated into opposing liposomes[131] to help stimulate fusion and counteract the negative charge of the azido-tagged lipid used in the study. As mentioned before, this strategy is likely to struggle in a biological setting due to the need for the copper catalyst. Therefore, biorthogonal strategies, such as oxyamine formation and copper-free click offer the possibility for improvement.

In 2014, Yousaf and coworkers[132-136] reported the use of keto-analogues in the presence of oxyamines ($R\text{-}ONH_2$) to drive cell-liposome fusion. Oxyamine conjugated liposomes reacted with those bearing ketones, forming an oximine (R-ON=R') functionality that caused liposome proximity and fusion. Herein, we describe the pursuit of an alternate bioorthogonal method for triggering membrane fusion driven by copper-free click chemistry using cyclooctyne- and azido-lipids.

Membrane bilayers do not always spontaneously fuse once they are brought into proximity, which impacts the selectivity of liposomal delivery. For fusion to occur, the lipid components must overcome the energy barrier of lipid mixing. This can be exploited by controlling the lipid composition within the membrane. PC is considered to be a bilayer forming lipid and PE is considered to be a non-bilayer

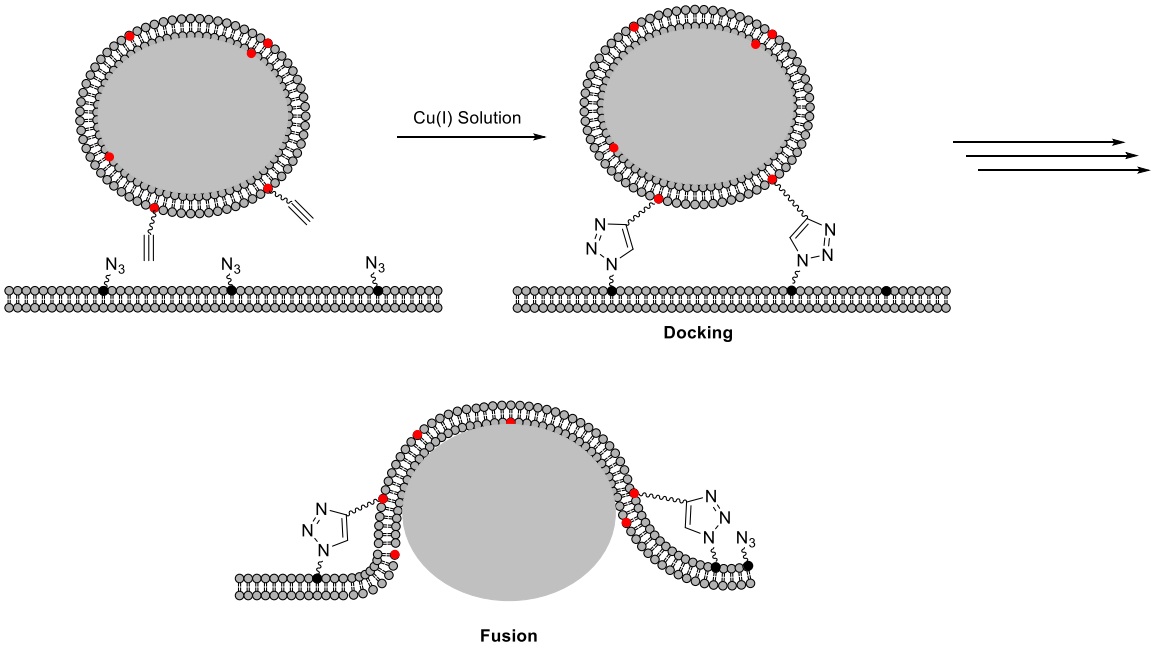

Figure 1.8 Representation of vesicle-vesicle fusion directed by copper-catalyzed click chemistry.

forming lipid. Altering the percentage of these two lipids can affect the curvature of the membranes in which they exist. When the curvature exhibits a negative curvature shape, i.e. folds outwards, this can lead to a higher propensity for fusion, due to the desire relieve curvature strain. It is thus desirable to achieve a proper ratio of PC and PE lipid in the membrane in order to stimulate fusion such that the vesicles are stable enough to remain intact while in the bloodstream but also destabilized to promote fusion.

1.10 Metabolic labeling as a tool for targeted delivery and fusion

Metabolic labeling has revolutionized the ability to label specific molecules with click chemistry tags in cells. In this process, simple biological substrates are strategically modified with tags, and in particular clickable groups. Since the azide used for click chemistry is very small, the addition of this group often can be performed in a way that does not impact the activity of the modified structure. When fed to cells, these compounds can enter normal biosynthetic pathways and produce labeled versions of products. This enables the selective labeling of particular cell types. While this approach has previously been performed to image specific biomolecules, clickable tags contained on specific cells, and in particular diseased cells, could be exploited for drug delivery to that site. Thus, metabolic labeling in combination with membrane fusion driven by copper-free click chemistry described in this dissertation shows strong promise for directed drug delivery.

The metabolic labeling approach was initially demonstrated for the tagging of sugars. Cell glycans are composed of an assortment of saccharide units that often reside on the cell membrane as glycoproteins or glycolipids. These structures mediate cellular recognition and binding events, thus providing a connecting point for pathogenic organisms.[137] However, biological studies have to circumvent the oligosaccharide heterogeneity of the glycan and the multiple enzymes needed in its biosynthesis.[138] Fortunately, evidence has been shown that nonphysiological, modified sugars can be incorporated into the cell, infiltrate sugar biosynthetic pathways, and be secreted into the cell membrane in the form of sialic residues.[139-140] The modified sugar substrate often often consists of an N-acetylated precursor of D-mannosamine or D-glucosamine into which an azide group is introduced to label sialic acid residues.[140]

These saccharides can be modified to include a variety of functional groups, most notably for the purposes to chemoselectively labeling glycoproteins.[141-145] In 1997, Bertozzi and coworkers submitted the first report of chemoselective live-cell labeling by using N-levulinoyl mannosamine (ManLev), a synthetic analogue with a ketone functionality.[76] Its presence was determined by the ligation of a biotinylated hydrazine-based probe, and upon conjugation the biotin tag was subjected to an avidin stain resulting in an increase in fluorescence intensity. However, this system is limited by the presence of the ketone functionality. There are a variety of ketone-containing small molecules inside the cell, which could prevent selective targeting by the hydrazine probe.[146]

Although work was shown to mitigate this issue, the focus shifted to finding new cell-compatible chemoselective techniques for targeting sialic residues. The azide group became a prevalent tag for this type of work[64, 147-148] owing to its inert reactivity *in vivo*. Over the years, Bertozzi and coworkers have used azides in the form of the Staudinger ligation as a method for labeling live cells with azido-tagged sugars.[148-151] They used the unnatural sugar N-azidoacetylmannosamine (Ac_4ManNAz) and delivered it live cells, where it became metabolically incorporated to label sialic acid containing glycoproteins (Figure 1.9). A phosphine moiety containing a fluorescence tag could be introduced to successfully label the cell glycan. It should be noted that these authors admitted the protocol is limited by the number of glycans that can be labeled. This is due to the low tolerance of a large number of glycoproteins for functionalized sugars.

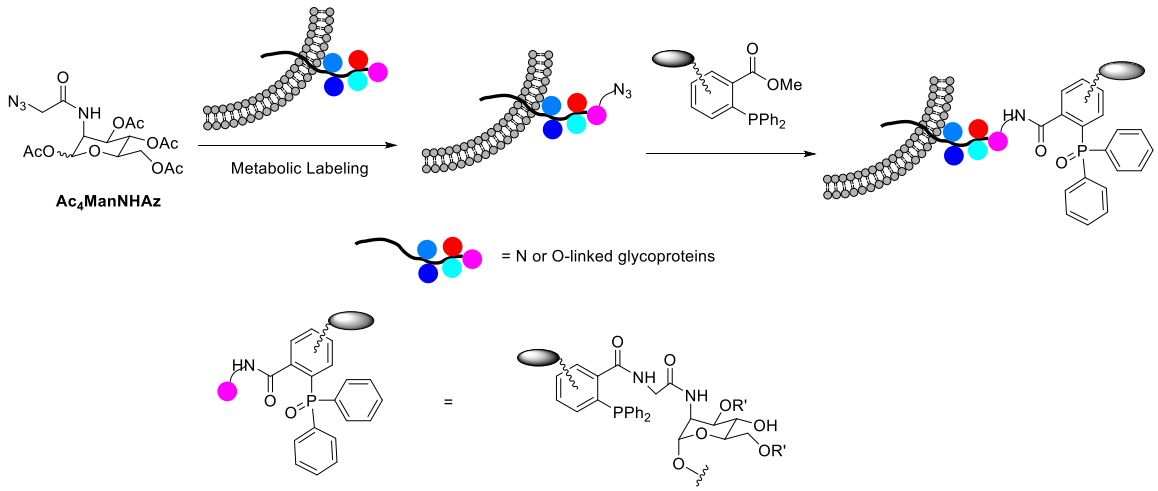

Figure 1.9 Metabolically labeling with azido-tagged glycoproteins. Cell glycans derivatized with azides target phosphine reagents for live-cell labeling.

In 2010, Finn and coworkers utilized azide-alkyne click chemistry as a tool for labeling live cells with Ac_4ManNAz-labeled sugars.[115] This method improved on the reaction kinetics seen in the studies with the Staudinger ligation, and since the copper (I) catalyst is known to be a detriment to cells, they used a THPTA ligand to quench the production of reactive oxygen species (ROS) brought on by copper (I). Additionally, Bertozzi and coworkers have reported the use of cyclooctynes as a carrier for labeling live cells coated with Ac_4ManNAz.[152-153] Both copper-catalyzed and copper-free click chemistry perform better as a method compared to the Staudinger ligation because of faster reaction kinetics, but the copper-free click reaction stands out as a more attractive option for in vivo imaging and targeting because it does not require the delivery of copper catalyst.

As previously introduced, metabolic labeling opens enables the selective labeling of biomolecules or cells, which could then be exploited for targeted delivery. Through the selective labeling of disease-associated biomolecules with azide in this manner, liposomes carrying a cyclooctyne moiety could selectively target the reactive functional group along the cell surface. Due to the close proximity between the liposome and cell, fusion could be triggered, and liposomes carrying encapsulated drug could be delivered to the cell. Cancer cells contain a more abundant range of sialic acid residues,[154] and other biomolecules, and therefore metabolic labeling, and subsequently fusion, at these sites could be beneficial targeted delivery. The projects described in this dissertation provide the

first steps for this selective drug delivery via click chemistry by analyzing the molecular determinants for membrane fusion by copper-free click chemistry.

Chapter 2: Design and Synthesis of Copper-Free Clickable Lipids for Membrane Derivatization and Triggered Fusion

2.1 Background and Significance

The design for the synthetic lipids presented in this document is largely inspired by work in past groups, who have attached a variety of ligands and reactive groups onto lipids to drive fusion. Since phospholipids are abundant in nature, a significant amount of work has been reported on the successful functionalization of phospholipids to produce functionalized lipids. In particular, PE is commonly used to generate derivatized lipids through the amine moiety on the head group. The modifications are made with the intention of mimicking cellular functions and exploiting pathways inside the membrane. Some of these modifications include the introduction of azides,[116, 155-159] alkynes,[158-162] DNA nucleotides,[163-165] and tri-dentate ligands.[166-168]

One of these biological processes, membrane fusion, has been mimicked through the aid of synthetic analogues capped with an azide and linear alkyne, respectively. Most synthetic lipids found in the literature contain a phosphate head group and long acyl chains, often derived from phosphatidylethanolamine (PE). Since PE contains a terminal amino group, this is commonly functionalized through reaction with carboxylic acid moieties through amide bond forming coupling reactions, akin to the formation of a peptide bond. PE constructs can be purchased through a commercial vendor, but the extreme polarity and charge of the phosphate head group makes the synthesis, purification and characterization of

phospholipids rather arduous. Thus, we have instead used the triazole group because it offers a more convenient path in synthesis.[156-157] The triazole can be synthesized by copper-catalyzed click chemistry, polar enough to reside at the aqueous interface,[108] and the compounds are easier to purify and characterize due to their lack of charge.

2.2 Design of ODIBO lipid 1

Since are goal has been to trigger membrane fusion via copper-free click, we set out to synthesize lipid analogues containing a cyclooctyne as well as those bearing an. For our own synthetic analogue, ODIBO lipid **1** (Figure 2.1), we used a similar approach to constructing this molecule to previous examples.[130] We incorporated long acyl chains to provide an anchor to embed these clickable lipids in the membrane. As previously described, the triazole group facilitates synthesis through click chemistry and is sufficiently polar to mimic the phosphate head group making the lipid amphiphilic.

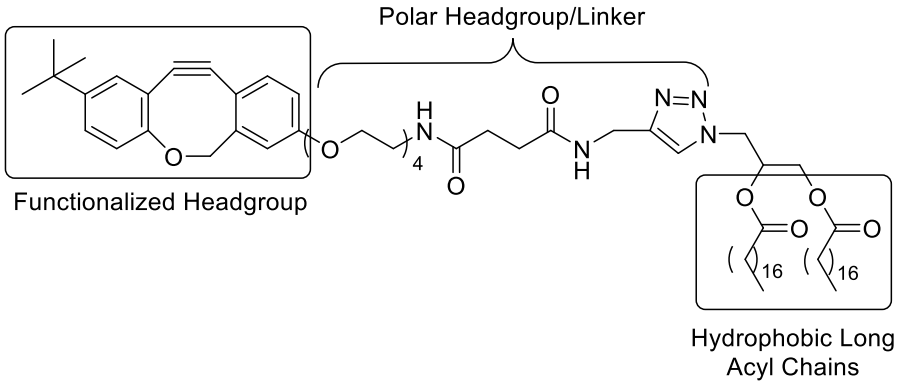

Figure 2.1 Design and structural components of ODIBO lipid **1**

The ODIBO group is linked to the lipid core using a tetra(ethylene) glycol (TEG) spacer. This was introduced to provide a flexible component to the headgroup, which allows the molecule to become more fluid and distance the reactive ODIBO functionality from the membrane surface. The TEG group is also polar, promoting presentation of the ODIBO away from the membrane core.

2.3 Design of ODIBO lipid 15 and Azide lipid 18

We discussed the aforementioned ODIBO lipid **1** as one of our synthetic targets. As an alternative to acyl groups, we also synthesized an analogue that includes ether linkages, ODIBO lipid **15**. This feature was included in our plan because ether linkages are more resistant to hydrolysis in both chemical synthesis and in biological systems.

We also designed an azido tagged lipid (**18**) (Figure 2.2), which unlike azido lipid **5** contains a triazole head group, and additionally includes an alkyl chain by which the azide is attached. A concern of this lipid is that, since this structure is fairly hydrophobic, the reactive azide group may be buried within the membrane when incorporated into liposomes. This could disallow the azide from reacting with the cyclooctyne moiety, rendering this azido-lipid less effective. However, spacing of the azide group further from the membrane surface compared to **5** could be beneficial. Therefore, we elected to evaluate both of these potential azido-lipids for membrane fusion.

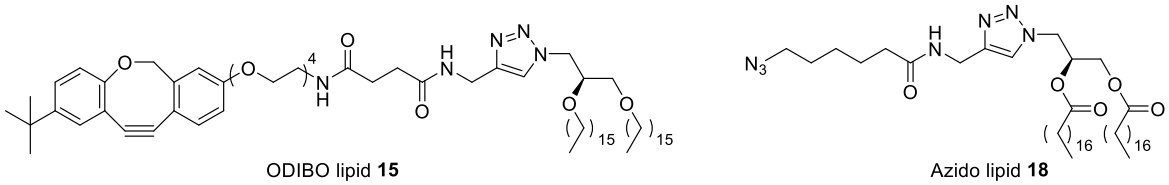

Figure 2.2 Structures of ODIBO lipid **15** and Azido-lipid **18**

2.4 Synthetic Procedure for ODIBO lipid 1

The synthetic scheme used to access both **5** and **1** began with commercially available (S)-glycerol acetonide **6**, which can be tosylated to produce **7** (Figure 2.3). The stereocenter present in reagent **6** matches natural phospholipid stereochemistry to avoid the potential perturbation of membrane properties. Next, tosyl acetonide **7** was treated with acid in methanol to deprotect the acetonide and produce diol **8**. This product was immediately treated with an excess amount of sodium azide (NaN_3) in dry and degassed dimethylforamide (DMF) to produce azido diol **9**. DMF has a tendency to decompose at high temperatures, and the reaction required heat as a catalyst. As a precaution, we distilled DMF under vacuum, let it sit in sieves for 24 hours, and then degassed it. The product could be easily traced on a TLC plate because the tosyl diol **8** is UV active, whereas the azido diol is not. Although the starting tosylate and product azide are similar in R_f value, the aforementioned difference in UV activity was used to track product formation.

Finally, azido diol **9** was treated with two equivalents of stearic acid and dicyclocarbodiimide (DCC) to produce azido lipid **5**. Azide lipid **5** could be used as a fusogenic lipid, since it possesses the necessary clickable group and simple

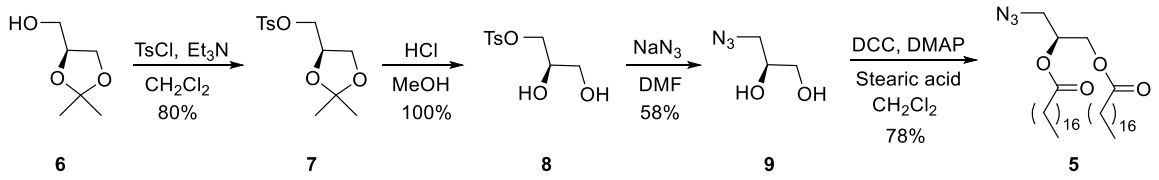

Figure 2.3 Synthetic Scheme for Azide lipid **5**

structure in the glycerol backbone. The small headgroup relative to the length of the acyl chains likely makes this a non-bilayer forming lipid, similar to the shape and properties of PE. Despite the simple structure, we elected to evaluate this compound for fusion since it is already made during the synthesis of ODIBO-lipid **1**.

The second stage of the synthesis began by reacting a boc-protected alkyne moiety (**10**) with azide lipid **5** by employing the copper-catalyzed click reaction (Figure 2.4). This reaction has shown to be compatible with the labeling of biomolecules, and the conditions under those circumstances call for the use of a catalytic amount of copper. Initial attempts to synthesize lipid **11** failed under these conditions, and instead we used excess amounts of copper reagent and sodium ascorbate. The copper solution was added dropwise to the reaction mixture containing all other reactants, and each drop resulted in the solution turning brown for a small amount of time. This transient color change indicated that copper (II) was being converted into copper (I), which is the active catalyst in this reaction. Lipid **11** was successfully obtained after purification. This analogue sets up the final synthesis steps to produce lipids **1** and **18** (Figure 2.5).

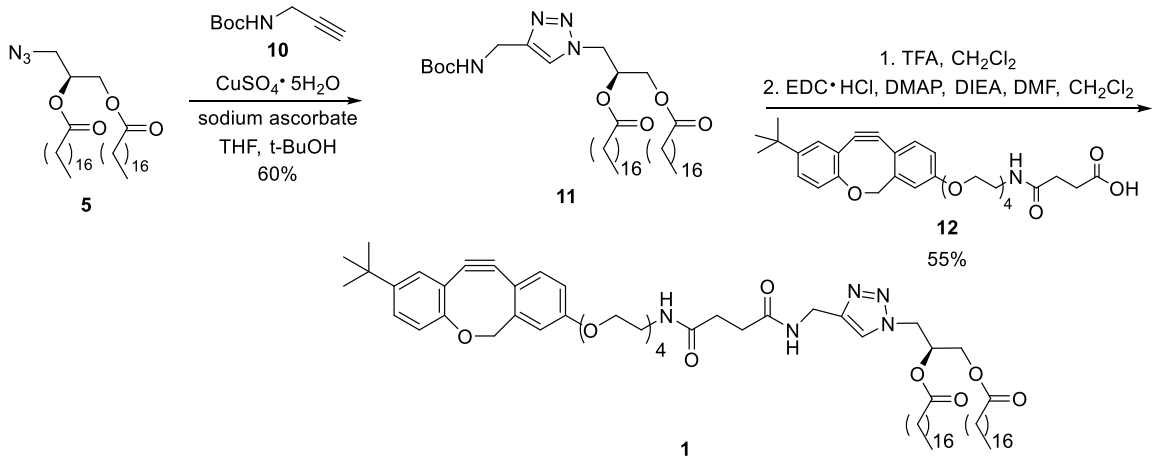

Figure 2.4 Synthetic Scheme for boc-lipid **11** and ODIBO lipid **1**

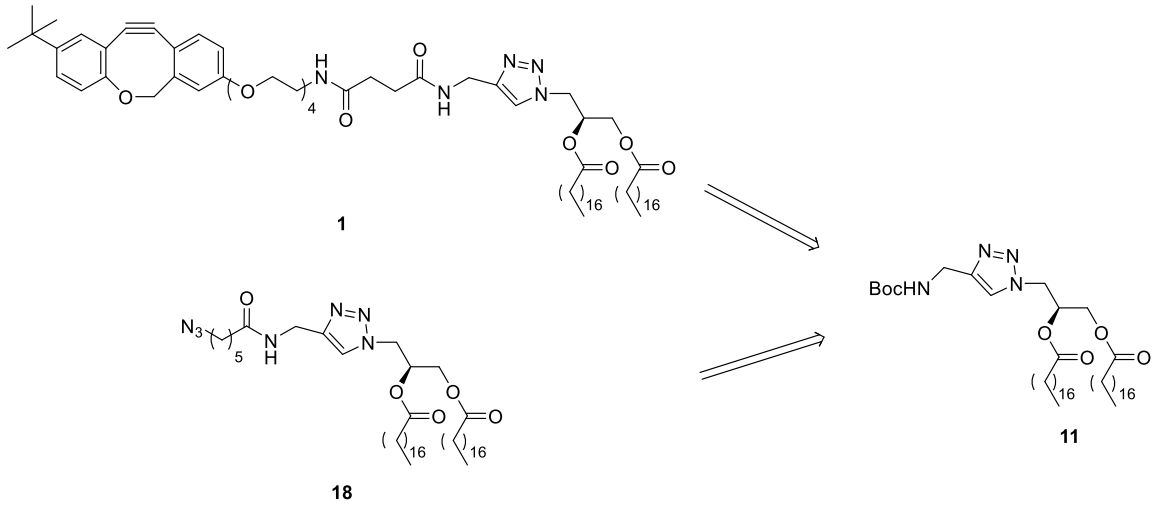

Figure 2.5 Retrosynthetic representation of Azido-lipid **18** and ODIBO lipid **1**

Next, we attempted to couple lipid **11** with ODIBO-TEG-COOH **12** which was synthesized by Christopher McNitt in Vladimir Popik's group at the University of Georgia. This reactant contains both the desired copper-free clickable ODIBO and the TEG spacer. We first intended to deprotect the boc group on lipid **11** and generate the amine analogue, and then react it with **12** by utilizing standard amide coupling reagents.

We first attempted to pre-mix **12** with base and coupling reagent to form the activated ester. We stirred this solution for 10 minutes before adding the amino lipid to the reaction in order to give enough time for the activated ester to form. Unfortunately, after 5 hours of stirring, there was no disappearance of any starting material on the TLC plate. We decided to optimize our amide coupling conditions using benzoic acid **13** (R-COOH) and 4-ethylaniline **14** (R'-NH_2) (Figure 2.6). We wanted to compare yields of a one-pot versus two-pot synthesis; the latter is what we initially used for **11** and **12**. Our strategy for employing a one-pot synthesis was to dissolve both the acid and amine in the same vial, then add the coupling reagent last. Using this procedure, we were able to obtain the amide product using the one-pot method in 69%, whereas the two-method did not produce any amide.

We incorporated this one-pot method into our attempt at synthesizing ODIBO lipid **1**. Consequently, we were able to observe a new spot on the TLC plate, and ODIBO lipid **1** was isolated in 55% yield. It should be noted that lipid **1** and ODIBO-TEG-COOH **12** are extremely close on the TLC plate, and can be tough to separate via column chromatography. Instead, we performed a sodium bicarbonate

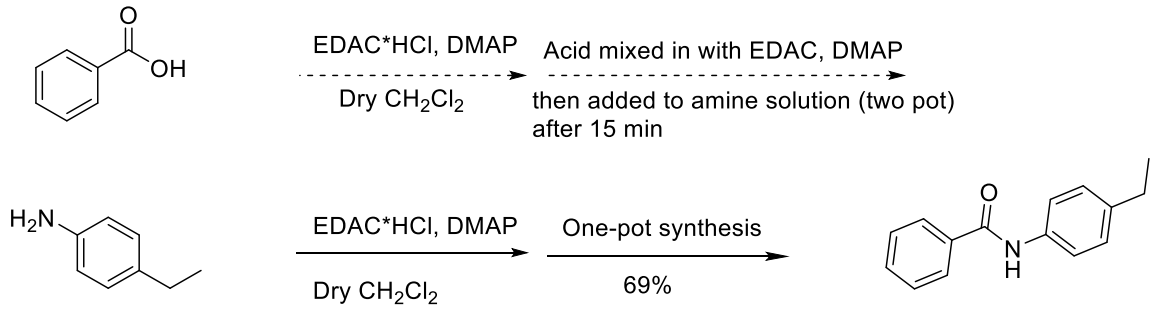

Figure 2.6 Synthetic scheme for the reaction of acid **13** and amine **14**; meant to optimize amide coupling conditions

($NaHCO_3$) extraction of the organic layer. This affects the acid by generating the sodium carboxylate and CO_2, while leaving the desired product unharmed. Additionally, an organic-soluble urea byproduct is generated over the course of this reaction and can remain hidden on a TLC plate and runs alongside ODIBO lipid **1** during column chromatography. This byproduct can be removed by dissolving the crude in ethyl acetate, and then siphoning off the liquid. NMR studies confirmed ODIBO lipid **1** as the major product upon concentration of the liquid and column chromatography.

2.5 Synthetic Procedure for ODIBO lipid 15

We also synthesized another ODIBO lipid with ether tails (**15**) as an additional target, particularly based on initial synthetic challenges in producing compound **1**. We outlined earlier how shorter tails in the hydrophobic region, as well as the incorporation of ether linkages, could alter the fluidity once embedded in a membrane. We set out to synthesize ODIBO lipid **15** using similar chemistry to the route developed to produce lipid **1**. Starting out with azide diol **9**, we performed a Williamson ether synthesis to produce azide lipid **16** (Figure 2.7). This reaction

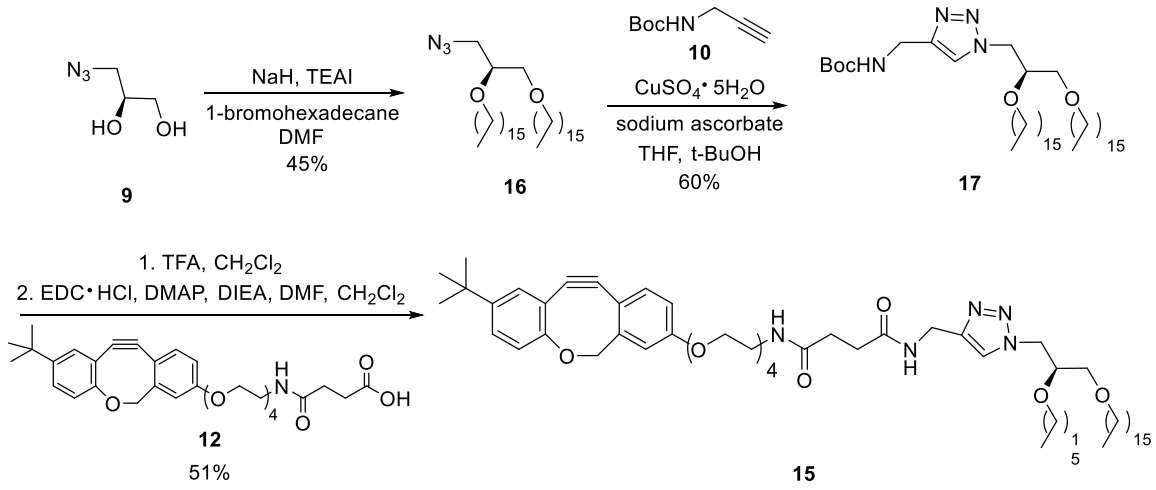

Figure 2.7 Synthetic scheme for making ODIBO lipid **15**

required the use of freshly distilled DMF to achieve completion, mainly due to the sensitive properties of sodium hydride (NaH) in water. We also included tetraethylammonium iodide (TEAI) as a catalyst in order to transform the 1-bromohexadecane reagent into a better electrophile. Next, **16** was reacted with boc-alkyne **10** using copper-catalyzed click conditions to produce **17**. Identical parameters were used for this step as they were for the production of lipid **11.**

Finally, boc lipid **17** was deprotected to give the amine analogue, and then reacted with ODIBO-TEG-COOH **12** to produce ODIBO lipid **15**. We used a different procedure for the deprotection of lipid **17** than that of lipid **11**. First, we dissolved lipid **17** in 50:50 trifluoroacetic acid (TFA)/CH_2Cl_2, and after 2 hours of stirring, the solution was poured into a 1 M ammonium hydroxide ($NH_4^+OH^-$) solution to quench the reaction. We could not use this step for lipid **11** because the ester tails are sensitive to strong base, but ethers are not. Therefore, the amino lipid analogue was extracted from this layer with CH_2Cl_2, and then isolated before

proceeding on to the coupling reaction. The benefit of this to ensure removal of all acid, save time, and eliminate the excess amount of tertiary amine that was used in the prior synthesis to neutralize the amine. This ensures the amino-lipid analogue is completely deprotonated and a strong nucleophile is available for the subsequent coupling step.

2.6 Synthetic procedure for azide lipid 18

We also synthesized azide lipid **18** to add to our library of fusogenic lipids due to concerns over the presentation of lipid **5**. First, we deprotected lipid **11** using the identical method seen with generating ODIBO lipid **1**. Immediately after collecting the amine analogue, azidohexanoic acid **19** was reacted with the amine under amide coupling conditions (Figure 2.8). We used the one-pot method as seen previously with the production of ODIBO lipids **1** and **15**. After completion of the reaction, the crude was subjected to another $NaHCO_3$ extraction because there was overlap between **18** and **19** on the TLC plate. This extraction successfully isolated lipid **18** as seen through NMR and mass spectrometry results.

2.7 Attempted Syntheses for Other Clickable Lipids

Before our success of synthesizing ODIBO-lipids, **1** and **15**, and azido-lipid **18**, we attempted to synthesize another cyclooctyne-labeled lipid. This lipid has the identical components as that seen with ODIBO lipids **1** and **15**: acyl chains anchoring as the hydrophobic backbone, a triazole and TEG linker for hydrophilicity, and the cyclooctyne moiety at the head of the compound. This compound contained an ADIBO moiety as this was designed prior to Popik's report

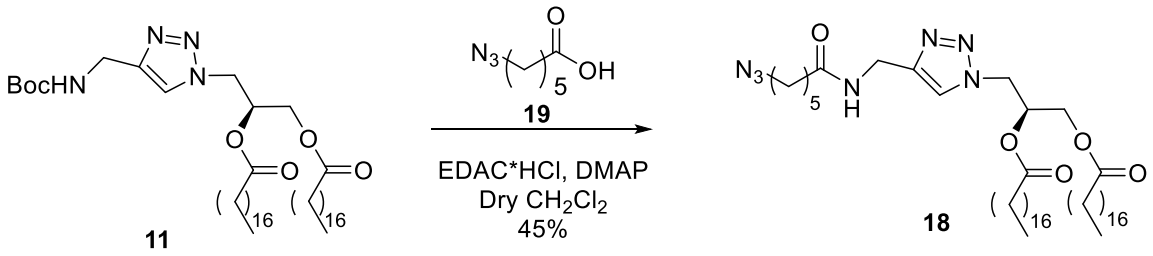

Figure 2.8 Synthetic scheme for azide lipid **18**

of the enhanced reactivity of ODIBO (Figure 2.9). We attempted to build this molecule up sequentially, similar to how we built ODIBO lipids **1** and **15**. We concentrated on synthesizing the hydrophobic backbone and TEG linkers individually, and then planned to couple these to generate the lipid scaffold.

2.7.1 Strategy for Synthesizing Cyclooctyne Lipid 20

Once azide lipid **5** was synthesized, we started to work on synthesizing the TEG linker. We synthesized boc-protected alkyne **21** by following a previously published procedure,[155] but made necessary modifications that we felt improved the yield of each step. We started with tetraethylene glycol **22** as our starting material in this scheme, and were able to functionalize one side of the molecule with diazoethylacetate to produce **23** (Figure 2.10). The reaction was controlled by cooling the temperature of the solution to prevent both alcohols from becoming functionalized. Mono-addition to TEG allowed the alcohol on the opposite side of the chain to be transformed into a mesylate, and then substituted with azide to produce **24**. The addition of mesyl chloride was controlled by cooling the temperature of the solution down to 0 ^{0}C because mesylates are susceptible to uncontrolled substitution at warm temperatures. As for azide introduction, we've

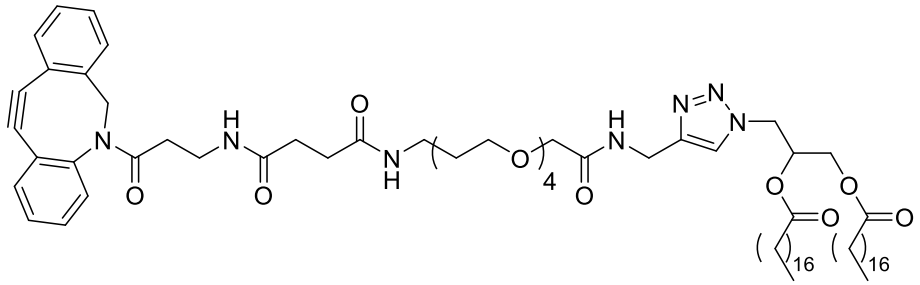

Figure 2.9 Structure of cyclooctyne lipid **20**

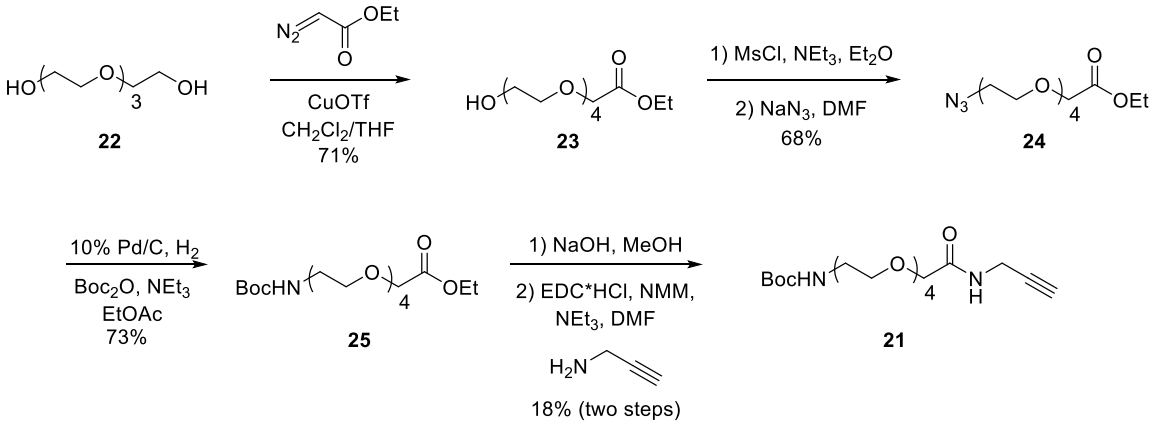

Figure 2.10 Synthetic scheme for boc-TEG alkyne **21**

shown before that azide substitution reaction works well with DMF as a solvent, however this particular compound reacted better with dry ethanol. This is likely due to better solubility of the mesylate compound.

Next, the azide was converted into the boc-protected amine **25** by simultaneous addition of palladium and hydrogen gas (Pd/H_2) and as well as di-*tert*-butyldicarbonate (Boc_2O). Hydrogen gas was added into the flask through a balloon, and then the system was evacuated. This cycle was repeated three times to ensure the reaction was stirred under a complete hydrogen atmosphere. After isolating **25**, we performed hydrolysis to produce the corresponding boc-protected carboxylic acid, which was then converted into boc-protected alkyne **21** by amide coupling conditions. We used the one-pot method for this reaction, which was controlled by cooling the solution down to 0 ^{0}C prior to adding EDC·HCl.

Next, we constructed our lipid component **26** by reacting azide lipid **5** with boc-protected alkyne **21** via the copper-catalyzed click reaction (Figure 2.11). We used similar conditions for this reaction as we did for the synthesis of lipid **11**, including excess amounts of copper (II) sulfate and sodium ascorbate. In the final step of this synthesis, attempted to deprotect boc-lipid **26** and couple the resulting amine with ADIBO-COOH **27** to form **20**. We were unsuccessful in producing this lipid. We believe in retrospect the reaction may not have worked due to the following possible reasons: the ammonium moiety formed by boc deprotection in acid may not have been full deprotonated for the subsequent coupling reaction, TFA/CH_2Cl_2 was left in the flask with lipid **26** for too long (potential ester hydrolysis), quenching

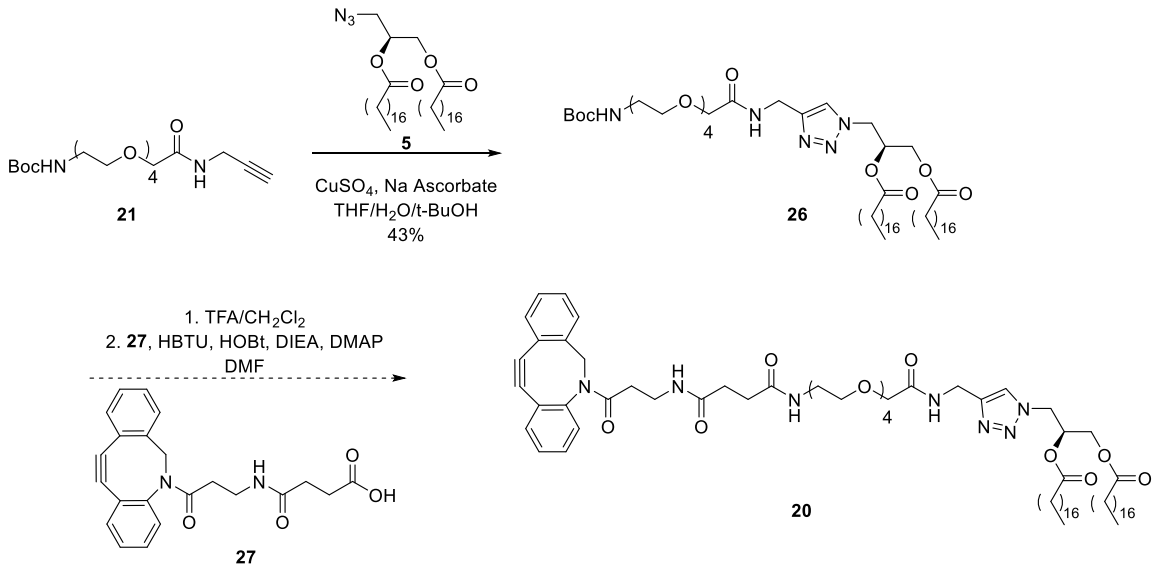

Figure 2.11 Synthetic scheme for ADIBO lipid **20**; boc-TEG-lipid **26** was isolated, but not successfully be converted into lipid **20**

with solid sodium carbonate ($NaCO_3$) led to a messy flask to clean up and potentially cleaved the ester tails in the hydrophobic backbone.

The reaction time was rectified when attempting to synthesize ODIBO lipid **1**. We used intermittent TLC analyses to track the original boc-protected lipid **11** on its course to the amine analogue. Leaving this acidic mixture stir for too long could have compromised other components of the molecule, such as cleaving the ester tails in the hydrophobic backbone. When synthesizing ODIBO lipid **1**, the quenching of the solution was kept in the same phase as the reaction, since we added liquid base to the reaction. Lastly, we outlined before the benefit of the one-pot method when performing amide coupling versus the two-pot method.

2.7.2 Strategy for Synthesizing ADIBO-COOH 28

We originally set out to synthesize ADIBO-COOH **28** to enable the synthesis of clickable lipids. However, due to challenges we encountered during this process, and since Dr. Vladimir Popik's group at the University of Georgia reported the enhanced reactivity of ODIBO around this time, we ultimately formed a collaboration in which they provided ODIBO-COOH **12**. Multiple groups have adapted their own methods for synthesizing ADIBO-COOH **28**, and we decided to follow the procedure from Chadwick and coworkers.[169] First, we obtained commercially available dibenzosuberone **29** and converted that into the oxime analogue **30** (Figure 2.12). This reaction required the use of dry pyridine for the best results. Upon workup, dilute acid (HCl) was used with the intention of only extracting the base out of the solution and not compromising the oxime product.

Next, oxime **30** underwent a ring expansion to cyclic amine **31** using DIBAL-H. This is a modification from other procedures that first convert to the amide product followed by reduction to generate the amine. Once **31** had been isolated, the acid chloride moiety **32** was coupled to generate amide **33**. This step was the most problematic because it required the initial production of acid chloride **32**. This reagent is derived from a succinyl ester and then reacted with neat sulfonyl chloride. We couldn't isolate the succinyl acid chloride, so it was immediately transferred to the reaction flask along with **31**. This reaction could've also been inhibited by residual sulfonyl chloride as well.

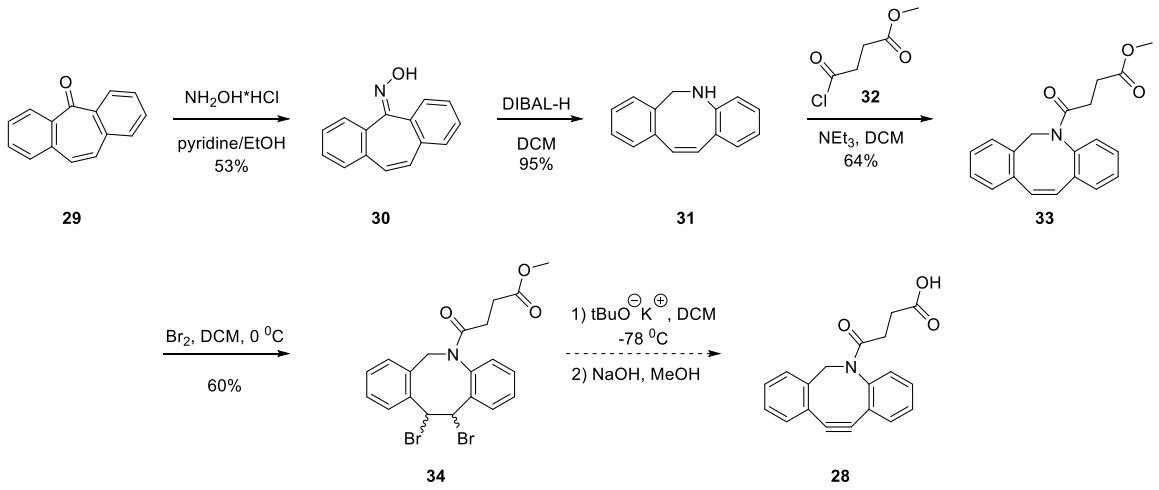

Figure 2.12 Synthetic scheme for ADIBO-COOH **28**; double elimination step from **34** to **28** could not be achieved

After isolation of amide **33**, the compound was subjected to bromine to produce the dibrominated product **34**. Next, we attempted to synthesize cycloalkyne **28** through double elimination in base to form the alkyne. This reaction was attempted with both potassium t-butoxide (KOt-Bu) and sodium amide ($NaNH_2$). The reaction proceeded by a fast initial elimination generating a vinyl bromide. The elimination of the second bromine atom was more challenging. We attempted a variety of conditions including the addition of excess strong base and initial elimination with KOt-Bu followed by treatment with $NaNH_2$ to promote the second elimination. Unfortunately, we were unable to isolate the cycloalkyne product. We attempted to add-in t-BuOH slowly with potassium metal (K^0) already in the flask, but we could not isolate the t-butoxide moiety. As for attempting the reaction with $NaNH_2$, we attempted the same strategy of generating the strong base by slow addition. This method did not produce the desired cycloalkyne functional group. Thus, we turned

our attention to ODIBO-COOH **12**, which was provided by Christopher McNitt in Dr. Popik's group.

2.8. Conclusions

The synthetic routes described in this chapter allowed us to access multiple ODIBO- and azide-containing lipids to pursue membrane fusion and derivatization driven by copper-free click chemistry. Many challenges were encountered during these syntheses, some of which were ultimately overcome to produce compounds for studies. In particular, the synthesis of ADIBO functionalities was not successful. For this reason, and since the ODIBO group was reported around this time, we turned our attention to ODIBO-lipids in collaboration with Dr. Popik's groups. Studies detailing the efficacies of these compounds for membrane derivatization and fusion are described in the following chapter.

2.9 Experimental Procedures

Reagents and solvents were generally purchased from Acros, Aldrich or Fisher Scientific and used as received. ^{1}H, ^{13}C, and MS data for compounds **5**, **7-10**, **12**, **19, 21, 23-26**, **30-34** matched reports found in the literature,[155, 169-170] but ^{1}H NMR values were listed below to confirm our scheme. ^{13}C NMR is provided for azido-diol **9** because we had trouble obtaining a clean ^{1}H NMR spectrum. Dry solvents were obtained from a Pure solvent delivery system purchased from Innovative Technology, Inc. Column chromatography was performed using 230-400 mesh silica gel purchased from Sorbent Technologies. NMR spectra were obtained using Varian Mercury 300 and 500 MHz spectrometers. Mass spectra were obtained with

JEOL DART-AccuTOF and ABI Voyager DE Pro MALDI mass spectrometers with high-resolution capabilities.

2.9.1 ODIBO Lipid 1 Synthesis

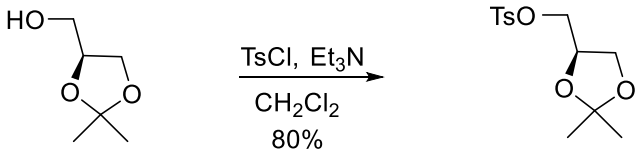

6 **7**

(R)-(2,2-dimethyl-1,3-dioxolan-4-yl)methyl-4-methylbenzenesulfonate (**7**): (S)-Glycerol acetonide **6** (1.00 mL, 8.09 mmol) was dissolved in dry CH_2Cl_2 (50 mL) and the reaction was allowed to stir at rt for 5 min. Next, triethylamine (NEt_3, 1.57 mL, 11.3 mmol) and tosyl chloride (TsCl, 2.15 g, 11.3 mmol) were added in succession and the solution changed from clear and colorless to a light yellow solution. The reaction was stirred at rt overnight under an Ar atmosphere. At completion, the solution was poured into 40 mL of 0.75 M hydrochloric acid (HCl). The organic layer was collected, and then washed with 2x 50 mL water (H_2O) and 1x 50 mL brine. The organic layer was dried with magnesium sulfate ($MgSO_4$), filtered, and the solvent was evaporated to produce a crude solution. The solution was purified via column chromatography with 10%EtOAc/hexane, and tosyl acetonide **7** was produced as a yellow oil in 80% yield (1.85 g). ^{1}H NMR (300 MHz, $CDCl_3$): 7.75 (d, J = 8.3 Hz, 2 H), 7.32 (d, J = 7.9 Hz, 2 H), 4.20-4.27 (m, 1 H), 3.96 (m, 3 H), 3.72 (m, 1 H), 2.41 (s, 3 H), 1.30 (s, 3 H), 1.27 (s, 3 H).

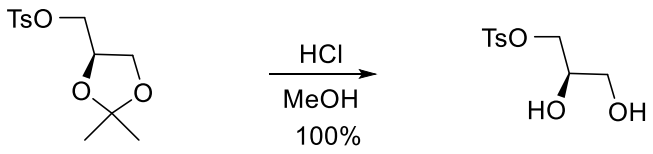

7 **8**

(R)-2,3-dihydroxypropyl 4-methylbenzenesulfonate (**8**): Tosyl acetonide **7** (1.50 g, 5.24 mmol) was dissolved in 0.5 M HCl/MeOH (15 mL). The solution was stirred at rt until the starting material disappeared on TLC (~3 hrs). The reaction was quenched with $NaHCO_3$ (0.3 g) and stirred for 25 min. Next, the solution was filtered, evaporated, and the flask was placed on the high vacuum. Tosyl diol **8** was isolated in quantitative yield (1.2 g) as a colorless oil. ^1H NMR (300 MHz, $CDCl_3$): 7.79 (d, J = 7.9 Hz, 2 H), 7.35 (d, J = 7.7 Hz, 2 H), 4.06 (m, 2 H), 3.94 (m, 1 H), 3.65 (m, 2 H), 2.45 (s, 3 H).

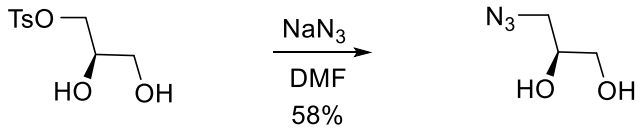

8 **9**

(S)-3-azidopropane-1,2-diol (**9**): Tosyl diol **8** (900 mg, 3.66 mmol) was dissolved in dry and degassed DMF (8 mL). As the solution was stirred, NaN_3 (951 mg, 14.6 mmol) was added to the flask. The solution was heated to 80 ^0C and refluxed overnight while stirring. Next, the solvent was evaporated, and the resulting crude was subjected to column chromatography (60% EtOAc/hexane) in order to purify the compound. Azido diol **9** was isolated in 58% yield (250 mg) as a yellow oil. ^1H

NMR (300 MHz, $CDCl_3$): 3.83 (d, J = 17.2 Hz, 2 H), 3.59-3.66 (m, 1 H), 3.37 (d, J = 6.0 Hz, 2 H). ^{13}C NMR (300 MHz, $CDCl_3$): 70.99, 63.97, 53.39.

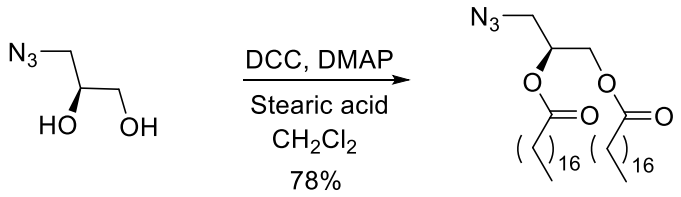

9 **5**

(S)-3-azidopropane-1,2-diyl distearate (**5**): Azide diol **9** (250 mg, 2.14 mmol) was dissolved in freshly distilled CH_2Cl_2 (20 mL). Stearic acid (1.34 g, 4.71 mmol) was added to the solution, then after 5 min. of stirring DCC (1.06 g, 5.14 mmol) and DMAP (130 mg, 1.07 mmol) were added. The solution was stirred at rt overnight, then the solvent was evaporated. The resulting crude mixture was purified via column chromatography (0-10% EtOAc/hexanes), and azido lipid **5** was produced in 78% yield (1.10 g) as a white solid. ^1H NMR (300 MHz, $CDCl_3$): 5.18 (m, 1 H), 4.26-4.32 (dd, J = 11.9, 4.6 Hz, 1 H), 4.12-4.17 (dd, J = 11.9, 5.6 Hz, 1 H), 3.46 (d, J = 4.7 Hz, 2 H), 2.29-2.37 (m, 4 H), 1.63 (m, 4 H), 1.25 (s, 56 H), 0.88 (t, J = 7.0 Hz, 6 H)

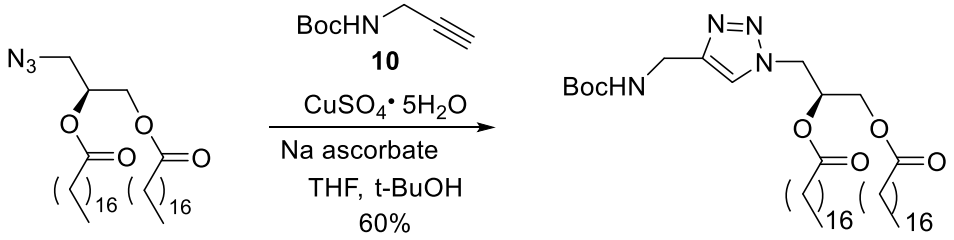

5 **11**

Synthesis of (S)-3-(4-(((tert-butoxycarbonyl)amino)methyl)-1H-1,2,3-triazol-1-yl)propane-1,2-diyl distearate (Boc-Triazole Lipid) (**11**): Azido lipid **5** (57.2 mg, 0.0876 mmol) and Boc-alkyne **10** (11.3 mg, 0.0730 mmol) were both dissolved in

a 2:1 mL mixture of THF/t-BuOH. Copper (II) sulfate pentahydrate ($CuSO_4 \cdot 5H_2O$, 72.9 mg, 0.292 mmol) and sodium ascorbate (115 mg, 0.584 mmol) were each dissolved in 0.5 mL of water in separate vials. The ascorbate solution was added to the THF/t-BuOH mixture slowly at rt. After 5 min of stirring, the copper (II) sulfate solution was added slowly (each drop changed the color of the solution from clear yellow to dark brown). After stirring for 16 h, the solvent was evaporated to yield a greenish blue solid. The crude solid was purified via column chromatography (1-2.5% MeOH/CH_2Cl_2) to give boc-triazole lipid **11** in 60% yield (58.1 mg) as white solid. ^{1}H NMR (300 MHz, $CDCl_3$): δ 7.55 ppm (s, 1H), 5.37 ppm (m, 1H), 5.07 ppm (bs, 1H), 4.59 ppm (s, 2H), 4.38 ppm (d, J = 5.9 Hz, 2H), 4.30 (dd, J = 12.0, 4.4 Hz, 1H), 4.00 ppm (dd, J = 11.1, 6.2, 1H), 2.33 ppm (m, 4H), 1.62 ppm (s, 4H), 1.44 ppm (s, 9H), 1.26 ppm (bs, 56H), 0.88 ppm (t, J = 6.5 Hz, 6H). ^{13}C NMR (75 MHz, $CDCl_3$): δ 173.06, 172.50, 157.81, 122.74, 109.99, 77.18, 69.30, 61.93, 50.08, 36.02, 34.01, 31.91, 29.69, 29.62, 29.47, 29.35, 29.24, 29.12, 29.02, 28.35, 24.83, 22.68, 14.10. calc. exact mass [M+H]: 805.6782 MS-DART-(+): 805.7267.

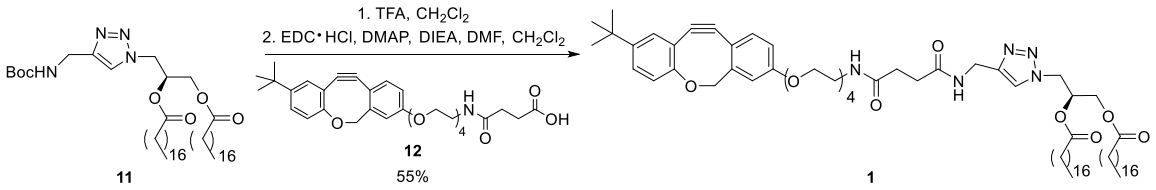

ODIBO-triazole-lipid (**1**): In a flame-dried flask, lipid **11** (12.0 mg, 0.0149 mg) was dissolved in freshly distilled CH_2Cl_2 (1 mL). TFA (1 mL) was slowly added at RT. The solution was stirred for 2 h or until the TLC showed complete removal of the starting material. The solvent was evaporated, and the resulting crude was

then re-dissolved in dry DMF (1 mL). DIEA (100 µL, 0.574 mmol) was added to the DMF solution and the reaction was allowed to stir until gas production subsided. To a flame-dried vial containing ODIBO-TEG-COOH **12** (8.01 mg, 0.0144 mmol) the DMF solution was added. Next, the solution was suspended in an ice bath, and DMAP (1.99 mg, 0163 mmol) was added. After 10 min of stirring in an ice bath, EDC·HCl (3.12 mg, 0163 mmol) was added. The solution was stirred for 10 min, and then removed from the ice bath with continued stirring overnight. The DMF was removed using a rotary evaporator, and the crude was then re-dissolved in chloroform ($CHCl_3$) (5 mL). The organic solution was washed with 2x 5 mL $NaHCO_3$, 1x 5mL H_2O, and 1x 5 mL brine. The organic layer was dried with magnesium sulfate, filtered, and then concentrated under nitrogen (N_2) gas. The crude was purified via column chromatography (2.5-3% MeOH/CH_2Cl_2) to produce ODIBO-lipid **1** in 55% yield (10.1 mg). ^{1}H NMR (500 MHz, $CDCl_3$): δ 7.55 ppm (s, 1H), 7.27 (s, 1H), 7.22-7.25 (dd, *J* = 8.8, 2.4 Hz, 2H), 7.07-7.11 (dd, *J* = 9.2, 2.3 Hz, 1H), 7.01-7.02 (d, J = 2.5 Hz, 1H), 6.87-6.92 (m, 1H), 6.66 (bs, 1H), 5.35 (s, 1H), 5.17 (d, J = 12.0 Hz, 1H), 5.11 (dd, J = 6.6, 3.1 Hz, 1H), 4.52-4.55 (d, J = 12.0 Hz, 1H), 4.45-4.47 (m, 2H), 4.26-4.30 (dd, J = 10.9, 4.9 Hz, 1H) 4.17 (t, J = 4.5 Hz, 2H), 4.04 (dd, J = 11.1, 6.2, 2H), 3.88 (t, J = 4.4 Hz, 2H), 3.51-3.76 (m, 10H), 3.42-3.45 (m, 2H), , 2.49 (s, 4H), 2.32 ppm (m, 4H), 1.62 ppm (m, 4H), 1.31 ppm (s, 9H), 1.26 (bs, 56H), 0.88 ppm (t, J = 6.5 Hz, 6H). ^{13}C NMR (125 MHz): δ183.13, 173.08, 172.55, 172.28, 167.07, 158.44, 148.92, 145.12, 126.70, 125.42, 123.53, 122.97, 121.18, 119.43, 117.66, 117.42, 114.42, 113.87, 110.64,

109.99, 77.81, 70.77, 70.50, 70.13, 69.89, 69.62, 69.29, 67.67, 61.97, 50.01, 39.27, 35.38, 35.07, 34.36, 34.00, 33.98, 31.91, 31.36, 29.69, 29.65, 29.48, 29.35, 29.26, 29.13, 29.03, 28.13, 24.83, 24.73, 22.68, 14.10. ESI-MALDI calculated exact mass [M+H] 1240.87 MS-ESI-(+): found 1240.8828

2.9.2 ODIBO lipid 15 Synthesis

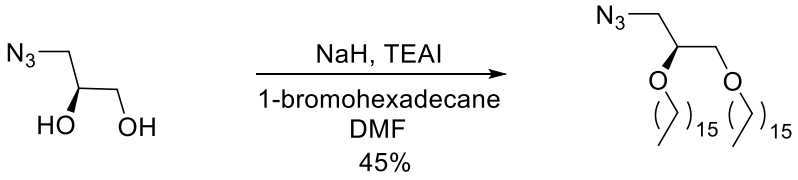

9 **16**

(S)-1-(3-azido-2-(hexadecyloxy)propoxy)hexadecane (**16**): Sodium hydride (NaH, 209 mg, 8.72 mmol) was added to a flame-dried flask, then placed under vacuum for 25 min. Dry DMF (1.5 mL) was next added and the flask was cooled to 0 ^{0}C. After stirring for 5 min, a solution of azido diol **9** (120 mg, 1.03 mmol) in dry DMF (1.5 mL) was added dropwise to the NaH solution at 0 ^{0}C. Once bubbling ceased in the flask, a solution of TEAI (45.0 mg, 0.175 mmol) and 1-bromohexadecane (700 µL, 2.26 mmol) in dry DMF (1 mL) was added dropwise. After 10 min of stirring, the ice bath was removed and the solution was stirred overnight at rt. Next, the solution was poured into 20 mL H_2O, which was then extracted with CH_2Cl_2 (3x 20 mL). The organic extracts were collected, then washed with H_2O (2x 60 mL) and brine (1x 60 mL). The organic layer was dried with $MgSO_4$, filtered, and then evaporated to produce a crude mixture. The mixture was purified via column chromatography (0% - 10% EtOAc/hexanes) to yield azido lipid **16** in 45% (300 mg) as a white solid. ^{1}H NMR (300 MHz): 3.34-3.57 (m, 9 H),

1.58-1.60 (m, 4 H), 1.26 (s, 48 H), 0.88 (t, J = 6.7 Hz, 6 H). ^{13}C (500 MHz): 77.88, 71.77, 70.64, 70.11, 52.07, 31.91, 30.01, 29.69, 29.67, 29.66, 29.64, 29.61, 29.59, 29.45, 29.35, 26.01, 22.68, 14.10. MS-DART (+) [M – N_2] calc. exact mass: 538.5558 found: 538.5365

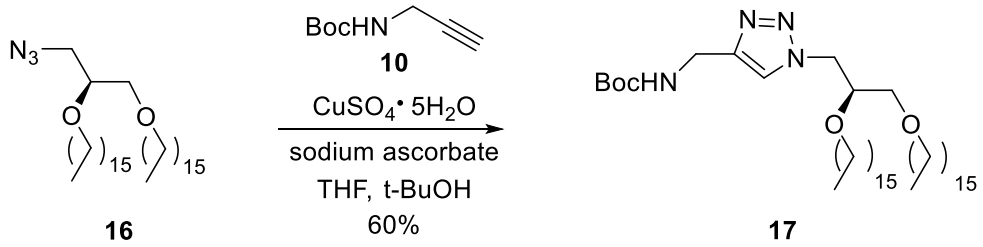

tert-Butyl-(S)-((1-(2,3-bis(hexadecyloxy)propyl)-1*H*-1,2,3-triazol-4-yl)methyl)carbamate (**17**): Azido lipid **16** (57.0 mg, 0.101 mmol) and Boc-alkyne **10** (17.2 mg, 0.110 mmol) were added to a flame-dried flask and dissolved in THF (2 mL). The solution was stirred at rt while $CuSO_4 \cdot 5H_2O$ (10.1 mg, 0.0403 mmol) and sodium ascorbate (20.0 mg, 0.101 mmol) were dissolved in 1:1 mixture of H_2O and t-BuOH (0.75 mL) in separate vials. First, the sodium ascorbate was added to the THF solution, and the resulting solution was stirred for 5 min. Next, the copper solution was added dropwise to the reaction mixture, and the color changed from dark yellow to brown after each drop. The solution stirred for 15 h at rt, and then the solvent was evaporated. The crude solid was purified via column chromatography using a gradient of 3% MeOH/CH_2Cl_2, and lipid **17** was isolated in 60% (43.7 mg) yield as a yellow solid. ^{1}H (300 MHz): 7.58 (s, 1 H), 5.10 (bs, 1 H), 4.37 (s, 2 H), 3.27-3.48 (m, 9 H), 1.53-1.55 (m, 4 H), 1.43 (s, 9 H), 1.25 (s, 48 H), 0.88 (t, J = 5.5 Hz, 6 H). ^{13}C (500 MHz): 154.95, 122.09, 109.98, 77.32, 71.90,

70.66, 69.60, 51.72, 36.16, 31.91, 29.69, 29.35, 28.36, 25.96, 22.67, 14.10. MS-DART (+) $[M+H]^+$ calc. exact mass: 721.6565 found: 721.5721

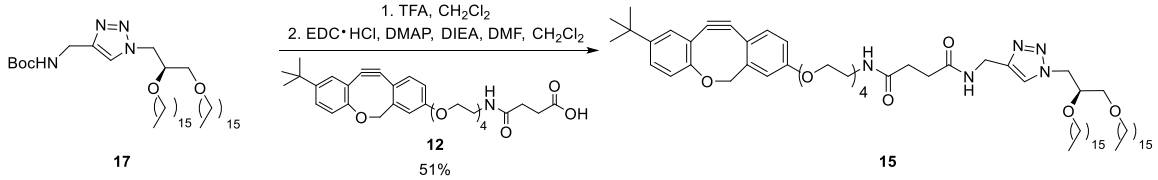

ODIBO-TEG-lipid **15**: Lipid **17** (40 mg, 0.056 mmol) was dissolved in dry CH_2Cl_2 (1 mL) and TFA (1 mL). The solution was stirred at rt for 2.5 h, and then poured into 1 M ammonium hydroxide (4 mL). The product was extracted with CH_2Cl_2 (3x 5 mL), then washed with H_2O (3x 10 mL) and 10 mL brine (1x 10 mL). The organic layer was dried with $MgSO_4$, filtered, and then evaporated to isolate the amine derivative. This product was subsequently dissolved in dry DMF (1.5 mL) and DIEA (55 µL, 0.32 mmol). This solution was added to a flame-dried vial containing ODIBO-TEG-COOH (22 mg, 0.040 mmol), and stirred for 5 min. The solution was cooled to 0 ^{0}C, and DMAP (6.3 mg, 0.051 mmol) was added. After 5 min, EDC·HCl (9.9 mg, 0.051 mmol) was added. The solution was stirred at 0 ^{0}C for 5 min, and then the ice bath was removed and the solution was stirred at rt overnight. The DMF was removed in a rotary evaporator, and the crude was re-dissolved in $CHCl_3$ (5 mL). The organic solution was washed with $NaHCO_3$ (2x 5 mL), H_2O (2x 5 mL), and brine (1x 5 mL). The organic layer was dried with magnesium sulfate, filtered, and then concentrated under N_2 gas. The crude was purified via column chromatography (2.5-3% MeOH/ CH_2Cl_2) to produce ODIBO-lipid **15** as a yellow-orange solid in 51% (23 mg) yield. ^{1}H NMR (500 MHz): 7.57 (s, 1 H), 7.20-7.25

(m, 3 H), 7.09 (d, J = 8.6 Hz, 1 H), 7.02 (s, 1 H), 6.90 (d, J = 8.3 Hz, 1 H), 6.62 (bs, 1 H), 6.37 (bs, 1 H), 5.16-5.18 (d, J = 12.1 Hz, 1 H), 5.10-5.12 (d, 9.3 Hz, 1 H), 4.49-4.52 (m, 2 H), 4.12 (s, 2 H), 3.86 (s, 2 H), 3.29-3.74 (m, 21 H), 2.63 (d, J = 4.2 Hz, 2 H), 2.48 (d, J = 9.0 Hz, 1 H), 1.55 (m, 4 H), 1.32 (s, 9 H), 1.25 (s, 48 H), 0.88 (t, J = 6.7 Hz, 6 H). ^{13}C NMR (500 MHz): 172.80, 172.01, 170.19, 148.92, 136.83, 128.44, 127.75, 125.41, 123.51, 121.17, 117.66, 114.43, 77.90, 73.86, 71.55, 70.64, 70.24, 69.61, 67.69, 45.32, 39.29, 34.36, 31.91, 31.36, 29.69, 29.35, 26.09, 22.67, 14.10. ESI-MALDI (+) $[M + H]^+$ calc. exact mass: 1156.8538 found: 1156.8416

2.9.3 Azido-lipid 18 Synthesis

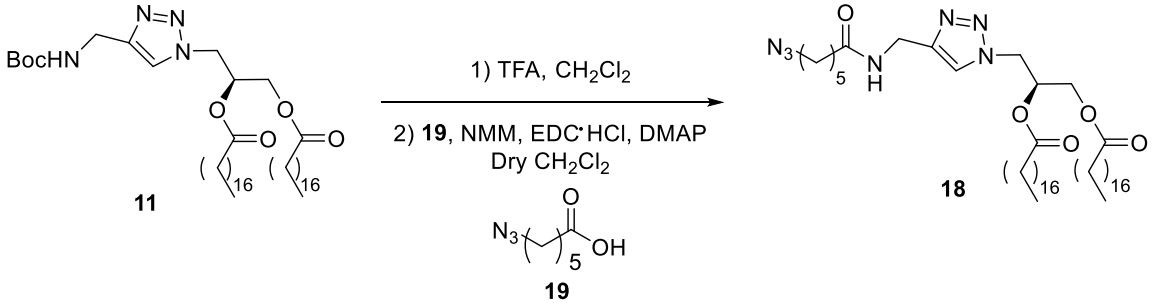

(*S*)-3-(4-((5-Azidopentanamido)methyl)-1*H*-1,2,3-triazol-1-yl)propane-1,2-diyl distearate (**18**): Boc-triazole-diastearate lipid **11** (28 mg, 0.035 mmol) was dissolved in freshly distilled CH_2Cl_2 (1 mL) and TFA (1 mL). The solution was stirred for 3 h and the solvent was evaporated with N_2 gas to yield the corresponding deprotected amine analogue. The crude was re-dissolved in dry DMF (1 mL) and NMM (38 µL, 0.35 mmol). The resulting amine solution was transferred to a flame-dried vial containing azido-hexanoic acid **19** (7.1 mg, 0.045

mmol), and the solution was cooled to 0 ^{0}C. After 5 min of stirring, DMAP (5.5 mg, 0.045 mmol) and EDC·HCl (8.7 mg, 0.045 mmol) were added in succession. The solution was stirred for 10 min before the ice bath was removed, and stirring continued overnight at rt under inert atmosphere (N_2 gas). The solvent was evaporated, and the crude solid was re-dissolved in H_2O (10 mL). The product was extracted using CH_2Cl_2 (3x 10 mL). The organic layers were collected, and were washed with 5.5% w/v $NaHCO_3$ (1x 25 mL), 0.75 M HCl (1x 25 mL), H_2O (2x 25 mL), brine (1x 25 mL). The organic layer was dried with $MgSO_4$, filtered, and then isolated to a give a crude product. The product was purified using column chromatography (1.5%-2.5% MeOH/CH_2Cl_2) to give azido-lipid **18** as a white-brownish solid in 45% (16 mg). ^{1}H NMR (300 MHz): 7.56 (s, 1 H), 6.12 (bs, 1 H), 5.38 (m, 1 H), 4.58 (m, 2 H), 4.48 (d, J = 5.5 Hz, 2 H), 4.26 (dd, J = 12.1, 4.5 Hz, 2 H), 4.07 (dd, J = 12.2, 5.2 Hz , 2 H), 3.26 (t, J = 6.8 Hz, 2 H), 2.35 (m, 4 H), 2.17 (t, J = 7.5 Hz , 2 H), 1.58 (m, 8 H), 1.26 (s, 56 H), 0.88 (t, J = 6.7 Hz, 6 H). ^{13}C NMR (500 MHz): 173.07, 172.50, 122.99, 111.77, 69.29, 61.92, 51.20, 50.11, 36.19, 34.83, 33.98, 31.91, 29.69, 29.35, 28.58, 26.33, 24.96, 22.68, 14.10. MS-ESI: calc. exact mass [M+H]: 844.69 found: 844.6958

2.9.4 Boc-TEG-alkyne 21

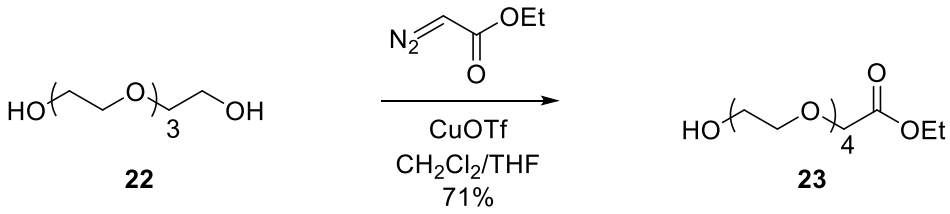

Ethyl 14-hydroxy-3,6,9,12-tetraoxatetradecanoate (**23**): Tetraethylene glycol (TEG) **22** (48.6 g, 0.251 mol) was dissolved in dry CH_2Cl_2 (25 mL) in a three-neck flask. A solution of copper (II) triflate (CuOTf) (904 mg, 2.51 mmol) in THF (5 mL) was added to the TEG solution, which was then stirred for 5 min. The flask was placed in an ice bath to cool the solution to ~0 ^{0}C. Ethyl diazoacetate (5.31 mL, 50.0 mmol) was added dropwise to the cold solution and over time the color of the solution changed from blue into darkish yellow. The reaction was stirred at rt under an N_2 atmosphere overnight. The solution was quenched by pouring into H_2O (150 mL), and the product was extracted using CH_2Cl_2 (3 x 100 mL). The organic extracts were collected and washed with H_2O (2x 100 mL) and brine (1x 100 mL). The organic solution was dried with $MgSO_4$, filtered, and then the solvent was removed by rotary evaporation to afford a yellow oil. The crude was purified via column chromatography using 3.5% MeOH/EtOAc, and **23** was produced in 71% (9.95 g) yield as a yellow oil. ^{1}H NMR (300 MHz, $CDCl_3$): 4.19 (q, J = 7.1 Hz, 2 H), 4.13 (s, 2 H), 3.60-3.71 (m, 16 H), 1.27 (t, J = 7.1 Hz, 3 H).

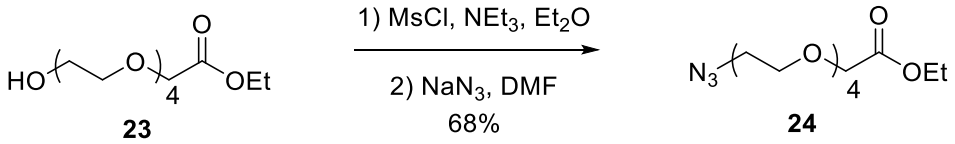

Ethyl 14-azido-3,6,9,12-tetraoxatetradecanoate (**24**): Hydroxy-TEG-ester **23** (1.42 g, 5.04 mmol) and NEt_3 (2.44 mL, 17.5 mmol) were dissolved in anhydrous ether (10 mL), and then immediately cooled down to 0 ^{0}C and placed under an N_2 atmosphere. Mesyl chloride (MsCl) (429 μL, 5.54 mmol) was added to the cold solution dropwise, and afterwards the solution was warmed back to rt. The solution was stirred for 2 h and the solvent was then evaporated to produce a white solid. The solid was re-dissolved in dry EtOH (10 mL), and subsequently NaN_3 (975 mg, 15 mmol) was added. The solution was stirred for 5 h at reflux (85 ºC), and the solvent was then evaporated. CH_2Cl_2 (100 mL) was added to crude, which was next washed with H_2O and brine (2 x 75 mL each). The organic layer was dried with $MgSO_4$, filtered, and evaporated to produce azido-TEG-ester **24** as a yellow oil in 68% (1.05 g) yield. ^{1}H NMR (300 MHz, $CDCl_3$): 4.22 (q, J = 7.2 Hz, 2 H), 4.16 (s, 2 H), 3.67-3.73 (m, 14 H), 3.40 (t, J = 7.3 Hz, 2 H), 1.29 (t, J = 7.1 Hz, 3 H).

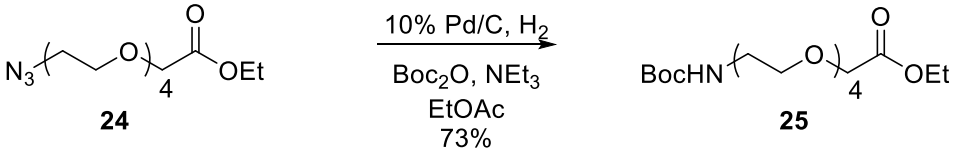

Ethyl 2,2-dimethyl-4-oxo-3,8,11,14,17-pentaoxa-5-azanonadecan-19-oate (**25**): Azido-TEG-ester **24** (450 mg, 1.48 mmol) was dissolved in EtOAc (5 mL). Boc_2O (480 mg, 2.19 mmol), NEt_3 (305 μL, 2.19 mmol), and 10% palladium on carbon (Pd/C) (50 mg) were all added to the solution. The flask was next

evacuated and refilled with Hydrogen (H_2) via balloon 3x. The solution was stirred under H_2 atmosphere at rt overnight. The Pd catalyst was removed by filtering the solution through a pad of celite (Ce). The collected organic layer was evaporated to give a yellow crude oil. The oil was purified via column chromatography using a gradient of 20-35% acetone/$CHCl_3$, and **25** was produced as a yellow oil in 73% (390 mg). ^{1}H NMR (300 MHz, $CDCl_3$): 5.13 (bs, 1 H), 4.22 (q, J = 7.1 Hz, 2 H), 4.15 (s, 2 H), 3.54-3.72 (m, 14 H), 3.30-3.32 (m, 2 H), 1.43 (s, 9 H), 1.28 (t, J = 7.1 Hz, 3 H).

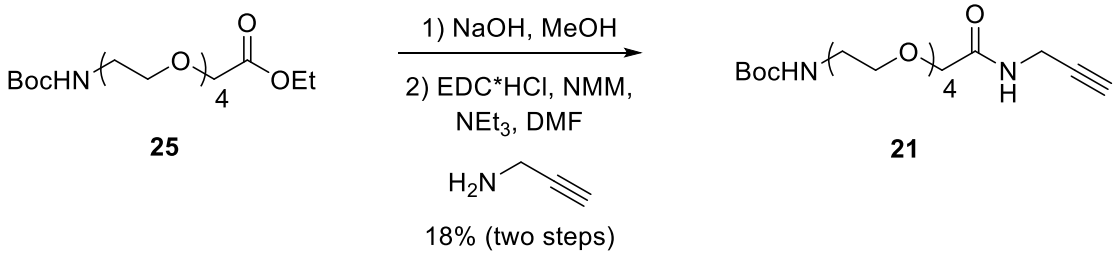

tert-Butyl (14-oxo-3,6,9,12-tetraoxa-15-azaoctadec-17-yn-1-yl)carbamate (**21**): Boc-TEG-ester **25** (200 mg, 0.569 mmol) was dissolved in MeOH (3 mL). A 2M solution of sodium hydroxide (NaOH) (1.5 mL) was added to the solution, and stirring took place for 2 h. The solution was quenched using Dowex 50WX8 (50-100 resin), which was continuously added until the pH of the solution reached ~5.5 (indicated by litmus paper). The solution was filtered through a pipette plugged by a cotton ball, and the solvent was evaporated using N_2 gas. The product was obtained as a brown solid in quantitative yield (195 mg), and then it was dissolved in dry DMF (5 mL). Propargylamine (40.0 μL, 0.631 mmol), NMM (81.0 μL, 0.736 mmol), and DMAP (77.1 mg, 0.631 mmol) were added to the solution, and then

the flask was placed in an ice bath to cool the solution to ~0 ^{o}C and a balloon filled with N_2 was inserted through a septum. After 5 min of stirring under these conditions, EDC·HCl (141 mg, 0.736 mmol) was added in small increments. The flask was immediately removed from the ice bath and the solution stirred at rt overnight. The solution was evaporated to produce a dark red crude oil. The oil was re-dissolved in 30 mL EtOAc, and washed with H_2O (2 x 30 mL) and brine (30 mL). The organic layer was dried with $MgSO_4$, filtered, and evaporated to produce a red oil. The crude was purified via column chromatography using a gradient of 20-25% acetone/$CHCl_3$, and boc-TEG-alkyne **21** was obtained in 21% (43.0 mg) yield. ^{1}H NMR (300 MHz, $CDCl_3$): 7.41 (bs, 1 H), 5.03 (bs, 1 H), 4.09 (dd, J = 5.6, 2.5 Hz, 2 H), 4.02 (s, 2 H), 3.63-3.69 (m, 12 H), 3.54 (t, J = 5.1 Hz, 2 H), 3.31 (m, 2 H), 2.22 (t, J =2.5 Hz, 1 H), 1.44 (s, 9 H).

2.9.5 ADIBO-COOH 28

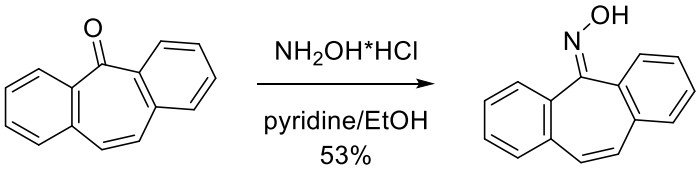

29 **30**

5H-Dibenzo[a,d][7]annulen-5-one oxime (**30**): Dry pyridine (4 mL) and dry EtOH (7 mL) were mixed together in a flame-dried flask and heated up to ~75 ^{o}C. Hydroxylamine hydrochloride ($NH_2OH·HCl$) (800 mg, 11.5 mmol) was added to the hot mixture, and the solution was stirred for ~10 min. Dibenzosuberone **29** (678 mg, 3.29 mmol) was dissolved in dry pyridine (2 mL), and then this solution was

added dropwise to the hydroxylamine solution. A condensing column was added to the setup, and the mixture was stirred for 5 h at reflux. After TLC showed disappearance of **29**, the solution was cooled to rt. Next, the solvent was evaporated to produce a viscous green oil. The oil was re-dissolved in CH_2Cl_2 (150 mL) and then washed with H_2O (2x 150 mL) and brine (1x 150 mL). The organic layer was dried with $MgSO_4$, filtered, and the solvent was evaporated to give a green oil. The oil was purified via column chromatography using 25% EtOAc/hexanes, and oxime **30** was produced as a white solid in 53% yield (380 mg). ^{1}H NMR (300 MHz, $CDCl_3$): 7.64-7.66 (m, 1 H), 7.57-7.60 (m, 1 H), 7.51 (s, 1 H), 7.38-7.44 (m, 6 H), 6.91-6.92 (m, 2 H).

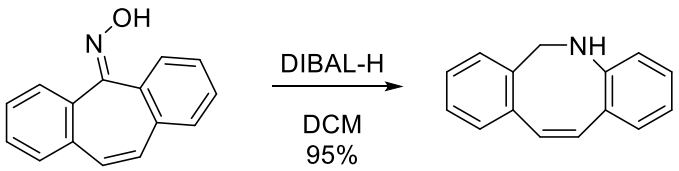

30 **31**

(Z)-5,6-Dihydrodibenzo[b,f]azocine (**31**): Oxime **30** (210 mg, 0.950 mmol) was dissolved in dry and distilled CH_2Cl_2 (10 mL). The flask was placed in an ice bath and the solution stirred for 10 min. DIBAL-H (1 M solution in hexanes, 6 mL) was added dropwise to the cold solution. After addition, the solution was gradually warmed to rt and stirred for 4 hrs. The solution was cooled to ~5 ^{o}C and was quenched with H_2O (3 mL) and sodium fluoride (500 mg), which turned the solution into a lime green slurry. The solution continued to stir for ~15 min at ~5 ^{o}C, and was afterwards was filtered through a pad of celite. EtOAc (50 mL) was poured

onto the celite to collect any remaining product. The organic layer was evaporated to produce amine **31** as a yellow solid in 95% (185 mg). ^{1}H NMR (300 MHz, $CDCl_3$): 7.15-7.24 (m, 4 H), 6.97 (d, J = 8.2 Hz, 1 H), 6.87 (m, 1 H), 6.59 (d, J = 8.8 Hz, 1 H), 6.52 (d, J = 2.3 Hz, 1 H), 6.47 (d, J =10.4 Hz, 1 H), 6.35 (d, J = 13.9 Hz, 1 H), 4.59 (s, 2 H).

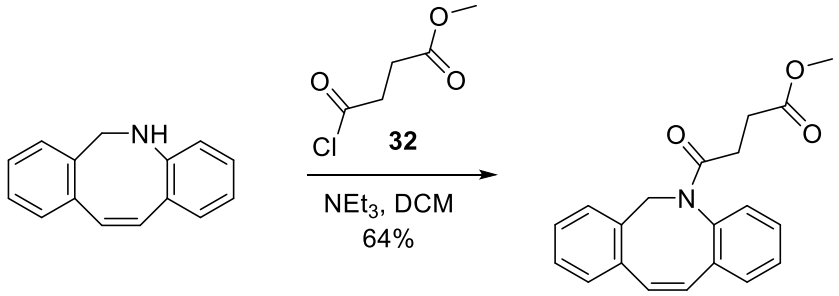

31 **33**

Methyl (Z)-4-(dibenzo[b,f]azocin-5(6H)-yl)-4-oxobutanoate (**33**): Amine **31** (160 mg, 0.780 mmol) was dissolved in dry and distilled CH_2Cl_2 (5 mL) and then brought to 0 ^{o} C. NEt_3 (270 µL, 1.95 mmol) was added to the cold solution, and after 10 min of stirring, methyl succinyl chloride **32** (193 µL, 1.56 mmol) was added dropwise. After 20 min of stirring at 0 ^{o} C, the solution was warmed up to RT and stirring continued overnight. The solution was quenched with H_2O (2 mL) and then diluted with CH_2Cl_2 (10 mL). The organic layer was washed with $NaHCO_3$ (2 x 10 mL), 0.75 M HCl (1 x 10 mL), H_2O (2 x 10 mL), and brine (1 x 10 mL). The organic layer was dried with $MgSO_4$, filtered, and the solvent was evaporated to produce a red oil. The crude oil was purified via column chromatography using 40% EtOAc/hexanes, and dibenzosuccinyl amide **33** was isolated as a brownish-white solid in 64% (160 mg). ^{1}H NMR (300 MHz, $CDCl_3$): 7.33 (m, 1 H), 7.26 (m, 1 H),

7.07-7.20 (m, 6 H), 6.81 (d, J = 13.0 Hz, 1 H), 6.61 (d, J = 13.0 Hz, 1 H), 5.89 (d, J = 14.9 Hz, 1 H), 4.30 (d, J =14.9 Hz, 1 H), 3.54 (s, 3 H), 2.81-2.89 (m, 1 H), 2.50-2.69 (m, 2 H), 2.06-2.15 (m, 1 H).

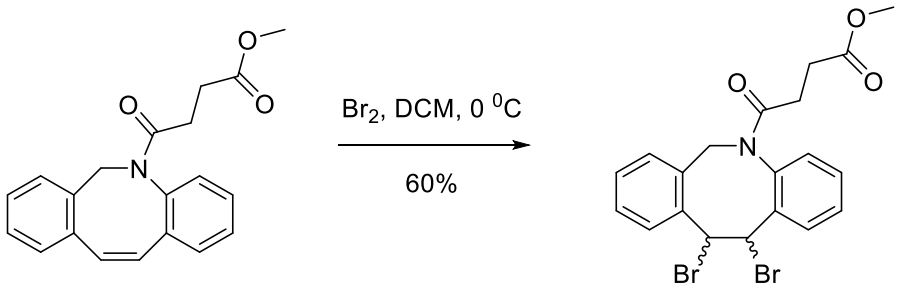

33 **34**

Methyl 4-(11,12-dibromo-11,12-dihydrodibenzo[b,f]azocin-5(6*H*)-yl)-4-oxobutanoate (**34**): Dibenzo succinyl amide **33** (100 mg, 0.310 mmol) was dissolved in dry CH_2Cl_2 (5 mL), and then the flask was placed in an ice bath. Bromine (Br_2) (liq., 40.0 µL, 0.620 mmol) was added dropwise to the cold solution, and the resulting mixture was kept at 0 ^oC as the solution stirred vigorously for 2.5 hrs. The reaction was quenched by adding sat. sodium sulfite (Na_2SO_3) (2 mL), which changed the color of the solution from dark orange to yellow. After stirring for 15 min at 0 ^oC, the mixture was diluted with CH_2Cl_2 (20 mL). The organic layer was washed with sat. Na_2SO_3 (3x 20 mL), H_2O (2x 20 mL), and brine (1x 15 mL). The organic layer was then dried with $MgSO_4$, filtered, and concentrated to give a yellow oil. The oil was purified via column chromatography using 25% EtOAc/hexanes, and dibromosuccinyl amide **34** was afforded as a yellow solid in 60% (89.2 mg) yield. ^1H NMR (300 MHz, $CDCl_3$): 7.72 (d, J = 7.8 Hz, 1 H), 7.09-

7.25 (m, 5 H), 7.02-7.04 (m, 2 H), 6.89 (d, J = 7.5 Hz, 1 H), 5.92 (d, J = 9.9 Hz, 1 H), 5.82 (d, J = 14.9 Hz, 1 H), 5.16 (d, J = 10.0 Hz, 1 H), 2.80-2.89 (m, 1 H), 2.56-2.63 (m, 2 H), 2.46-2.52 (m, 1 H).

2.9.6 ADIBO lipid 20

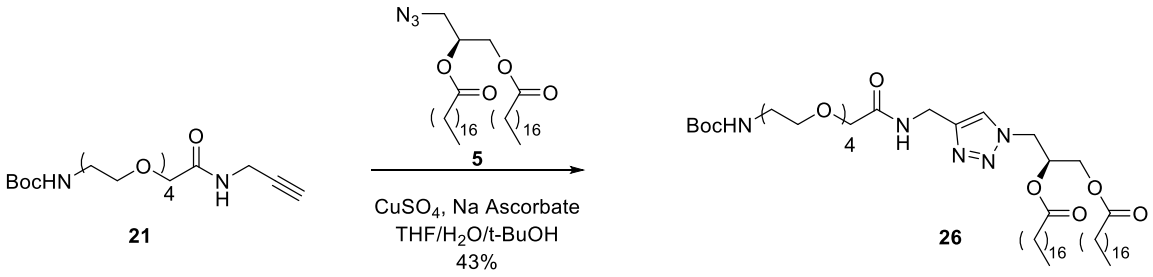

(S)-3-(4-(20,20-dimethyl-3,18-dioxo-5,8,11,14,19-pentaoxa-2,17-diazahenicosyl)-1H-1,2,3-triazol-1-yl)propane-1,2-diyl distearate (**26**): Azido lipid **5** (37.0 mg, 0.0570 mmol) and boc-TEG-alkyne **21** (20.0 mg, 0.0510 mmol) were dissolved in THF (2 mL). $CuSO_4 \cdot 5H_2O$ (115 mg, 0.460 mmol) and sodium ascorbate (153 mg, 0.770 mmol) were each dissolved in separate vials with H_2O (0.2 mL) and t-BuOH (0.5 mL). First, the ascorbate solution was added to the THF solution, and then the copper solution was added dropwise. Each drop of the copper solution elicited a change of color to dark brown. The solution was stirred at rt overnight, and afterwards it was evaporated to produce a greenish blue crude solid. The crude was purified via column chromatography using a gradient of 5% MeOH/CH_2Cl_2, and lipid **26** was produced as a yellowish white solid in 43% (23.0 mg). ^{1}H NMR (500 MHz, 95% $CDCl_3$, 5% MeOD): 8.07 (bs, 1 H), 7.73 (s, 1 H), 5.78 (bs, 1 H), 5.41 (m, 1 H), 4.62-4.66 (m, 2 H), 4.52 (d, J = 5.7 Hz, 2 H), 4.36 (dd, J = 12.1, 4.0 Hz, 1 H), 4.08 (dd, J = 12.2, 5.5 Hz, 1 H), 4.02 (s, 2 H), 3.65-3.71

(m, 12 H), 3.54 (m, 2 H), 3.27 (m, 2 H), 2.34 (m, 4 H), 1.63 (m, 4 H), 1.45 (s, 9 H), 1.25 (s, 56 H), 0.88 (t, J = 6.9 Hz, 6 H).

Chapter 3: Membrane Fusion Triggered by Copper-Free Click Chemistry

3.1 Background and Significance

Functionalized lipids are used to mimic certain biological processes in membranes. The development of artificial methods for triggering membrane fusion is an important goal as this would advance targeted drug delivery. In this chapter, we will describe the development of selective fusion between separate liposome samples bearing partner cyclooctyne and azide functional groups displayed on their surfaces. Copper-free click chemistry has a significant advantage as a tool for promoting membrane fusion because of its fast reaction kinetics, the lack of copper catalyst requirement, and its bioorthogonal nature.

We present copper-free click chemistry as a hopeful and innovative method in targeted membrane fusion that overcomes longstanding challenges associated with the application of chemically driven membrane fusion to drug delivery. A successful fusion mechanism will simultaneously require successful conjugation of liposomes and overcoming the energy barrier associated with lipid mixing. The product of the click reaction between cyclooctyne and azide groups brings the liposomes into proximity, which can trigger membrane fusion depending on the properties of the membranes (Figure 3.1).[130, 133]

Liposome-liposome adhesion will lead to translocation of lipids within the membrane; mixing the lipids from the two complementary liposomes. This will reorganize the membrane and result in the formation of a larger vesicle. This is

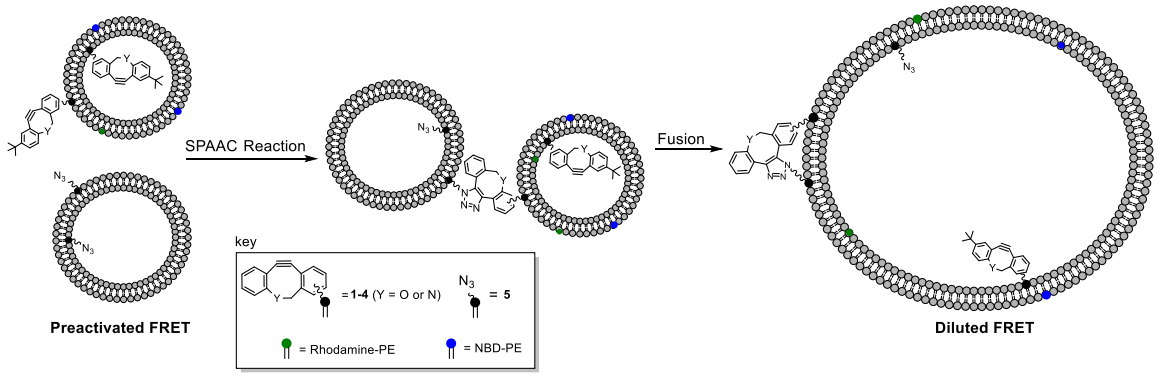

Figure 3.1 FRET assay for detecting membrane fusion based on the dilution of FRET pairs in original liposomes, leading to an increase in the NBD-PE/rhodamine-PE emission ratio.

designed to mimic the action of SNARE proteins on the surfaces of cells, which promote the fusion of specific vesicles and delivery of contents into the cells. This has been useful for drug delivery to cancer cells.[133, 171]

3.2 Membrane Derivatization of Cyclooctyne Lipids

In this project, we first we set out to confirm that our new ODIBO-lipids lipids are effective for copper-free click chemistry reactions to derivatize the membrane surface. To do so, we set out to compare the derivatization of liposomes into which a variety of cyclooctyne lipids (**1**-**4**, **15**) (Figure 3.2) were incorporated. For these purposes, a convenient method for tracking conjugation via the click reaction was to implement assays that cause fluorescence changes when the reaction occurs. In particular, Förster Resonance Energy Transfer (FRET) was employed for many of the assays we used to study membrane derivatization and fusion since it provides sensitive detection of changes in proximity of molecules during these processes. In addition to ODIBO-lipids **1** and **15**, we also evaluated ADIBO-lipids

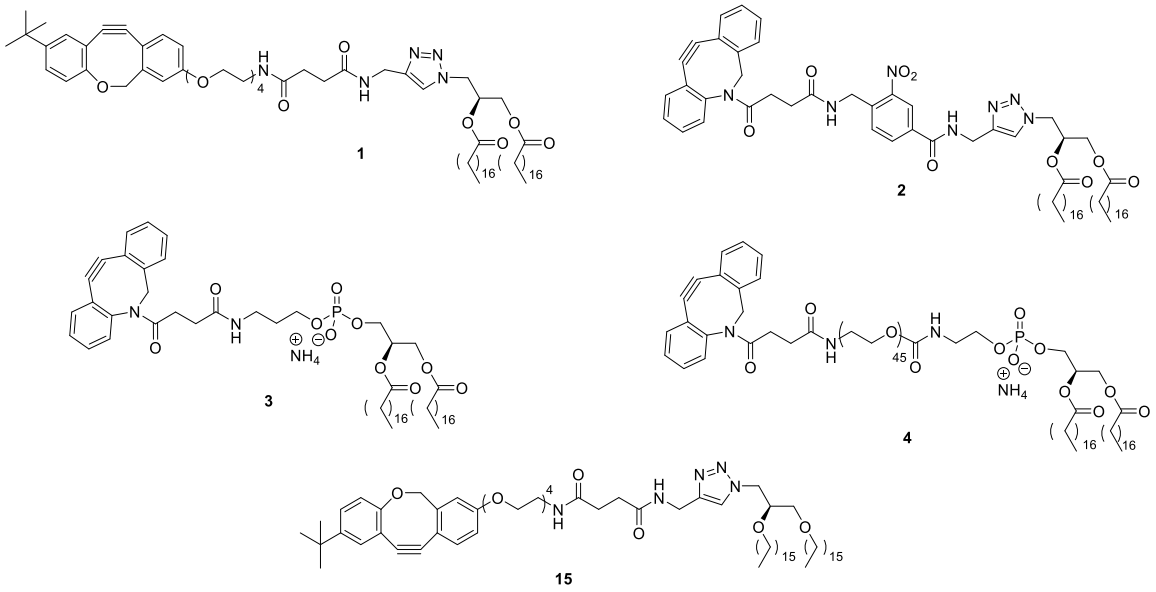

Figure 3.2 List of cyclooctyne lipids used for membrane fusion assays: ODIBO-lipids **1** and **15** and ADIBO-lipids **2-4**

2-4, which were synthesized by others (**2**) or became commercially available (**3**-). During the course of our studies, these compounds each have different structural features, which will be discussed later.

To study membrane derivatization through copper-free click chemistry, we chose to employ a FRET-based assay driven by the convergence of FRET donor and acceptor molecules on the surface of the membrane upon conjugation (Figure 3.3). To do so, we decorated our liposomes with “donor” lipid, NBD-PE (λ_{ex} = 470 nm, λ_{em} = 520 nm). This is a commercially available phospholipid that has a fluorescent moiety (NBD) attached at the headgroup. We subjected these liposomes to an “acceptor” molecule, rhodamine (λ_{ex} = 540 nm, λ_{em} = 588 nm), with an azide moiety attached to it (**35**). When this is added to the liposome solution,

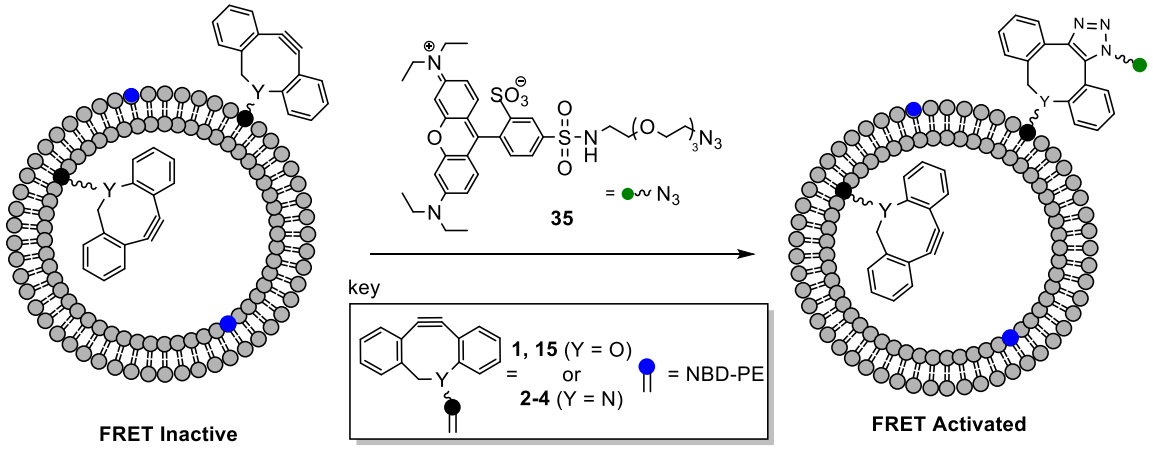

Figure 3.3 FRET assay for detection of membrane derivatization by copper-free click chemistry using ODIBO-lipids (**1**, **15**) and ADIBO-lipids (**2**-**4**)

a click reaction will attach the rhodamine to the surface of the liposome. Consequently, a FRET signal will be produced due to the enhanced proximity of the rhodamine and NBD on the membrane surface. A control experiment was also run in which liposomes lacking cyclooctyne were treated with rhodamine azide **35**.

We composed our liposomes with 90% PC, 9% cyclooctyne lipid (**1**-**4, 15**), and 1% NBD-PE. Rhodamine-azide (1.5 equivalents with respect to cyclooctyne) was added to a cuvette, after which the cyclooctyne-tagged liposomes were introduced. After a few mixes with the pipette, fluorescence spectra were collected over time through excitation of NBD donor at 460 nm and tracking of the NBD/Rhd emission signals over time. As seen in Figure 3.4, all liposomes containing cyclooctyne lipids showed continual decreases in the NBD/Rhd emission ratio signal. This is expected since the convergence of the dyes should cause both a decrease in the donor emission and increase of the acceptor emission, which indicates FRET activation. We see in the graph that liposomes containing the ODIBO moiety

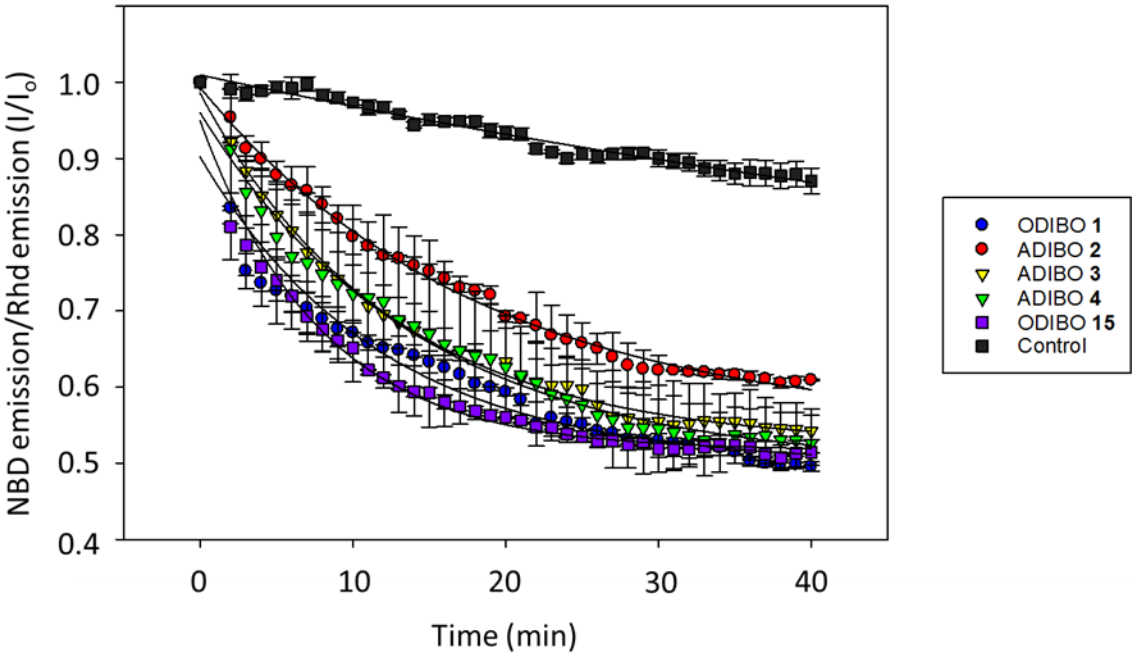

Figure 3.4 Change in FRET (NDB/rhodamine emission ratio) as a function of time upon treatment of liposomes containing ODIBO-lipid (**1**, **15**), ADIBO-lipid (**2**-**4**) or control lacking cyclooctyne with rhodamine-azide **35**. Error bars denote standard errors calculated from at least three replicate experiments.

exhibited greater change in the NBD/Rhd signal than those containing the ADIBO moiety (Figure 3.4), which we attribute to the ODIBO component having faster reaction kinetics than the ADIBO. Liposomes containing no cyclooctyne (control) exhibited a lesser amount of change over time. We attribute the minor signal to non-covalent interactions between rhodamine and the membrane, even perhaps with the rhodamine penetrating the bilayer and inserting into the vesicle. We have previously observed a similar result in fluorescence membrane studies.[170]

3.3 Triggering Membrane Fusion

Now that we had confirmed the derivatization of cyclooctyne lipids, we next worked to promote membrane fusion between vesicles containing cyclooctyne and azido lipids. The cyclooctyne lipids used in this study ranged in terms of substitution around the cyclooctyne moiety, headgroup size/polarity, and hydrophobic chain length. We mentioned the design of ODIBO **1** in an earlier chapter; it has a highly reactive cyclooctyne moiety and tetraethylene glycol linker, which can give the molecule flexibility upon the transition phases occurring in membrane fusion. Additionally, ADIBO **2**, another synthetic lipid, consists of a nitrophenyl moiety that links an ADIBO group to a triazole-lipid backbone. The photocleavable nitrophenyl group was incorporated for a separate project aimed at light-initiated drug release.[170] We also obtained ADIBO lipids **3** and **4** from Avanti lipids, a commercial vendor, which became available during the course of these studies. ADIBO **3** has the cyclooctyne moiety directly linked to the phosphate headgroup, and ADIBO **4** has a long polyethylene glycol chain in its

backbone. This PEG chain should distance the ADIBO group further away from the membrane surface. and we sought to determine the effect this has on membrane fusion.

We modeled our system for detecting membrane fusion after multiple reports.[126, 172-175] This particular model incorporated both donor and acceptor (NBD and Rhd, respectively) labeled lipids within the same vesicle, which also included the cyclooctyne-lipids. These are then treated with liposomes containing no fluorescent dyes, but bearing azido-lipid **5**. Upon fusion, a larger vesicle is created in which the fluorescent lipids originating from the cyclooctyne liposomes are distributed throughout a greater area, and thus these fluorophores undergo dilution within the membrane. This leads to decreased proximity of these fluorescent lipids, and thus the FRET signal is diminished. The expected result is the inverse of what we explained before, showing in an increase in NBD emission and a decrease in Rhd emission. Below is an example of the fluorescence spectrum for liposomes containing PC, PE, **1**, Rhd-PE, NBD-PE (45/45/8/1/1, respectively) (Figure 3.5). We can see the increase in the NBD emission signal and decrease in Rhd emission over time, eventually plateauing between 60-90 minutes. We first used low concentrations of PE (~20%) in our studies, and that did not produce any change in FRET. Thus, we decided to focus on how PE, a non-bilayer forming lipid, could affect the change in FRET over time, and hence the rate of fusion.

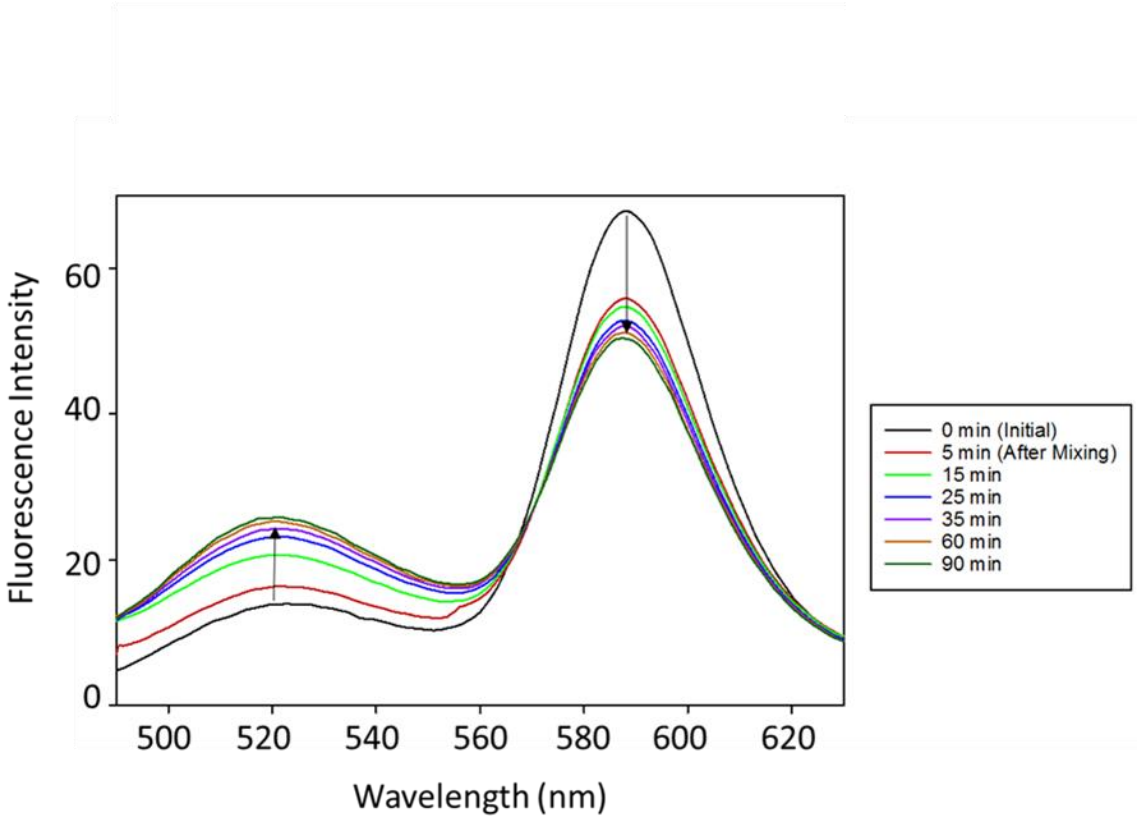

Figure 3.5 Representative overlay of spectra showing the change in emission properties over time for the PC/PE/**1**/NBD-PE/rhodamine-PE 45/45/8/1/1 samples.

3.3.1 Effect of PE Liposome Percentage on Fusion

We set out to optimize the bulk lipid concentration that yielded the greatest change in FRET signal attributed to fusion. We considered the respective concentrations of PC and PE in the membrane, and how that relationship could impact the rate of fusion. PC is classified as a bilayer forming lipid, where PE is a non-bilayer forming lipid. Therefore, increased percentages of PE in the membrane should promote fusion by destabilizing the membrane bilayer and thereby lowering the barrier for fusion. However, increasing PE may also increase non-specific fusion that is not driven by the click reaction, and liposomes containing greater than 50% PE are not particularly stable.

In this experiment, one set of liposomes contained a fixed amount of ODIBO lipid **1** (8%), NBD-PE (1%), and Rhd-PE (1%), and the other contained a fixed amount of PC (46%), PE (46%), and azide lipid **5**. In the liposome set containing ODIBO lipid **1**, studies were taken at various concentrations of PC (60, 50, and 45%) and PE (30, 40, and 45%, respectively). We ran control studies with the aforementioned liposomes containing the variety of PC/PE concentrations along with ODIBO-lipid **1** against liposomes lacking any azide lipid **5**.

We performed many experiments where heat was not used during the mixing process, and we were unsuccessful in observing any FRET change. Indeed, numerous trials were attempted before fusion was successful, as will later be summarized. We eventually decided to heat the cuvette in between collecting data points as this would be expected to increase fluidity of the liposome membrane, as

a result of the lipids transitioning from gel to liquid phase. This could in turn promote fusion and lipid mixing. We experienced success when we heated the cuvette up to slightly above physiological temperature (~40 ^{o}C).

In the results from this study, the curve (Figure 3.6) corresponding to 45% PC/45% PE showed the biggest change in the NBD/Rhd signal over time, followed by 50% PC/45% PE, and finally 60% PC/30% PE. This sequential order of reactivity indicates tight balance between membrane destabilization being beneficial for promoting fusion and detrimental for producing liposomes that are too unstable. The results also indicate that fusion can be tuned using this ratio of PC and PE.

Additionally, while the control studies showed lesser activity, it should be noted how similar the curves are for control studies with liposomes containing 45% PC/45% PE versus study liposomes containing 60% PC/30% PE mixed with azido-liposomes. This could be an indication that the liposomes containing 45% PC/45% PE participate in some non-specific membrane fusion driven by the membrane instability caused by increased PE incoporation. It could also be an indication that the high PE composition is shortening the lifespan of small unilamellar vesicles, and thus increasing the propensity to undergo fusion and relieve the membrane strain. Not pictured are the studies containing liposomes with PE compositions exceeding 45% in the membrane.

We observed a diminishing returns effect with these concentrations; falling along the same path as seen with 50% PC/40% PE study. This also provides

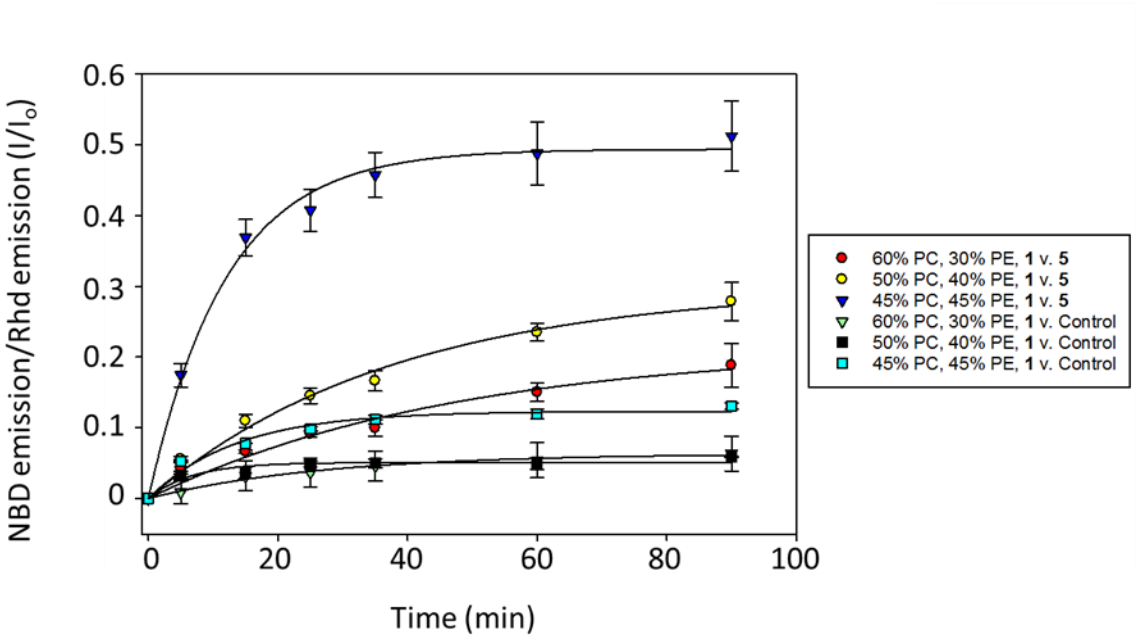

Figure 3.6 FRET assay results for fusion using ODIBO-lipid **1** containing liposomes at various PC/PE percentages (60/30 (red circle), 50/40 (yellow circle), 45/45 (blue triangle)) and their corresponding controls (green triangle, black square, light blue square, respectively) mixed with azido-lipid **5** labeled containing liposomes.

further evidence that having too much PE in the membrane can cause too much destabilization of the bilayer. This result could be caused by a mixture of lipids breaking into small micelles or undergoing non-targeted fusion with other vesicles, and this could potentially explain why we don't observe significant changes in the NBD/Rhd signal.

3.3.2 Cyclooctyne Lipid Effects on Fusion

Now that we had optimized the conditions to promote membrane fusion, we next moved to study the effects that different cyclooctyne and azide lipids have on the fusion rate. We outlined the four cyclooctyne lipids we used in these studies earlier in the chapter: ODIBO **1** and ADIBO **2**-**4**. We were excited to test azide lipid **5** because it is the most synthetically accessible azide lipid target. It is expected to present similar properties to diacylglyerol (DAG) due to its small headgroups, which should augment the curvature in a membrane. This is beneficial to us as this effect on membrane curvature could decrease the energy barrier to stimulate fusion.

In this series of studies, we can see the effect ODIBO lipid **1** has on the NBD/Rhd signal compared to other cyclooctyne lipids (Figure 3.7). This is likely caused by the fast kinetics of ODIBO. When we compare the change seen with ODIBO **1** to ADIBO **2**, we did not see the same sort of reactivity and what essentially seemed to fall in line with the control study. This could be attributed to the hydrophobicity and rigidity of lipid **2**, which may not provide an effective presentation of the cyclooctyne group for conjugation. We believe this aspect of

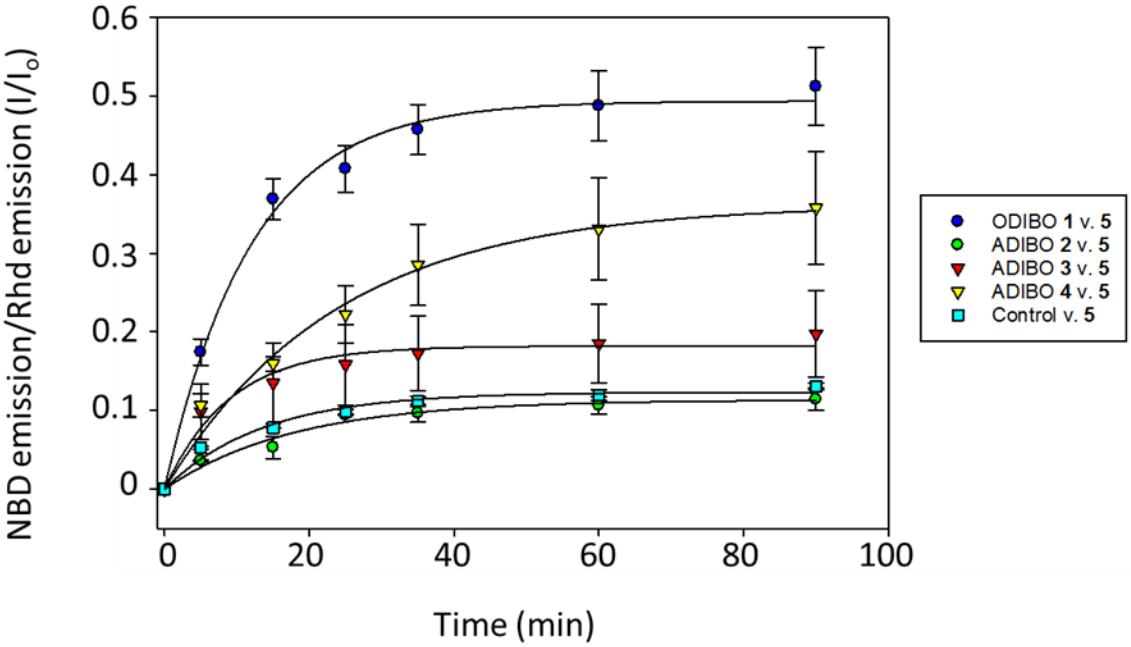

Figure 3.7 FRET fusion assay results as a function of cyclooctyne-lipid using ODIBO (**1**, blue circle), ADIBO **2** (green circle), **3** (red triangle) or **4** (yellow triangle)) or control liposomes (light blue square) lacking cyclooctyne-lipid. Error bars denote standard errors calculated from at least three replicate experiments.

ADIBO lipid **2** was more prohibitive to promoting fusion than the switch to the ADIBO moiety based on the other compounds that were studied.

Although ADIBO lipids **3** and **4** did not show the same degree of change in the NBD/Rhd signal, these sets of data provided valuable insight nonetheless. We discussed earlier the prospect of ADIBO lipid **4** being affected by the long PEG chain causing the triazole formation to occur away from the membrane. We also expected ADIBO lipid **3** to be an extremely effective fusogenic lipid due to the presence of the phosphate head group, which could enhance presentation at the aqueous interface. Our results show that ADIBO lipid **4** exhibited greater change over time than ADIBO lipid **3**. In fact, ADIBO lipid **3** barely climbed above the control curve. ADIBO **4** also exhibited greatest amount of volatility between trials, as seen by by the large error bars in both the derivatization and fusion studies.

We have a few theories as to why we observed the results we did. First, the ADIBO lipid **3** has an alkyl group branching off the phosphate group of around seven carbons. Granted, there are amide linkages in the middle of the chain, but this chain does have discernable hydrophobic character. This observation revisits an initial concern of ours when designing these functionalized lipids. There was a chance that the hydrophobic character of the ADIBO moiety could induce the cyclooctyne to bury itself in the membrane bilayer, rendering it unavailable for reaction. This could explain the limited reactivity of this lipid in the study.

Secondly, ADIBO lipid **4** has a long, bulky PEG chain its headgroup, and PEG lipid (with no functional group) is meant to stabilize membrane bilayers and inhibit

fusion events. Since PEG is hydrophilic, it prefers to reside along the outer leaflet of the membrane, and with enough PEG composition in the membrane this can prevent opposing membranes from interacting with lipids. However, having the cyclooctyne attached to a long PEG chain may work to its advantage because it is more likely to reside outside the membrane, unlike the case with ADIBO lipid **3**. It should be noted that with the azide lipid **5**, the triazole will form along the edge of one liposome, and may mitigate the effect of the cyclooctyne being removed from its own liposomal membrane. Perhaps instead of blocking any contact between membranes normally seen by PEG, the reaction between the azide lipid **5** and ADIBO-PEG lipid **4** does bring the membranes close enough to promote fusion.

When membranes are decorated with reactive functional groups, they are included such that multiple functional groups are available to react. This opens the possibility that a network of reactions can be accomplished between liposomes. In other words, two liposomes can fuse to form a vesicle twice the size, but this can be repeated such that one liposome could potentially react with 4 or 5 complementary liposomes. This networking effect could be involved in the reactivity pattern seen with ADIBO lipid **4**. The PEG component could still have an inhibitory effect on fusion between azido-tagged liposomes and cyclooctyne-tagged liposomes, but this doesn't prevent a number of azido-tagged liposomes from being docked to surface in close proximity. This swarming of the liposomes could break down the PEGylated surface and fusion could be stimulated. It could be an interesting prospect to design and synthesize a lipid with an ODIBO moiety

as the reactive partner and a PEG linker in the backbone, since it has been shown that the PEG linker does not seem to diminish the fusion properties of the lipid.

3.3.3 Azide Lipid Effects on Fusion

We also studied the effects of incorporating azido-lipids with different headgroup linkers on FRET changes attributed to membrane fusion in this assay. For this experiment, we compared azido-lipids **5** and **36** (Figure 3.8) to both ODIBO-lipid **1** and ADIBO-lipid **3**. Lipid **36** contains a phosphate headgroup and lengthy alkyl chain branching off of the phosphate, so it contains a different makeup in the headgroup than **5**. We purchased lipid **36** through a commercial vendor before we synthesized azido-lipid **18**.

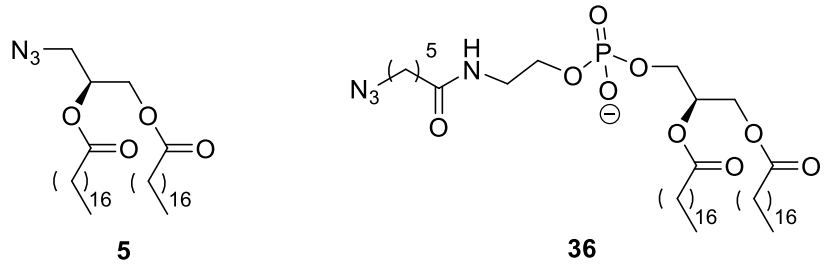

5 **36**

Figure 3.8 Structures for azido-lipid's **5** and **36**

In these studies, liposomes were composed of the lipid percentages that had been optimized in the aforementioned studies (46% PC, 46%, PE, and 8% azide-lipid (**5** or **36**)).These were then mixed with liposomes composed of 45% PC, 45% PE, 1% each of NBD-PE and Rhd-PE, and 8% (**1** or **3**). According to Figure 3.9, there wasn't much difference in the change of FRET between azido-lipids **5** and

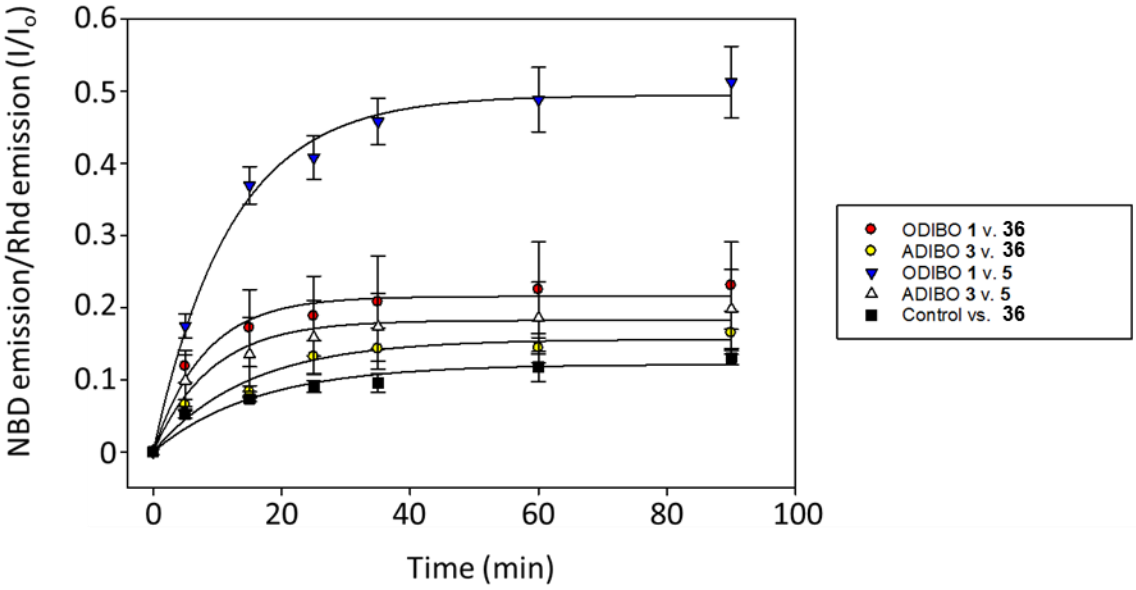

Figure 3.9 FRET fusion assay as a function of cyclooctyne-lipid using ODIBO **1** mixed with azide lipid **5** (blue triangle) or azide lipid **36** (red circle), and ADIBO **3** mixed with azide lipid **5** (white triangle) or azide lipid **36** (yellow circle). Control liposomes lacking cyclocytne were mixed with azide lipid **36** (black square).

36 when mixed with ADIBO-lipid **3**, but a significantly greater change occurred when liposomes containing azido-lipids **5** and **36** were mixed with ODIBO-lipid **1**.

We saw similar results when comparing various cyclooctyne labeled liposomes when mixed with those containing azide lipid **5**, again supporting the faster reaction kinetics of ODIBO compared to ADIBO. However, when we substituted azido-lipid **36** into the membrane, the change in FRET narrowed between ODIBO **1** and ADIBO **3**. This could indicate that the azido-alkyl linker branching off of the phosphate headgroup in **36** has an inhibitive effect on the rate of fusion. The linker could have enough hydrophobic character that the azide tag becomes buried underneath the outer leaflet of the membrane, thus limiting the efficacy of the reaction.

3.4 DLS and STEM Use for Detecting Fusion

Other than FRET, there has been significant contribution to studying membrane fusion from other prominent methods. This list of methods includes dynamic light scattering (DLS) and transmission electron microscopy (TEM). DLS is a scattering technique that indicates the size of molecules in solution by cross-referencing the profile of the solution with the size distribution of the particles. Given the method of this technique, we can track the liposome size in the solution upon mixing of complementary vesicles and detect the distribution of various sizes over time. Unfortunately, we did not obtain any results conducive to tracking membrane fusion.

Basically, the two initial readings of each respective liposome will determine if the filter used in extruding yielded the proper size of liposomes, and also the level of polydispersity. Over time, as these two solutions mix, we should see a second peak arise that indicates a larger sized particle has emerged, and a larger polydispersity index that confirms an increased variance in the size of the particles. While we did eventually observe an increase in liposome size during studies, it was not as great of a change as expected from membrane fusion.

We were able to gather images of our liposome solutions using the scanning transmission electron microscopy (STEM) method (Figure 3.10). We isolated two different types of solutions onto a copper-coated plate for scanning purposes: azido-tagged liposomes only (control), and cyclooctyne-tagged liposomes mixed with azido-tagged liposomes (study). After a drop (~10 µL) of each solution was placed onto separate plates, a drop of KHPTA stain was placed onto each plate. The purpose of the stain was to be encapsulated within the membrane bilayer, which will allow the detection of liposomes on the plate surface. In the images of the azido-tagged liposomes, a clear depiction of small, unilamellar vesicles (~100-200 nm) was captured (Figure 3.10A). It should also be noted how focused the KHPTA stain is along the membrane surface, capturing the clear divide between inside and outside of the liposome.

Upon mixing the azido-tagged liposomes with ODIBO-labeled liposomes, we could see on multiple images larger vesicles being formed. Some vesicles were measured to be 4x the size of the extrusion, along with the imperfection of the

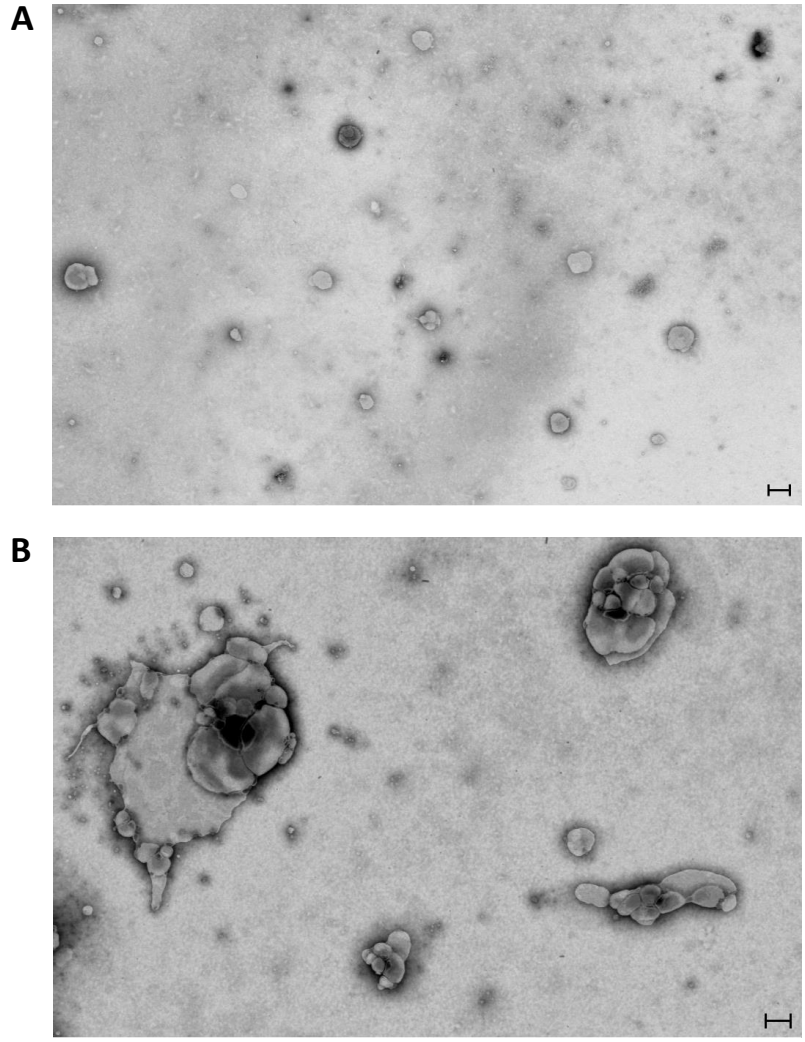

Figure 3.10 STEM images of liposomes before and after fusion driven by SPAAC. A. Images of azido-liposomes (46/46/8 PC/PE/5) show ~200 nm liposomes. B. Images after mixing of azido- (46/46/8 PC/PE/5) and ODIBO- (46/46/8 PC/PE/1) containing liposomes indicate much larger and multilamellar assemblies, indicating fusion and incomplete lipid mixing. All scale bars correlate with 200 nm.

vesicle membrane (according to the stain) (Figure 3.10B). These images support our FRET studies by confirming that the liposomes are fusing when the azide- and ODIBO-lipids are incorporated into liposomes. The large sizes of the structures seen in the STEM study image supports that multiple liposomes are fusing and mixing lipid contents. These structures do, however, contain multiple compartments in which not all lipid contents have mixed. It is possible that the large assemblies result from the high percentage of azido- and ODIBO-lipids in the liposomes. Future work could be performed to vary these percentages and see the effect this has on the ultimate membrane size.

Additionally, we subjected liposomes containing azido-lipids to those lacking the ODIBO-lipid (additional control). In this experiment, we did not see the same evidence that fusion had taken place. However, according to these images, we did see the aggregation of liposomes around one another, but the presence of the stain clearly divided each individual membrane surface. The congregation of liposomes, not resulting in fusion, could be attributed to van der Waals forces driving aggregation of unlike liposomes. In this control sample, the ODIBO-lipid that was removed was replaced with PC and PE. It is possible that the extra PE content is triggering non-specific fusion, as was seen in the previous studies. Therefore, a control should be run in which the ODIBO-lipid that is removed is replaced by PC.

3.5 Additional attempts at instigating fusion

Prior to our discovery of the conditions that promote membrane fusion by copper-free click chemistry, as previously described, numerous unsuccessful attempts were made. In many of these cases, we employed conditions that were later shown to be ineffective for promoting fusion. For example, many initial liposome studies utilized ADIBO-lipid **2** and/or azido-lipid **36**, which were ultimately shown to be ineffective in comparison to ODIBO-lipid **1** and azido-lipid **5**, respectively. In addition, many experiments were performed in the absence of heat, which was later identified to be necessary. While these studies typically provided no change during fluorescence studies, we will now discuss a few examples in which experiments provided insights into the system.

3.5.1. Effect of Cholesterol on Membrane Fusion

Before we attempted to promote membrane fusion by using non-bilayer lipids, we studied the effects of membrane penetrating additives. Membrane penetrating molecules such as detergents and peptides have the ability to insert into the bilayer and disrupt membrane fluidity. For example, the addition of Triton-X lowers the critical micelle concentration (CMC) of lipid assemblies, which diminishes liposome viability in solution. Cholesterol is a popular compound to be paired with PE in the membrane, especially when inducing membrane fusion. Cholesterol is a rigid structure that increases the hexagonal shape, H_{II}, of the membrane. In other words, it can augment the negative curvature strain on the membrane and increase the propensity to form inverse micelles (polar head groups facing inward).

We incorporated various amounts of cholesterol (0%, 10%, and 20%) in each liposome containing ODIBO-lipid **1** and azido lipid **5**, respectively, while maintaining the same ratio of PC/PE (1:1). Figures 3.11 and 3.12 show the results from studies in which we mixed liposomes solutions containing 45:45:0:8:1:1 (PC:PE:Cholesterol:**1**:NBD-PE:Rhd-PE), 40:40:10:8:1:1, and 35:35:20:8:1:1 with liposome solutions containing 46:46:8:0 (PC:PE:**5**:Cholesterol), 41:41:8:10, and 36:36:8:20. We mixed each possible combination at 40 ^{o}C to obtain results for a variety of cholesterol-containing liposomes (0%, 10%, and 20%). We also made liposomes that lacked ODIBO **1** to be used as the control, and mixed those solutions with the aforementioned liposomes containing azido lipid **5** and cholesterol.

In Figure 3.11, the results of the fusion mixes (cyclooctyne liposomes vs. azide liposomes) and the control mixes (no cyclooctyne vs. azide) suggest that cholesterol inhibits the change in FRET over time. In Figure 3.12, we compared the two best fusion mixes (10% vs. 10% and 0% vs. 20%) with the mix containing no cholesterol, and the change in FRET seen by the fusion mix with no cholesterol involved was much greater. It appears in Figure 3.11 that the mixes containing less cholesterol generally displayed the greatest change in FRET, aside from the mix of 0% and 10% in the cyclooctyne and azide liposomes, respectively. Although we are maintaining the concentration of PE equal to the PC, a combination that produced the greatest change in FRET (Figure 3.6), these studies suggest that fusion is largely contributed by the absolute amount of PE present in the liposome.

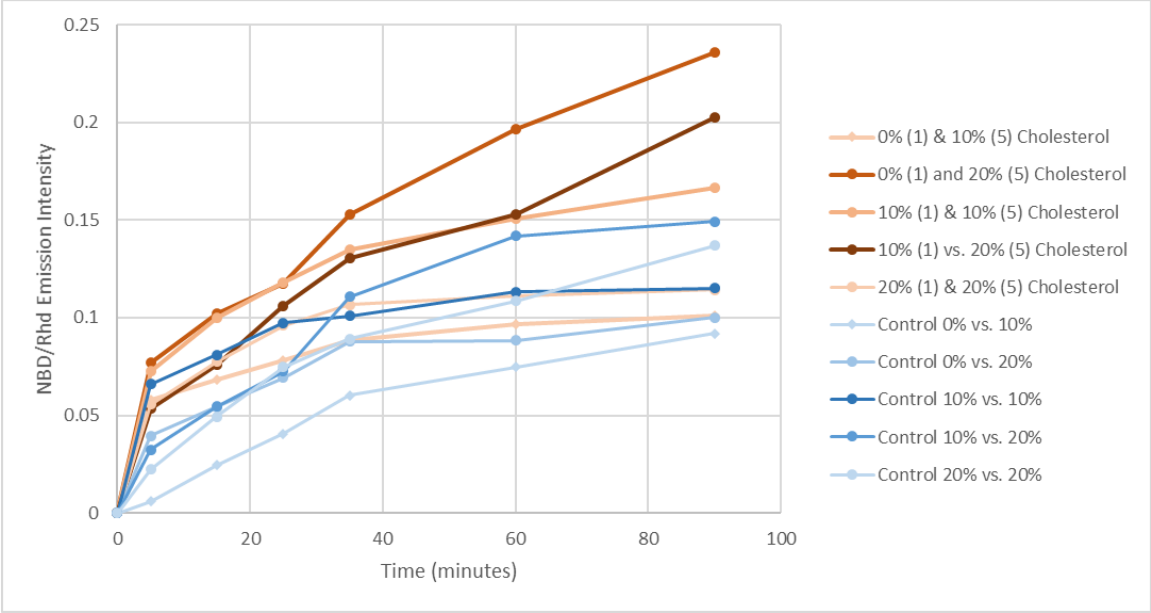

Figure 3.11 FRET studies for ODIBO **1**-labeled liposomes mixed with N_3 **5**-labeled liposomes and control liposomes mixed with N_3 **5**-labeled liposomes. All combinations of liposomes were studied in which the cholesterol was varied (0, 10, and 20%).

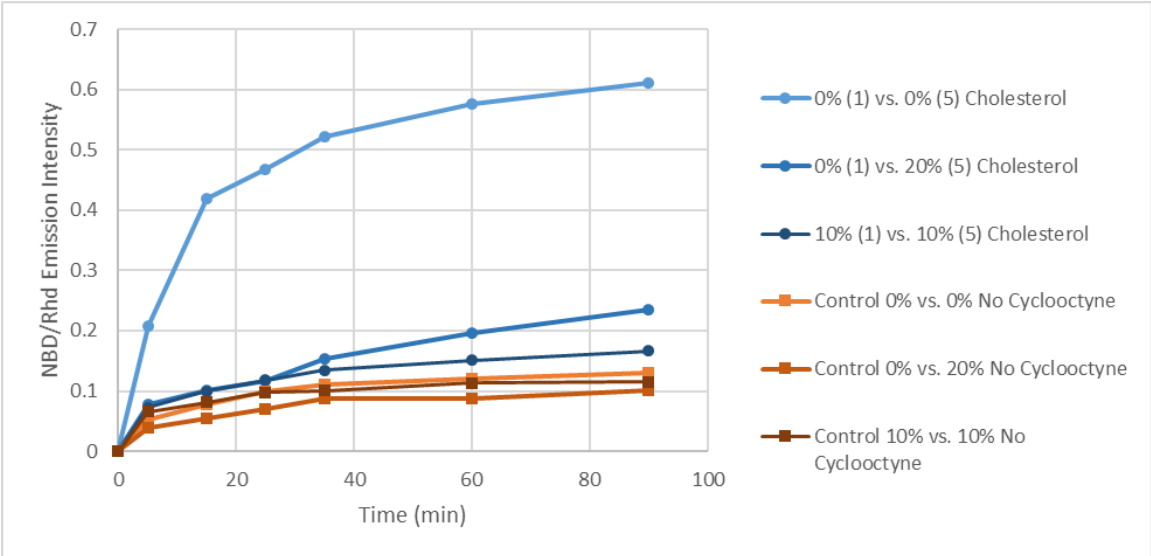

Figure 3.12 FRET studies comparing the best liposome mixtures with and without cholesterol. Control liposome mixtures were also placed in this graph.

3.5.2. Effect of Detergent on Membrane Fusion

We also attempted to initiate membrane fusion by adding small aliquots of Triton-X into the solution. Triton-X, a detergent, is an amphiphilic entity that can penetrate membranes through insertion, but can also promote lipid mixing between aggregated vesicles by destabilizing the bilayer.[176] When the membranes are in close proximity to each other, the Triton-X was expected to assist in initiating fusion through the mechanism we just described. We composed liposomes with 87:11:1:1 (PC:ADIBO **2**:NBD-PE:Rhd-PE) and 89:11 (PC:Azide **36**) and mixed them at room temperature. Upon addition of 4% (w/v) Triton-X, the results showed that this additive did not cause changes in FRET between the fused liposomes and control studies. We should note that this study likely suffered from the choice of clickable lipids used, ADIBO **2** and azide **36**, since we had not yet synthesized/incorporated ODIBO **1**, ADIBO's **3** and **4**, and azide **5**. In Figure 3.7, we showed that ADIBO **2** contributed little change in FRET compared to the other lipids used, and in Figure 3.9 we observed that azide **36** facilitated less change in FRET than azide **5**. It is worth revisiting this experiment with the clickable lipids ODIBO **1** and azide **5** and observing if any difference between the fusion and control studies is detected.

We attempted these experiments before investigating the effect PE on fusion rate, but we did incorporate minor amounts of PE (~30%) into the liposomes by replacing the PC percentage. This resulted in liposomes composed of 57:30:11:1:1 (PC:PE:ADIBO **2**:NBD-PE:Rhd-PE) and 59:30:11 (PC:PE:Azide **36**).

As with studies that did not include PE in the liposomes, there was no difference seen between the fused and control liposomes.

3.5.3. Effect of Oppositely Charged Lipids on Fusion

A popular method for stimulating membrane fusion involves the use of charge disparity on opposing liposomes to further promote an interaction.[177-183] This can be achieved by introducing cationic lipids into one liposome accompanied by negatively-charged liposomes in the fusion partner. The ionic relationship will enhance attraction and may also destabilize the membrane and allow lipids from different bilayers to mix more readily. In our studies, the incorporation of opposite charges in the form of a positively-charged lipid (DOTAP) in one liposome and negatively-charged lipid (either PA or PS) in opposing liposomes was ineffective for promoting membrane fusion. In addition to having a negatively-charged phosphate, PA contains a small headgroup, thus giving it a small surface area relative to the hydrophobic tails. This lipid can thus induce negative curvature strain, and promote destabilization in the membrane. We anticipated the click reaction, again, to dock these liposomes on the surface. This final step is to cross over the energy barrier and finalize the path to membrane fusion.

We originally created liposomes with 78:10:10:1:1 (PC:DOTAP:ADIBO **2**:NBD-PE:Rhd-PE) and 80:10:10 (PC:(PS or PA):Azide **36**), as well as control liposomes composed of 88:10:1:1 (PC:DOTAP:NBD-PE:Rhd-PE). We did not detect any changes in FRET with fused liposomes (cyclooctyne and azide) nor the control liposomes (control and azide). We attempted to add Triton-X to the mixture in

order to induce fusion, but again no change was observed in the FRET studies. In the next batch of liposomes, we made two changes: (1) we incorporated the fluorescent lipids (NBD-PE and Rhd-PE) into the azido-tagged liposomes instead of the cyclooctyne-tagged liposomes. The purpose of this alteration was to pair the negatively-charged headgroup of Rhd-PE with the negatively-charged PS (or PA) in order to reduce self-aggregation of liposomes, (2) we incorporated PE into the liposomes as means to augment fusion rate, so now we have liposomes composed of 47:35:10:8 (PC:PE:DOTAP:ADIBO **2**), 50:32:9:8:0.5:0.5 (PC:PE:(PS or PA):Azide **36**:NBD-PE:Rhd-PE), and 58:32:9:0.5:0.5 (PC:PE:(PS or PA):NBD-PE:Rhd-PE). In Figure 3.13, we are comparing the fluorimeter results of the fused liposomes and control liposomes by displaying the change in absolute intensity of the NBD emission (518 nm) and Rhd emission (590 nm). We do observe a change in the NBD emission intensity over time in the fused mixture (3.13A) and no change in the control mixture (3.13B), but the Rhd emission does not waver from the initial intensity in both the fused and control liposomes over time.

After synthesizing ODIBO **1** and obtaining ADIBO **3**, we started to use this lipid in our studies and we continued with attempting to facilitate fusion using oppositely charged lipids in opposing liposomes. We composed liposomes with 40:40:10:8:1:1 (PC:PE:PA:(ODIBO **1** or ADIBO **3**):NBD-PE:Rhd-PE), 40:40:10:10 (PC:PE:DOTAP:Azide **36**), and 43:43:12:1:1 (PC:PE:PA:NBD-PE:Rhd-PE). As seen in Figure 3.14, we observed no difference in the FRET change between the fused liposomes and control liposomes. In this graph, we are presenting the

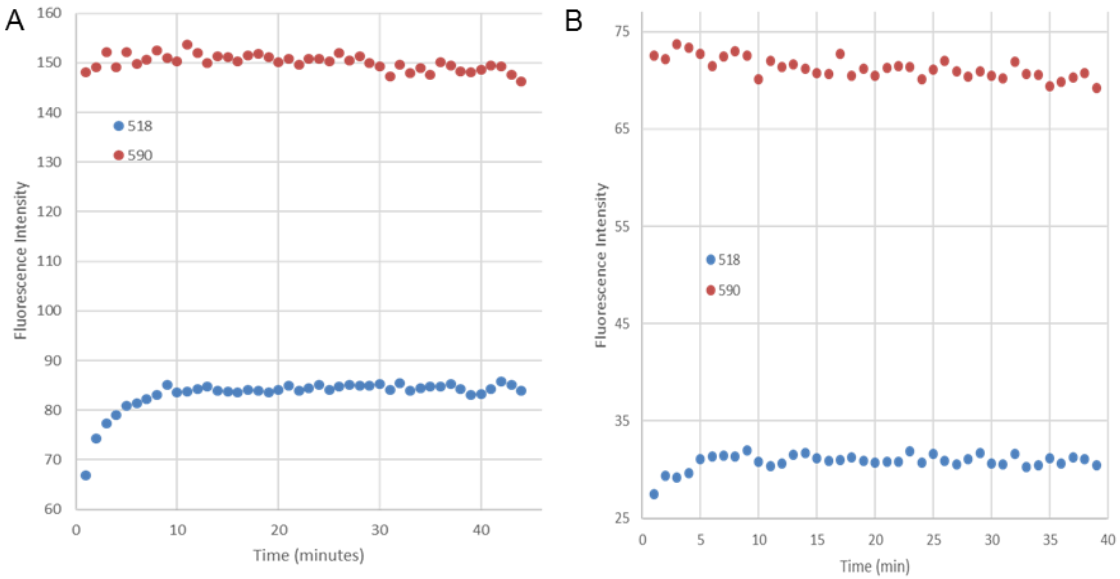

Figure 3.13 FRET Studies of ADIBO **2**-labeled liposomes mixed with azide **36**-labeled liposomes (A) and control liposomes mixed with azide **36**-labeled liposomes (B). In addition to PC & PE, liposomes were composed of PA in one solution and DOTAP in the other solution. Emission intensities for NBD (518 nm) and Rhd (590 nm) were plotted.

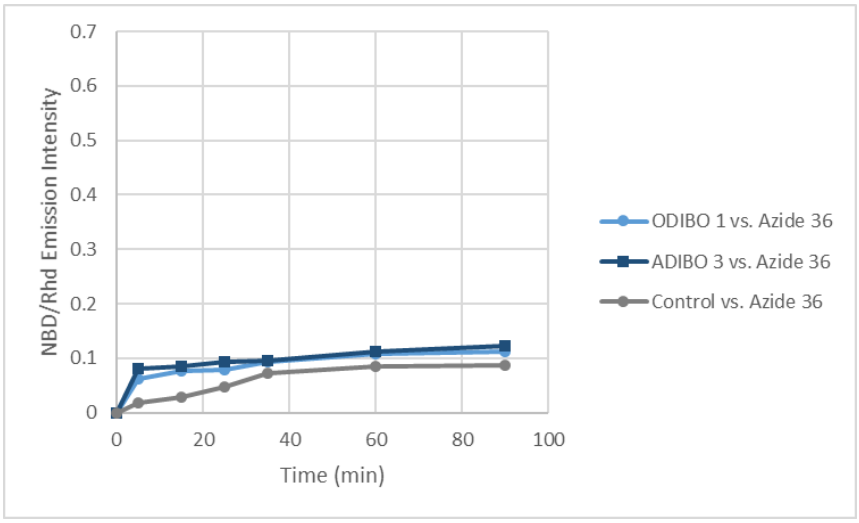

Figure 3.14 FRET Studies of cyclooctyne-labeled (ODIBO **1**, ADIBO **3**) liposomes mixed with azide **36**-labeled liposomes (blue curves) and control liposomes mixed with azide **36**-labeled liposomes (grey curve). Cyclooctyne and control liposomes contain PA while azido-tagged liposomes contain DOTAP.

NBD/Rhd emission ratio over time, which is the relationship we presented in Figures 3.4, 3.6, 3.7, and 3.9. There is some separation seen between the fused liposomes and control liposomes within the first 20 minutes of the experiment, but compared to the results we observed in Figures 3.6 and 3.7 we don't see quite the same change. Subsequently, we were able to experience better FRET results in our fused liposomes by optimizing the PE concentration, utilizing azide lipid **5**, and mixing the liposomes in a ~40 ^{o}C water bath.

3.6. Conclusions

In the work described in this chapter, we identified and optimized conditions for liposome-liposome fusion driven by copper-free click chemistry. In doing so, we optimized the structure of the cyclooctyne- and azido-lipid components, the temperature of the reaction, and the percentages of bulk lipids including PC and PE. Fusion was found to be most effective when using ODIBO-lipid **1**, azido-lipid **5**, a reaction temperature of 40 ^{o}C, and PC/PE percentages of 45% in the liposomes. However, the inclusion of 45% PE was pushing it as this began to increases non-specific fusion. This system provides an initial model for targeted drug delivery using copper-free click chemistry. Prior to identifying successful conditions, many experiments were unsuccessful since they involved compounds that ultimately proved unsuccessful or only slightly effective for fusion (ADIBO **2** and azido **36**), were run at room temperature, or were run with lipids that appeared to inhibit fusion (cholesterol).

3.7 Experimental Procedures

PC (L-*α*-Phosphatidylcholine, mixed isomers from chicken egg), PE (1,2-dioleoyl-*sn*-glycero-3-phosphoethanolamine), 1,2-dioleoyl-*sn*-glycero-3-phosphoethanolamine-*N*-(7-nitro-2-1,3-benzoxadiazol-4-yl) (NBD-PE), 1,2-dioleoyl-*sn*-glycero-3-phosphoethanolamine-*N*-(lissamine rhodamine B sulfonyl) (rhodamine-PE), ADIBO-lipids **3** and **4**, and azido-lipid **36** were purchased from Avanti Polar Lipids, Inc. Liposome extruder and polycarbonate membranes were obtained from Avestin (Ottawa, Canada). Ultrapure water was purified via a Millipore water system (≥ 18 MΩ·cm triple water purification system). Small quantities (< 5 mg) were weighed on a OHRUS analytical-grade mass balance. Fluorescence studies were performed using a Perkin Elmer LS55 fluorimeter. Plots were generated using SigmaPlot 13, and curves in Figure 3 were fitted using an exponential decay function, while those in Figures 5A and 6 were fitted using an exponential growth to maximum function. All errors bars in plots include error bars depicting the standard errors of at least three experimental replicates.

3.7.1 Liposome preparation

Stock solutions of lipids **1** and **2,** PC, NBD-PE, and rhodamine-azide **35 (**Rhd-N_3) were made in chloroform for fluorimeter studies. Examples of these stock solutions were prepared as follows: 6 mg of ODIBO-lipid **1,** 1.2 mg of ADIBO-lipid **2**, 100 mg of PC, 1 mg of NBD-PE, and 1.8 mg of Rhd-N_3 **35** were dissolved in 1 mL, 1 mL, 4 mL, 1.5 mL, and 2 mL of chloroform, respectively, to form stock solutions of 4.83 mM lipid **1**, 0.970 mM lipid **2**, 32.5 mM PC, 0.720 mM NBD-PE,

and 1.18 mM Rhd-N_3 **16**. In three separate separate vials, we used these stock solutions to add the following: 11.8 µL PC (90%), 8 µL lipid **1** (9%), and 5.8 µL NBD-PE (1%) in vial A; 11.9 µL PC (90%), 40 µL lipid **2** (9%), and 5.9 µL NBD-PE (1%) in vial B; and 11.9 µL PC (99%) and 5.4 µL (1%) in vial C. Each lipid solution was evaporated using argon gas to generate a solid lipid film. All vials were placed under vacuum for 4 h and then dissolved in Tris-HCl buffer (10 mM)/NaCl (90 mM)/EDTA (1 mM) to produce 2 mM liposome solutions. The solutions were hydrated for 1 h at 50 ^{o}C, and then subjected to 10 freeze/thaw cycles to form unilamellar vesicles. Next, the liposome solutions were extruded 15 times using a 200 nm polycarbonate membrane. Other liposomes used for studies were produced in the same manner using different percentages of the appropriate lipids.

3.7.2 Membrane derivatization studies

Rhodamine-azide **35** (48.96 µL, 58.0 nmol) was added to the two separate microcuvettes, and then evaporated with Ar gas to leave solid Rhd-N_3. Using the ODIBO **1** liposome solution (22 µL) was added to one of the cuvettes, and then diluted with Tris buffer (300 µL) to give a final total concentration of 220 µM. An initial reading was collected; the resulting solution was mixed thoroughly with a pipette for 5 minutes, and the cuvette was then placed in the fluorimeter. The fluorimeter was set to scan an excitation wavelength of 460 nm and with emission and excitation slits of 9.5 nm and 7.5 nm, respectively. Fluorescent readings were collected for ~40 min. This procedure was repeated for the studies of ADIBO lipid(s) **2**, **3**, **4**, and ODIBO **15**.

3.7.3 Membrane fusion FRET dilution studies using ODIBO-lipid 1 by varying PC/PE percentages.

PE (5 mg), azido-lipid **5** (2.3 mg), and rhodamine-PE (2 mg) were dissolved in 1.5 mL, 2 mL, and 675 µL of chloroform, respectively, to form stock solutions of 4.48 mM PE, 5.24 mM lipid **5**, and 0.77 mM rhodamine-PE. These stock solutions along with the stock solutions of PC (32.46 mM), ODIBO lipid **1** (4.83 mM), and NBD-PE (0.72 mM) were used to make lipid solutions of 60:30:8:1:1 (PC:PE:**1**:NBD-PE:Rhd-PE), 50:40:8:1:1 (PC:PE:**1**:NBD-PE:Rhd-PE), 45:45:8:1:1 (PC:PE:**1**:NBD-PE:Rhd-PE), 46:46:8 (PC:PE:**5**), and 50:50 (PC:PE). Each lipid solution was converted into a 2 mM liposome solution by employing a similar protocol outlined in the liposome preparation section using 100 nm polycarbonate membranes for extrusion. Cyclooctyne-labeled liposome solution (20 µL) was added to a microcuvette and diluted with Tris buffer (420 µL), and an initial reading was taken on the fluorimeter (0 min). Next, azido-labeled liposome solution (60 µL) was added to the cuvette to give a final total concentration of 250 µM. The solution was mixed thoroughly with a pipette for ~ 2 min while the cuvette was submerged in a warm water bath (~ 40 ^{0}C). Fluorescence measurements were taken at 5, 15, 25, 35, 60, and 90 minutes after mixing, with heating in between each fluorescence scan. The ratio of fluorescence intensities at NBD emission (520 nm) and Rhd emission (588 nm) was calculated, and each ratio was normalized by subtracting the initial NBD/Rhd ratio from each measurement.

3.7.4 FRET Dilution Studies using Cyclooctyne-lipids 1-4

ADIBO-PEG-lipid **4** (5 mg), and ADIBO-lipid **3** (5 mg) were dissolved in 400 µL and 1 mL of chloroform, respectively, to form stock solutions of 4.44 mM of ADIBO **4** and 5.02 mM of ADIBO **3**. These stock solutions and the stock solutions of PC (32.46 mM), PE (4.48 mM), lipids **1**, **2**, and **5** (4.83 mM, 0.97 mM, and 5.24 mM, respectively), NBD-PE (0.72 mM), and Rhd-PE (0.77 mM) were used to make lipid solutions of 45:45:8:1:1 (PC:PE:cyclooctyne-lipid:NBD-PE:Rhd-PE), 46:46:8 (PC:PE:azide **5**), and 49:49:1:1 (PC:PE:NBD-PE:Rhd-PE). One lipid solution was made for each cyclooctyne lipid (**1**-**4**). Each lipid solution was converted into a 2 mM liposome solution by employing a similar protocol outlined in the previous liposome preparation protocol using 100 nm polycarbonate membranes for extrusion. Cyclooctyne-labeled liposome solution (20 µL) was added to a microcuvette and diluted with Tris buffer (420 µL), and an initial reading was taken on the fluorimeter (0 min). Next, azido-labeled liposome solution (60 µL) was added to the cuvette to give a final total concentration of 250 µM. The solution was mixed thoroughly with a pipette for ~ 2 min while the cuvette was submerged in a warm water bath (40 ^{0}C). Fluorescence measurements were taken at 5, 15, 25, 35, 60, and 90 minutes after mixing, with heating in between each fluorescence scan. The ratio of fluorescence intensities at NBD emission (520 nm) and Rhd emission (588 nm) was calculated, and each ratio was normalized by subtracting the initial NBD/Rhd ratio from each measurement.

3.7.5 FRET Dilution Studies using Cholesterol

In addition to the solutions of PC, PE, ODIBO **1**, Azide **5**, NBD-PE, and Rhd-PE described earlier, a stock solution of cholesterol (5 mg/mL, 12.93 mM) was made. Liposomes composed of 45:45:0:8:1:1 (PC:PE:Cholesterol:**1**:NBD-PE:Rhd-PE), 40:40:10:8:1:1, 35:35:20:8:1:1 and 46:46:8:0 (PC:PE:**5**:Cholesterol), 41:41:8:10, and 36:36:8:20 were made according to the procedure listed above. Control liposomes consisting of 49:49:0:1:1 (PC:PE:Cholesterol:NBD-PE:Rhd-PE), 44:44:10:1:1, and 39:39:20:1:1 were also made. Cyclooctyne-tagged liposomes (labeled) were thoroughly mixed with azido-tagged liposomes (unlabeled) in a 1:3 ratio, respectively, at ~40 ºC (final concentration: 250 μM). Prior to addition of unlabeled liposomes, an initial fluorescent reading was taken, and fluorescent measurements (post-mixing) were subsequently taken at 5, 15, 25, 35, 60, and 90 minutes. Studies were repeated with control liposomes instead of cyclooctyne-tagged liposomes.

3.7.6 FRET Dilution Studies using PS, PA, and DOTAP

In addition to the solutions of PC, PE, ODIBO **1**, ADIBO **2** and **3**, NBD-PE, and Rhd-PE described earlier, stock solutions of PS (5 mg/1.5 mL, 4.04 mM), PA (5 mg/mL, 7.08 mM), DOTAP (16 mg/mL, 22.90 mM), and azide **36** (5 mg/mL, 5.98 mM) were made. Liposomes consisting of 40:40:10:8:1:1 (PC:PE:PA:ODIBO **1**:NBD-PE:Rhd-PE), 40:40:10:10 (PC:PE:DOTAP:Azide **36**), and 43:43:12:1:1 (PC:PE:PA:NBD-PE:Rhd-PE) were made according to the procedure described above. Solutions containing fused liposomes (cyclooctyne and azide) and control

liposomes (control and azide) were made by mixing 3 equivalents of unlabeled liposomes with 1 equivalent of labeled liposomes at room temperature into a cuvette (final concentration: 250 μM). Prior to adding the unlabeled liposomes, an initial reading of the labeled liposomes was recorded. Fluorescence measurements were taken at 5, 15, 25,35, 60, and 90 minutes after mixing.

3.7.7 Scanning Transmission Electron Microscopy (STEM) Experiment Assays

Liposomes consisting of Azido lipid **5**, ODIBO **1**, and control were prepared using the procedure listed above. Three separate solutions were prepared for study: **5**, **5** mixed with **1**, and **5** mixed with control. Each solution was measured to a total concentration of 400 μM. The latter solutions were mixed and heated (submerged in water bath of ~35 ºC) for 5 minutes, and then allowed to sit at room temperature for 1 hr. A drop (5-10 μL) from each solution was immobilized onto three separate carbon filters. Each filter was stained using a 5% (w/v) solution of phosphotungstic acid, and the filter was stored in a desiccator overnight prior to experiment. Images were collected using the Zeiss Auriga at the Joint Institute of Advanced Materials in Knoxville, TN. The electron beam was set at 25 eV, and images were detected using an Everhardt-Thornley SE2 detector.

Chapter 4: Miscellaneous Projects

4.1 PSII Inhibitor Synthesis

Photosynthesis is an important and necessary process to preserve plant life on this planet. Two proteins in particular, photosystem I (PSI) and photosystem II (PSII), are prevalent in maintaining this cycle in perpetuity. When sunlight is makes contact with the plant, a variety of pigment molecules absorb the light and are excited. This excitation energy is transferred to light-harvesting pigments and goes through a series of electron-transfer processes at the reactive center site, where ultimately the PSI and PSII reside.[184-186] These photosystems consist of supermolecules that contain a vast array of pigment-protein interactions and chlorophyll molecules. Inhibition of these pathways could lead to plant death, but there are benefits to this process as well. This could be aided by disrupting the photosynthetic pathway of certain bacterial strains; allowing us to improve plant viability.

A variety of novel small synthetic molecules have been designed to inhibit the PSII complex in plants and weeds. These synthetic analogues were designed to displace pigment-protein interactions and disrupt the flow of electrons photosynthesis. Examples of these novel molecules include hydroquinolines, ureas, and amides.[187-190] There have also been studies using halides as inhibitors in solution with PSII. This is due to the strong binding affinity between calcium, a popular ion present in the PSII complex, and specifically, fluoride. This was the inspiration behind this particular group of PSII inhibitors in a collaborative effort

with Dr. Gregory Armell, formerly of the UT Institute of Agriculture and currently at BASF Corporation. The trifluoromethyl substituent is perhaps meant to be the primary inhibitive portion of the molecule, and although it doesn't exist as an ion, the electron pairs on each of the fluorides are able to coordinate with the reactive core and label it as a dual site inhibitor.[191] Studies on these molecules will be necessary to understand the full capabilities of both the trifluoromethyl and urea substituents.

We began the synthesis for PSII inhibitors with commercially available 3-trifluorophenol **39** and 4-chloro-1-nitrobenzene **38** (Figure 4.1). These two reagents were coupled using an Ullman type reaction, which produces the ether linkage between the two benzene moieties. We originally designed the synthesis to generate biphenyl urea **37** in one step using the Ullman reaction from **39** and a urea chlorobenzene moiety. This reaction suffered from degradation of the urea compound, which was confirmed by mass spectrometry. Consequently, we decided to generate the ether linkage first. Compound **38** has the nitro functional group, and in the para position on the ring can withdraw a lot of electron density from the C-Cl bond. The Ullman reaction has shown limited reactivity when using chlorine as the halogen, as opposed to the bromine or iodine.[192-194] Having an electronegative halogen substituted on the benzene and using it as the electrophilic piece in the Ullman reaction could lead to lower yields. Adding the nitro functional group onto the ring weakens the bond between C-Cl, and thus could increase the reactivity of the electrophile. Another addition we made to the

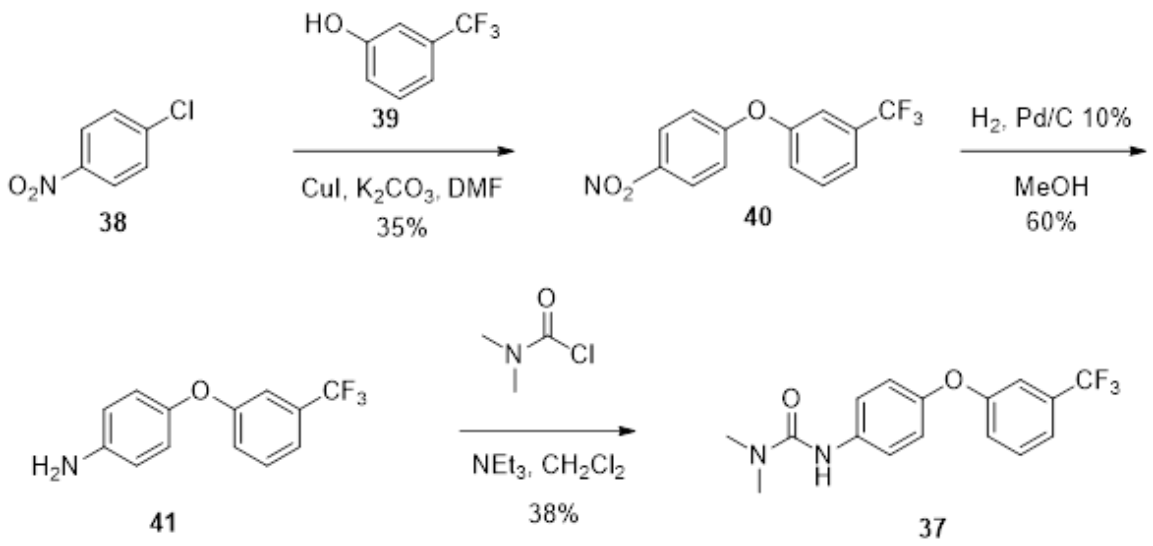

Figure 4.1 Synthetic scheme for producing biphenyl ether **37**

reaction was to use dry and degassed DMF as the solvent. Since we heated the reaction to high temperatures, this could've led to DMF decomposing in the flask and produce unnecessary byproducts. Degassing solvents inhibits the solvent to be exposed to oxidation in the flask. Taking into account all of these details, we were able to isolate the biphenyl ether adduct **40**.

We subjected this to hydrogen and palladium catalyst to generate amine **41**. We were able to obtain the commercially available dimethylcarbomoyl chloride, and after slow addition at 0 ^{o}C and basic conditions we generated urea **37**. This final reaction also required dry and distilled dicholoromethane (CH_2Cl_2) to obtain a modest yield. This is likely due to the moisture sensitive nature of dimethylcarbomyl chloride. We produced compound **37** in 8% overall yield with respect to nitrobenzene **38**, and 300 mg total of **37**. This scheme was limited by both the first step (Ullman Reaction), which could be because the electrophile likely

wasn't sufficiently reactive, and the final, which may suffer from the moisture sensitivity of the dimethylcarbamoyl chloride reagent. Another possibility is that the reactivity of the phenol, which is the nucleophile in this case, could be limited by the presence of the trifluoromethyl group substituent. This is a strong electron withdrawing group that can decrease the nucleophilicty of the phenol, and hinder its ability to attack the chlorobenzene moiety.

We've also designed a class of molecules that contain a heteroatom in one or each of the benzene rings. Heteroaromatics are a class of compounds that can be useful for designing biological inhibitors. These functional groups have especially been prominent in manufacturing herbicides for plant and weed diseases.

4.2 Coumarin-Azide Synthesis

Coumarins are useful, versatile, and small molecules that contribute to fluorescent labeling of organic entities. The assistance of coumarins is a popular entity used in labeling live cells, and for reacting with derivatized liposomes.[195-200] A variety of coumarins have been synthesized by adding on different substituents to cater to different functional groups. These groups include thiols,[201-202] acids, alkynes, and azides. The latter of which has been most prominently utilized as a fluorogenic dye through the use of the copper-catalyzed click reaction.[203]

2,4-Dihydroxybenzaldehyde **43** was purchased through a commercial vendor, and then reacted with *N*-acetylglycine **44** (Figure 4.2). The reaction proceeded through a Robinson annulation in order to form the bicyclic component. In addition

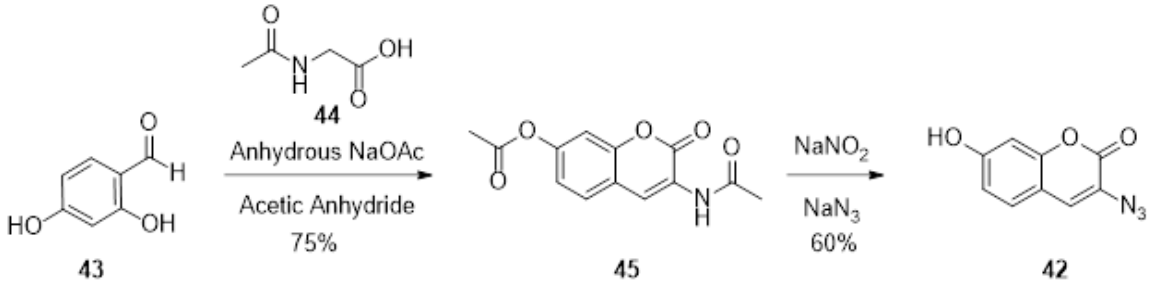

Figure 4.2 Synthetic scheme for producing azido-coumarin **42**

to this reaction closing up the ring, the hydroxyl group at the 4-position was acetyl protected. Coumarin analogue **45** was collected and moved to the next step without further purification. Next, **45** was reacted with sodium nitrite to form the nitrosamine derivative, and then sodium azide was added to produce the coumarin azide **42**. The product was isolated via crystallization with H_2O and characterized by infrared spectroscopy. This compound is defined by the strong peak at 2140 cm^{-1}, which signifies the presence of the azide functional group.

Coumarin analogues have been useful for fluorescence detection, particularly for in vitro studies. These dyes have the ability to act as 'on/off' fluorophore in which fluorescence is activated upon reaction. Multiple functional groups have been added on coumarin to optimize fluorogenic properties for this purpose. A number of chemical methods have been implemented to expose this 'on/off' attribute, most notably azide-alkyne click chemistry, thiolene click chemistry, and oxazine moieties. Recently, we incorporated this coumarin-azide probe as a method to derivative membranes decorated with a photocleavable lipid.[170] The coumarin probe for this system was introduced into a microplate containing liposomal solution with and without cyclooctyne lipid. Upon mixing with the solution

containing the cyclooctyne lipid (Figure 4.3), the results show a steady increase in fluorescence. Liposomes lacking the cyclooctyne (control) showed an initial increase in fluorescence, but it tapered off quickly.

All of these methods are likely to suffer when it comes to selective targeting in vivo. Thiolene chemistry involves the use of cysteine residues, and although it has been shown to have good selectivity with this coumarin analogue, it was matched against one cell solution. Given the robust variety of cells, there is skepticism whether this method will have any success in labeling a specific type of cell. Azide-alkyne click chemistry offers the best approach because of the orthogonal nature invoked by each functional group. With Bertozzi and coworkers fabricating the method of metabolically labeling live cells with azido-tagged glycoproteins, this offers potential in selectively targeting functionalized cells with fluorescent probes.

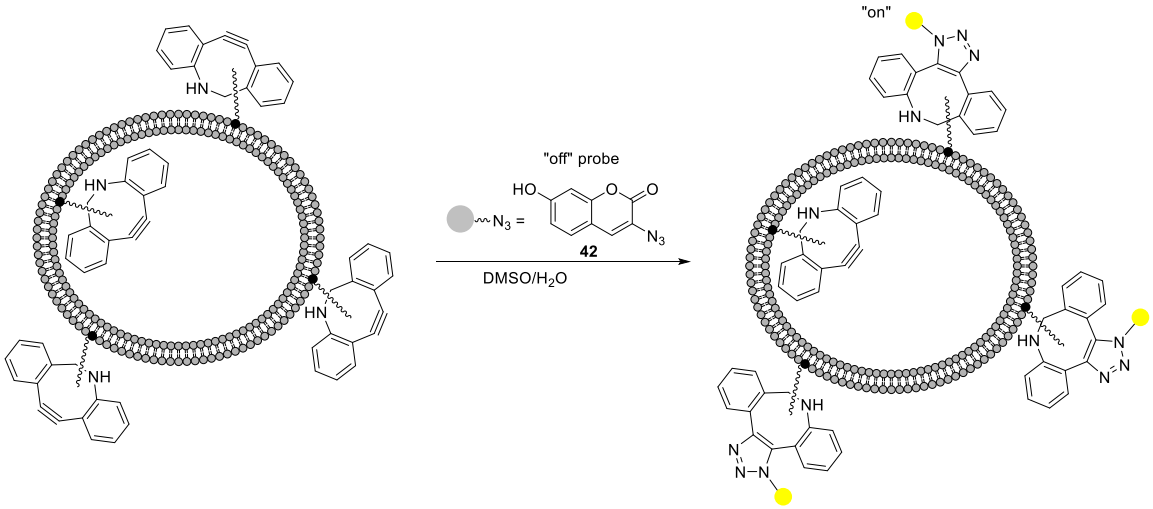

Figure 4.3 Strategy for implementing azido-coumarin **42** into derivatized liposomes.

4.3 Porphyrin lipid Project

Porphyrins are photosensitive molecules utilized for the absorption of reactive oxygen species. They have received a lot of attention for their potential in biological and biochemical processes,[204] specifically for materials to combat issues in photonics and electronics. The pervasive feature of these porphyrin substrates is the large planar pi-conjugation they possess at the core of the structure.[205-206] They also provide good thermal stability and photodynamic properties, which are attractive to material scientists.

The synthesis for porphyrin related materials is an important exercise is well published in the literature.[207-210] The structure has been exploited to convert the singlet oxygen state into triplet oxygen, a process that can benefit photosynthetic pathways (Figure 4.4).[211-212] It can be helpful to bind porphyrin to a variety of biomolecules because of their chemotherapeutic applications, since they can also absorb radiation and inhibit reactive oxygenated products.

We attempted to synthesize porphyrin lipid **46** via copper-catalyzed click chemistry (Figure 4.5). The availability we had with azide lipid **5** made for an appealing component in the collaborative work between us and the supplier of porphyrin alkyne **47**, Reza Ghiladi from North Carolina State University.[213] With porphyrin lipid available, we could incorporate this lipid into a bilayer membrane and undergo non-specific cell therapy. Given the experience and success we've had in the laboratory with utilizing copper-catalyzed click reactions between terminal alkynes and azides, we figured to employ the same tactics with this

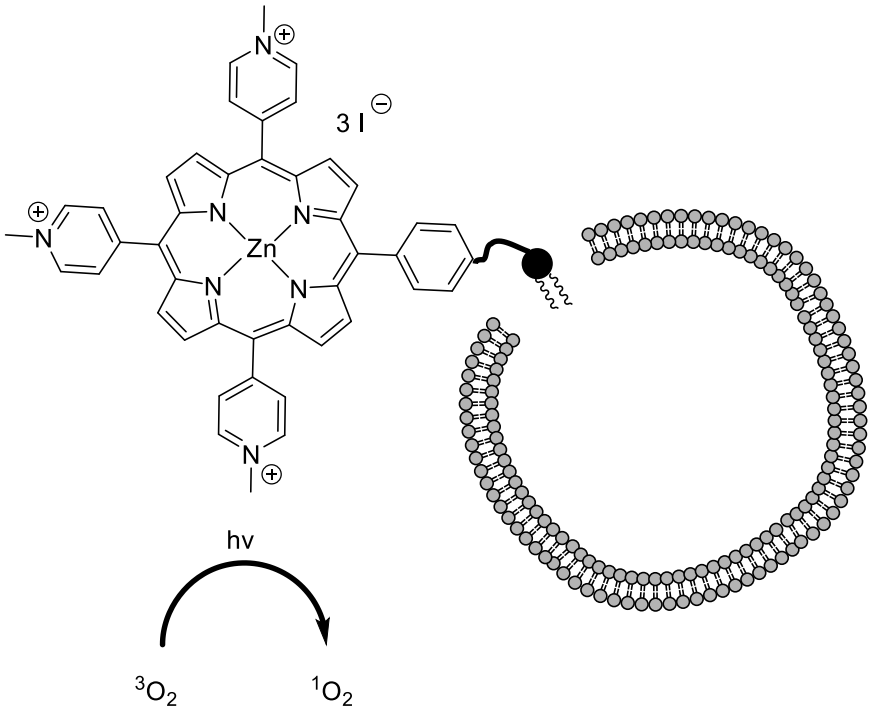

Figure 4.4 Potential application of porphyrin lipid **46** being incorporated into vesicles and converting triplet oxygen into singlet oxygen.

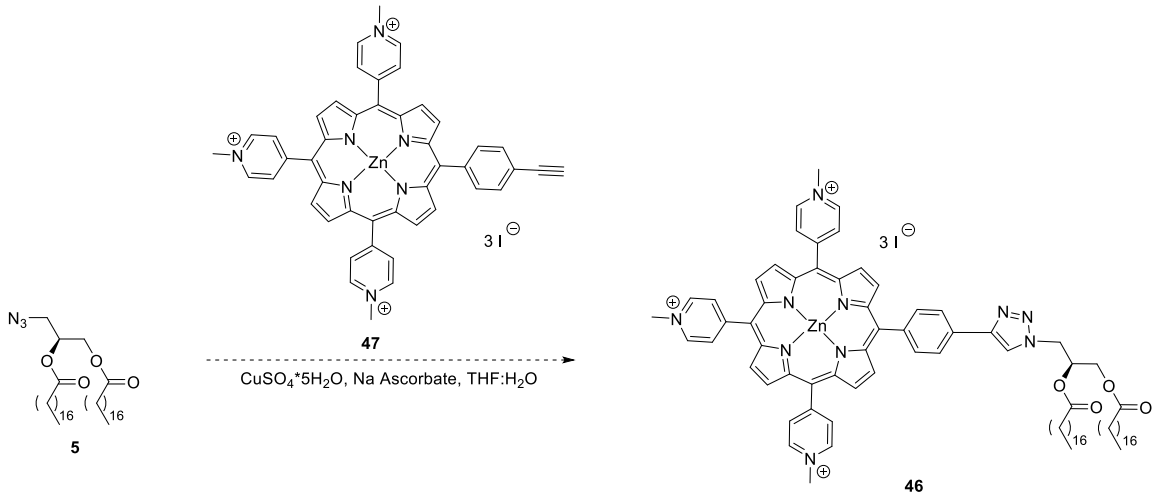

Figure 4.5 Synthesis scheme for porphyrin lipid **46**. Lipid could not be isolated.

particular scheme. We dissolved both the porphyrin alkyne moiety and azide lipid **5** in THF, and then mixed in an aqueous solution of copper (II) sulfate ($CuSO_4$) and sodium ascorabate (Na Ascorbate). We experimented with catalytic and stoichiometric amounts of this copper solution, and found THF to be a desirable solvent for both azide lipid **5** and porphyrin alkyne **47**.

We believe the desired product was not amenable to normal phase column, so we attempted a reverse phase column instead. We analyzed a variety of fractions from this column on the HPLC instrument, and compared the results to the porphyrin alkyne moiety. We found there to be no change between any of the fractions with the starting alkyne. Based on the literature precedent with producing porphyin derived molecules, introducing heat did yield some success with the reaction.

4.4 Conclusions

We described in this chapter the various side projects we worked on while attempting to synthesize lipid analogues for the promotion SPAAC driven membrane fusion. We synthesized one potential PSII dual-site inhibitor, biphenyl ether urea **37**, from trifluoromethyl phenol in a collaborative work with Dr. Gregory Armel from BASF. We originally intended to synthesize **37** by the Ullman reaction in one step, but found the urea starting was susceptible to decomposition during this reaction. Instead, this led to a multistep synthesis that saved the generation of urea moiety until after the Ullman coupling step. We also synthesized coumarin-azide analogue (**42**) to be used in the derivatization of cyclooctyne-tagged

liposomes through exploiting the SPAAC reaction. We found this fluorogenic analogue to be extremely selective in targeting these functionalized liposomes over control liposomes (lacking cyclooctyne). Finally, we attempted to synthesize a porphyrin lipid (**46**) by clicking on azido-lipid **5** with a porphyrin alkyne (**47**) in a collaborative work with Dr. Reza Ghiladi from the North Carolina State University. We found the porphyrin alkyne moiety and porphyrin lipid analogue to be tough to distinguish between each other during characterization. Given the large polarity difference between azido-lipid **5** and porphyrin alkyne **47**, this reaction could be improved by increasing the solubility of both components. We could've experimented with different concentrations of aqueous and organic solvents in solution to achieve this.

4.5 Experimental Procedures

4.5.1 Biphenylether urea 37 Synthesis

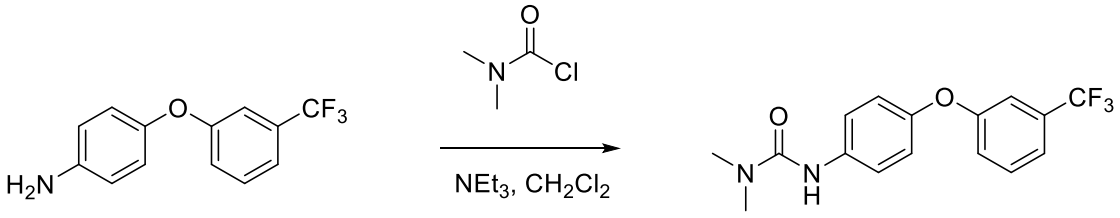

41 **37**

1-(4-nitrophenoxy)-3-(trifluoromethyl)benzene (**40**): 1-chloro-4-nitrobenzene **38** (1.03 g, 6.51 mmol), 3-(trifluoromethyl)phenol **39** (948 µL, 7.82 mmol), potassium carbonate (1.08 g, 7.82 mmol), and copper (I) iodide (37.0 mg, 0.200 mmol) were added to a flame dried flask and capped with a rubber septum. Next, 4 mL of dry and degassed DMF was added to the flask via syringe. The flask was evacuated

and refilled with nitrogen gas three times, and the solution was stirred at reflux (120 ^{0}C) overnight. The solution gradually cooled down to room temperature, and then added to 50 mL ethyl acetate. The organic layer was washed with 2x 50 mL H_2O and 1x 50 mL brine. The organic layer was collected and dried with $MgSO_4$, filtered, and concentrated using a rotary evaporator. The green-blue solid was purified via column chromatography (3.5% EtOAc/Hexanes), and nitro-biphenyl ether **40** was produced as a yellow solid in 45% yield (830 mg). ^{1}H NMR (300 MHz, $CDCl_3$): 8.23-8.26 (d, J = 9.1 Hz, 2H), 7.50-7.57 (m, 2H), 7.35 ppm (s, 1H), 7.26-7.29 (d, J = 9.5 Hz, 1H), 7.04-7.07 (d, J = 9.1 Hz, 2H). ^{13}C NMR (75 MHz, $CDCl_3$): 162.27, 155.27, 130.99, 126.13, 123.55, 121.93, 117.72, 117.30. MS-DART(+) [M+H] calc. exact mass: 284.05, found: 284.00

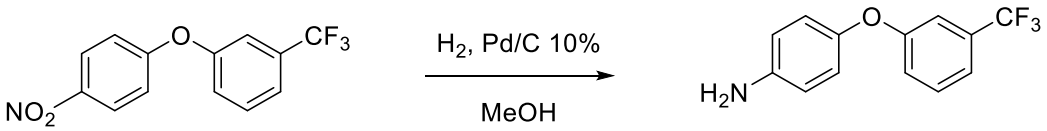

40 **41**

4-(3-(trifluoromethyl)phenoxy)aniline (**41**): Nitro-biphenyl ether **40** (500 mg, 1.76 mmol) and 10% Pd/C (20 mg) were dissolved in 5 mL of dry MeOH in a flame-dried flask. The flask was evacuated and refilled with hydrogen gas, and the solution was stirred at room temperature for 6 hr. The solution was filtered through a pad of celite, and liquid was concentrated on a rotary evaporator to produce a crude oil. The oil was purified via column chromatography (15% EtOAc/Hexanes) to produce amino-biphenyl ether **41** as a dark yellow oil (60%, 267 mg). ^{1}H NMR

(300 MHz, $CDCl_3$): 7.38 (t, J = 8.0 Hz, 1 H), 7.25-7.27 (d, J = 7.0 Hz, 1H), 7.16 (s, 1 H), 7.08-7.10 (d, J = 8.2 Hz, 1H), 6.87-6.90 (d, J = 8.9 Hz, 2 H), 6.69-6.72 (d, J = 8.9 Hz, 2 H), 3.59 (bs, 2H). ^{13}C NMR: 159.36, 147.51, 143.38, 130.05, 121.43, 120.11, 118.51, 116.36, 113.69. MS-DART(+) [M+H] calc. exact mass: 254.07, found: 254.0464.

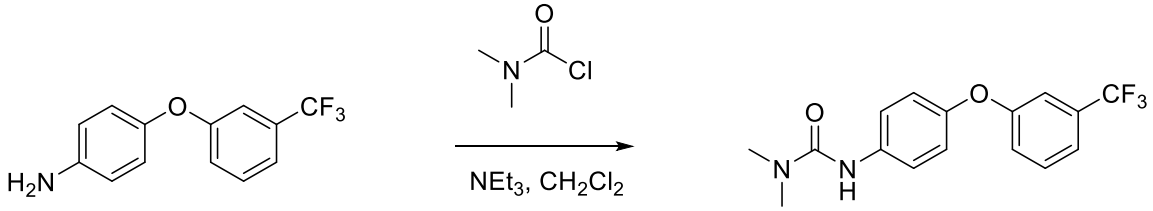

41 **37**

1,1-dimethyl-3-(4-(3-(trifluoromethyl)phenoxy)phenyl)urea (**37**): Amino-biphenyl ether **41** (200 mg, 0.790 mmol) and NEt_3 (440 µL, 3.16 mmol) were dissolved in dry & distilled CH_2Cl_2 (5 mL). The solution was cooled to 0 ^0C before dimethylcarbamoyl chloride (87.0 µL, 0.948 mmol) was added dropwise via syringe. The ice bath was removed after 10 minutes and stirring continued for 7 hr. The solution was poured into 10 mL H_2O, and then extracted with 3x 10 mL EtOAc. The organic layers were collected and washed with 1x 20 mL 0.75 M HCl, 2x 20 mL H_2O, and 1x 20 mL brine. The organic solution was dried with $MgSO_4$, filtered, and evaporated to produce a red solid. The solid was purified via column chromatography (35-50% EtOAc/Hexanes) to produce biphenyl ether urea **37** as a brownish white solid in 38% yield (97.0 mg). ^1H NMR: 7.40 (d, J = 6.2 Hz, 2H), 7.28-7.31 (d, J = 7.4 Hz, 2H), 7.20 (s, 1H), 7.11-7.13 (d, J = 8.0 Hz, 1H), 6.95-7.00 (m, 2H), 6.40 (bs, 1H), 3.04 (s, 6H). ^{13}C NMR (125 MHz, $CDCl_3$): 158.49, 155.78,

151.17, 135.69, 130.17, 121.83, 120.28, 114.58, 36.44. MS-DART(+) [M+H] calc. exact mass: 325.11, found: 325.07199.

4.5.2 Synthetic Scheme of Coumarin Azide 42[203]

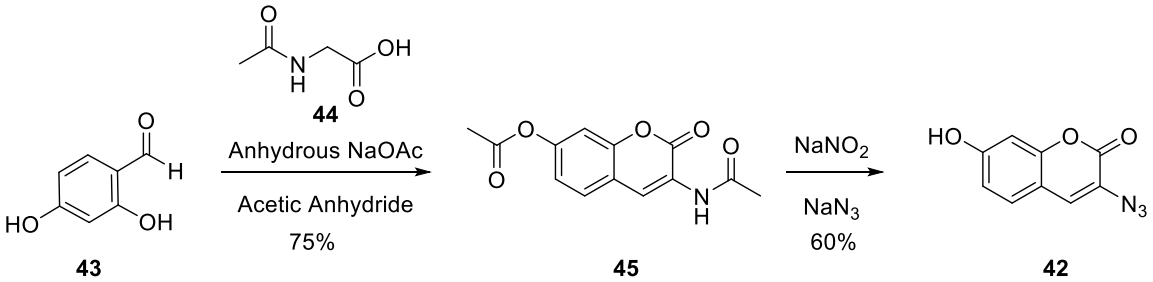

N-[7-(Acetyloxy)-2-oxo-2H-1-benzopyran-3-yl]acetamide (**45**): 2,4-dihydroxybenzaldehyde **43** (1.38 g, 10.0 mmol), *N*-acetylglycine **44** (1.17 g, 10.0 mmol), and anhydrous NaOAc (2.46 g, 30.0 mmol) were dissolved in Acetic Anhydride (50 mL). This mixture was put under reflux and N_2 atmosphere for 4 hours. The solution was poured onto crushed ice and a yellow precipitate developed. This precipitate was collected via filtration, and dried to produce 1.96 g (75%) of a yellow solid. This solid was carried through to the next step without further purification.

3-Azido-7-hydroxycoumarin (**42**): 3-Acetamido-7-acetoxycoumarin **45** (170 mg, 0.650 mmol) was dissolved in conc. HCl:EtOH (15 mL, 2:1, respectively), and then stirred at reflux for 1 hr. Ice water was added dropwise to the solution. The flask was then put into an ice bath, and as the solution was cooling down, sodium nitrite (90.0 mg, 1.30 mmol) was added; solution stirred in ice bath for ~10 minutes. While still stirring in an ice bath, sodium azide (130 mg, 2.00 mmol) was added in small increments over 5 minutes. The solution was stirred in an ice bath for an

additional 5 minutes, and then warmed up to room temperature and stirred for an additional 1 hr. A brown precipitate developed over the course of this last stage of stirring, and it was collected via filtration. After drying, azido-coumarin **42** was isolated in 60% yield (79.0 mg) as a brown solid. ^{1}H NMR (300 MHz, MeOD): 7.40 (s, 1 H), 6.80-6.81 (dd, J = 2.3, 0.5 Hz, 1 H), 6.77 (dd, J = 2.3, 0.5 Hz, 1 H), 6.72 (d, J = 2.1 Hz, 2 H). IR (cm^{-1}): 2107 (s), 1676 (s), 1620 (s), 1321 (s).

List of References

1. Lipowsky, R., The morphology of Lipid Membranes. *Current Opinion in Structural Biology* **1995,** *5*, 531-540.
2. Dietrich, C.; Bagatolli, L. A.; Volovyk, Z. N.; Thompson, N. L.; Levi, M.; Jacobson, K.; Gratton, E., Lipid rafts reconstituted in model membranes. *Biophysical Journal* **2001,** *80* (3), 1417-1428.
3. Voskuhl, J.; Ravoo, B. J., Molecular recognition of bilayer vesicles. *Chem Soc Rev* **2009,** *38* (2), 495-505.
4. Luisi, P. L.; Walde, P.; Oberholzer, T., Lipid vesicles as possible intermediates in the origin of life. *Curr. Opin. Colloid Interface Sci.* **1999,** *4* (1), 33-39.
5. Binder, W. H.; Barragan, V.; Menger, F. M., Domains and rafts in lipid membranes. *Angewandte Chemie-International Edition* **2003,** *42* (47), 5802-5827.
6. Bevers, E. M., Comfurius, E.M., Dekkers, P., & Zwaal, Lipid translocation across the plasma membrane of mammalian cells. *Biochimica et. biophysica acta* **1999,** *1439*, 317-330.
7. Daleke, D. I., Regulation of transbilayer plasma membrane phospholipid asymmetry. *Journal of lipid research* **2003,** *44*, 233-242.
8. Hope, M. J., Bally, M.B., Madden, T.D., & Mayer, L.D., Influence of pH gradients on the transbilayer transport of drugs, lipids, peptides, and metal ions into large unilamellar vesicles. *Biochimica et. biophysica acta* **1997,** *1331*, 199-203.
9. Brown, M. F., Modulation of rhodopsin function by properties of the membrane bilayer. *Chemistry and physics of lipids* **1994,** *73*, 159-161.
10. van Meer, G.; de Kroon, A., Lipid map of the mammalian cell. *J. Cell Sci.* **2011,** *124* (1), 5-8.
11. van Meer, G.; Voelker, D. R.; Feigenson, G. W., Membrane lipids: where they are and how they behave. *Nature Reviews Molecular Cell Biology* **2008,** *9* (2), 112-124.
12. Vance, J. E.; Steenbergen, R., Metabolism and functions of phosphatidylserine. *Prog. Lipid Res.* **2005,** *44* (4), 207-234.
13. Suetsugu, S.; Kurisu, S.; Takenawa, T., Dynamic shaping of cellular membranes by phospholipids and membrane-deforming proteins. *Physiol Rev* **2014,** *94* (4), 1219-48.
14. Janmey, P. A.; Kinnunen, P. K. J., Biophysical properties of lipids and dynamic membranes. *Trends Cell Biol.* **2006,** *16* (10), 538-546.
15. Svenson, S., Dendrimers as versatile platform in drug delivery applications. *european journal of pharmaceutics and biopharmaceutics* **2009,** *71*, 445-462.
16. Allen, T. M., Cullis, P.R., Drug delivery systems: Entering the mainstream. *Science* **2004,** *303*, 1818-1822.
17. Torchilin, V. P., Structure and design of polymeric surfactant-based drug delivery systems. *Journal of Controlled Release* **2001,** *73*, 137-172.
18. Langer, R., Drug delivery and targeting. *Nature* **1998,** *392*, S5-10.

19. Chan, Y. H.; Boxer, S. G., Model membrane systems and their applications. *Curr Opin Chem Biol* **2007,** *11* (6), 581-7.
20. Lee, J. L., B.R., Evolution of Lipidic Structures during Model Membrane Fusion and the Relation of This Process to Cell Membrane Fusion. *biochemistry* **1997,** *36*, 6251-6258.
21. Yong, M., Jiang, R., Zhang, H., Gruzdys, V., & Sun, X., Chemoselectively surface functionalizable tethered bilayer lipid membrane for versatile membrane mimetic systems fabrication. *Journal of Materials Chemistry* **2012,** *22*, 6148-6155.
22. Atanasov, V., Atanasova, P.P., Vockenroth, I.K., Knorr, N., & Koper, I., A molecular toolkit for highly insulating tethered bilayer lipid membranes on various substrates. *Bioconjuate Chemistry* **2006,** *17*, 631-637.
23. Santonicola, M. G., Memesa, M., Meszynska, A., Ma, Y.J., & Vancso, G.J., Surface-grafted zwitterionic polymers as platforms for functional supported phospholipid membranes. *Soft Matter* **2012,** *8*, 1556-1562.
24. de Groot, G. W., Demarche, S., Tiefenauer, L., & Vancso, G.J., Smart polymer brush nanostructures guide the self-assembly of pore-spanning lipid bilayers with integrated membrane proteins. *Nanoscale* **2014,** *6*, 2228-2237.
25. Liu, Y., Young, M.C., Moshe, O., Cheng, Q., & Hooley, R.J., A membrane-bound synthetic receptor that promotes growth of a polymeric coating at the bilayer-water interface. *Angew Chem Int Ed* **2012,** *51*, 7748-7751.
26. Jackman, J. A., Tabaei, S.R., Zhao, Z.L., Yorulmaz, S., & Cho, N.J., Self-assembly formation of lipid bilayer coatings on bare aluminum oxide: overcoming the force of interfacial water. *ACS Applied Materials & Interfaces* **2015,** *7*, 959-968.
27. Tabaei, S. R., Vafaei, S., Cho, N. J., Fabrication of charge membranes by the solvent-assisted lipid bilayer formation method on SiO2 and Al2O3. *Physical Chemistry Chemical Physics* **2015,** *17*, 11546-11552.
28. Cho, N. J. F., C.W., Fabrication of a planar zwitterionic lipid bilayer on titanium oxide. *Langmuir* **2010,** *26*, 15706-15710.
29. Venkatesan, B. M., Polans, J., Comer, J., et. al., Lipid bilayer coated Al2O3 nanopore sensors: towards a hybrid biological solid-state nanopore. *Biomedical Microdevices* **2011,** *13*, 671-682.
30. Trubetskoy, V. S. T., V. P., Use of polyoxyethylene-lipid conjugates as long-circulating carriers for delivery of therapeutic and diagnostic agents. *Adv. Drug Deliv. Rev.* **1995,** *16*, 311-320.
31. Kwon, G. S. K., K., Block copolymer micelles as long-circulating drug vehicles. *Adv. Drug Deliv. Rev.* **1995,** *16*, 295-309.
32. Soo, P. L., Luo, L., Maysinger, D., & Eisenberg, A, Incorporation and release of hydrophobic probes in biocompatible polycaprolactone-block-poly(ethylene oxide) micelles: Implications for drug delivery. *Langmuir* **2002,** *18*, 9996-10004.

33. Kwon, G. S., Polymeric micelles for delivery of poorly water-soluable compounds. *Critical Reviews in Therapeutic Drug Carrier Systems* **2003,** *20*, 357-403.
34. Torchilin, V. P., Micellar nanocarriers: Pharmaceutical perspectives. *Pharmaceutical Research* **2007,** *24*, 1-16.
35. Tengamnuay, P. M., A.K., Bile salt-fatty acid mixed micelles as nasal absorption promoters of peptides. *Pharm. Res.* **1990,** *7*, 127-133.
36. Magnusson, G., Olsson, T., & Nyberg, J.A., Toxicty of Pluronic F-68. *Toxicol. Lett.* **1986,** *30*, 203-207.
37. Schmolka, I. R., A review of block polymer surfactants. *J. Am. Oil Chem. Soc.* **1977,** *54*, 110-116.
38. Port, C. D., Garvin, P.J., & Ganote, C.E., The effect of Pluoronic F-38 (poloxamer 108) administered intravenously in rats. *Toxicol. Appl. Pharmacol.* **1978,** *44*, 401-411.
39. Nasongkla, N., Bey, E., Ren, J., Hua, A., Khemtong, C., Guthi, J.S., Chin, S., Sherry, A.D., Boothman, D.A., Gao, J., Multifunctional Polymeric Micelles as Cancer-Targeted, MRI-Ultrasensitive Drug Delivery Systems. *Nano Letters* **2006,** *6*, 2427-2430.
40. Soppimath, K. S., Tan, D.C., & Yang, Y., pH-Triggered Thermally Responsive Polymer Core-Shell Nanoparticles for Drug Delivery. *Adv. Mater.* **2005,** *17*, 318-323.
41. Pourmoazzen, Z., Bagheri, M., & Entezami, A.A., Cholesterol-modified poly (monomethyl itaconate)s micelles as nano-carriers for pH-responsive drug delivery. *Polymer Journal* **2014,** *46*, 806-812.
42. Liu, G. Y., Li, M., Zhu, C.S., Jin, Q., Zhang, Z.C., & Ji, J., Charge-conversional and pH-sensitive PEGylated polymeric micelles as efficient nanocarriers for drug delivery. *Macromolecular Bioscience* **2014,** *14*, 1280-1290.
43. Rezaei, S. J. T., Abandansari, H.S., Nabi, M.R., & Niknejad, H., pH-responsive unimolecular micelles self-assembled from amphiphilic hyperbranched block copolymer for efficient intracellular release of poorly water-soluble anticancer drugs. *Journal of Colloid and Interface Science* **2014,** *425*, 27-35.
44. Ye, L., Gao, Z.M., Zhou, Y., Yin, X., Zhang, X.P., Zhang, A.Y., Feng, Z.G., A pH-sensitive binary drug delivery system based on poly(caprolactone)-heparin conjugates. *Journal of Biomedical Materials* **2014,** *102*, 880-889.
45. Nie, S. Y., Sun, Y., Lin, W.J., Wu, W.S., Guo, X.D., Qian, Y., & Zhang, L.J., Dissipative particle dynamics studies of doxorubicin-loaded micelles assembled from four-arm star triblock polymers 4AS-PCL-b-PDEAEMA-b-PPEGMA and their pH-release mechanism. *Journal of Physical Chemistry* **2013,** *117*, 13688-13697.
46. Ravazzolo, E., Salmaso, S., Mastrotto, F., Bersani, S., Gallon, E., & Caliceti, P., pH-responsive lipid core micelles for tumour targeting. *European journal of pharmaceutics and biopharmaceutics* **2013,** *83*, 346-357.

47. Jiang, X. L., Li, L.H., Liu, J., Hennink, W.E., & Zhuo, R.X., Facile fabrication of thermo-responsive and reduction-sensitive polymeric micelles for anticancer drug delivery. *Macromolecular Bioscience* **2012,** *12*, 703-711.
48. Zhang, F., Wu, Q., Liu, L.J., Chen, Z.C., & Lin, X.F., Thermal treatment of galactose-branched polyelectrolyte microcapsules to improve drug delivery with reserved targetability. *International Journal of Pharmaceutics* **2008,** *357*, 22-31.
49. Wu, Q. G., Du, F., Luo, Y., Lu, W., Huang, J., Yu, J.H., & Liu, S.Y., Poly(ethylene glycol) shell-sheddable nanomicelle prodrug of camptothecin with enhanced cellular uptake. *Colloids and Surfaces B-Biointerfaces* **2013,** *105*, 294-302.
50. Ishii, T., Miyata, K., et. al., Enhanced target recognition of nanoparticles by cocktail PEGylation with chains of varying lengths. *Chemical Communications* **2016,** *52*, 1517-1519.
51. Lu, J. Q., Huang, Y.X., et. al., PEG-derivatized embelin as a nanomicellar carrier for delivery of paclitaxel to breast and prostate cancers. *Biomaterials* **2013,** *34*, 1591-1600.
52. Ding, H., Yong, K.T., Roy, I., et. al., Bioconjugated PLGA-4-arm-PEG branched polymeric nanoparticles as novel tumor targeting carriers. *Nanotechnology* **2011,** *22*, 1-12.
53. Ji, T. J., Ding, Y.P., Zhao, Y., et. al., Peptide assembly integration of fibroblast-targeting and cell-penetration features for enhanced antitumor drug delivery. *Advanced Materials* **2015,** *27*, 1865-1873
54. Sutton, D.; Nasongkla, N.; Blanco, E.; Gao, J. M., Functionalized micellar systems for cancer targeted drug delivery. *Pharmaceutical Research* **2007,** *24* (6), 1029-1046.
55. Farokhzad, O. C.; Karp, J. M.; Langer, R., Nanoparticle-aptamer bioconjugates for cancer targeting. *Expert Opinion on Drug Delivery* **2006,** *3* (3), 311-324.
56. Sofou, S.; Sgouros, G., Anti body-targeted liposomes in cancer therapy and imaging. *Expert Opinion on Drug Delivery* **2008,** *5* (2), 189-204.
57. Torchilin, V., Antibody-modified liposomes for cancer chemotherapy. *Expert Opinion on Drug Delivery* **2008,** *5* (9), 1003-1025.
58. Wu, X. L.; Kim, J. H.; Koo, H.; Bae, S. M.; Shin, H.; Kim, M. S.; Lee, B.-H.; Park, R.-W.; Kim, I.-S.; Choi, K.; Kwon, I. C.; Kim, K.; Lee, D. S., Tumor-Targeting Peptide Conjugated pH-Responsive Micelles as a Potential Drug Carrier for Cancer Therapy. *Bioconjugate Chemistry* **2010,** *21* (2), 208-213.
59. Arap, W.; Pasqualini, R.; Ruoslahti, E., Cancer treatment by targeted drug delivery to tumor vasculature in a mouse model. *Science* **1998,** *279* (5349), 377-380.
60. Accardo, A.; Tesauro, D.; Morelli, G., Peptide-based targeting strategies for simultaneous imaging and therapy with nanovectors. *Polymer Journal* **2013,** *45* (5), 481-493.

61. Kim, H.; Kang, Y. J.; Min, J.; Choi, H.; Kang, S., Development of an antibody-binding modular nanoplatform for antibody-guided targeted cell imaging and delivery. *Rsc Advances* **2016,** *6* (23), 19208-19213.
62. Hudson, P. J.; Souriau, C., Engineered antibodies. *Nature Medicine* **2003,** *9* (1), 129-134.
63. von Mehren, M.; Adams, G. P.; Weiner, L. M., Monoclonal antibody therapy for cancer. *Annual Review of Medicine-Selected Topics in the Clinical Sciences* **2003,** *54*, 343-369.
64. Baskin, J. M.; Bertozzi, C. R., Bioorthogonal click chemistry: Covalent labeling in living systems. *Qsar & Combinatorial Science* **2007,** *26* (11-12), 1211-1219.
65. Saxon, E. B., C. R., Cell Surface Engineering by a Modified Staudinger React. *Science* **2000,** *287*, 2007-2010.
66. Prescher, J. A.; Bertozzi, C. R., Chemistry in living systems. *Nature Chemical Biology* **2005,** *1* (1), 13-21.
67. Wittrock, S.; Becker, T.; Kunz, H., Synthetic vaccines of tumor-associated glycopeptide antigens by immune-compatible thioether linkage to bovine serum albumin. *Angewandte Chemie-International Edition* **2007,** *46* (27), 5226-5230.
68. Jonkheijm, P.; Weinrich, D.; Koehn, M.; Engelkamp, H.; Christianen, P. C. M.; Kuhlmann, J.; Maan, J. C.; Nuesse, D.; Schroeder, H.; Wacker, R.; Breinbauer, R.; Niemeyer, C. M.; Waldmann, H., Photochemical surface patterning by the thiol-ene reaction. *Angewandte Chemie-International Edition* **2008,** *47* (23), 4421-4424.
69. Agarwal, P.; Bertozzi, C. R., Site-Specific Antibody-Drug Conjugates: The Nexus of Bioorthogonal Chemistry, Protein Engineering, and Drug Development. *Bioconjugate Chemistry* **2015,** *26* (2), 176-192.
70. Cornish, V. W.; Hahn, K. M.; Schultz, P. G., Site-specific protein modification using a ketone handle. *Journal of the American Chemical Society* **1996,** *118* (34), 8150-8151.
71. Rose, K.; Vizzavona, J., Stepwise solid-phase synthesis of polyamides as linkers. *Journal of the American Chemical Society* **1999,** *121* (30), 7034-7038.
72. Yousaf, M. N.; Mrksich, M., Diels-Alder reaction for the selective immobilization of protein to electroactive self-assembled monolayers. *Journal of the American Chemical Society* **1999,** *121* (17), 4286-4287.
73. de Araujo, A. D.; Palomo, J. M.; Cramer, J.; Kohn, M.; Schroder, H.; Wacker, R.; Niemeyer, C.; Alexandrov, K.; Waldmann, H., Diels-Alder ligation and surface immobilization of proteins. *Angewandte Chemie-International Edition* **2006,** *45* (2), 296-301.
74. Seelig, B.; Jaschke, A., Site-specific modification of enzymatically synthesized RNA: Transcription initiation and Diels-Alder reaction. *Tetrahedron Letters* **1997,** *38* (44), 7729-7732.
75. Latham-Timmons, H. A.; Wolter, A.; Roach, J. S.; Giare, R.; Leuck, M., Novel method for the covalent immobilization of oligonucleotides via Diels-Alder

bioconjugation. *Nucleosides Nucleotides & Nucleic Acids* **2003,** *22* (5-8), 1495-1497.
76. Mahal, L. K.; Yarema, K. J.; Bertozzi, C. R., Engineering chemical reactivity on cell surfaces through oligosaccharide biosynthesis. *Science* **1997,** *276* (5315), 1125-1128.
77. Bertozzi, C. R., Guest Editorial: A Decade of Bioorthogonal Chemistry. *Accounts of Chemical Research* **2011,** *44* (9), 651-653.
78. Lim, R. K. V.; Lin, Q., Bioorthogonal chemistry: a covalent strategy for the study of biological systems. *Science China-Chemistry* **2010,** *53* (1), 61-70.
79. Soellner, M. B., Nilsson, B. L., & Raines, R. T., Staudinger Ligation of a-Azido Acids Retains Stereochemistry. *J. Org. Chem* **2002,** *67*, 4993-4996.
80. Tam, A., Soellner, M. B., & Raines, R. T., Water-Soluble Phosphinothiols for Traceless Staudinger Ligation and Integration with Expressed Protein Ligation. *J Am Chem Soc* **2007,** *129*, 11421-11430.
81. Tam, A.; Raines, R. T., Coulombic effects on the traceless Staudinger ligation in water. *Bioorg Med Chem* **2009,** *17* (3), 1055-63.
82. Tam, A.; Soellner, M. B.; Raines, R. T., Electronic and steric effects on the rate of the traceless Staudinger ligation. *Org Biomol Chem* **2008,** *6* (7), 1173-5.
83. Tsao, M. L.; Tian, F.; Schultz, P. G., Selective staudinger modification of proteins containing p-azidophenylalanine. *Chembiochem* **2005,** *6* (12), 2147-2149.
84. Lin, F. L., Hoyt, H. M., van Halbeek, H., Bergman, R. G., & Bertozzi, C. R., Mechanistic Investigation of the Staudinger Ligation. *J Am Chem Soc* **2005,** *127*, 2686-2695.
85. Nilsson, B. L., Kiessling, L. L., & Raines, R. T., High-Yielding Staudinger Ligation of a Phosphinothioester and Azide To Form a Peptide. *Organic Letters* **2001,** *3*, 9-12.
86. Tornoe, C. W., Christensen, C., and Meldal, M., *J. Org. Chem* **2002,** *67*, 3057-3062.
87. Rostovtsev, V. V., Green, L. G., Fokin, V. V., and Sharpless, K. B., *Angew Chem Int Ed* **2002,** *41*, 2596-2599.
88. Huisgen, R., *Angew Chem Int Ed* **1963,** *2*, 565-598.
89. Himo, F., Lovell, T., Hilgraf, R., Rostovtsev, V.V., Noodleman, L,; Sharpless, K. B., and Fokin, V.V., *J Am Chem Soc* **2005,** *127*, 210-216.
90. Devaraj, N. K. C., J. P., Copper catalyzed azide-alkyne cycloadditions on solid surfaces: Applications and future directions. *QSAR & Combinatorial Science* **2007,** *26*, 1253-1260.
91. Berg, R. S., B.F., Advancements in the mechanistic understanding of the copper-catalyzed azide-alkyne cycloaddition. *Beilstein Journal of Organic Chemistry* **2013,** *9*, 2715-2750.
92. Angell, Y. L. B., K, *Chemical Society Reviews* **2007,** *36*, 1674-1689.
93. Gramlich, P., Wirges, CT, Manetto, A, & Carell, T., *Angewandte chemie-international edition* **2008,** *47*, 8350-8358.

94. Tunca, U., *Journal of polymer science* **2014,** *52*, 3147-3165.
95. Agard, N. J., Prescher, J. A., & Bertozzi, C. R., A Strain-Promoted [3 + 2] Azide-Alkyne Cycloaddition for Covalent Modification of Biomolecules in Living Systems. *J Am Chem Soc* **2004,** *126*, 15046-15047.
96. Ess, D. H.; Jones, G. O.; Houk, K. N., Transition states of strain-promoted metal-free click chemistry: 1,3-dipolar cycloadditions of phenyl azide and cyclooctynes. *Organic Letters* **2008,** *10* (8), 1633-1636.
97. Baskin, J. M.; Prescher, J. A.; Laughlin, S. T.; Agard, N. J.; Chang, P. V.; Miller, I. A.; Lo, A.; Codelli, J. A.; Bertozzi, C. R., Copper-free click chemistry for dynamic in vivo imaging. *Proc Natl Acad Sci U S A* **2007,** *104* (43), 16793-7.
98. van Geel, R., Pruijn, GJM, van Delft, FL, & Boelens, WC, *Bioconjugate Chemistry* **2012,** *23*, 392-398.
99. Prim, D., Rebeaud, F, Cosandey, V., Marti, R., Passeraub, P, & Pfeifer, M.E., *Molecules* **2013,** *18*, 9833-9849.
100. Yao, J., Uttamapinant, C, Poloukhtine, A, Baskin, JM, Codelli, JA, Sletten, EM, Bertozzi, CR, Popik, VV, Ting, Ay, **2012,** *134*, 3720-3728.
101. McNitt, C. D.; Popik, V. V., Photochemical generation of oxa-dibenzocyclooctyne (ODIBO) for metal-free click ligations. *Org. Biomol. Chem.* **2012,** *10* (41), 8200-8202.
102. Yuan, L., Lin, W.Y., Zheng, K.B., and Zhu, S.S., *Accounts of Chemical Research* **2013,** *46*, 1462-1473.
103. Lebrun-Chirio, M. C. P., M., *Biochemical Education* **1998,** *26*, 320-323.
104. Wallrabe, H. P., A, *Current Opinion in Biotechnology* **2005,** *16*, 19-27.
105. Clapp, A. R., Medintz, I.L., and Mattoussi, H, *ChemPhysChem* **2006,** *7*, 47-57.
106. Hassane, F. S., Frisch, B., & Schuber, F., Targeted Liposomes: Convenient Coupling of Ligands to Preformed Vesicles Using “Click Chemistry”. *Bioconjugate Chemistry* **2006,** *17*, 849-854.
107. Cavalli, S.; Tipton, A. R.; Overhand, M.; Kros, A., The chemical modification of liposome surfaces via a copper-mediated [3 + 2] azide-alkyne cycloaddition monitored by a colorimetric assay. *Chem Commun (Camb)* **2006,** (30), 3193-5.
108. O'Neil, E. J., DiVittorio, K. M., & Smith, B. D., Phosphatidylcholine-Derived Bolaamphiphiles via Click Chemistry. *Organic Letters* **2007,** *9*, 199-202.
109. Cameron, L. M., Fyles, T.M., and Hu, C.W., Synthesis and membrane activity of a bis(metacyclophane)bolaamphiphile. *Journal of Organic Chemistry* **2002,** *67*, 1548-1553.
110. Forbes, C. C., DiVittorio, K.M., & Smith, B.D., Bolaamphiphiles promote phospholipid translocation across vesicle membranes. *Journal of American Chemical Society* **2006,** *128*, 9211-9218.
111. Lutz, J.-F., Borner, H. G., & Weichenhan, K., Combining ATRP and “Click” Chemistry: a Promising Platform toward Functional Biocompatible Polymers and Polymer Bioconjugates. *Macromolecules* **2006,** *39*, 6376-6383.

112. Lallana, E., Fernandez-Trillo, F., et. al., Click chemistry with polymers, dendrimers, and hydrogels for drug delivery. *Pharmaceutical Research* **2012,** *29*, 902-921.
113. Wang, L. L., Kiemle, D.J., Boyle, C.J., Connors, E.L., & Gitsov, I., "Click" synthesis of intrinsically hydrophilic dendrons and dendrimers containing metal binding moieties at each branching unit. *Macromolecules* **2014,** *47*, 2199-2213.
114. Houghton, E. A.; Nicholas, K. M., In vitro reactive oxygen species production by histatins and copper(I,II). *Journal of Biological Inorganic Chemistry* **2009,** *14* (2), 243-251.
115. Hong, V.; Steinmetz, N. F.; Manchester, M.; Finn, M. G., Labeling Live Cells by Copper-Catalyzed Alkyne-Azide Click Chemistry. *Bioconjugate Chemistry* **2010,** *21* (10), 1912-1916.
116. Bostic, H., Smith, MD, Poloukhtine, AA, Popik, VV, & Best, MD., *Chemical Communications* **2012,** *48*, 1431-1433.
117. Oude Blenke, E.; Klaasse, G.; Merten, H.; Pluckthun, A.; Mastrobattista, E.; Martin, N. I., Liposome functionalization with copper-free "click chemistry". *J Control Release* **2015,** *202*, 14-20.
118. Kumar, P.; Guha, S.; Diederichsen, U., SNARE protein analog-mediated membrane fusion. *J Pept Sci* **2015,** *21* (8), 621-9.
119. Nordlund, G.; Brzezinski, P.; von Ballmoos, C., SNARE-fusion mediated insertion of membrane proteins into native and artificial membranes. *Nat Commun* **2014,** *5*, 4303.
120. Tareste, D.; Shen, J.; Melia, T. J.; Rothman, J. E., SNAREpin/Munc18 promotes adhesion and fusion of large vesicles to giant membranes. *Proc Natl Acad Sci U S A* **2008,** *105* (7), 2380-5.
121. Robson Marsden, H.; Korobko, A. V.; Zheng, T.; Voskuhl, J.; Kros, A., Controlled liposome fusion mediated by SNARE protein mimics. *Biomaterials Science* **2013,** *1* (10), 1046.
122. Paleos, C. M. T., D., Interaction between complementary liposomes: a process leading to multicompartment systems formation. *Journal of Molecular Recognition* **2006,** *19*, 60-67.
123. Tarafdar, P. K., Chakraborty, H., Dennison, S. M., & Lentz, B. R., Phosphatidylserine Inhibits and Calcium Promotes Model Membrane Fusion. *Biophysical Journal* **2012,** *103*, 1880-1889.
124. Richard, A., Marchi-Artzner, V., Lalloz, M-N., Brienne, M. J., Artzner, F., Gulik-Krzywicki, T., Guedeau-Boudeville, M. A., and Lehn, J. M., Fusogenic supramolecular vesicle systems induced by metal ion binding to amphiphilic ligands. *Proc. Natl. Acad. Sci. U.S.A.* **2004,** *101*, 15279-15284.
125. Lentz, B. R., PEG as a tool to gain insight into membrane fusion. *Eur Biophys Journal* **2007,** *36*, 315-326.
126. Stengel, G., Simonsson, L., Campbell, R. A., & Hook, F., Determinants for Membrane Fusion Induced by Cholesterol-Modified DNA Zippers. *J. Phys. Chem. B.* **2008,** *112*, 8264-8274.

127. Chan, Y. H.; van Lengerich, B.; Boxer, S. G., Effects of linker sequences on vesicle fusion mediated by lipid-anchored DNA oligonucleotides. *Proc Natl Acad Sci U S A* **2009,** *106* (4), 979-84.
128. van Lengerich, B.; Rawle, R. J.; Bendix, P. M.; Boxer, S. G., Individual vesicle fusion events mediated by lipid-anchored DNA. *Biophys J* **2013,** *105* (2), 409-19.
129. Jahn, R.; Lang, T.; Sudhof, T. C., Membrane fusion. *Cell* **2003,** *112* (4), 519-533.
130. Loosli, F., Doval, DA, Grassi, D, Zaffalon, PL, Favarger, F, & Zumbuehl, A, *Chemical Communications* **2012,** *48*, 1604-1606.
131. Menger, F. M.; Zhang, H. L., Self-adhesion among phospholipid vesicles. *Journal of the American Chemical Society* **2006,** *128* (5), 1414-1415.
132. Luo, W.; Pulsipher, A.; Dutta, D.; Lamb, B. M.; Yousaf, M. N., Remote control of tissue interactions via engineered photo-switchable cell surfaces. *Sci Rep* **2014,** *4*, 6313.
133. O'Brien, P. J.; Luo, W.; Rogozhnikov, D.; Chen, J.; Yousaf, M. N., Spheroid and Tissue Assembly via Click Chemistry in Microfluidic Flow. *Bioconjugate Chemistry* **2015,** *26* (9), 1939-1949.
134. Pulsipher, A.; Dutta, D.; Luo, W.; Yousaf, M. N., Cell-surface engineering by a conjugation-and-release approach based on the formation and cleavage of oxime linkages upon mild electrochemical oxidation and reduction. *Angew Chem Int Ed Engl* **2014,** *53* (36), 9487-92.
135. Park, S., Westcott, S.P., Luo, W., Dutta, D., and Yousaf, M.N., General Chemoselective and Redox-Responsive Ligation and Release Strategy. *Bioconjug Chem* **2014,** *25*, 543-551.
136. Elahipanah, S.; Radmanesh, P.; Luo, W.; O'Brien, P. J.; Rogozhnikov, D.; Yousaf, M. N., Rewiring Gram-Negative Bacteria Cell Surfaces with Bio-Orthogonal Chemistry via Liposome Fusion. *Bioconjug Chem* **2016,** *27* (4), 1082-9.
137. Dube, D. H.; Bertozzi, C. R., Metabolic oligosaccharide engineering as a tool for glycobiology. *Curr. Opin. Chem. Biol.* **2003,** *7* (5), 616-625.
138. Saxon, E.; Bertozzi, C. R., Chemical and biological strategies for engineering cell surface glycosylation. *Annu. Rev. Cell Dev. Biol.* **2001,** *17*, 1-23.
139. Kayser, H.; Zeitler, R.; Kannicht, C.; Grunow, D.; Nuck, R.; Reutter, W., Biosynthesis of a nonphysoiological sialic-acid in different rat organs, using N-propanoyl-D-hexosamines. *Journal of Biological Chemistry* **1992,** *267* (24), 16934-16938.
140. Keppler, O. T.; Horstkorte, R.; Pawlita, M.; Schmidts, C.; Reutter, W., Biochemical engineering of the N-acyl side chain of sialic acid: biological implications. *Glycobiology* **2001,** *11* (2), 11R-18R.
141. Hang, H. C.; Bertozzi, C. R., Chemoselective approaches to glycoprotein assembly. *Accounts of Chemical Research* **2001,** *34* (9), 727-736.
142. Cheng, L. W.; Zhang, X. X.; Zhang, Z. Y.; Chen, H.; Zhang, S.; Kong, J. L., Multifunctional phenylboronic acid-tagged fluorescent silica nanoparticles via

thiol-ene click reaction for imaging sialic acid expressed on living cells. *Talanta* **2013,** *115*, 823-829.
143. Zhang, Y.; Yuan, J. B.; Song, J. J.; Wang, Z. F.; Huang, L. J., An efficient method for selectively imaging and quantifying in situ the expression of sialylated glycoproteins on living cells. *Glycobiology* **2013,** *23* (6), 643-653.
144. Spate, A. K.; Schart, V. F.; Schollkopf, S.; Niederwieser, A.; Wittmann, V., Terminal Alkenes as Versatile Chemical Reporter Groups for Metabolic Oligosaccharide Engineering. *Chem.-Eur. J.* **2014,** *20* (50), 16502-16508.
145. Hanson, S. R.; Hsu, T. L.; Weerapana, E.; Kishikawa, K.; Simon, G. M.; Cravatt, B. F.; Wong, C. H., Tailored glycoproteomics and glycan site mapping using saccharide-selective bioorthogonal probes. *Journal of the American Chemical Society* **2007,** *129* (23), 7266-+.
146. Chen, I.; Howarth, M.; Lin, W. Y.; Ting, A. Y., Site-specific labeling of cell surface proteins with biophysical probes using biotin ligase. *Nature Methods* **2005,** *2* (2), 99-104.
147. Kiick, K. L.; Saxon, E.; Tirrell, D. A.; Bertozzi, C. R., Incorporation of azides into recombinant proteins for chemoselective modification by the Staudinger ligation. *Proceedings of the National Academy of Sciences of the United States of America* **2002,** *99* (1), 19-24.
148. Saxon, E.; Luchansky, S. J.; Hang, H. C.; Yu, C.; Lee, S. C.; Bertozzi, C. R., Investigating cellular metabolism of synthetic azidosugars with the Staudinger ligation. *Journal of the American Chemical Society* **2002,** *124* (50), 14893-14902.
149. Chang, P. V., Prescher, J. A., Hangauer, M. J., & Bertozzi, C. R., Imaging Cell Surface Glycans with Bioorthogonal Chemical Reporters. *J Am Chem Soc* **2007,** *129*, 8400-8401.
150. Saxon, E.; Bertozzi, C. R., Cell surface engineering by a modified Staudinger reaction. *Science* **2000,** *287* (5460), 2007-2010.
151. Laughlin, S. T.; Bertozzi, C. R., Metabolic labeling of glycans with azido sugars and subsequent glycan-profiling and visualization via Staudinger ligation. *Nature Protocols* **2007,** *2* (11), 2930-2944.
152. Baskin, J. M.; Prescher, J. A.; Laughlin, S. T.; Agard, N. J.; Chang, P. V.; Miller, I. A.; Lo, A.; Codelli, J. A.; Bertozzi, C. R., Copper-free click chemistry for dynamic in vivo imaging. *Proceedings of the National Academy of Sciences of the United States of America* **2007,** *104* (43), 16793-16797.
153. Agard, N. J.; Prescher, J. A.; Bertozzi, C. R., A strain-promoted 3+2 azide-alkyne cycloaddition for covalent modification of blomolecules in living systems. *Journal of the American Chemical Society* **2004,** *126* (46), 15046-15047.
154. Dube, D. H.; Bertozzi, C. R., Glycans in cancer and inflammation--potential for therapeutics and diagnostics. *Nat Rev Drug Discov* **2005,** *4* (6), 477-88.
155. Losey, E. A., Smith, M.D., Meng Meng, & Best, M.D., *Bioconjug Chem* **2009,** *20*, 376-383.

156. Smith, M. D.; Gong, D. H.; Sudhahar, C. G.; Reno, J. C.; Stahelin, R. V.; Best, M. D., Synthesis and convenient functionalization of azide-labeled diacylglycerol analogues for modular access to biologically active lipid probes. *Bioconjugate Chemistry* **2008,** *19* (9), 1855-1863.
157. Smith, M. D.; Sudhahar, C. G.; Gong, D. H.; Stahelin, R. V.; Best, M. D., Modular synthesis of biologically active phosphatidic acid probes using click chemistry. *Molecular Biosystems* **2009,** *5* (9), 962-972.
158. Zerkowski, J. A.; Nunez, A.; Strahan, G. D.; Solaiman, D. K. Y., Clickable Lipids: Azido and Alkynyl Fatty Acids and Triacylglycerols. *Journal of the American Oil Chemists Society* **2009,** *86* (11), 1115-1121.
159. Dauner, M.; Batroff, E.; Bachmann, V.; Hauck, C. R.; Wittmann, V., Synthetic Glycosphingolipids for Live-Cell Labeling. *Bioconjugate Chemistry* **2016,** *27* (7), 1624-1637.
160. Contal, E.; Klymchenko, A. S.; Mely, Y.; Meunier, S.; Wagner, A., Core functionalization of polydiacetylene micelles by a "click" reaction. *Soft Matter* **2011,** *7* (5), 1648-1650.
161. Sandbhor, M. S.; Key, J. A.; Strelkov, I. S.; Cairo, C. W., A Modular Synthesis of Alkynyl-Phosphocholine Headgroups for Labeling Sphingomyelin and Phosphatidylcholine. *Journal of Organic Chemistry* **2009,** *74* (22), 8669-8674.
162. Augustin, K. E.; Schafer, H. J., Alkynic fatty acids: omega-Arylation, methoxycarbonylation to alpha,beta-unsaturated esters, cyclotrimerization to pyridines and 2-pyridones. *European Journal of Lipid Science and Technology* **2011,** *113* (1), 72-82.
163. Gong, Y.; Ma, M.; Luo, Y.; Bong, D., Functional Determinants of a Synthetic Vesicle Fusion System. *JACS* **2008,** *130*, 6196-6205.
164. Ma, M., Paredes, A., & Bong, D., Intra- and Intermembrane Pairwise Molecular Recognition between Synthetic Hydrogen-Bonding Phospholipids. *J Am Chem Soc* **2008,** *130*, 14456-14458.
165. Ma, M., Gong, Y., & Bong, D., Lipid Membrane Adhesion and Fusion Driven by Designed, Minimally Multivalent Hydrogen-Bonding Lipids. *J Am Chem Soc* **2009,** *131*, 16919-16926.
166. Rani, R. S.; Rao, G. N., Influence of propylene glycol on chemical speciation of ternary complexes of bi- and tri-dentate ligands with some essential metal ions. *Journal of the Indian Chemical Society* **2014,** *91* (3), 455-463.
167. Wu, M. C.; Hu, T. C.; Lo, Y. C.; Lee, T. Y.; Lin, C. H.; Lu, W. Y.; Lin, C. C.; Datta, A.; Huang, J. H., New types of bi- and tri-dentate pyrrole-piperazine ligands and related zinc compounds: Synthesis, characterization, reaction study, and ring-opening polymerization of epsilon-caprolactone. *Journal of Organometallic Chemistry* **2015,** *791*, 141-147.
168. Hu, T. C.; Wu, M. C.; Wu, S. S.; Hu, C. H.; Lin, C. H.; Datta, A.; Lin, T. H.; Huang, J. H., Synthesis, characterization and reactivity study of aluminum compounds incorporating bi- and tri-dentate pyrrole-piperazine ligands. *Rsc Advances* **2016,** *6* (20), 16331-16339.

169. Chadwick, R. C.; Van Gyzen, S.; Liogier, S.; Adronov, A., Scalable Synthesis of Strained Cyclooctyne Derivatives. *Synthesis-Stuttgart* **2014,** *46* (5), 669-677.
170. Alam, S.; Alves, D. S.; Whitehead, S. A.; Bayer, A. M.; McNitt, C. D.; Popik, V. V.; Barrera, F. N.; Best, M. D., A clickable and photocleavable lipid analogue for cell membrane delivery and release. *Bioconjug Chem* **2015,** *26* (6), 1021-31.
171. Csiszar, A.; Hersch, N.; Dieluweit, S.; Biehl, R.; Merkel, R.; Hoffmann, B., Novel Fusogenic Liposomes for Fluorescent Cell Labeling and Membrane Modification. *Bioconjugate Chemistry* **2010,** *21* (3), 537-543.
172. Stengel, G.; Zahn, R.; Hook, F., DNA-Induced Programmable Fusion of Phospholipid Vesicles. *JACS* **2007,** *129*, 9584-9585.
173. Simonsson, L.; Jonsson, P.; Stengel, G.; Hook, F., Site-Specific DNA-Controlled Fusion of Single Lipid Vesicles to Supported Lipid Bilayers. *Chemphyschem* **2010,** *11* (5), 1011-1017.
174. Michanek, A.; Kristen, N.; Hook, F.; Nylander, T.; Sparr, E., RNA and DNA interactions with zwitterionic and charged lipid membranes - A DSC and QCM-D study. *Biochim. Biophys. Acta-Biomembr.* **2010,** *1798* (4), 829-838.
175. Ries, O.; Loffler, P. M. G.; Vogel, S., Convenient synthesis and application of versatile nucleic acid lipid membrane anchors in the assembly and fusion of liposomes. *Org. Biomol. Chem.* **2015,** *13* (37), 9673-9680.
176. Maru, N.; Shohda, K.-i.; Sugawara, T., Successive Fusion of Vesicles Aggregated by DNA Duplex Formation in the Presence of Triton X-100. *Chemistry Letters* **2008,** *37* (3), 340-341.
177. MarchiArtzner, V.; Jullien, L.; Belloni, L.; Raison, D.; Lacombe, L.; Lehn, J. M., Interaction, lipid exchange, and effect of vesicle size in systems of oppositely charged vesicles. *Journal of Physical Chemistry* **1996,** *100* (32), 13844-13856.
178. Pantazatos, D. P.; MacDonald, R. C., Directly observed membrane fusion between oppositely charged phospholipid bilayers. *Journal of Membrane Biology* **1999,** *170* (1), 27-38.
179. Pantazatos, D. P.; Pantazatos, S. P.; MacDonald, R. C., Bilayer mixing, fusion, and lysis following the interaction of populations of cationic and anionic phospholipid bilayer vesicles. *Journal of Membrane Biology* **2003,** *194* (2), 129-139.
180. Zhigaltsev, I. V.; Maurer, N.; Wong, K. F.; Cullis, P. R., Triggered release of doxorubicin following mixing of cationic and anionic liposomes. *Biochim. Biophys. Acta-Biomembr.* **2002,** *1565* (1), 129-135.
181. Biner, O.; Schick, T.; Muller, Y.; von Ballmoos, C., Delivery of membrane proteins into small and giant unilamellar vesicles by charge-mediated fusion. *Febs Letters* **2016,** *590* (14), 2051-2062.
182. Caschera, F.; Stano, P.; Luisi, P. L., Reactivity and fusion between cationic vesicles and fatty acid anionic vesicles. *Journal of Colloid and Interface Science* **2010,** *345* (2), 561-565.

183. Saeki, D.; Sugiura, S.; Baba, T.; Kanamori, T.; Sato, S.; Mukataka, S.; Chikawa, S., Dynamic interaction between oppositely charged vesicles: Aggregation, lipid mixing, and disaggregation. *Journal of Colloid and Interface Science* **2008,** *320* (2), 611-614.
184. Barber, J., Photosystem II: a multisubunit membrane protein that oxidises water. *Current Opinion in Structural Biology* **2002,** *12*, 523-530.
185. Croce, R.; van Amerongen, H., Light-harvesting and structural organization of Photosystem II: from individual complexes to thylakoid membrane. *J Photochem Photobiol B* **2011,** *104* (1-2), 142-53.
186. van Amerongen, H. C., R., Light harvesting in photosystem II. *Photosynth Res* **2013,** *116*, 251-263.
187. Cutulle, M. A.; Armel, G. R.; Brosnan, J. T.; Best, M. D.; Kopsell, D. A.; Bruce, B. D.; Bostic, H. E.; Layton, D. S., Synthesis and evaluation of heterocyclic analogues of bromoxynil. *J Agric Food Chem* **2014,** *62* (2), 329-36.
188. Jampilek, J.; Kralova, K.; Pesko, M.; Kos, J., Ring-substituted 8-hydroxyquinoline-2-carboxanilides as photosystem II inhibitors. *Bioorg Med Chem Lett* **2016,** *26* (16), 3862-5.
189. Liang, A.; Han, S.; Liu, Z.; Wang, L.; Li, J.; Zou, D.; Wu, Y.; Wu, Y., Regioselective Synthesis of N-Heteroaromatic Trifluoromethoxy Compounds by Direct O-CF3 Bond Formation. *Chemistry* **2016,** *22* (15), 5102-6.
190. Armel, G. R.; Rardon, P. L.; McComrick, M. C.; Ferry, N. M., Differential Response of Several Carotenoid Biosynthesis Inhibitors in Mixtures with Atrazine. *Weed Technology* **2007,** *21* (4), 947-953.
191. Lovyagina, E. R.; Semin, B. K., Mechanism of inhibition and decoupling of oxygen evolution from electron transfer in photosystem II by fluoride, ammonia and acetate. *J Photochem Photobiol B* **2016,** *158*, 145-53.
192. Ley, S. V.; Thomas, A. W., Modern synthetic methods for copper-mediated C(aryl)-O, C(aryl)-N, and C(aryl)-S bond formation. *Angewandte Chemie-International Edition* **2003,** *42* (44), 5400-5449.
193. Theil, F., Synthesis of diaryl ethers: A long-standing problem has been solved. *Angewandte Chemie-International Edition* **1999,** *38* (16), 2345-2347.
194. Maiti, D.; Buchwald, S. L., Cu-Catalyzed Arylation of Phenols: Synthesis of Sterically Hindered and Heteroaryl Diaryl Ethers. *Journal of Organic Chemistry* **2010,** *75* (5), 1791-1794.
195. Bharathi, M. V.; Chhabra, M.; Paira, P., Development of surface immobilized 3-azidocoumarin-based fluorogenic probe via strain promoted click chemistry. *Bioorg Med Chem Lett* **2015,** *25* (24), 5737-42.
196. Cusido, J.; Ragab, S. S.; Thapaliya, E. R.; Swaminathan, S.; Garcia-Amorós, J.; Roberti, M. J.; Araoz, B.; Mazza, M. M. A.; Yamazaki, S.; Scott, A. M.; Raymo, F. M.; Bossi, M. L., A Photochromic Bioconjugate with Photoactivatable Fluorescence for Superresolution Imaging. *The Journal of Physical Chemistry C* **2016,** *120* (23), 12860-12870.

197. Dandriyal, J.; Singla, R.; Kumar, M.; Jaitak, V., Recent developments of C-4 substituted coumarin derivatives as anticancer agents. *Eur J Med Chem* **2016,** *119*, 141-68.
198. Emami, S.; Dadashpour, S., Current developments of coumarin-based anti-cancer agents in medicinal chemistry. *Eur J Med Chem* **2015,** *102*, 611-30.
199. Lakshmi Ranganatha, V.; Zameer, F.; Meghashri, S.; Rekha, N. D.; Girish, V.; Gurupadaswamy, H. D.; Khanum, S. A., Design, synthesis, and anticancer properties of novel benzophenone-conjugated coumarin analogs. *Arch Pharm (Weinheim)* **2013,** *346* (12), 901-11.
200. Soh, N., Makihara, K., et. al., Phospholipid-linked Coumarin: A Fluorescent Probe for Sensing Hydroxyl Radicals in Lipid Membranes. *Analytical Sciences* **2008,** *24*, 293-296.
201. Liu, M.; Jiang, Q.; Lu, Z.; Huang, Y.; Tan, Y.; Jiang, Q., A coumarin-based fluorescent turn-on probe for detection of biothiols in vitro. *Luminescence* **2015,** *30* (8), 1395-402.
202. Sun, Q.; Sun, D.; Song, L.; Chen, Z.; Chen, Z.; Zhang, W.; Qian, J., Highly Selective Fluorescent Turn-On Probe for Protein Thiols in Biotin Receptor-Positive Cancer Cells. *Anal Chem* **2016,** *88* (6), 3400-5.
203. Sivakumar, K.; Xie, F.; Cash, B. M.; Long, S.; Barnhill, H. N.; Wang, Q., A fluorogenic 1,3-dipolar cycloaddition reaction of 3-azidocoumarins and acetylenes. *Organic Letters* **2004,** *6* (24), 4603-4606.
204. Berg, K., Selbo, P.K., et. al., Porphyrin-related photosensitizers for cancer imaging and therapeutic applications. *Journal of Microscopy* **2005,** *218*, 133-147.
205. Huang, X., Zhu, C., et. al., Porphyrin-Dithienothiophene π-Conjugated Copolymers: Synthesis and Their Applications in Field-Effect Transistors and Solar Cells. *Macromolecules* **2008,** *41*, 6895-6902.
206. Xing, C., Xu, Q., et. al., Conjugated Polymer/Porphyrin Complexes for Efficient Energy Transfer and Improving Light-Activated Antibacterial Activity. *Journal of American Chemical Society* **2009,** *131*, 13117-13124.
207. Anderson, H. L., Martin, S. J., & Bradley, D. D. C., Synthesis and Third-Order Nonlinear Optical Properties of a Conjugated Porphyrin Polymer. *Angew Chem Int Ed* **1994,** *33*, 655-657.
208. Taylor, P. N. A., H. L., Cooperative self-assembly of double-strand conjugated porphyrin ladders. *Journal of American Chemical Society* **1999,** *121*, 11538-11545.
209. Burrell, A. K., Officer, D. L., Plieger, P. G., & Reid, D. C. W., Synthetic routes to multiporphyrin arrays. *Chemical Reviews* **2001,** *101*, 2751-2796.
210. Lash, T., Porphyrin Synthesis by the “3 + 1” Approach: New Applications for an Old Methodology. *Chem Euro J* **1996,** *2*, 1197-1200.
211. Imahori, H., Giant Multiporphyrin Arrays as Artificial Light-Harvesting Antennas. *J. Phys. Chem. B.* **2004,** *108*, 6130-6143.

212. Balaban, T. S., Tailoring Porphyrins and Chlorins for Self-Assembly in Biomimetic Artificial Antenna Systems. *Accounts of Chemical Research* **2005,** *38*, 612-623.
213. Feese, E., Sadeghifar, H., Gracz, H.S., Argyropoulos, D.S., and Ghiladi, R.A., *Biomacromolecules* **2011,** *12*, 3528-3539.

Appendix

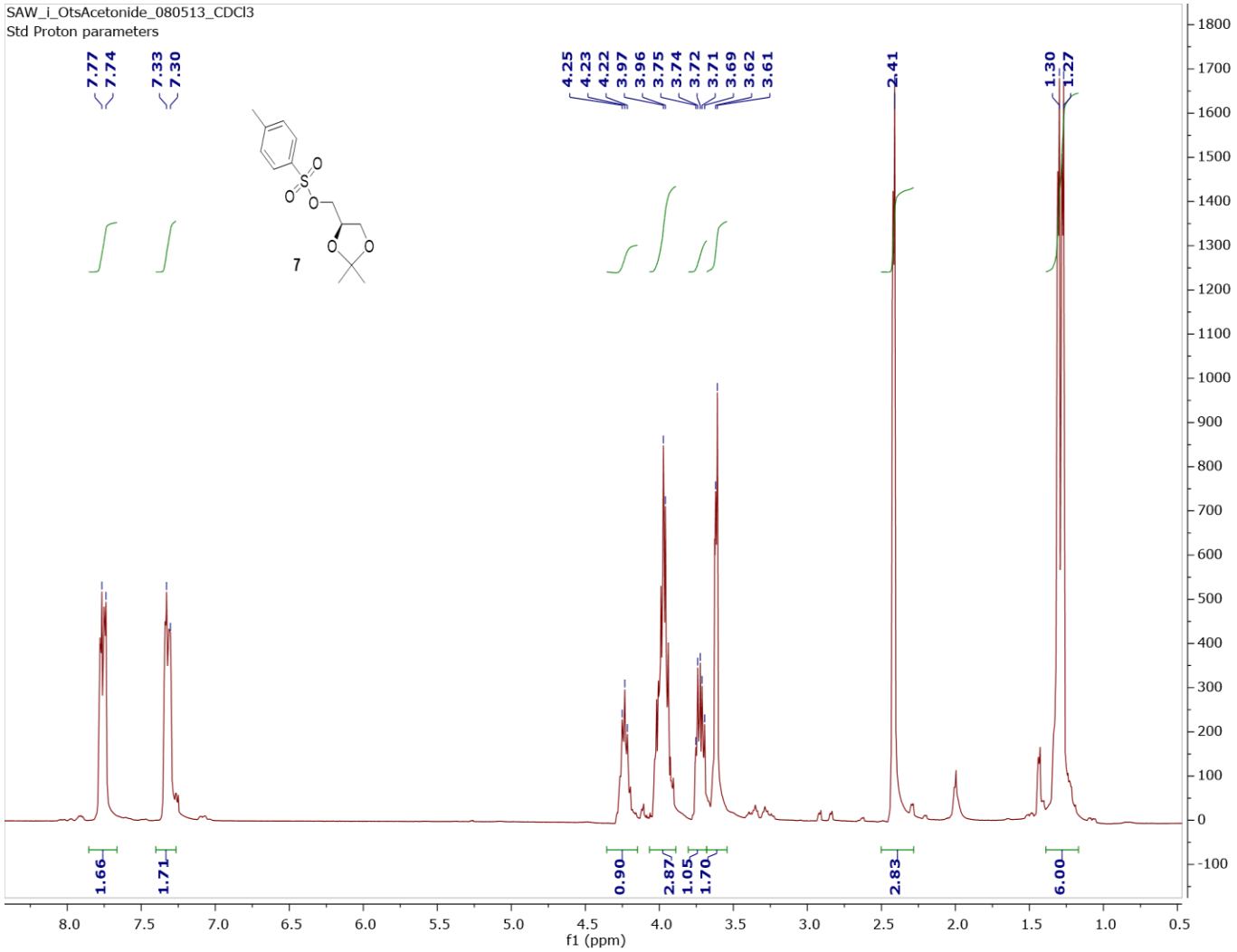
SAW_i_OtsAcetonide_080513_CDCl3
Std Proton parameters
7.77
7.74
7.33
7.30
4.25
4.23
4.22
3.97
3.96
3.75
3.74
3.72
3.71
3.69
3.62
3.61
2.41
1.30
1.27
7
1.66
1.71
0.90
2.87
1.05
1.70
2.83
6.00
f1 (ppm)

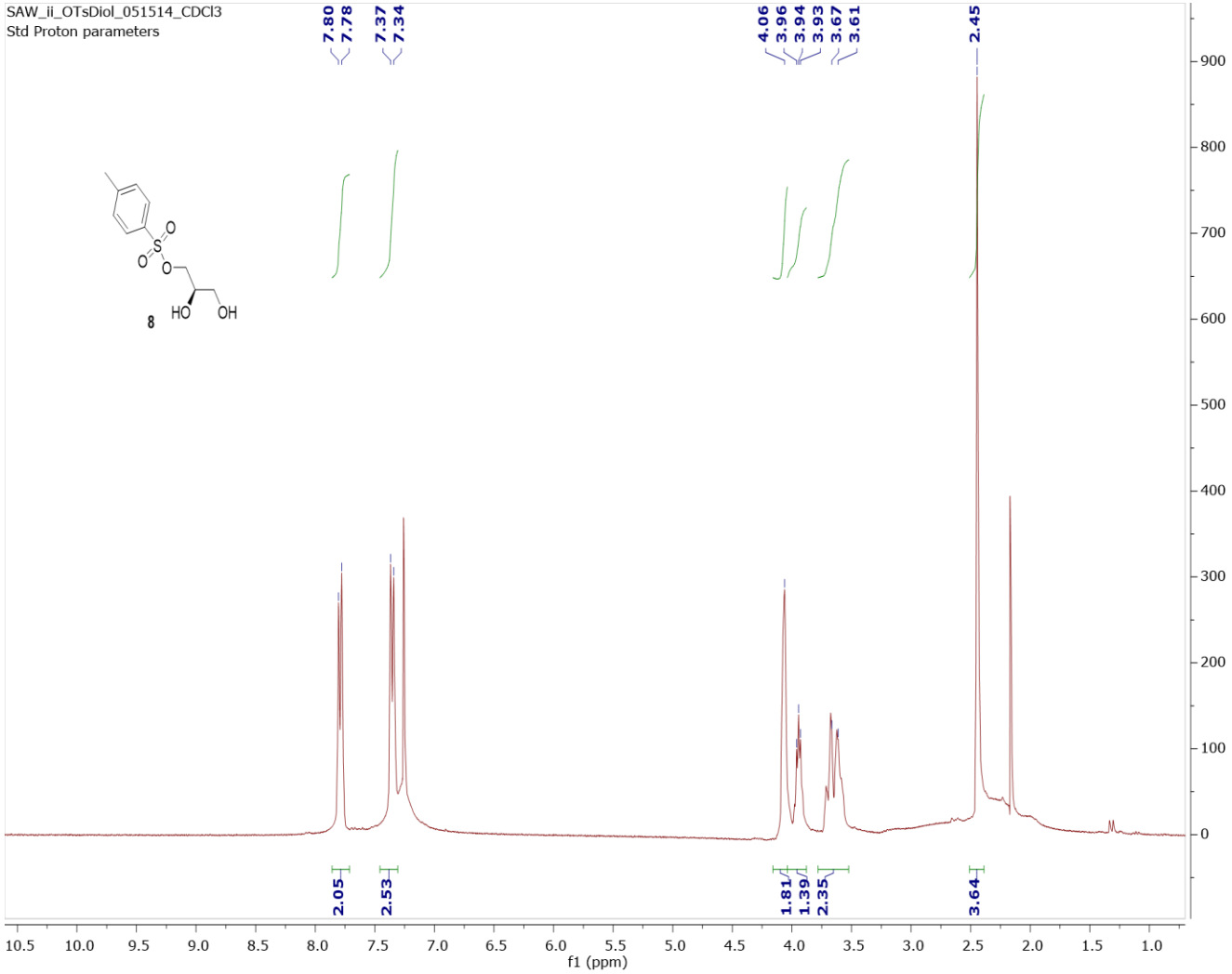
SAW_ii_OTsDiol_051514_CDCl3
Std Proton parameters
7.80
7.78
7.37
7.34
4.06
3.96
3.94
3.93
3.67
3.61
2.45
HO
OH
8
2.05
2.53
1.81
1.39
2.35
3.64
f1 (ppm)

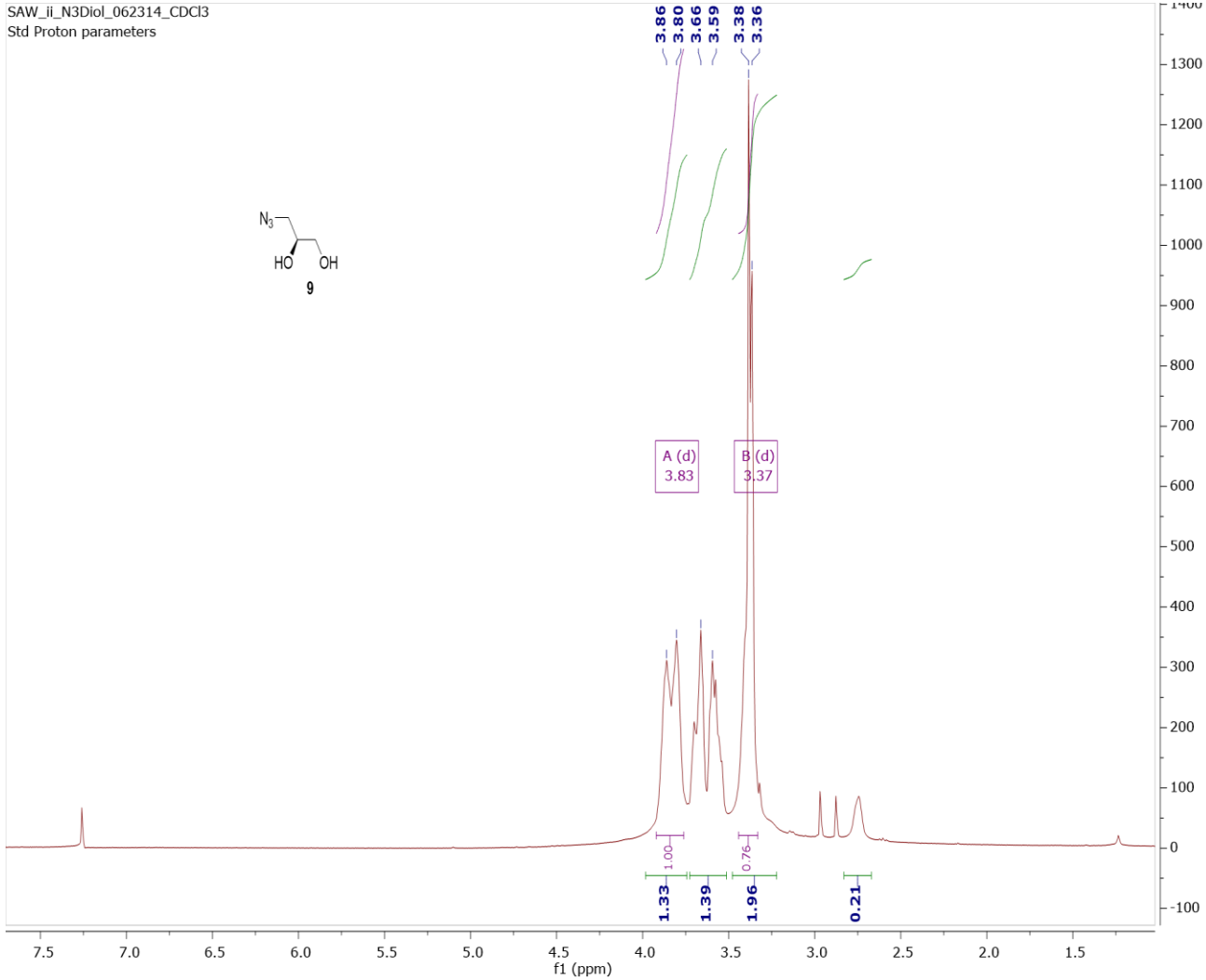
SAW_ii_N3Diol_062314_CDCl3
Std Proton parameters
3.86
3.80
3.66
3.59
3.38
3.36
N3
HO
OH
9
A (d)
3.83
B (d)
3.37
1.00
0.76
1.33
1.39
1.96
0.21
f1 (ppm)

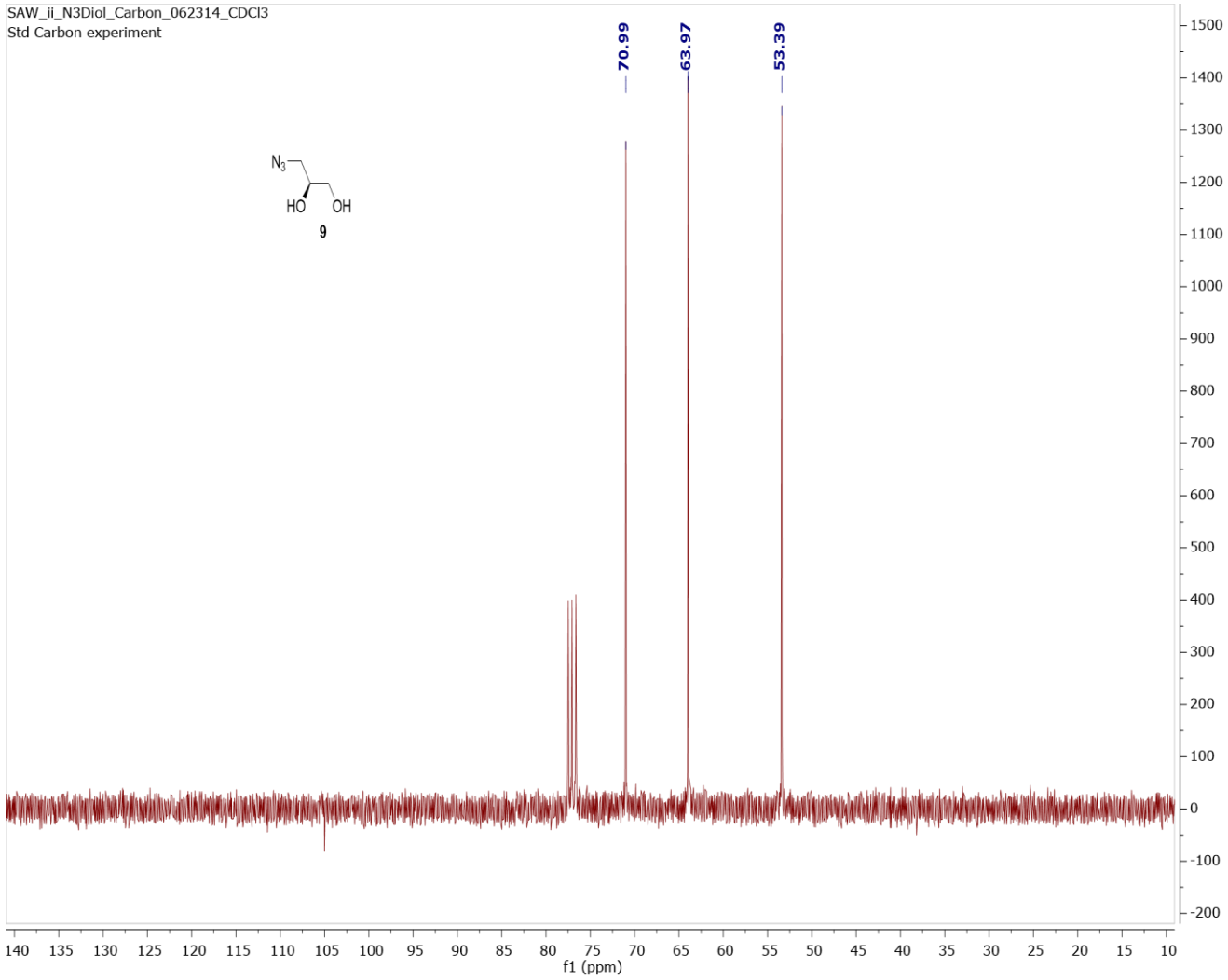
SAW_ii_N3Diol_Carbon_062314_CDCl3
Std Carbon experiment
70.99
63.97
53.39
N3
HO
OH
9
f1 (ppm)

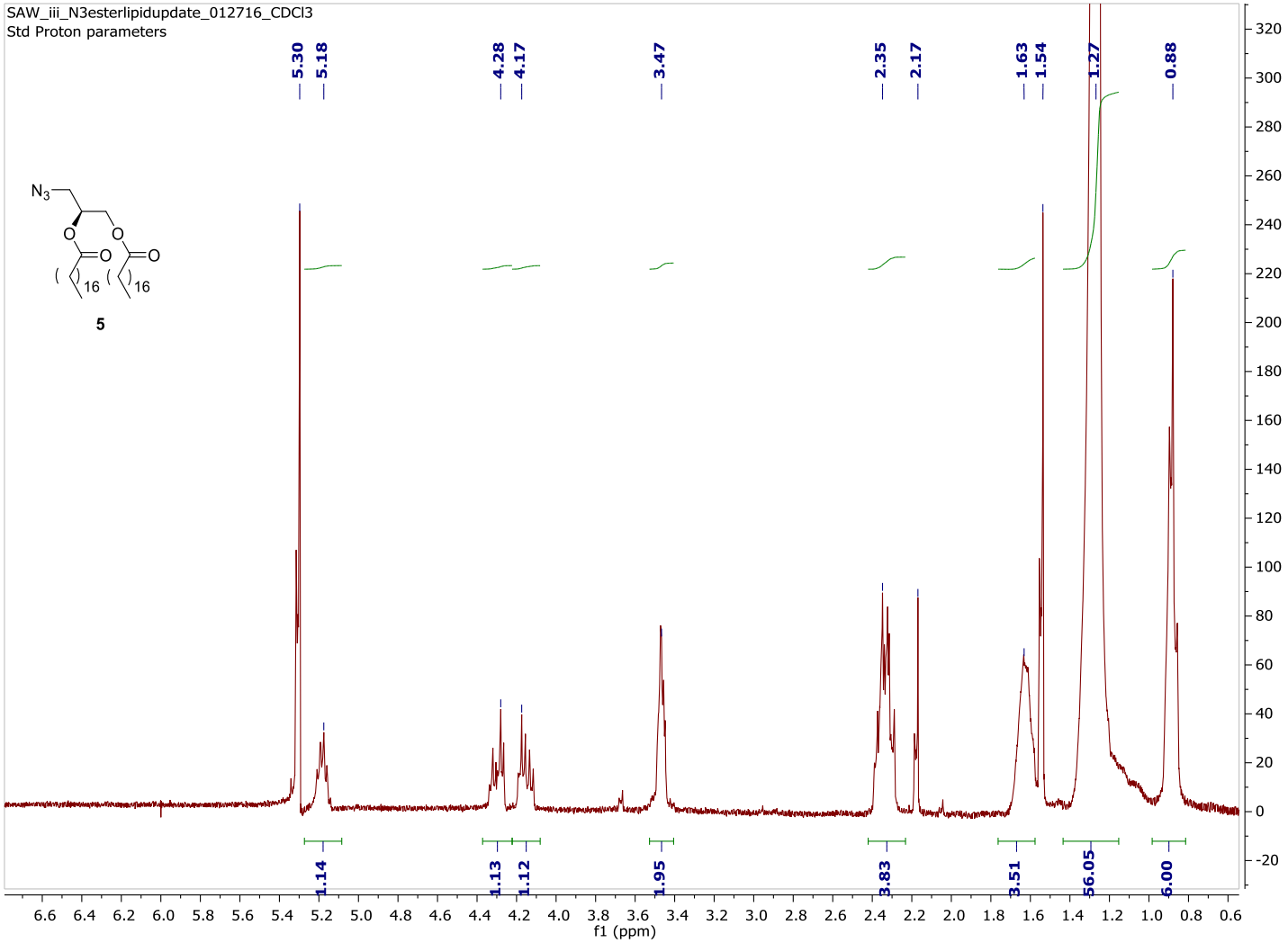
SAW_iii_N3esterlipidupdate_012716_CDCl3
Std Proton parameters
5.30
5.18
4.28
4.17
3.47
2.35
2.17
1.63
1.54
1.27
0.88
N3
O
O
O
O
16
16
5
1.14
1.13
1.12
1.95
3.83
3.51
56.05
6.00
f1 (ppm)

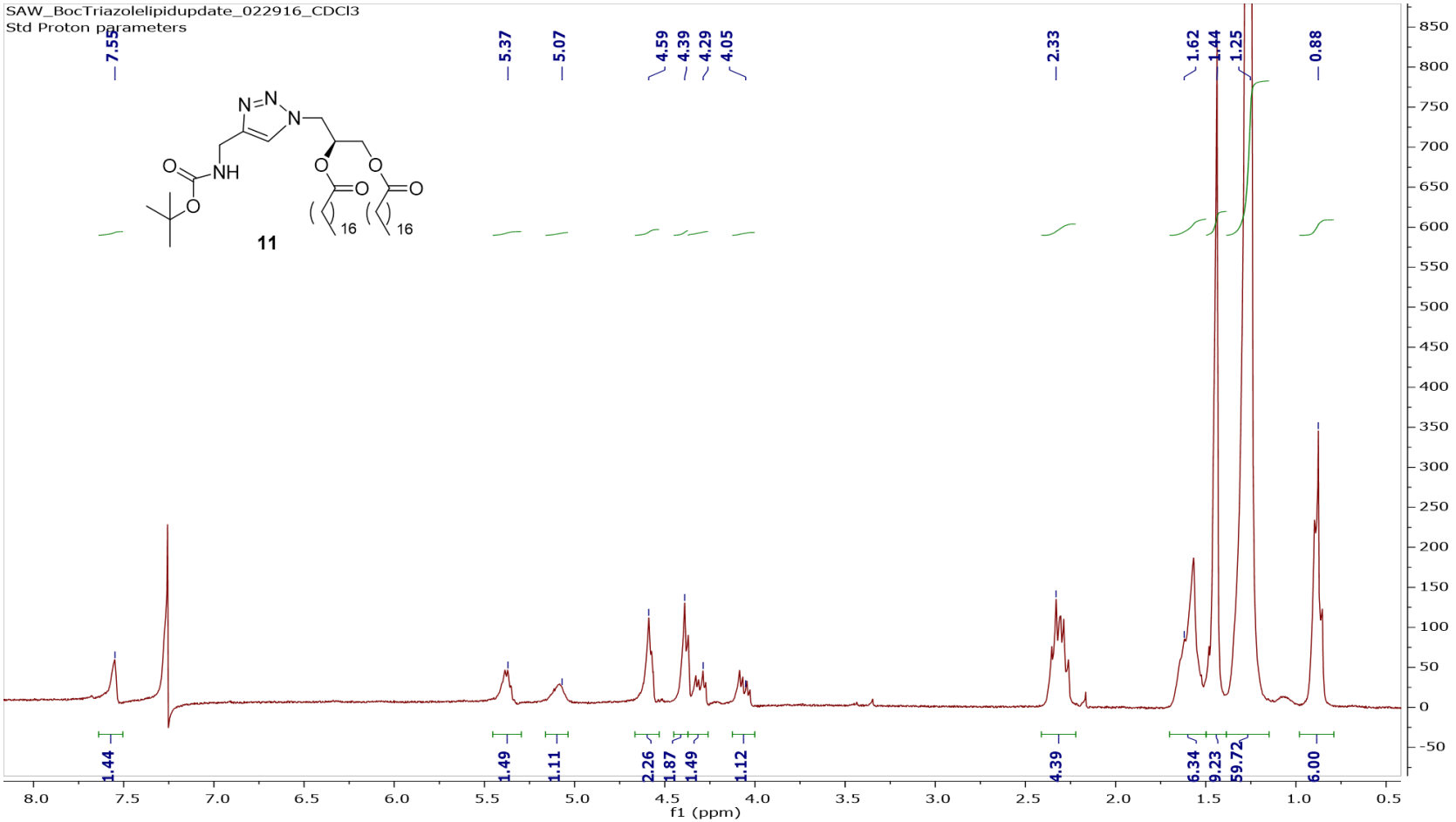
SAW_BocTriazolelipidupdate_022916_CDCl3
Std Proton parameters
7.55
5.37
5.07
4.59
4.39
4.29
4.05
2.33
1.62
1.44
1.25
0.88
11
16
16
1.44
1.49
1.11
2.26
1.87
1.49
1.12
4.39
6.34
9.23
59.72
6.00
f1 (ppm)

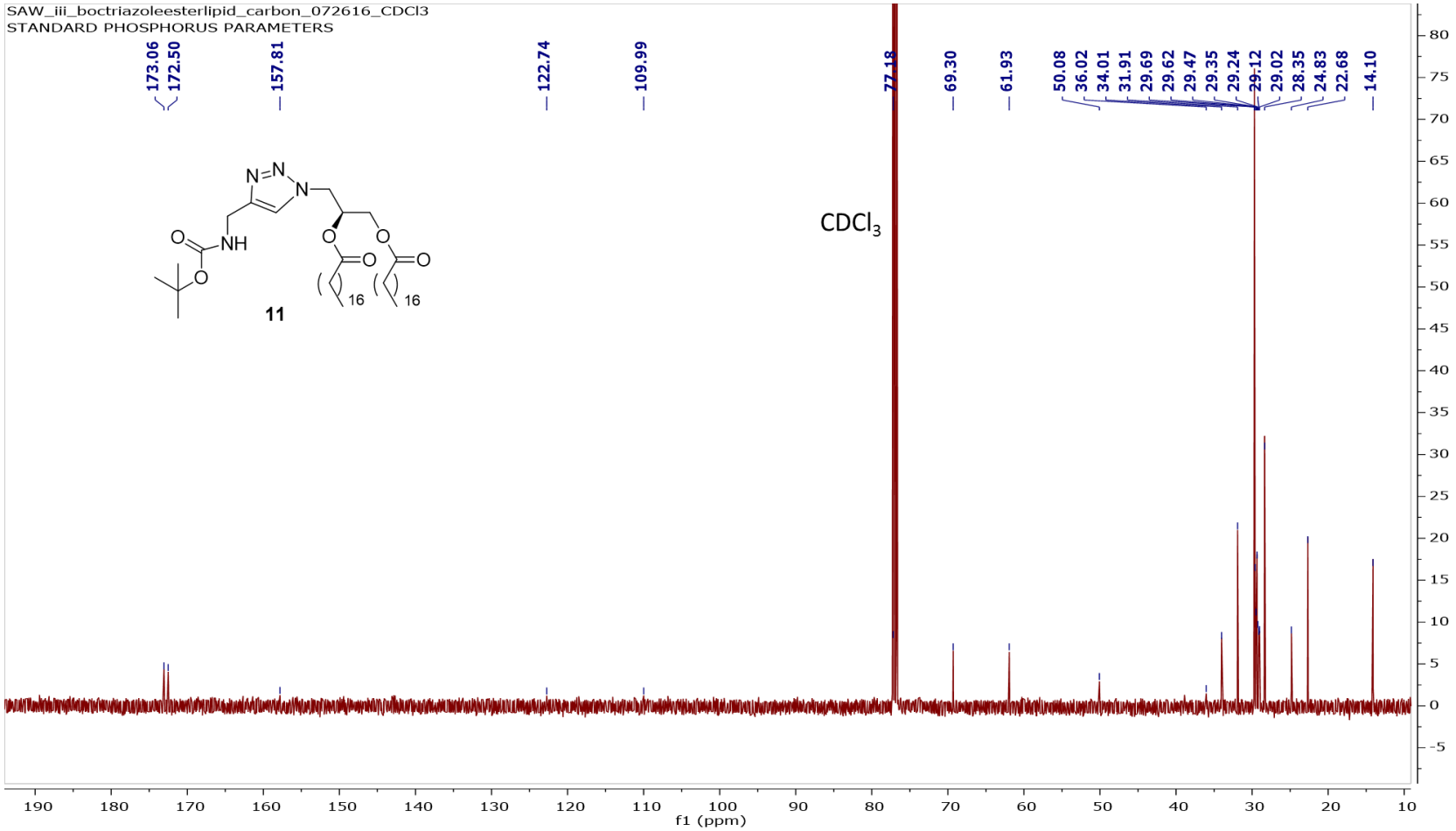
SAW_iii_boctriazoleesterlipid_carbon_072616_CDCl3
STANDARD PHOSPHORUS PARAMETERS
173.06
172.50
157.81
122.74
109.99
77.18
69.30
61.93
50.08
36.02
34.01
31.91
29.69
29.62
29.47
29.35
29.24
29.12
29.02
28.35
24.83
22.68
14.10
CDCl3
11
f1 (ppm)

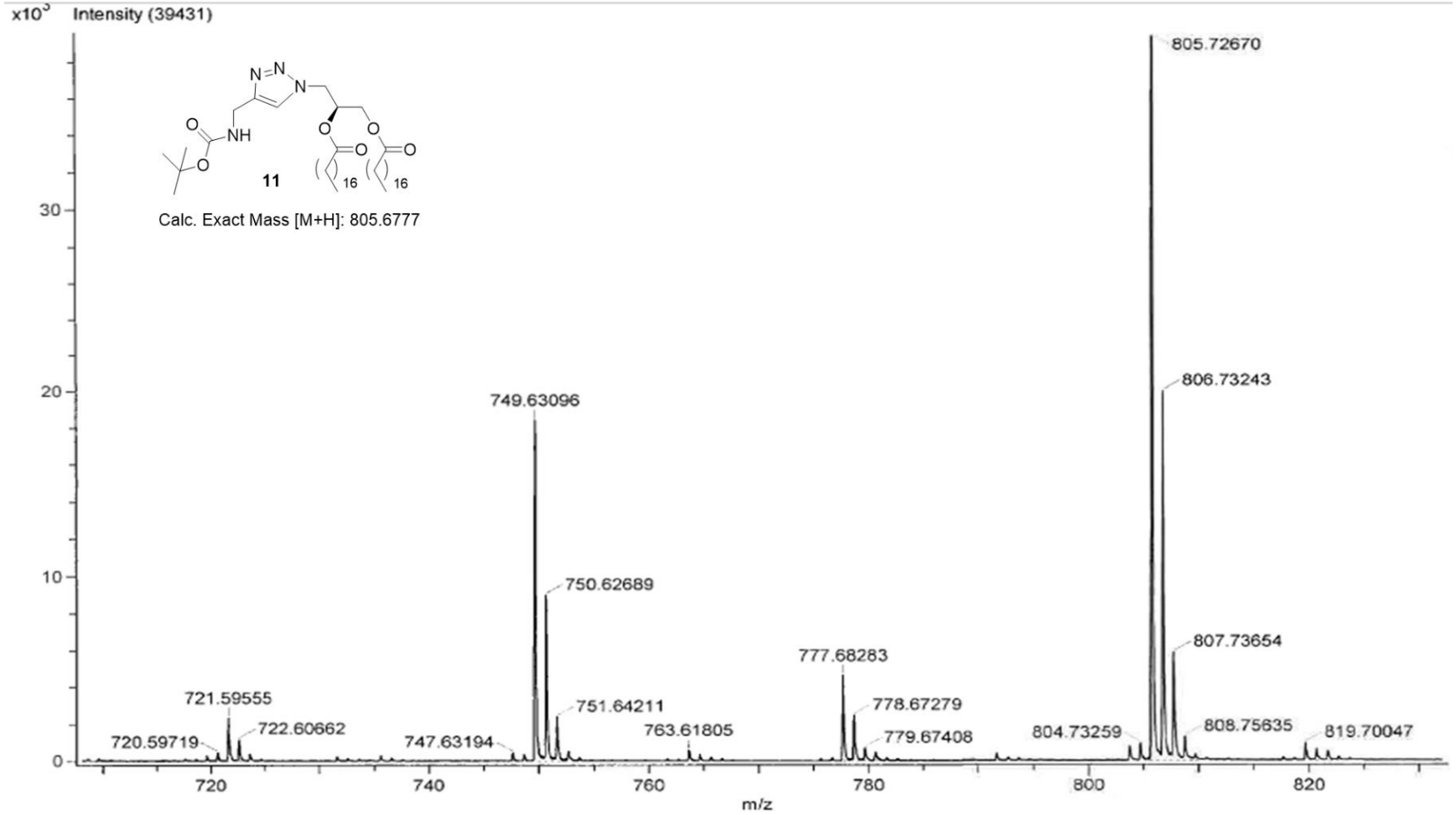
x10^5 Intensity (39431)
11
Calc. Exact Mass [M+H]: 805.6777
805.72670
806.73243
749.63096
750.62689
807.73654
777.68283
721.59555
778.67279
751.64211
722.60662
763.61805
808.75635
819.70047
720.59719
747.63194
779.67408
804.73259
30
20
10
0
720
740
760
780
800
820
m/z

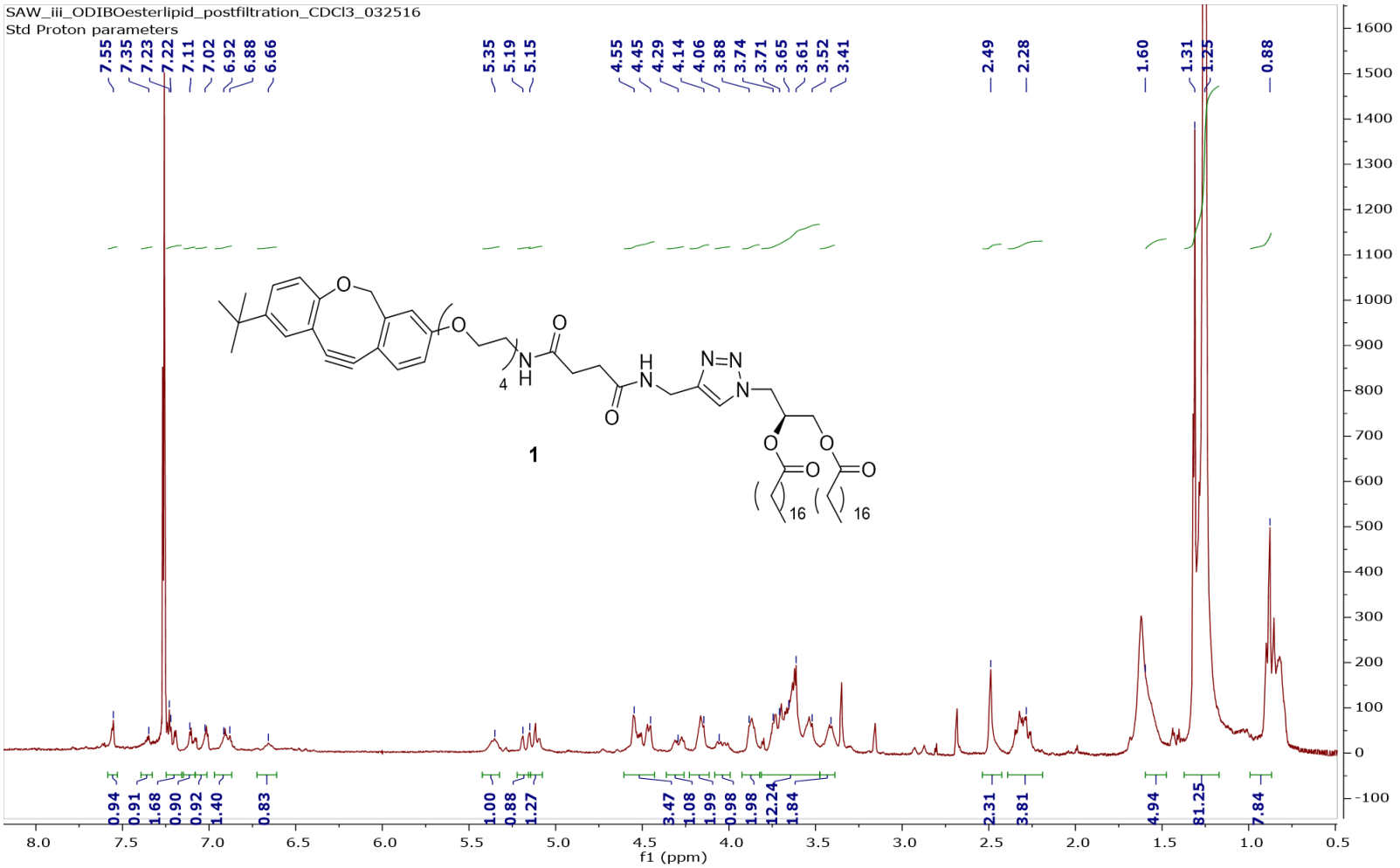
SAW_iii_ODIBOesterlipid_postfiltration_CDCl3_032516
Std Proton parameters
7.55 7.35 7.23 7.22 7.11 7.02 6.92 6.88 6.66
5.35 5.19 5.15
4.55 4.45 4.29 4.14 4.06 3.88 3.74 3.71 3.65 3.61 3.52 3.41
2.49 2.28
1.60 1.31 1.25
0.88
1
16
16
0.94 0.91 1.68 0.90 0.92 1.40 0.83
1.00 0.88 1.27
3.47 1.08 1.99 0.98 1.98 12.24 1.84
2.31 3.81
4.94 31.25
7.84
f1 (ppm)

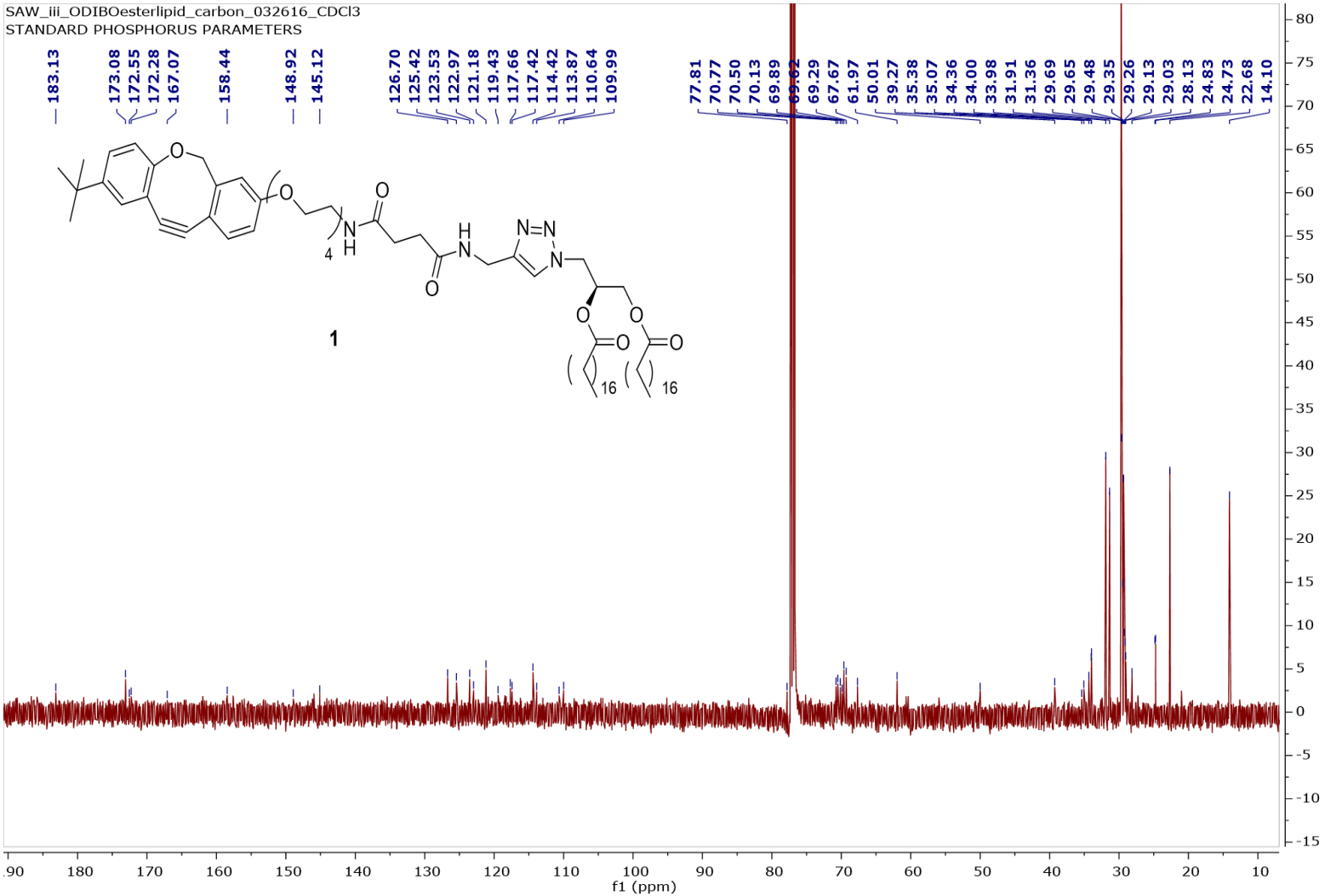
SAW_iii_ODIBOesterlipid_carbon_032616_CDCl3
STANDARD PHOSPHORUS PARAMETERS
183.13
173.08
172.55
172.28
167.07
158.44
148.92
145.12
126.70
125.42
123.53
122.97
121.18
119.43
117.66
117.42
114.42
113.87
110.64
109.99
77.81
70.77
70.50
70.13
69.89
69.62
69.29
67.67
61.97
50.01
39.27
35.38
35.07
34.36
34.00
33.98
31.91
31.36
29.69
29.65
29.48
29.35
29.26
29.13
29.03
28.13
24.83
24.73
22.68
14.10
1
f1 (ppm)

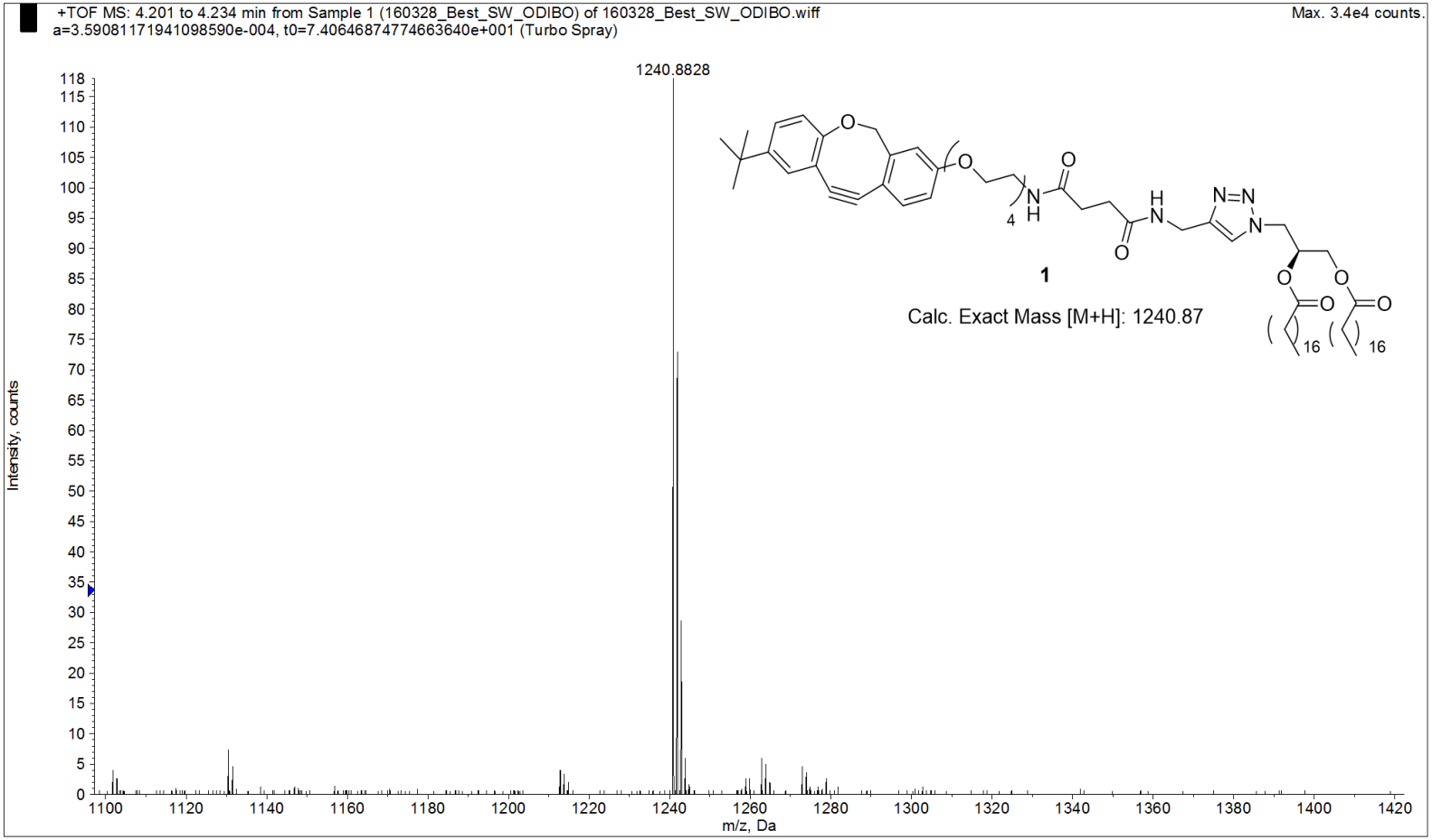
+TOF MS: 4.201 to 4.234 min from Sample 1 (160328_Best_SW_ODIBO) of 160328_Best_SW_ODIBO.wiff
a=3.59081171941098590e-004, t0=7.40646874774663640e+001 (Turbo Spray)
Max. 3.4e4 counts.
1240.8828
Intensity, counts
m/z, Da
1
Calc. Exact Mass [M+H]: 1240.87

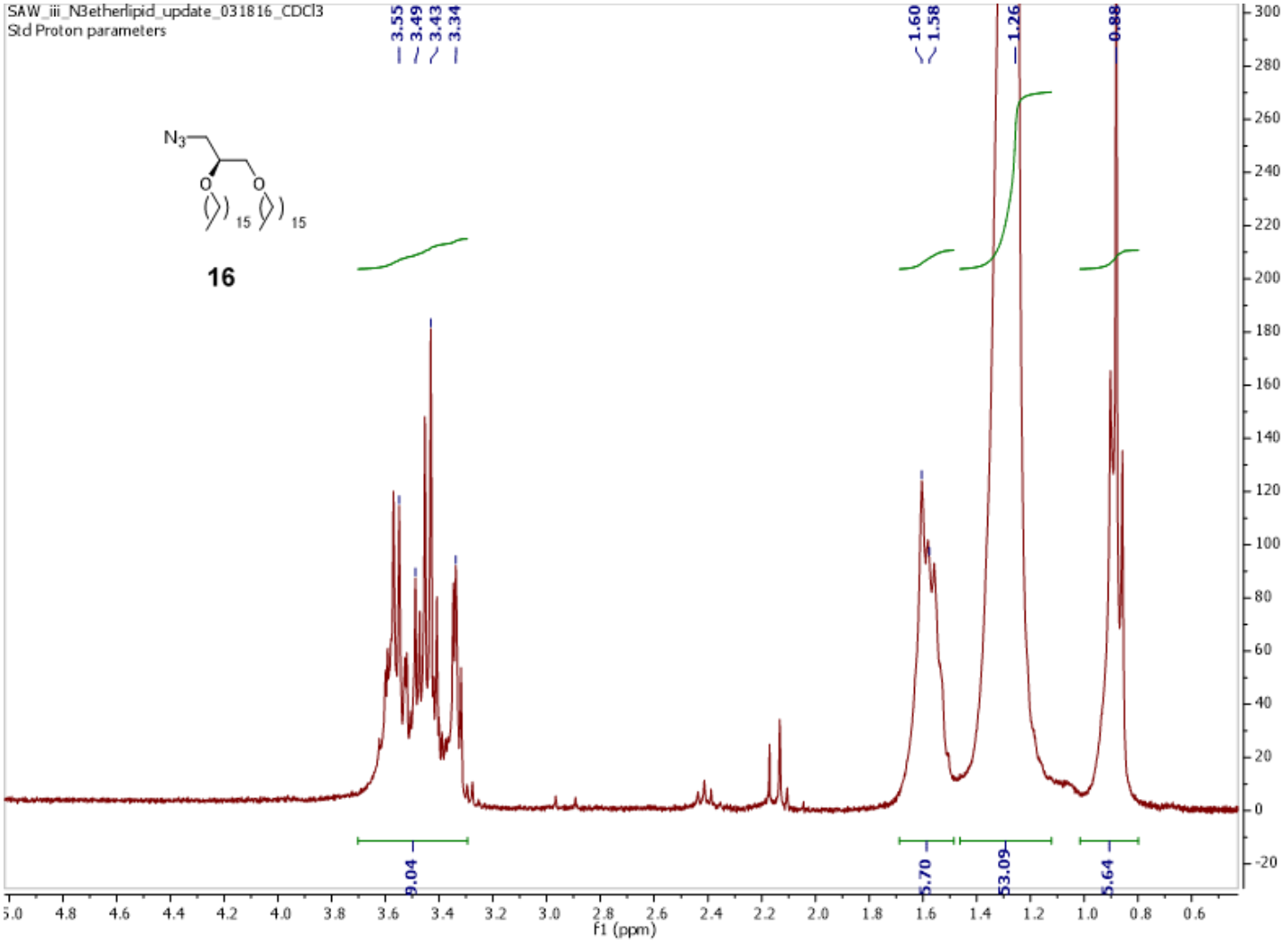
SAW_iii_N3etherlipid_update_031816_CDCl3
Std Proton parameters
3.55
3.49
3.43
3.34
1.60
1.58
1.26
0.88
16
9.04
5.70
53.09
5.64
F1 (ppm)

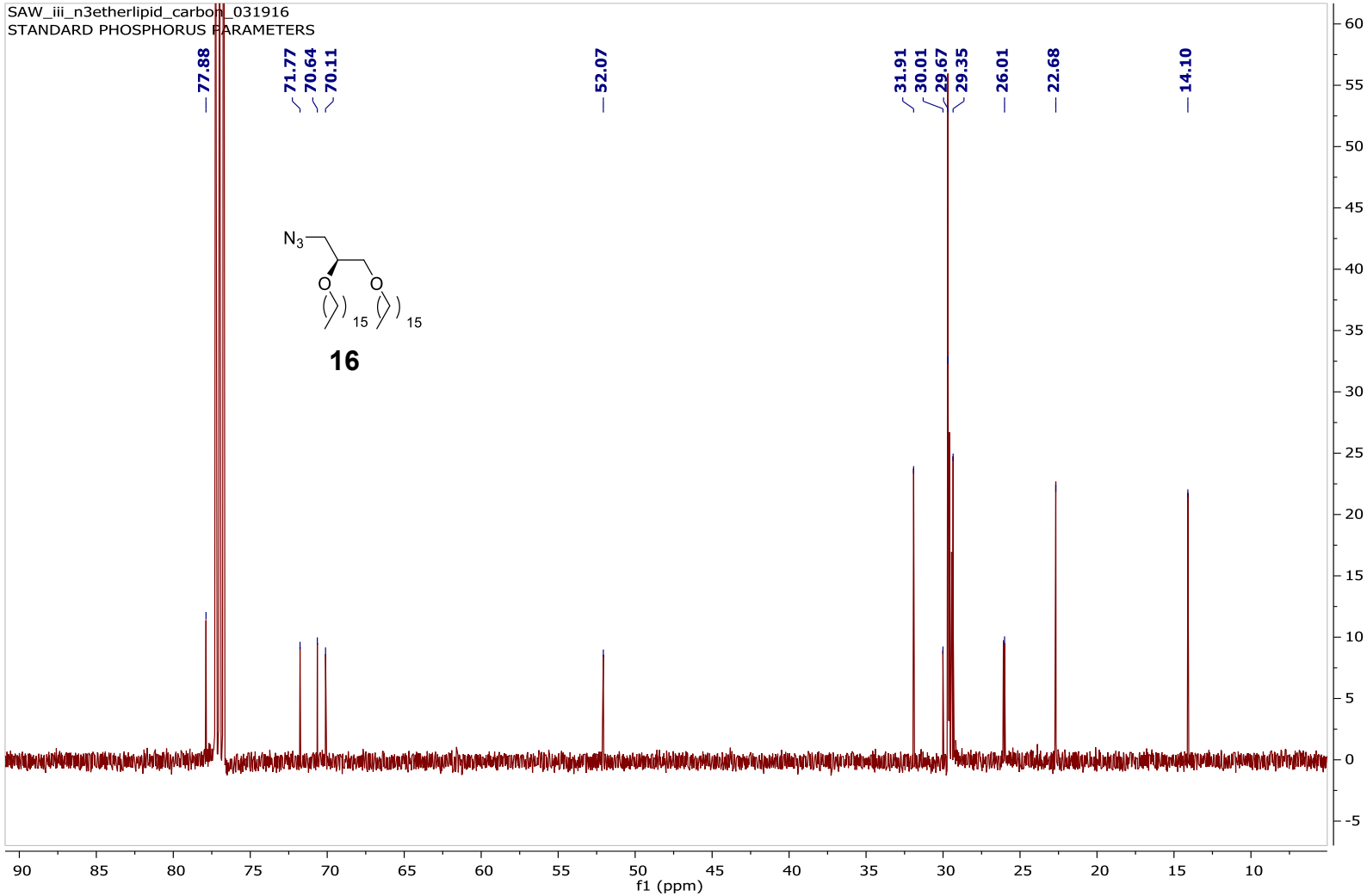
SAW_iii_n3etherlipid_carbon_031916
STANDARD PHOSPHORUS PARAMETERS
77.88
71.77
70.64
70.11
52.07
31.91
30.01
29.67
29.35
26.01
22.68
14.10
N3
O
O
15
15
16
f1 (ppm)

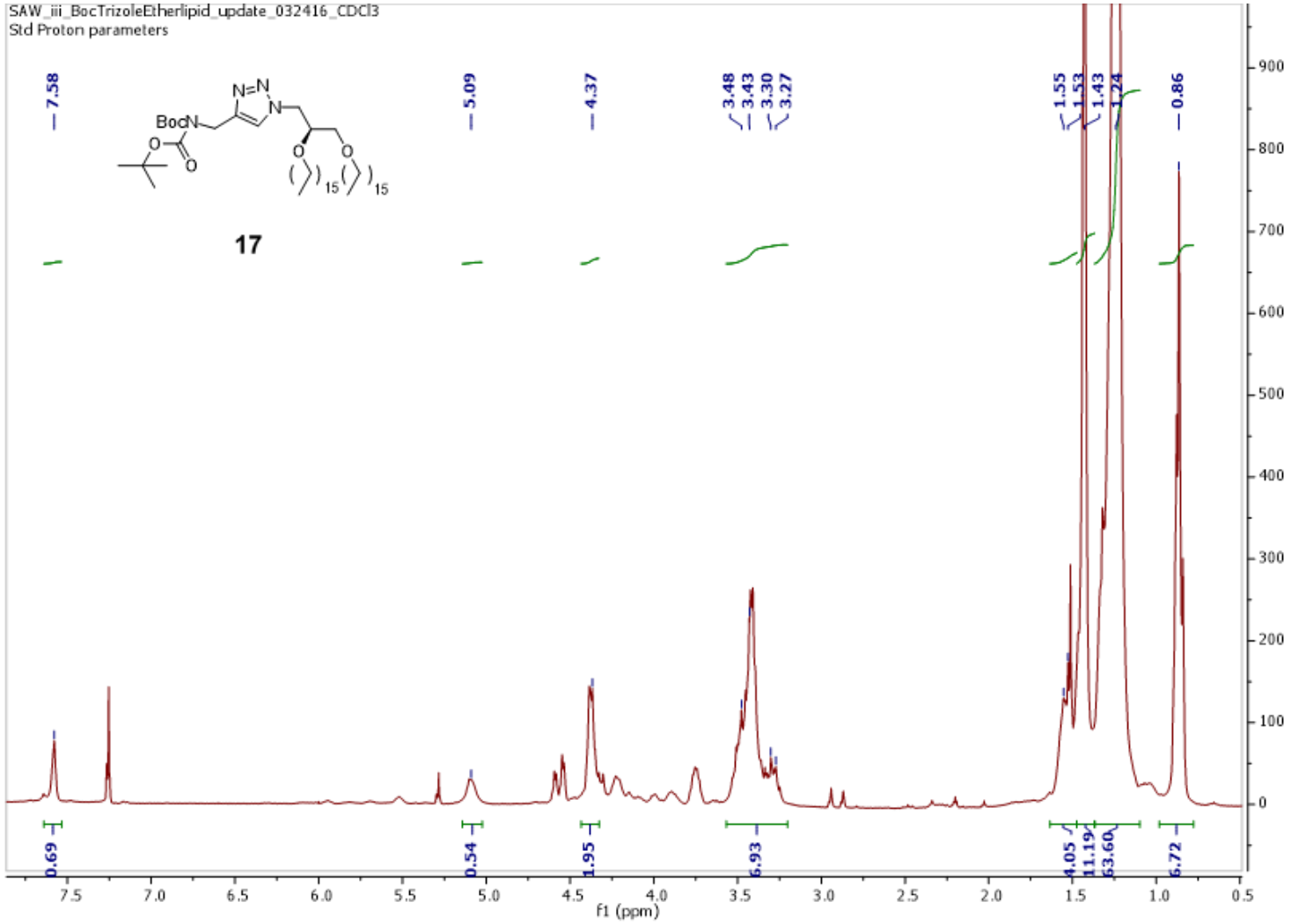
SAW_iii_BocTrizoleEtherlipid_update_032416_CDCl3
Std Proton parameters
7.58
5.09
4.37
3.48
3.43
3.30
3.27
1.55
1.53
1.43
1.24
0.86
BocN
17
0.69
0.54
1.95
6.93
4.05
11.19
3.60
6.72
f1 (ppm)

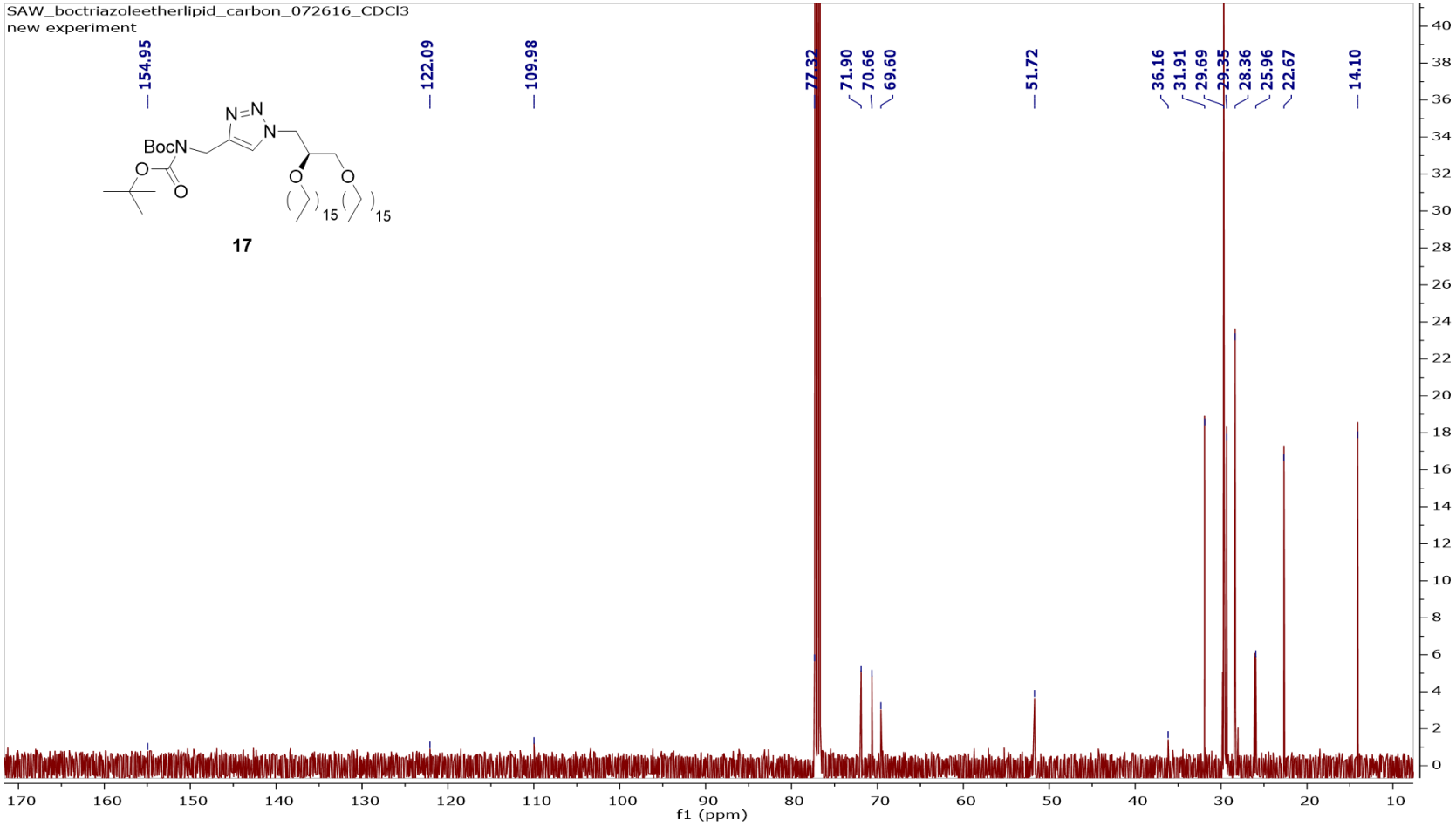
SAW_boctriazoleetherlipid_carbon_072616_CDCl3
new experiment
154.95
122.09
109.98
77.32
71.90
70.66
69.60
51.72
36.16
31.91
29.69
29.35
28.36
25.96
22.67
14.10
BocN
O
O
N=N
N
O
O
15
15
17
f1 (ppm)

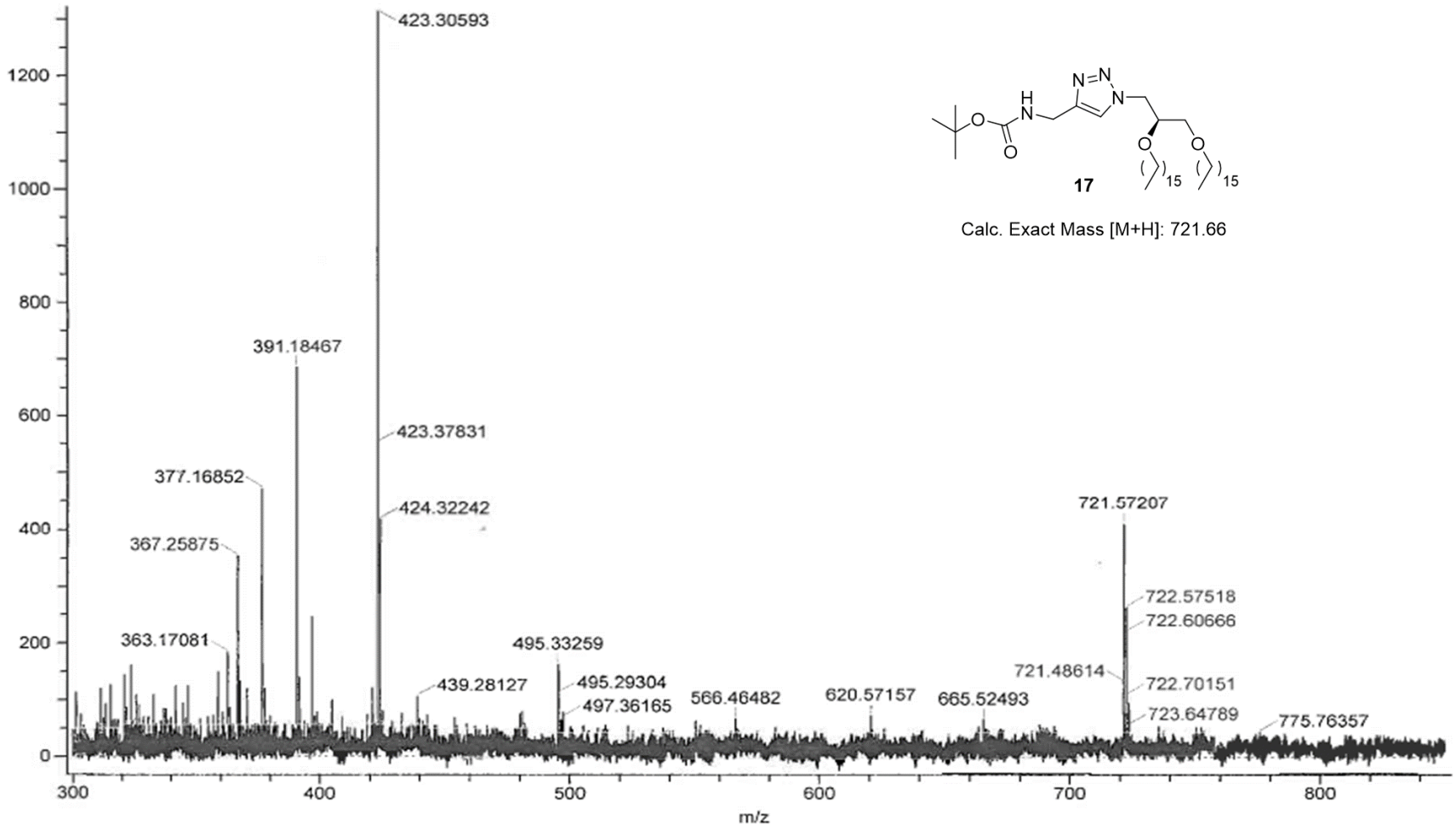

17

Calc. Exact Mass [M+H]: 721.66

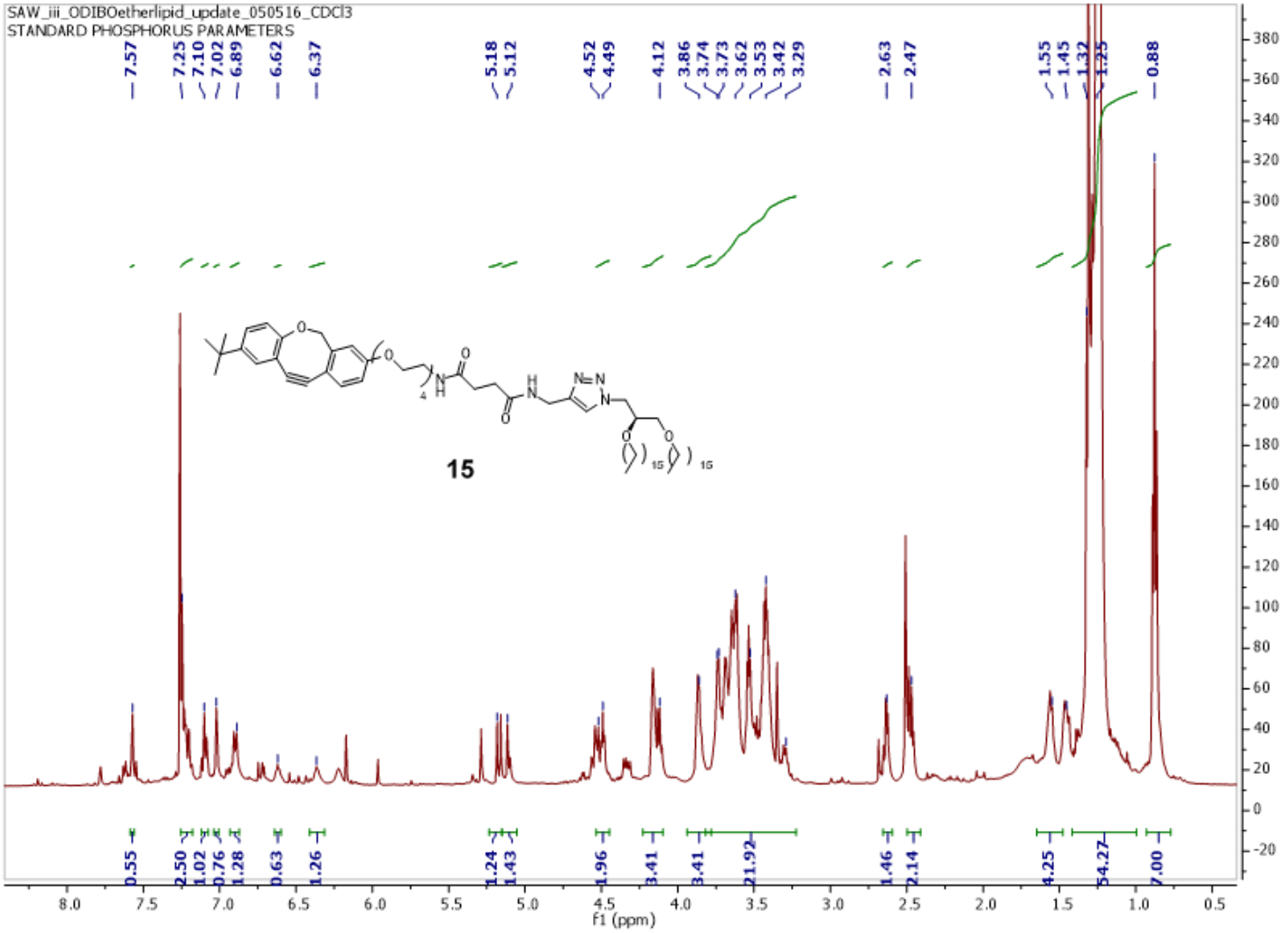
SAW_iii_ODIBOetherlipid_update_050516_CDCl3
STANDARD PHOSPHORUS PARAMETERS
7.57
7.25
7.10
7.02
6.89
6.62
6.37
5.18
5.12
4.52
4.49
4.12
3.86
3.74
3.73
3.62
3.53
3.42
3.29
2.63
2.47
1.55
1.45
1.32
1.25
0.88
15
0.55
2.50
1.02
0.76
1.28
0.63
1.26
1.24
1.43
1.96
3.41
3.41
21.92
1.46
2.14
4.25
54.27
7.00
F1 (ppm)

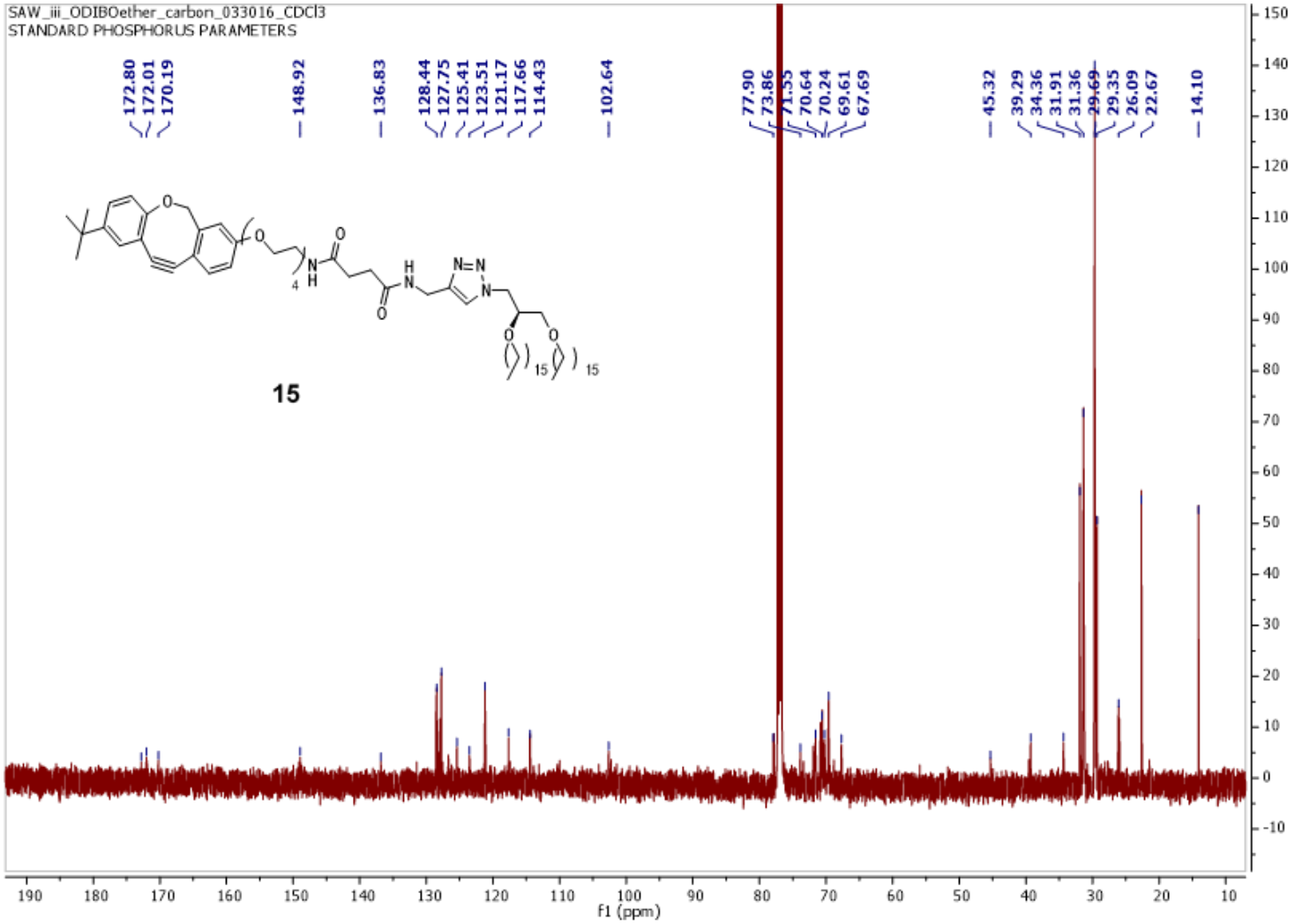
SAW_iii_ODIBOether_carbon_033016_CDCl3
STANDARD PHOSPHORUS PARAMETERS
172.80
172.01
170.19
148.92
136.83
128.44
127.75
125.41
123.51
121.17
117.66
114.43
102.64
77.90
73.86
71.55
70.64
70.24
69.61
67.69
45.32
39.29
34.36
31.91
31.36
29.69
29.35
26.09
22.67
14.10
15
f1 (ppm)

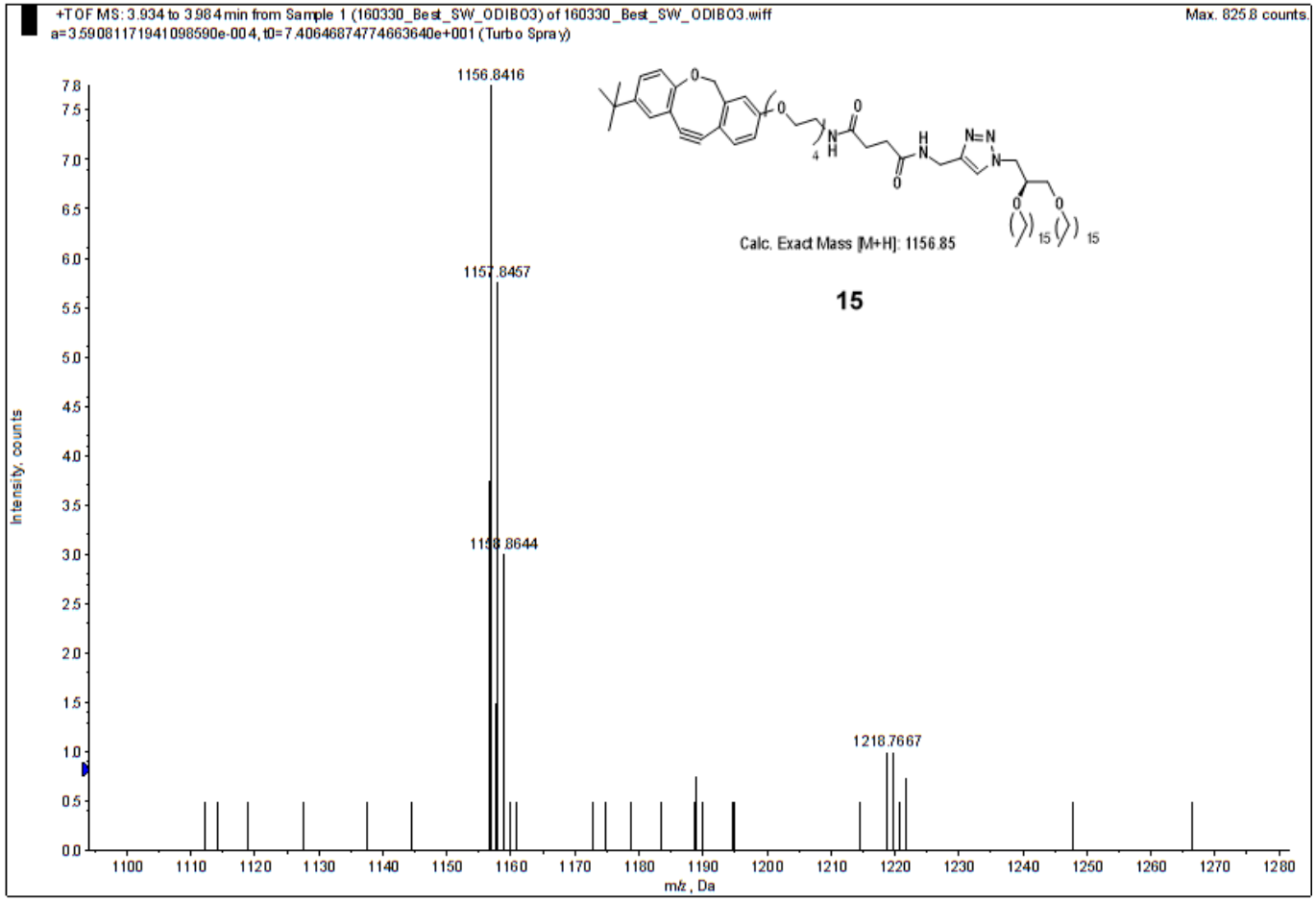
+TOF MS: 3.934 to 3.984 min from Sample 1 (160330_Best_SW_ODIBO3) of 160330_Best_SW_ODIBO3.wiff
a=3.590811719410985 90e-004, t0=7.406468747746636 40e+001 (Turbo Spray)
Max. 825.8 counts.
1156.8416
1157.8457
1158.8644
1218.7667
Calc. Exact Mass [M+H]: 1156.85
15
Intensity, counts
m/z, Da

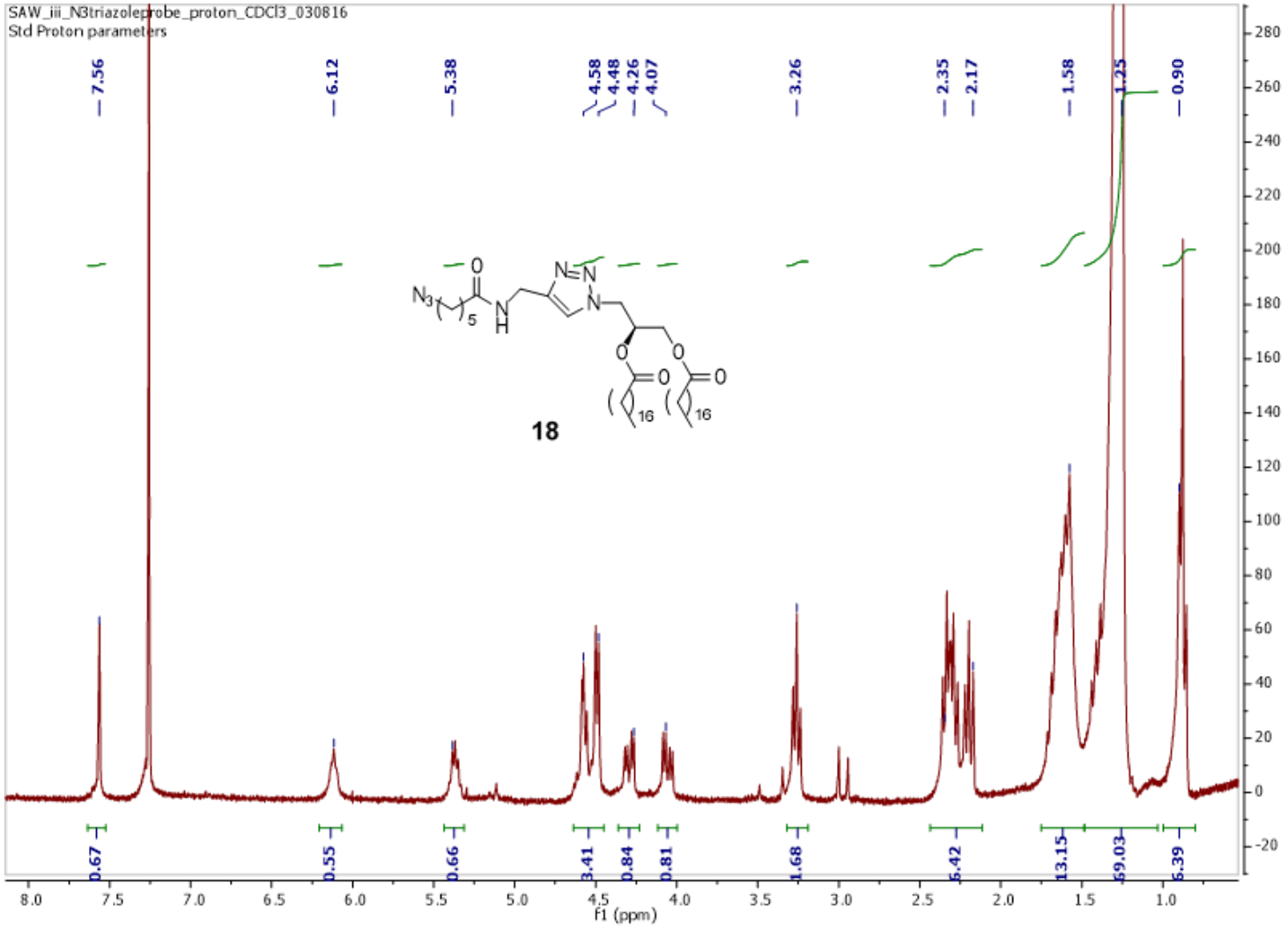
SAW_iii_N3triazoleprobe_proton_CDCl3_030816
Std Proton parameters
7.56
6.12
5.38
4.58
4.48
4.26
4.07
3.26
2.35
2.17
1.58
1.25
0.90
18
0.67
0.55
0.66
3.41
0.84
0.81
1.68
6.42
13.15
69.03
6.39
f1 (ppm)

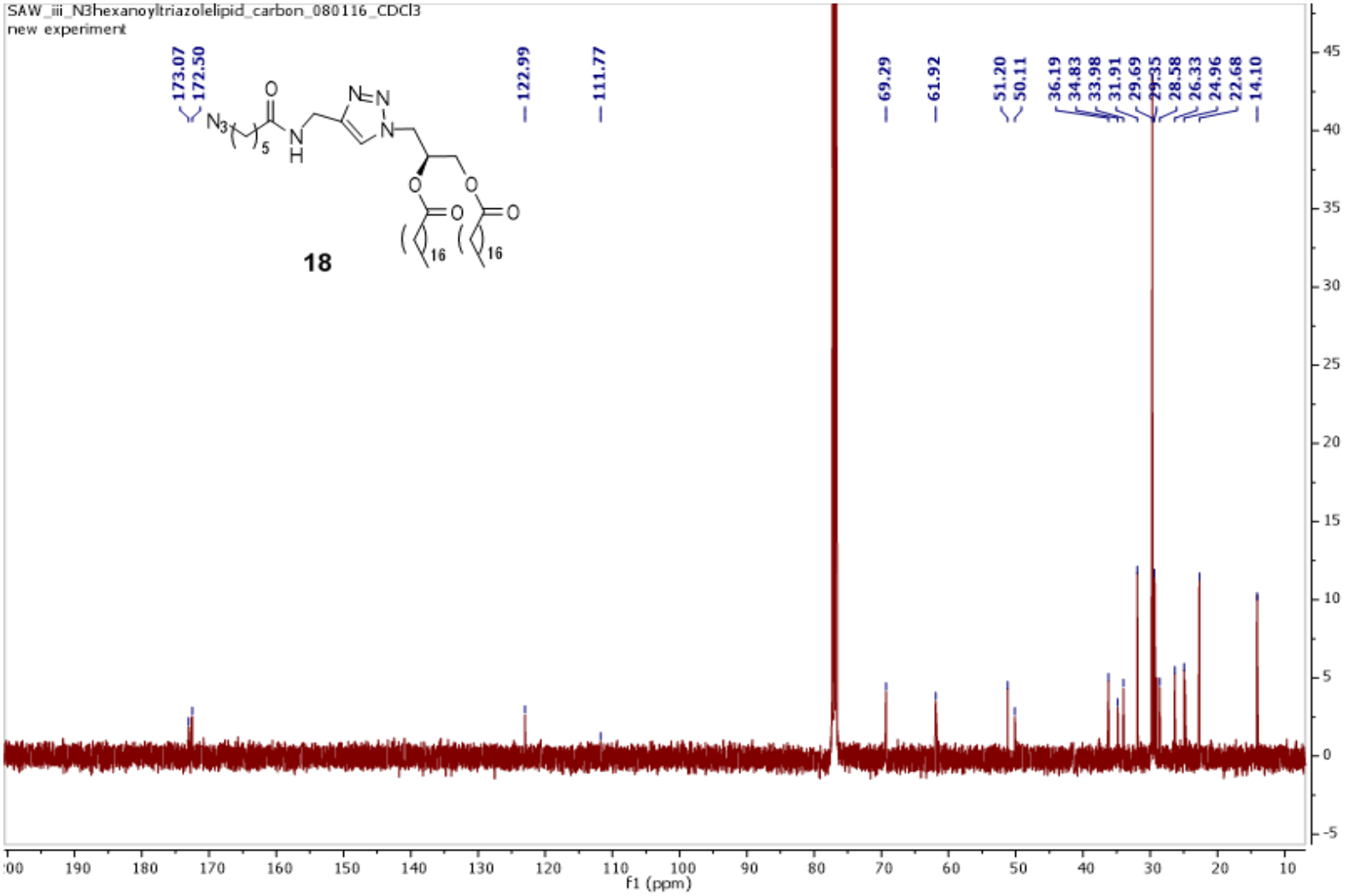
SAW_iii_N3hexanoyltriazolelipid_carbon_080116_CDCl3
new experiment
173.07
172.50
122.99
111.77
69.29
61.92
51.20
50.11
36.19
34.83
33.98
31.91
29.69
29.35
28.58
26.33
24.96
22.68
14.10
18
f1 (ppm)

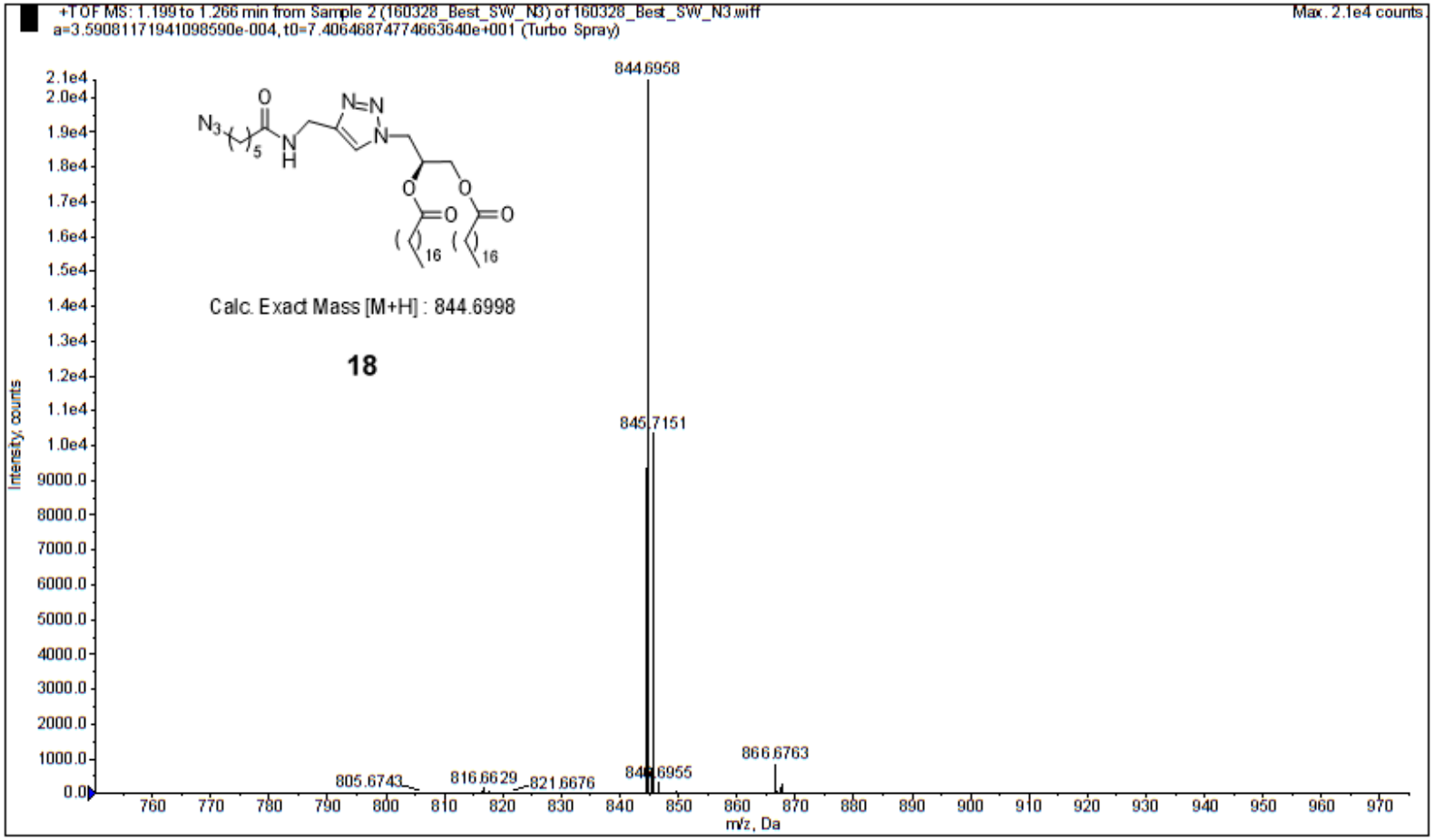
+TOF MS: 1.199 to 1.266 min from Sample 2 (160328_Best_SW_N3) of 160328_Best_SW_N3.wiff
a=3.59081171941098590e-004, t0=7.40646874774663640e+001 (Turbo Spray)
Max. 2.1e4 counts.
Intensity, counts
m/z, Da
844.6958
845.7151
866.6763
805.6743
816.6629
821.6676
Calc. Exact Mass [M+H] : 844.6998
18

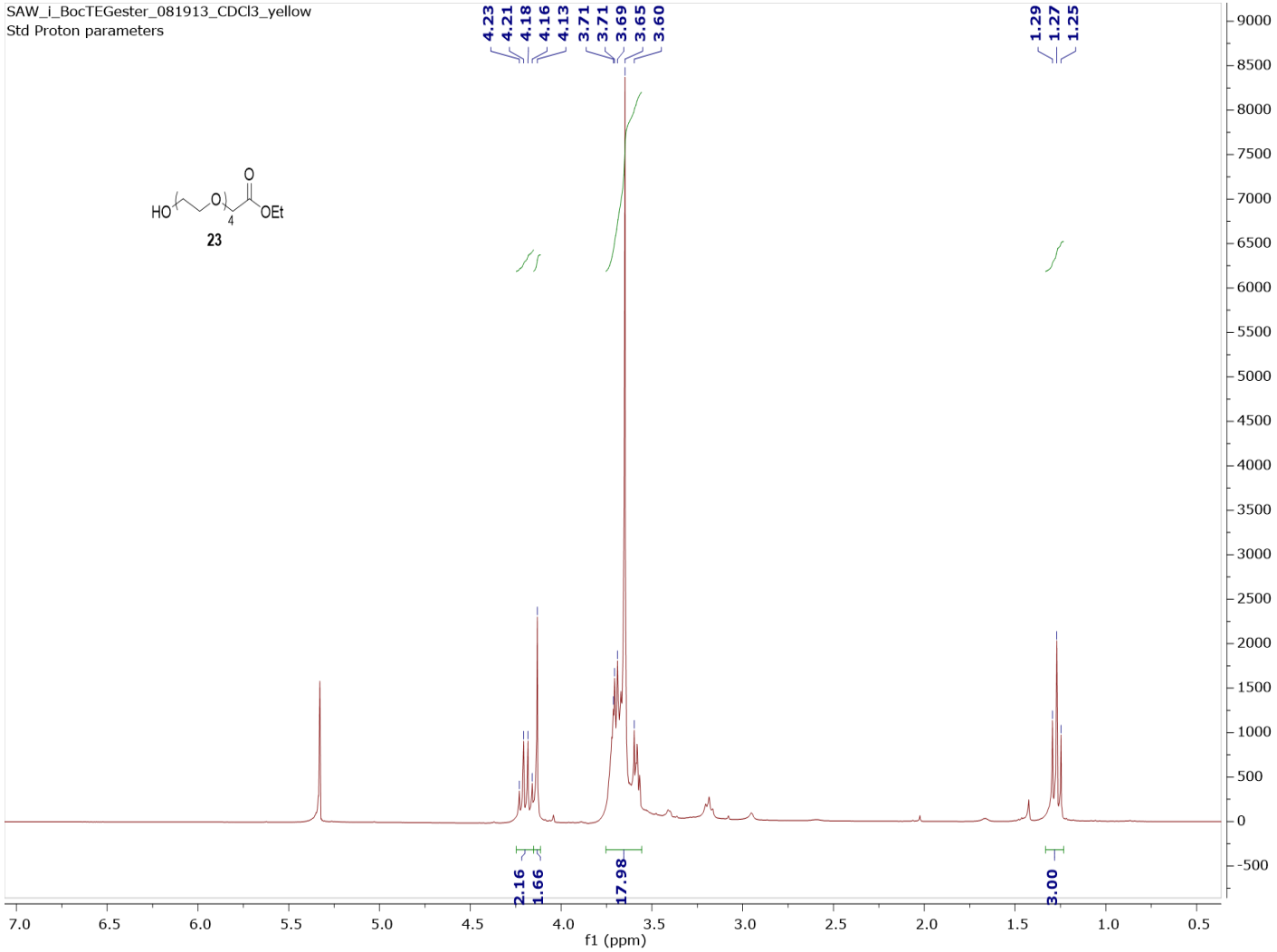
SAW_i_BocTEGester_081913_CDCl3_yellow
Std Proton parameters
4.23
4.21
4.18
4.16
4.13
3.71
3.71
3.69
3.65
3.60
1.29
1.27
1.25
HO
O
O
4
OEt
23
2.16
1.66
17.98
3.00
f1 (ppm)

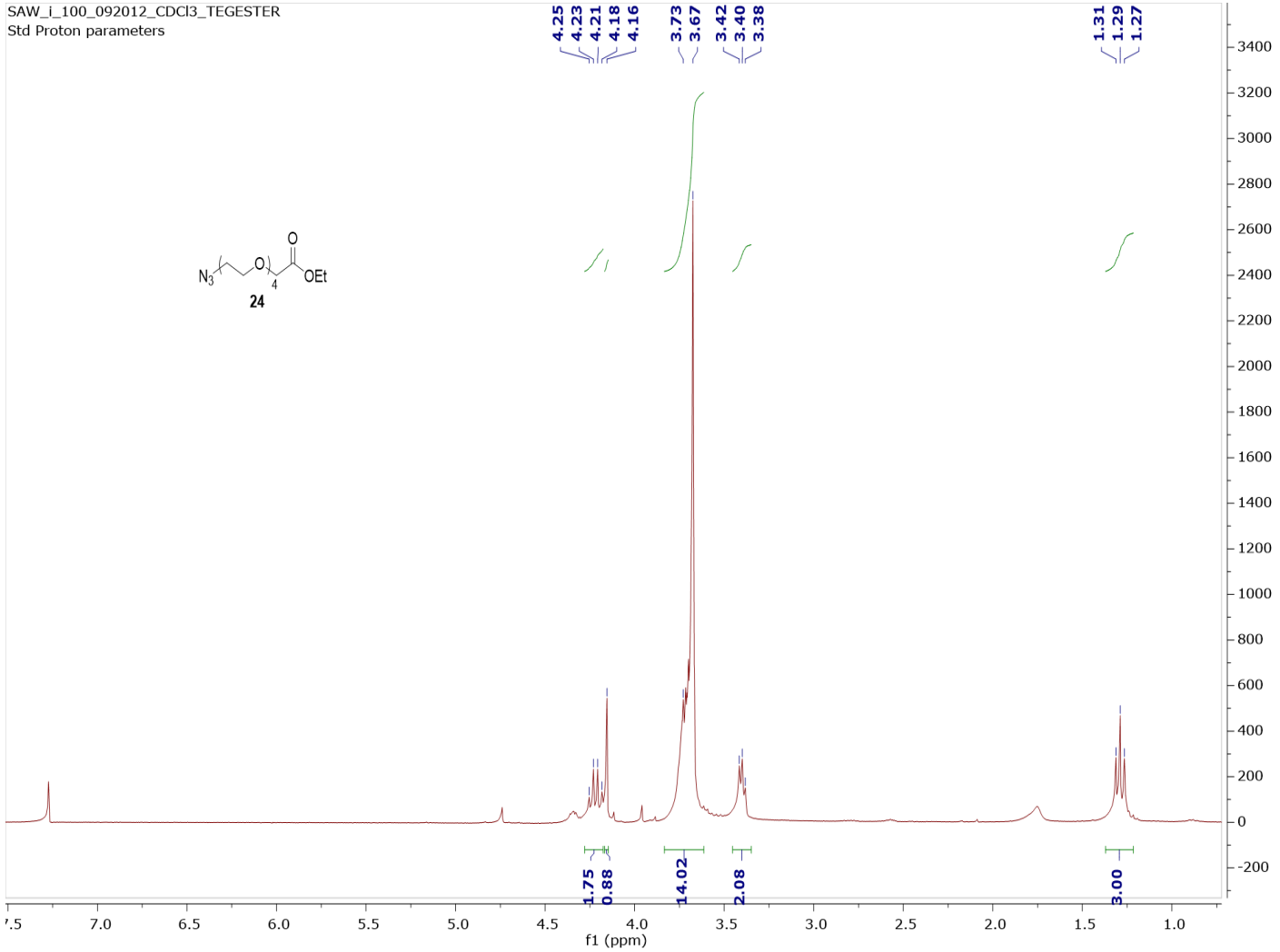
SAW_i_100_092012_CDCl3_TEGESTER
Std Proton parameters
4.25
4.23
4.21
4.18
4.16
3.73
3.67
3.42
3.40
3.38
1.31
1.29
1.27
N3
O
4
OEt
24
1.75
0.88
14.02
2.08
3.00
f1 (ppm)

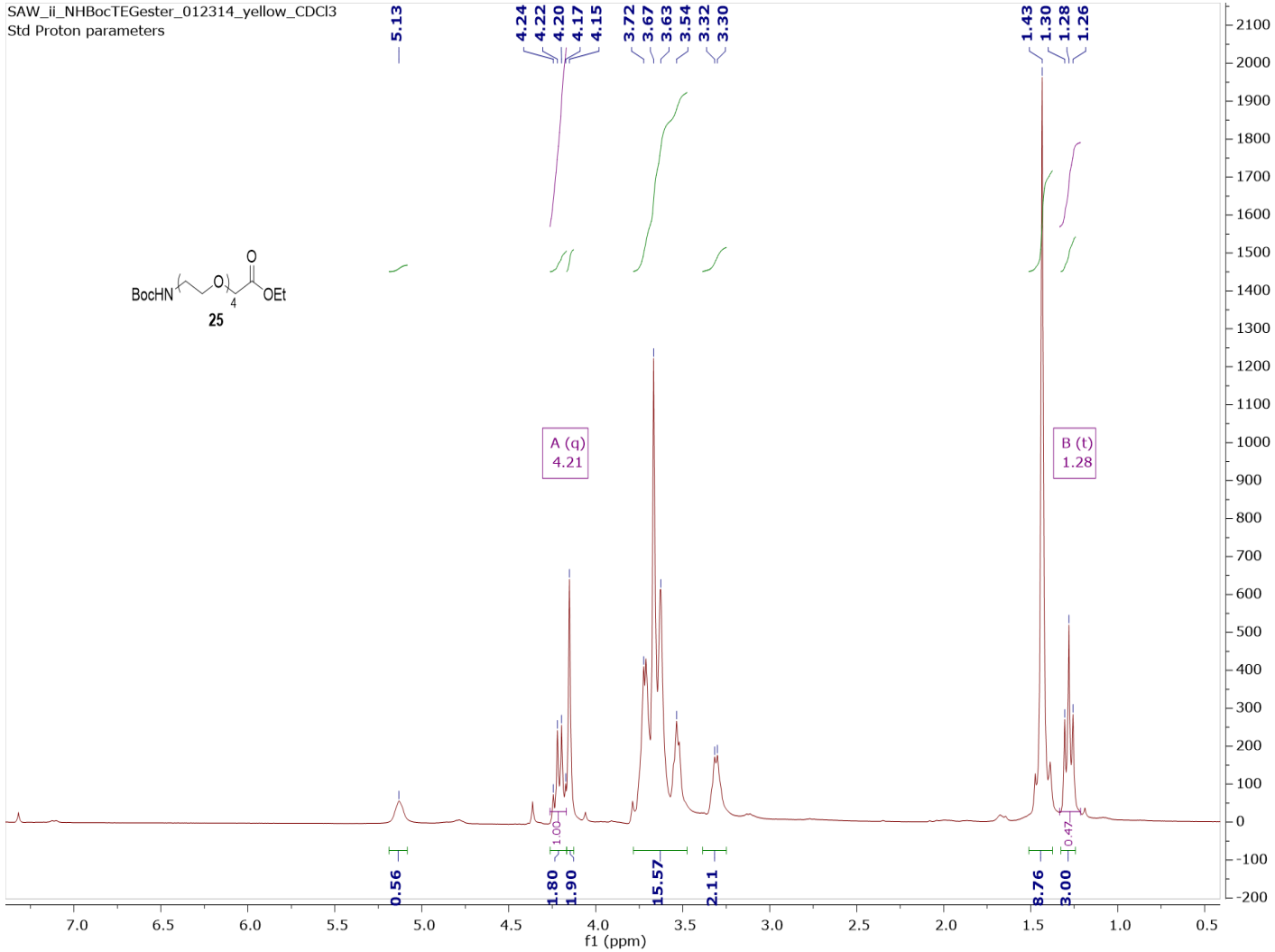
SAW_ii_NHBocTEGester_012314_yellow_CDCl3
Std Proton parameters
5.13
4.24
4.22
4.20
4.17
4.15
3.72
3.67
3.63
3.54
3.32
3.30
1.43
1.30
1.28
1.26
BocHN
O
O
4
OEt
25
A (q)
4.21
B (t)
1.28
1.00
0.47
0.56
1.80
1.90
15.57
2.11
8.76
3.00
f1 (ppm)

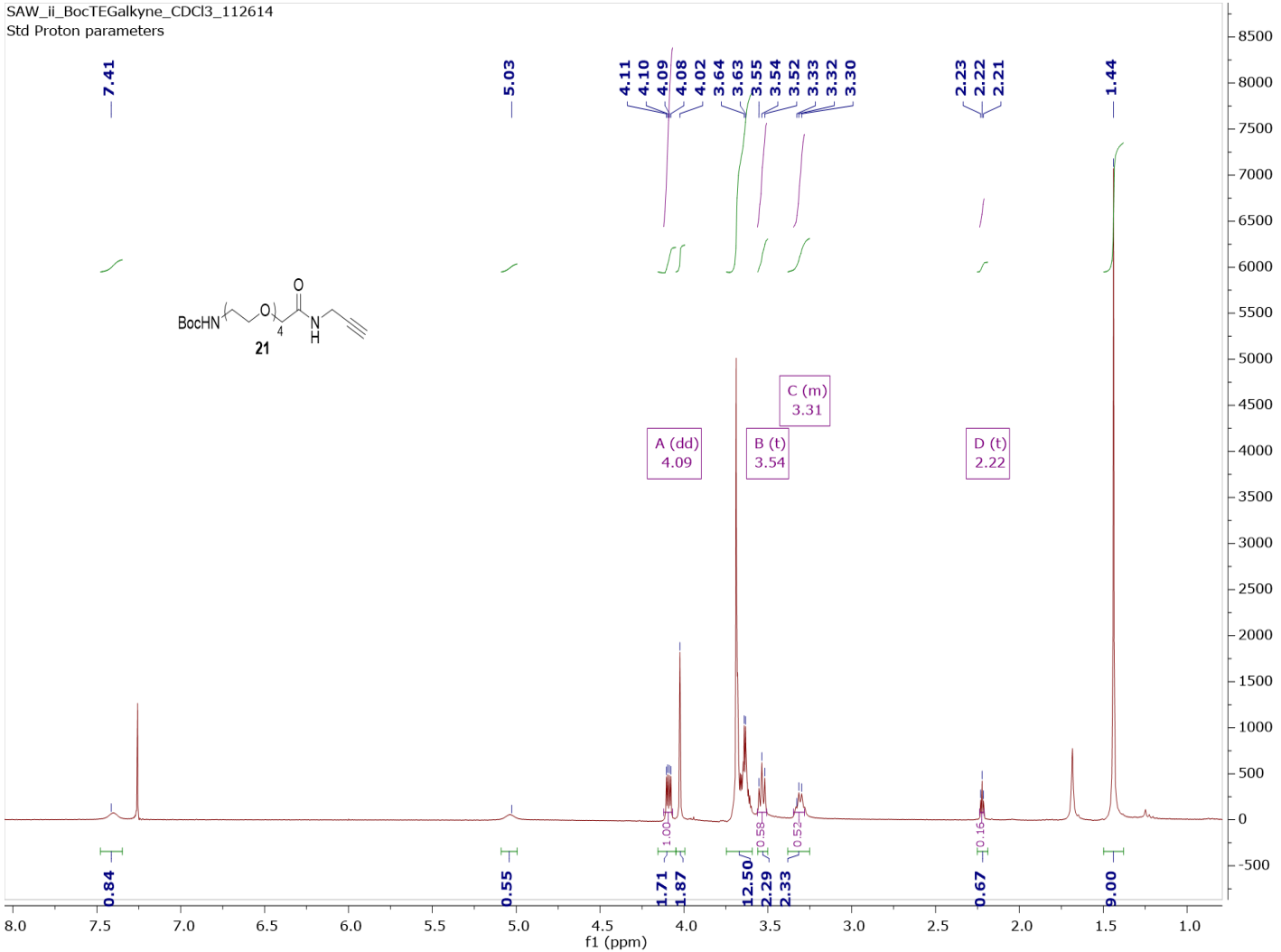
SAW_ii_BocTEGalkyne_CDCl3_112614
Std Proton parameters
7.41
5.03
4.11
4.10
4.09
4.08
4.02
3.64
3.63
3.55
3.54
3.52
3.33
3.32
3.30
2.23
2.22
2.21
1.44
BocHN
O
O
4
N
H
21
A (dd)
4.09
B (t)
3.54
C (m)
3.31
D (t)
2.22
0.84
0.55
1.71
1.87
12.50
2.29
2.33
0.67
9.00
1.00
0.58
0.52
0.16
f1 (ppm)

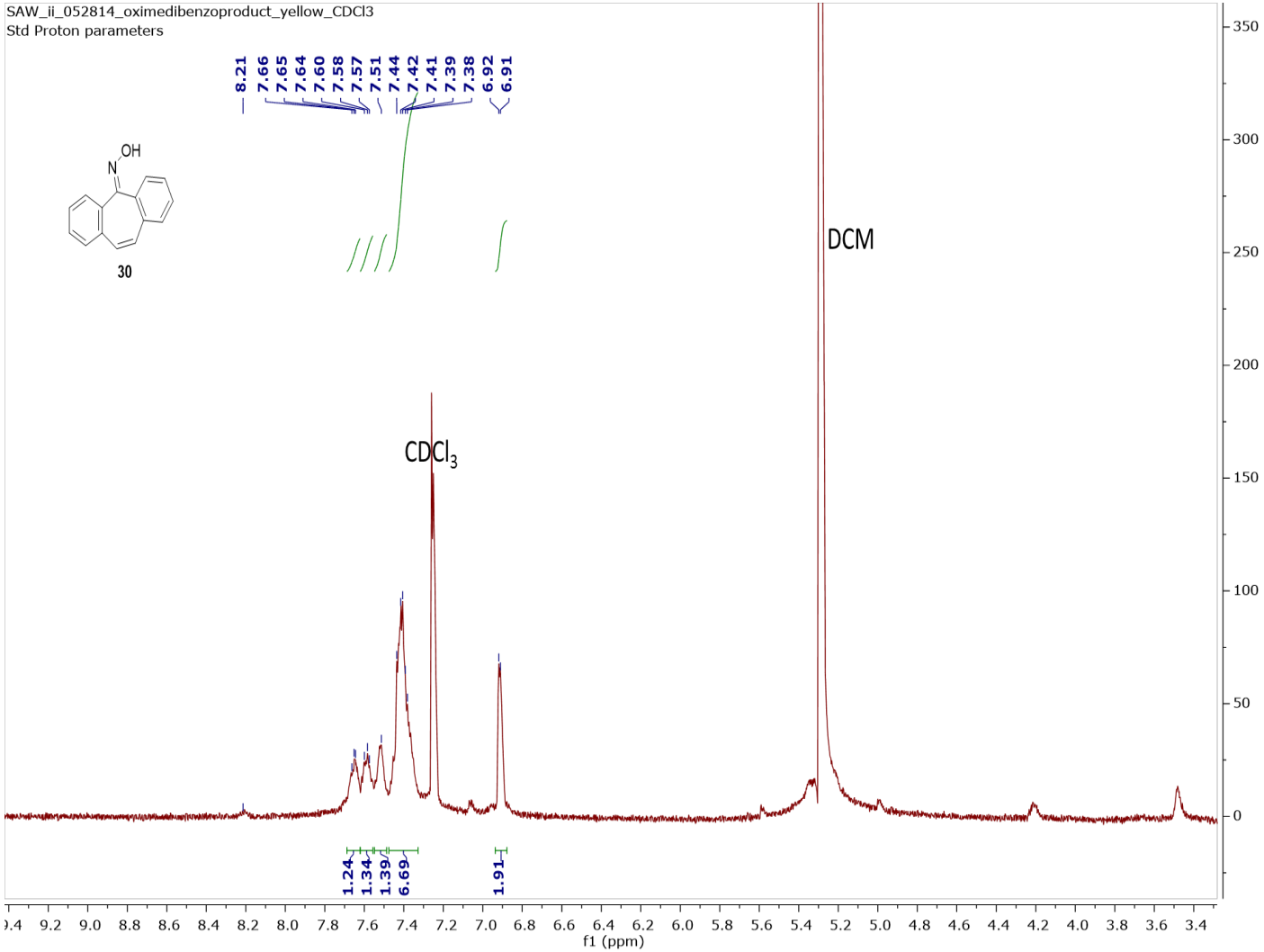
SAW_ii_052814_oximedibenzoproduct_yellow_CDCl3
Std Proton parameters
8.21
7.66
7.65
7.64
7.60
7.58
7.57
7.51
7.44
7.42
7.41
7.39
7.38
6.92
6.91
OH
N
30
DCM
CDCl3
1.24
1.34
1.39
6.69
1.91
f1 (ppm)

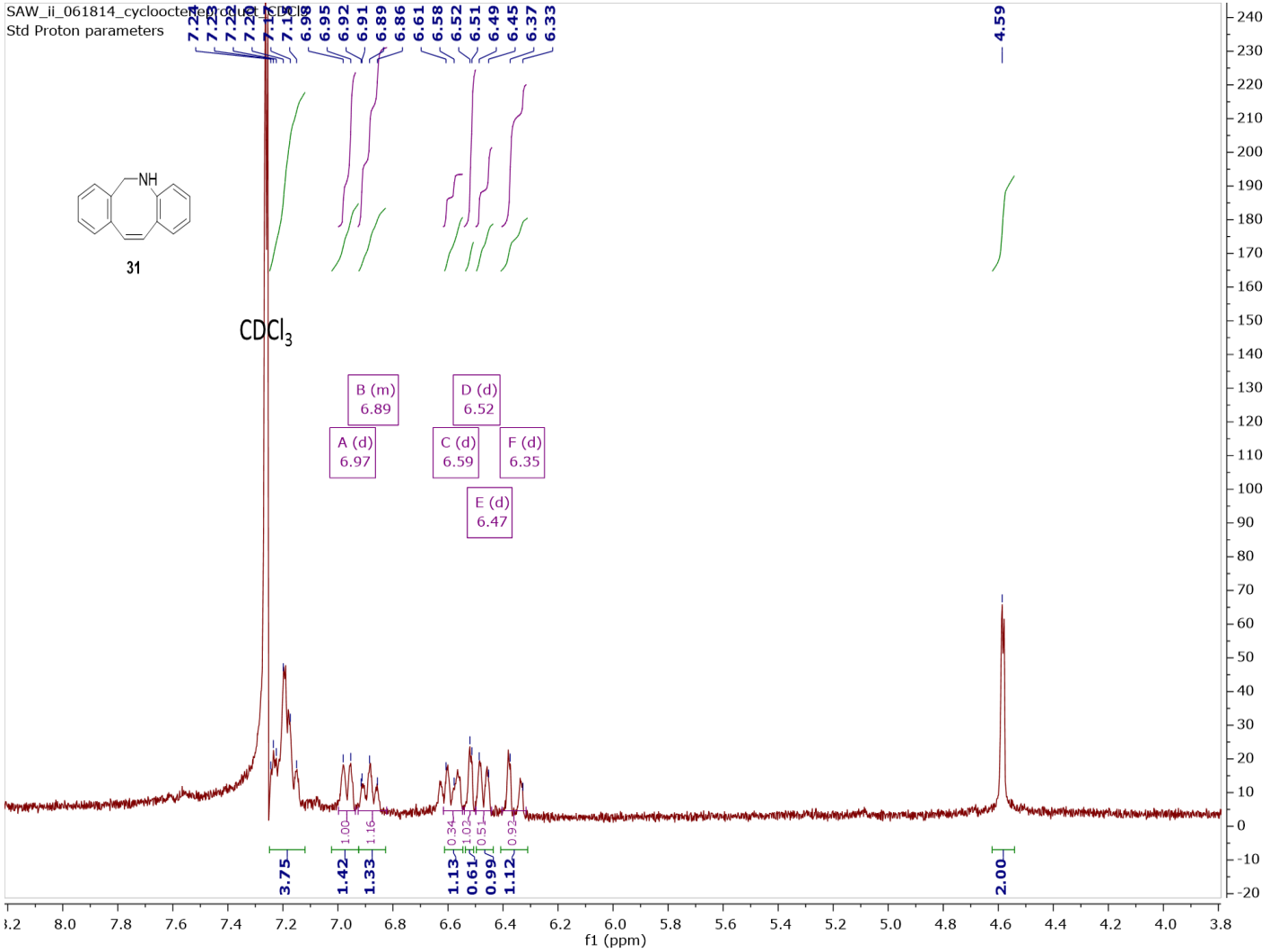
SAW_ii_061814_cyclooctene_quat_CDCl3
Std Proton parameters
7.24
7.23
7.22
7.20
7.17
7.15
6.98
6.95
6.92
6.91
6.89
6.86
6.61
6.58
6.52
6.51
6.49
6.45
6.37
6.33
4.59
NH
31
CDCl3
B (m)
6.89
D (d)
6.52
A (d)
6.97
C (d)
6.59
F (d)
6.35
E (d)
6.47
1.00
1.16
0.34
1.03
0.51
0.92
3.75
1.42
1.33
1.13
0.61
0.99
1.12
2.00
f1 (ppm)

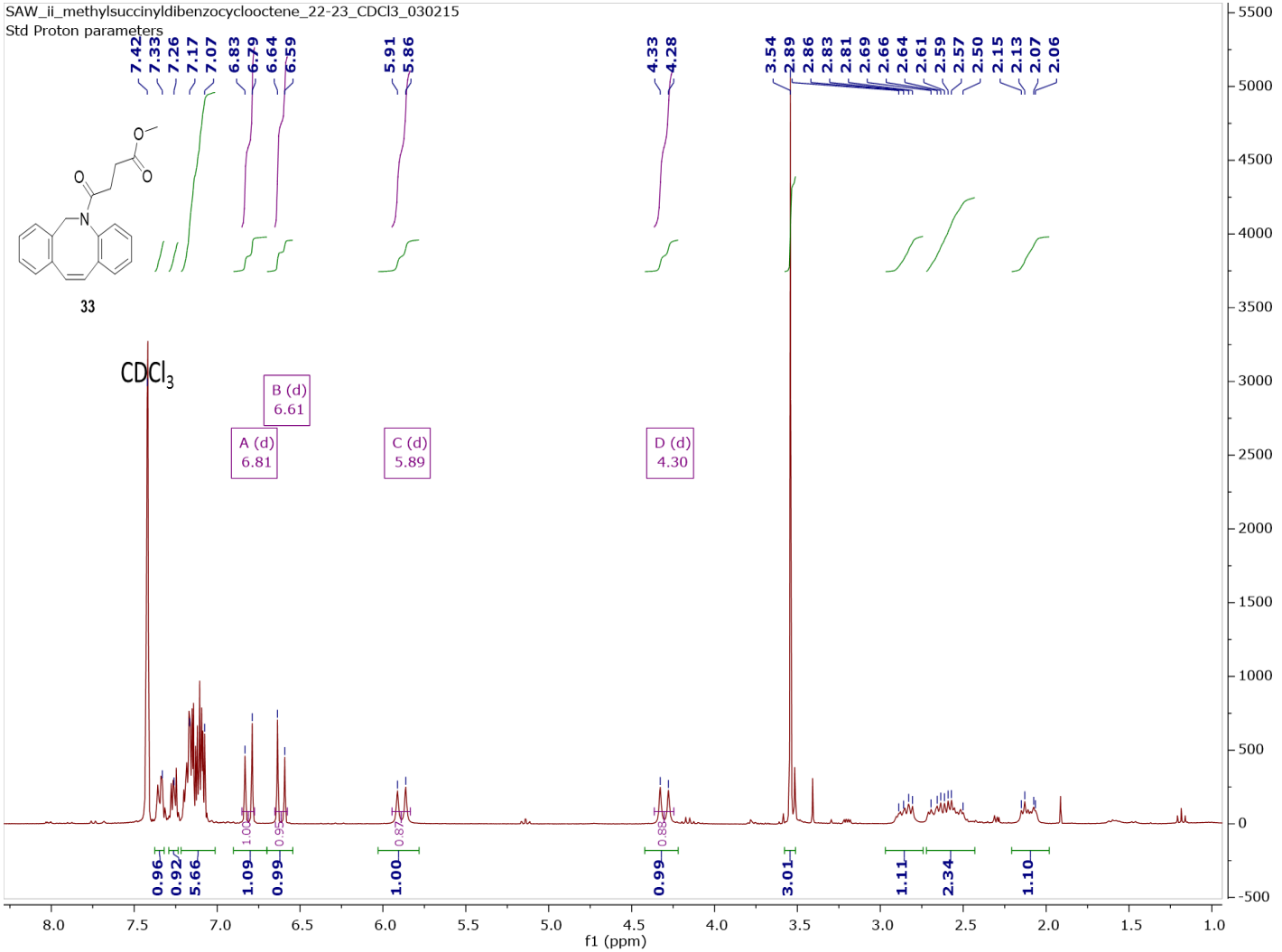
SAW_ii_methylsuccinyldibenzocyclooctene_22-23_CDCl3_030215
Std Proton parameters
7.42
7.33
7.26
7.17
7.07
6.83
6.79
6.64
6.59
5.91
5.86
4.33
4.28
3.54
2.89
2.86
2.83
2.81
2.69
2.66
2.64
2.61
2.59
2.57
2.50
2.15
2.13
2.07
2.06
33
CDCl3
B (d)
6.61
A (d)
6.81
C (d)
5.89
D (d)
4.30
0.96
0.92
5.66
1.09
0.99
1.00
0.99
3.01
1.11
2.34
1.10
f1 (ppm)

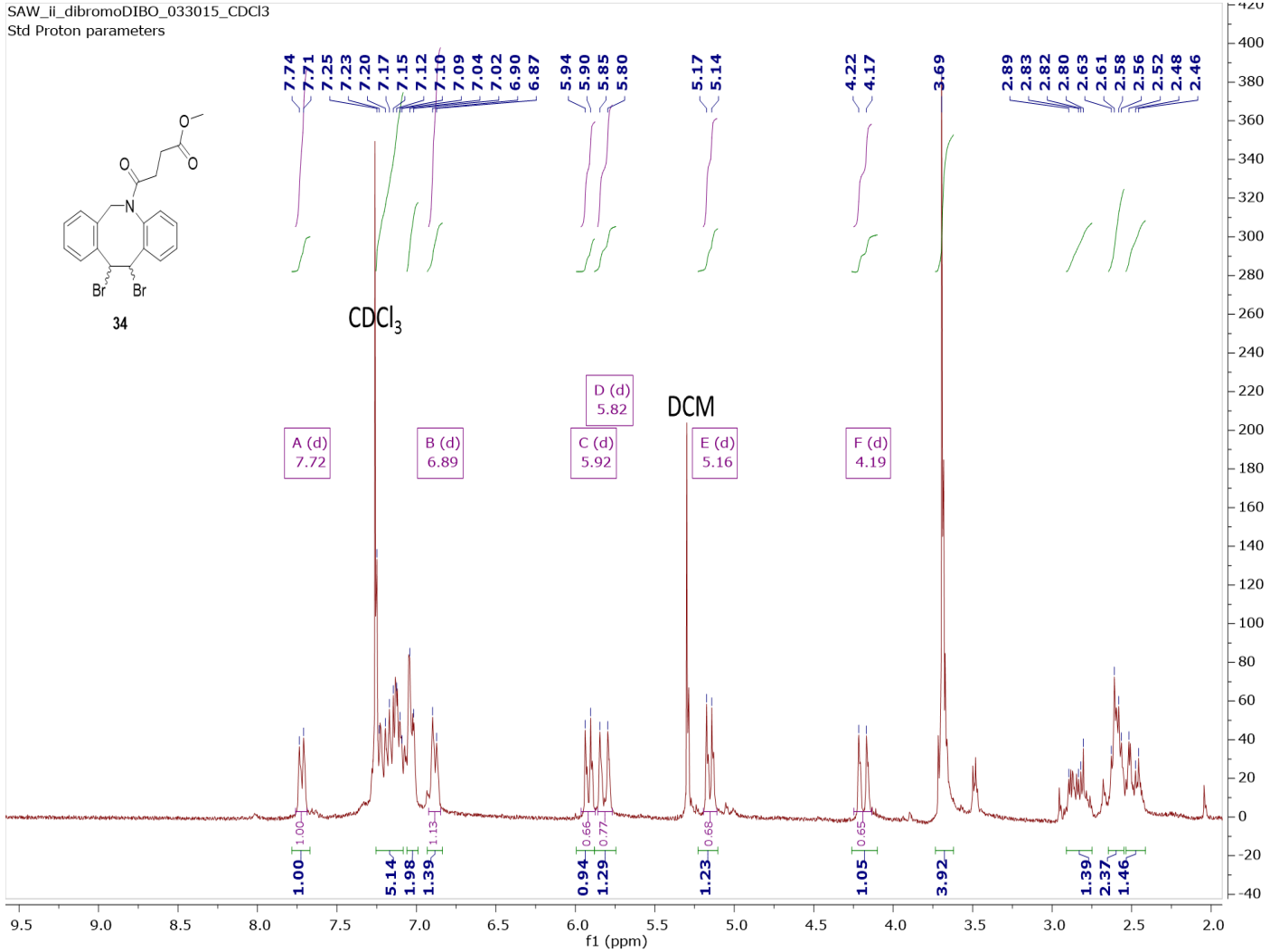
SAW_ii_dibromoDIBO_033015_CDCl3
Std Proton parameters
7.74
7.71
7.25
7.23
7.20
7.17
7.15
7.12
7.10
7.09
7.04
7.02
6.90
6.87
5.94
5.90
5.85
5.80
5.17
5.14
4.22
4.17
3.69
2.89
2.83
2.82
2.80
2.63
2.61
2.58
2.56
2.52
2.48
2.46
O
O
O
N
Br
Br
34
CDCl3
DCM
A (d) 7.72
B (d) 6.89
C (d) 5.92
D (d) 5.82
E (d) 5.16
F (d) 4.19
1.00
5.14
1.98
1.39
0.94
1.29
1.23
1.05
3.92
1.39
2.37
1.46
f1 (ppm)

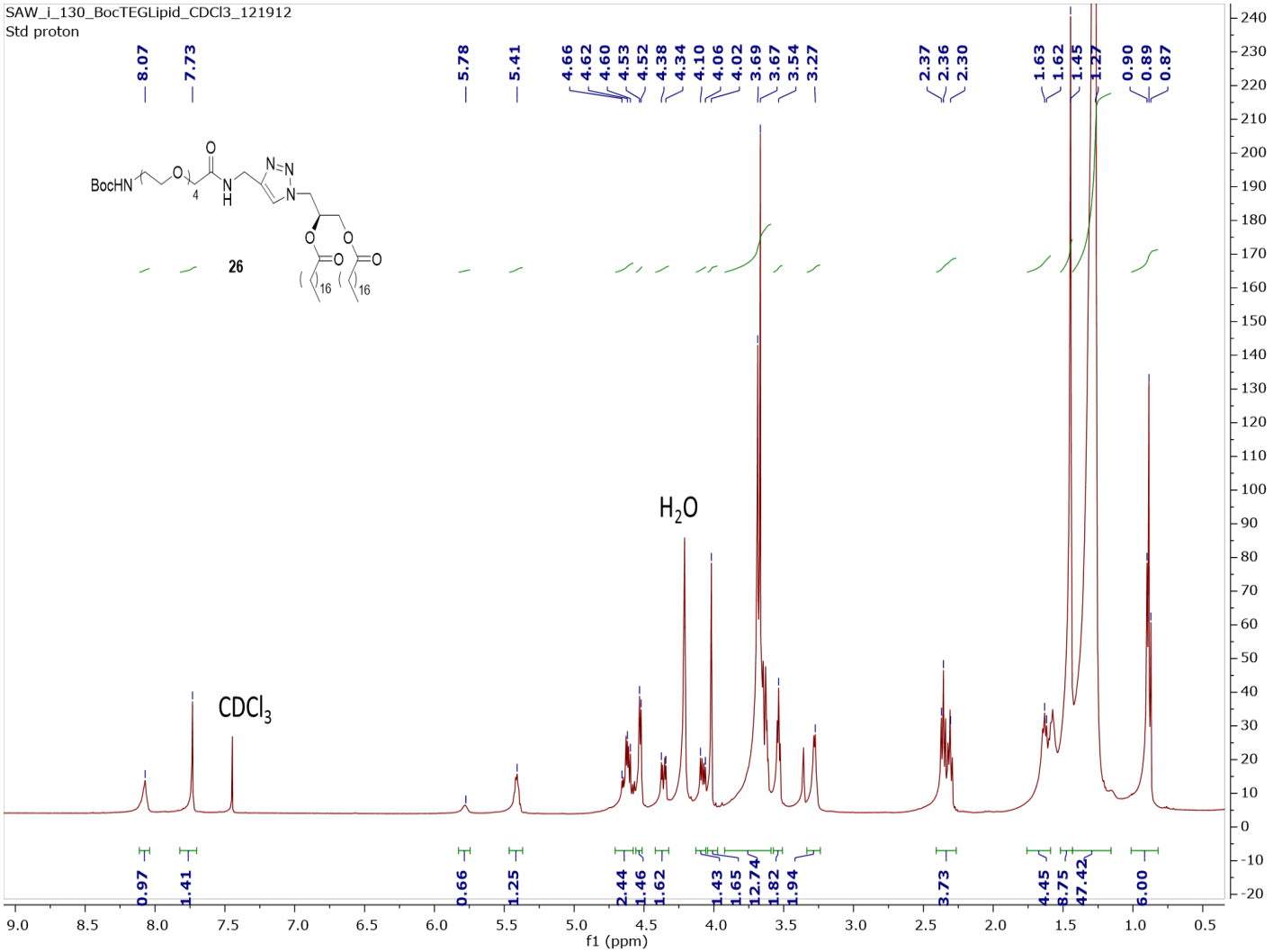
SAW_i_130_BocTEGLipid_CDCl3_121912
Std proton
8.07
7.73
5.78
5.41
4.66
4.62
4.60
4.53
4.52
4.38
4.34
4.10
4.06
4.02
3.69
3.67
3.54
3.27
2.37
2.36
2.30
1.63
1.62
1.45
1.27
0.90
0.89
0.87
BocHN
26
CDCl3
H2O
0.97
1.41
0.66
1.25
2.44
1.46
1.62
1.43
1.65
12.74
1.82
1.94
3.73
4.45
8.75
47.42
6.00
f1 (ppm)

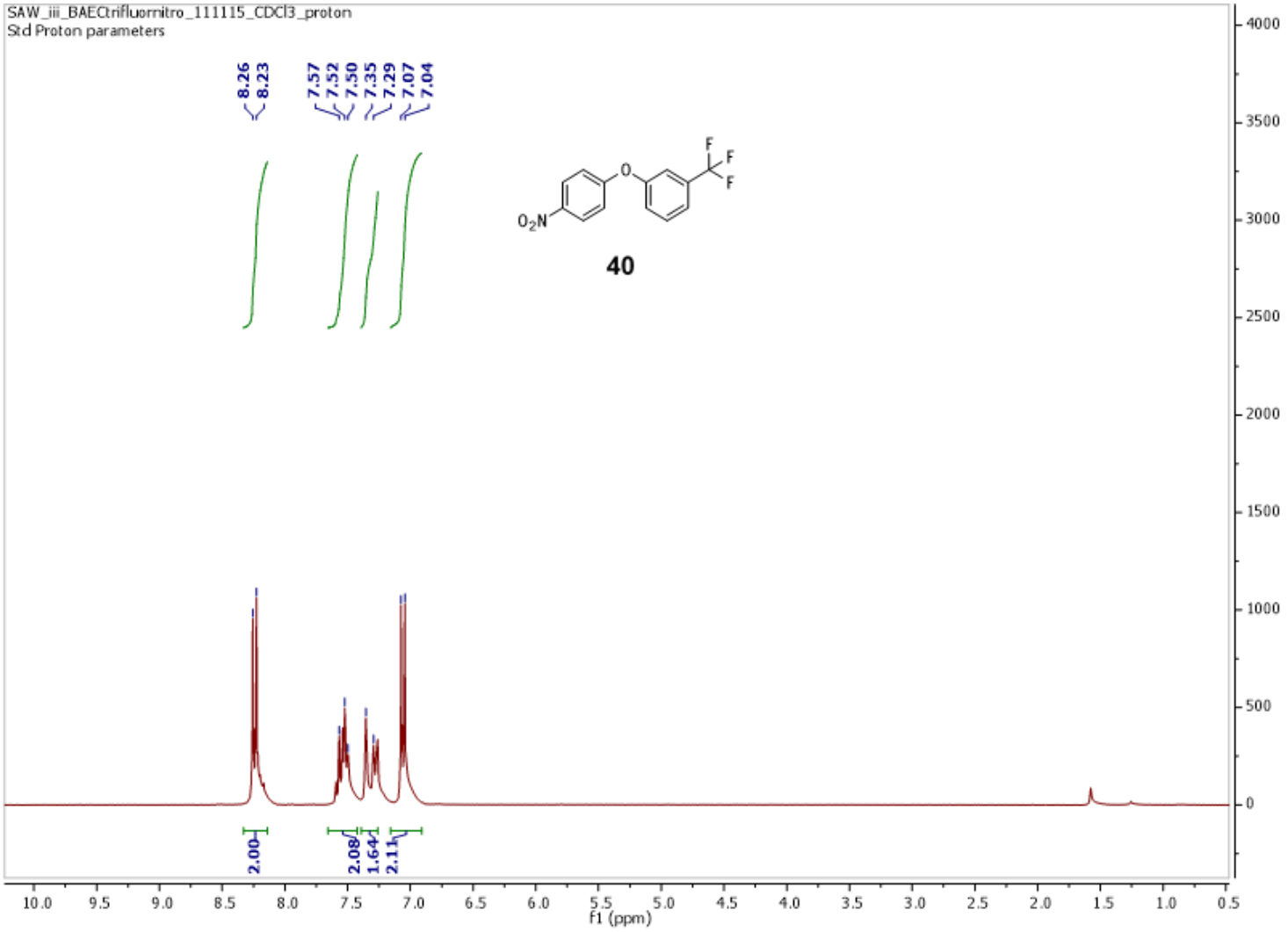
SAW_iii_BAECtrifluornitro_111115_CDCl3_proton
Std Proton parameters
8.26
8.23
7.57
7.52
7.50
7.35
7.29
7.07
7.04
F
F
F
O
O_2N
40
2.00
2.08
1.64
2.11
f1 (ppm)

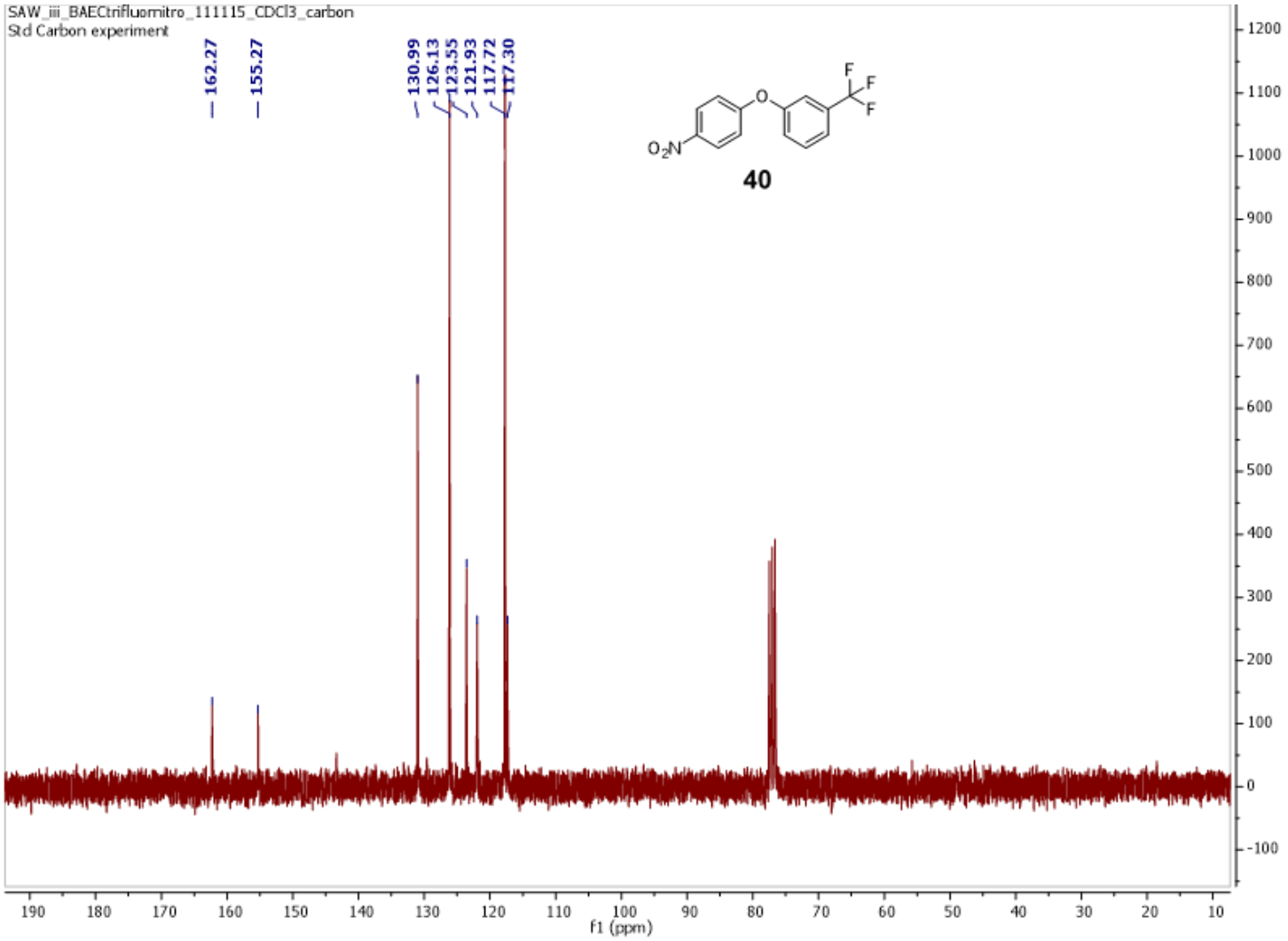
SAW_iii_BAECtrifluomitro_111115_CDCl3_carbon
Std Carbon experiment
162.27
155.27
130.99
126.13
123.55
121.93
117.72
117.30
O2N
O
F
F
F
40
f1 (ppm)

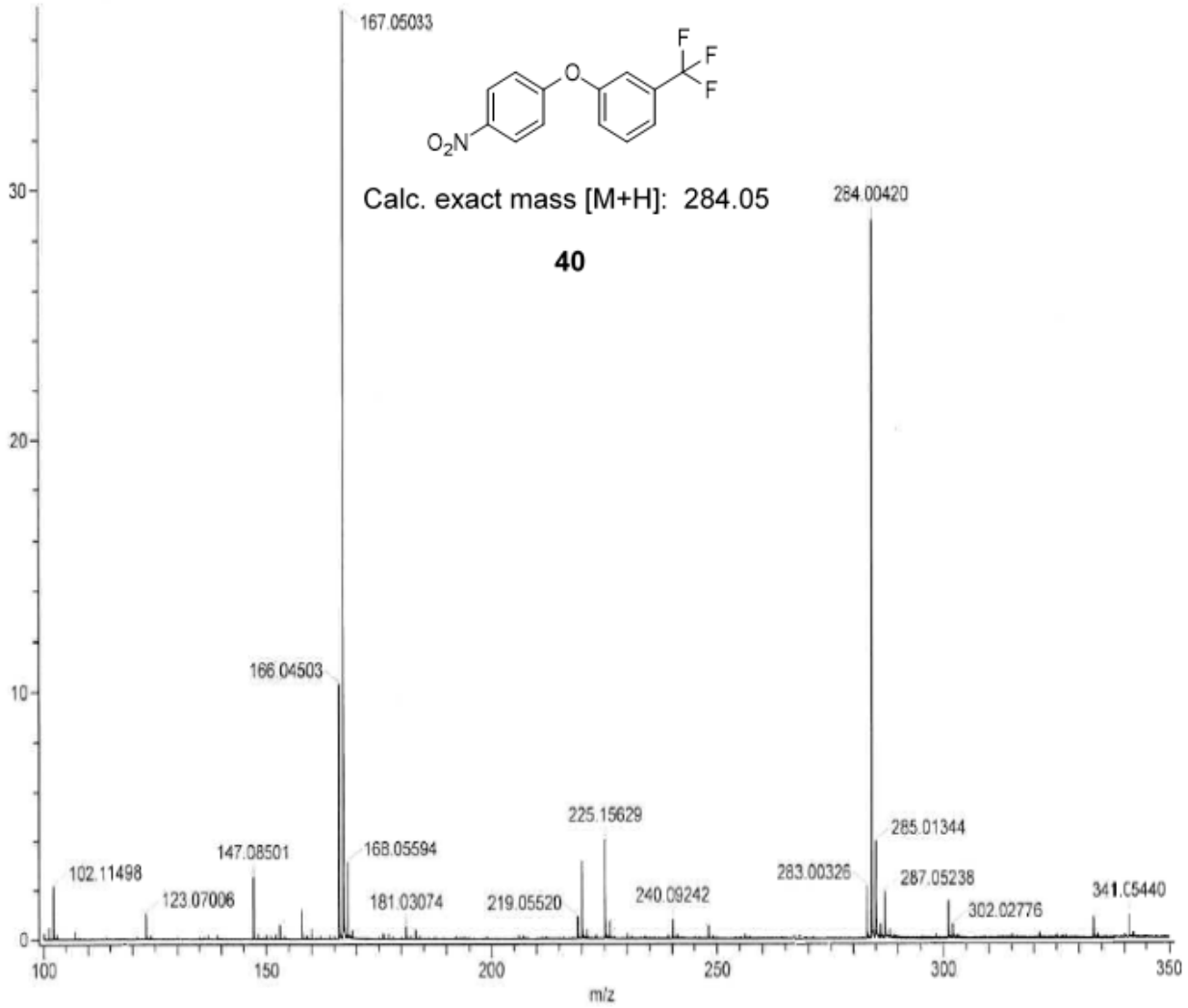
167.05033
F
F
F
O
O_2N
Calc. exact mass [M+H]: 284.05
40
284.00420
166.04503
225.15629
285.01344
147.08501
168.05594
102.11498
283.00326
287.05238
123.07006
181.03074
219.05520
240.09242
302.02776
341.05440
30
20
10
0
100
150
200
250
300
350
m/z

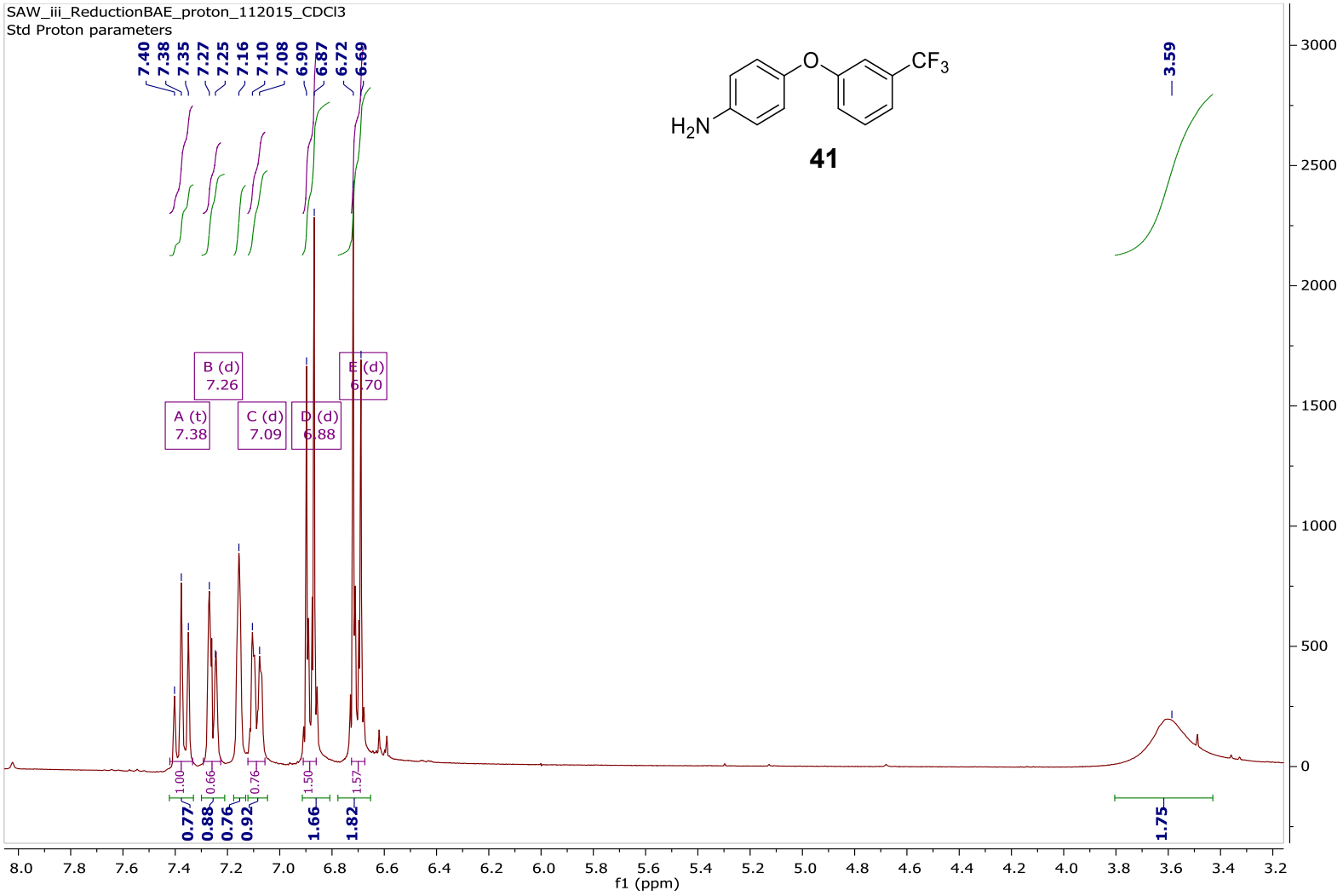
SAW_iii_ReductionBAE_proton_112015_CDCl3
Std Proton parameters
7.40
7.38
7.35
7.27
7.25
7.16
7.10
7.08
6.90
6.87
6.72
6.69
3.59
O
CF3
H2N
41
B (d)
7.26
E (d)
6.70
A (t)
7.38
C (d)
7.09
D (d)
6.88
1.00
0.66
0.76
1.50
1.57
0.77
0.88
0.76
0.92
1.66
1.82
1.75
f1 (ppm)

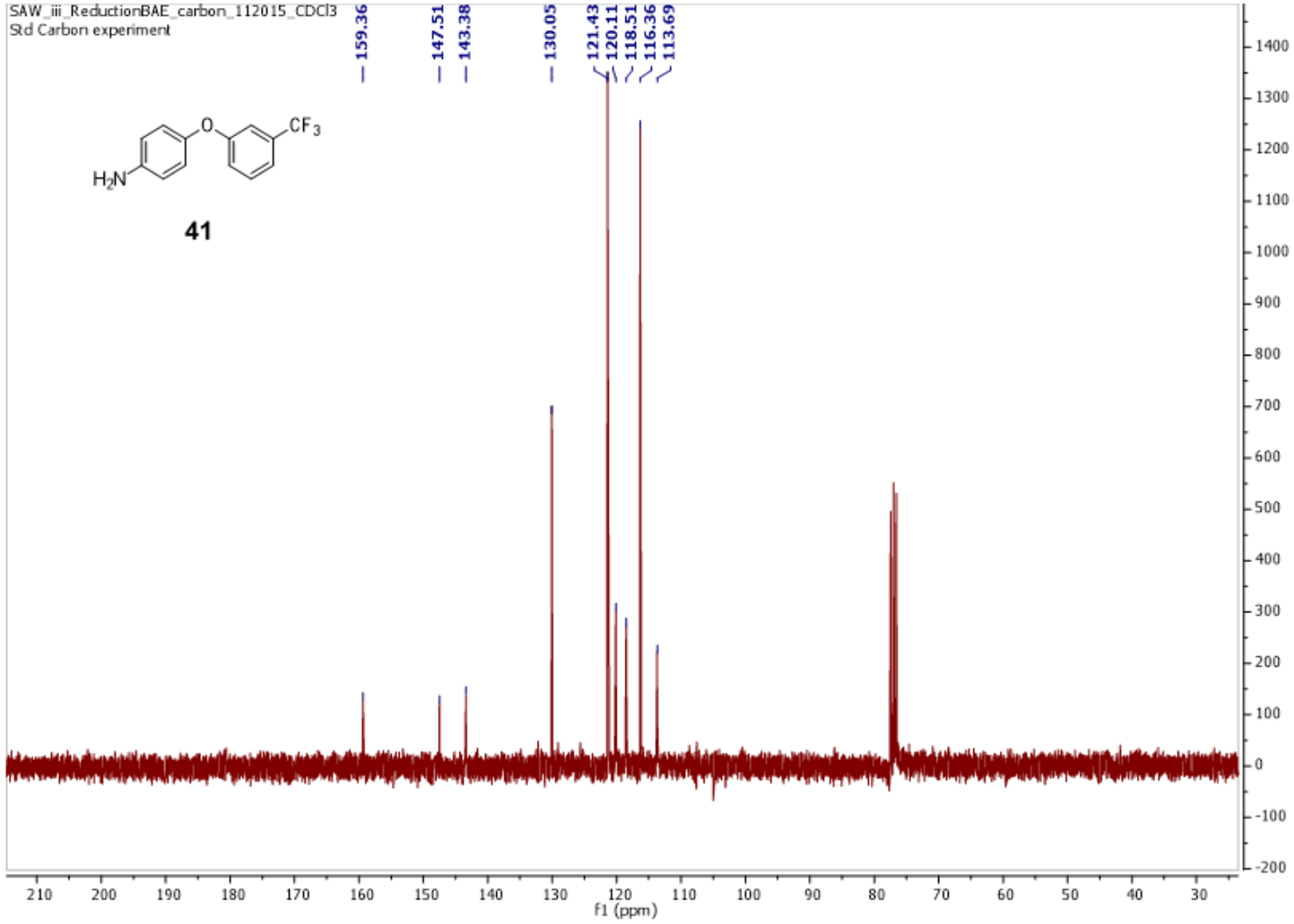
SAW_iii_ReductionBAE_carbon_112015_CDCl3
Std Carbon experiment
159.36
147.51
143.38
130.05
121.43
120.11
118.51
116.36
113.69
O
CF3
H2N
41
f1 (ppm)

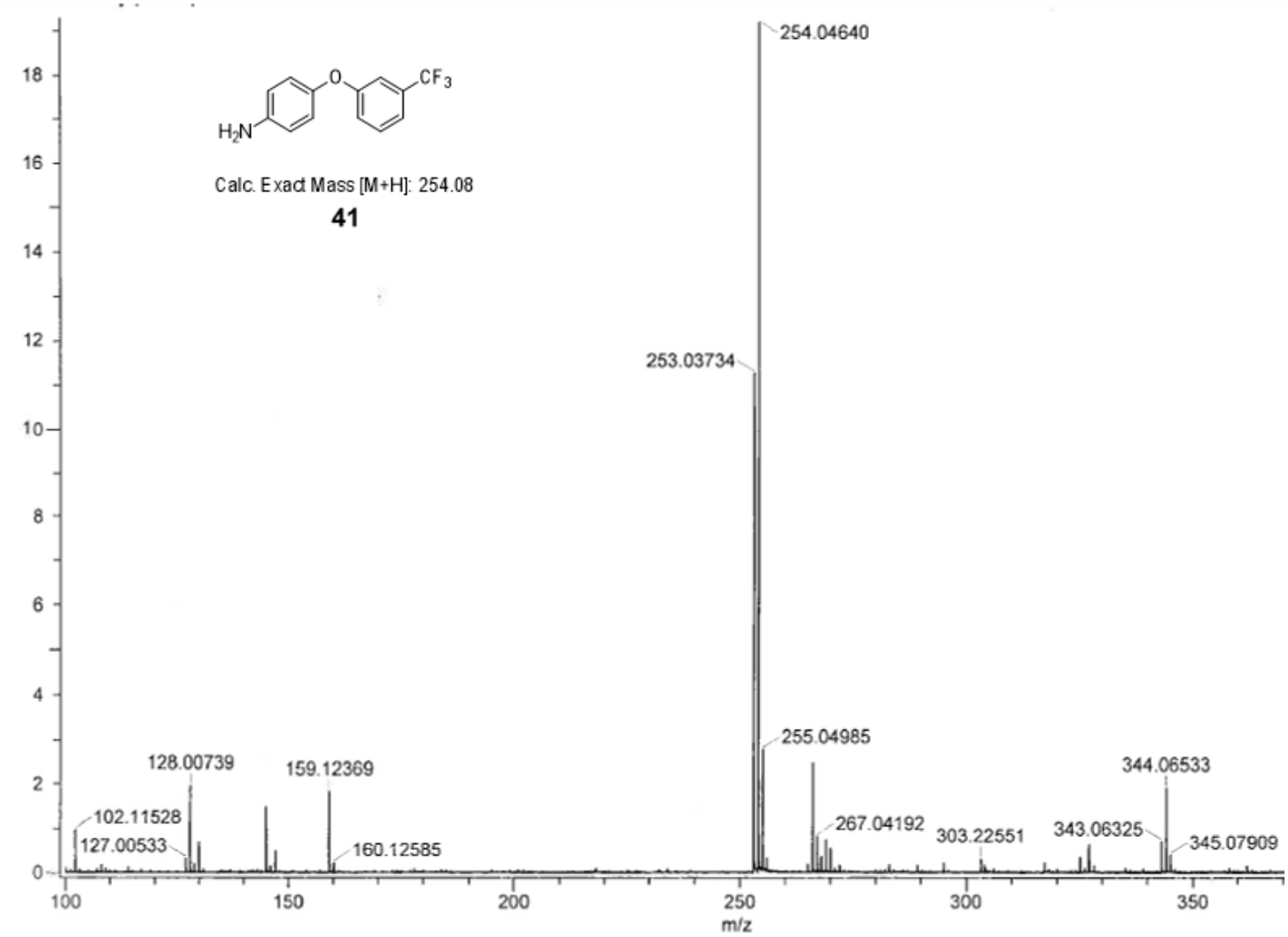
254.04640
253.03734
255.04985
128.00739
159.12369
102.11528
127.00533
160.12585
267.04192
303.22551
343.06325
344.06533
345.07909
Calc. Exact Mass [M+H]: 254.08
41
m/z

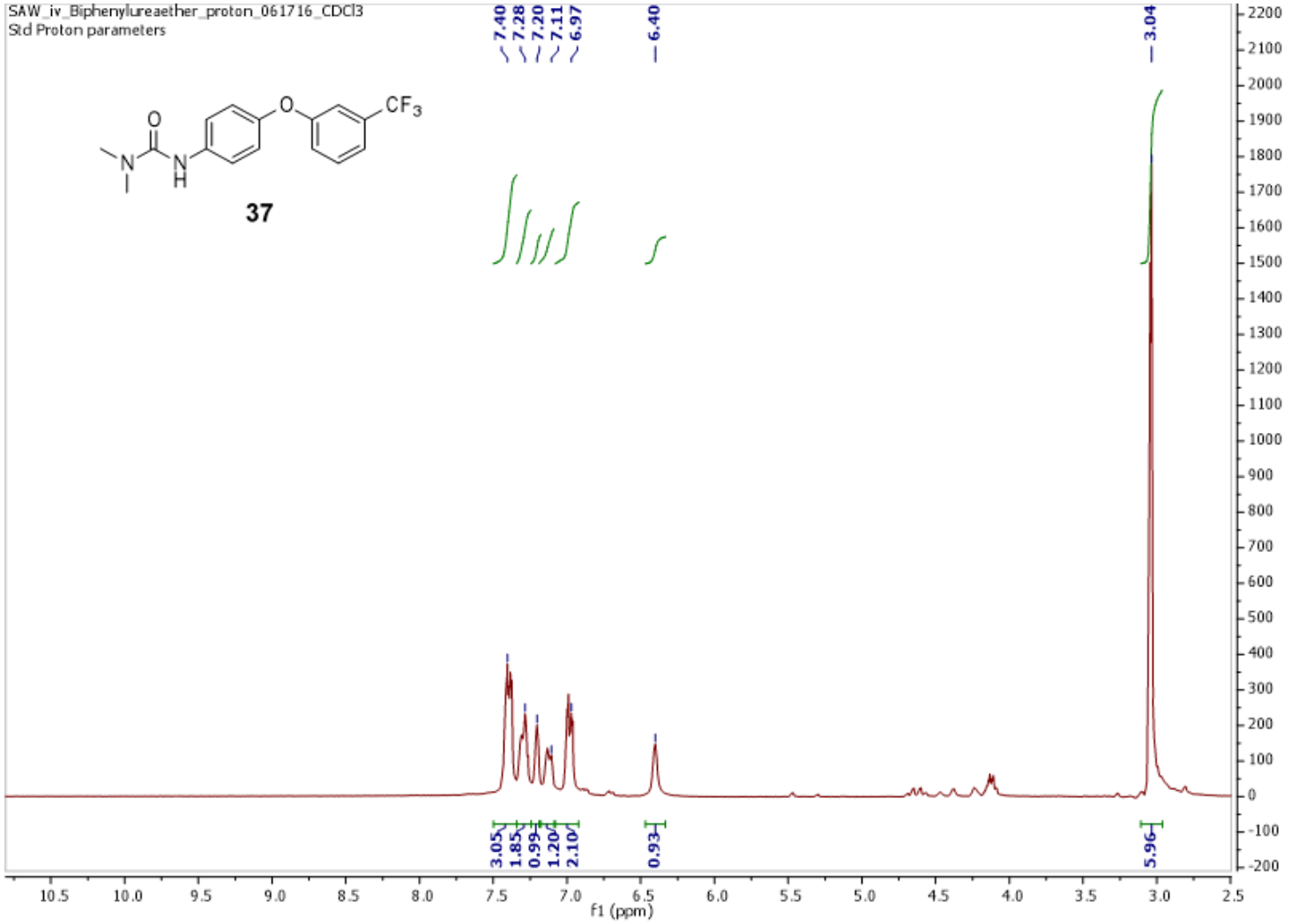
SAW_iv_Biphenylureaether_proton_061716_CDCl3
Std Proton parameters
37
7.40
7.28
7.20
7.11
6.97
6.40
3.04
3.05
1.85
0.99
1.20
2.10
0.93
5.96
f1 (ppm)

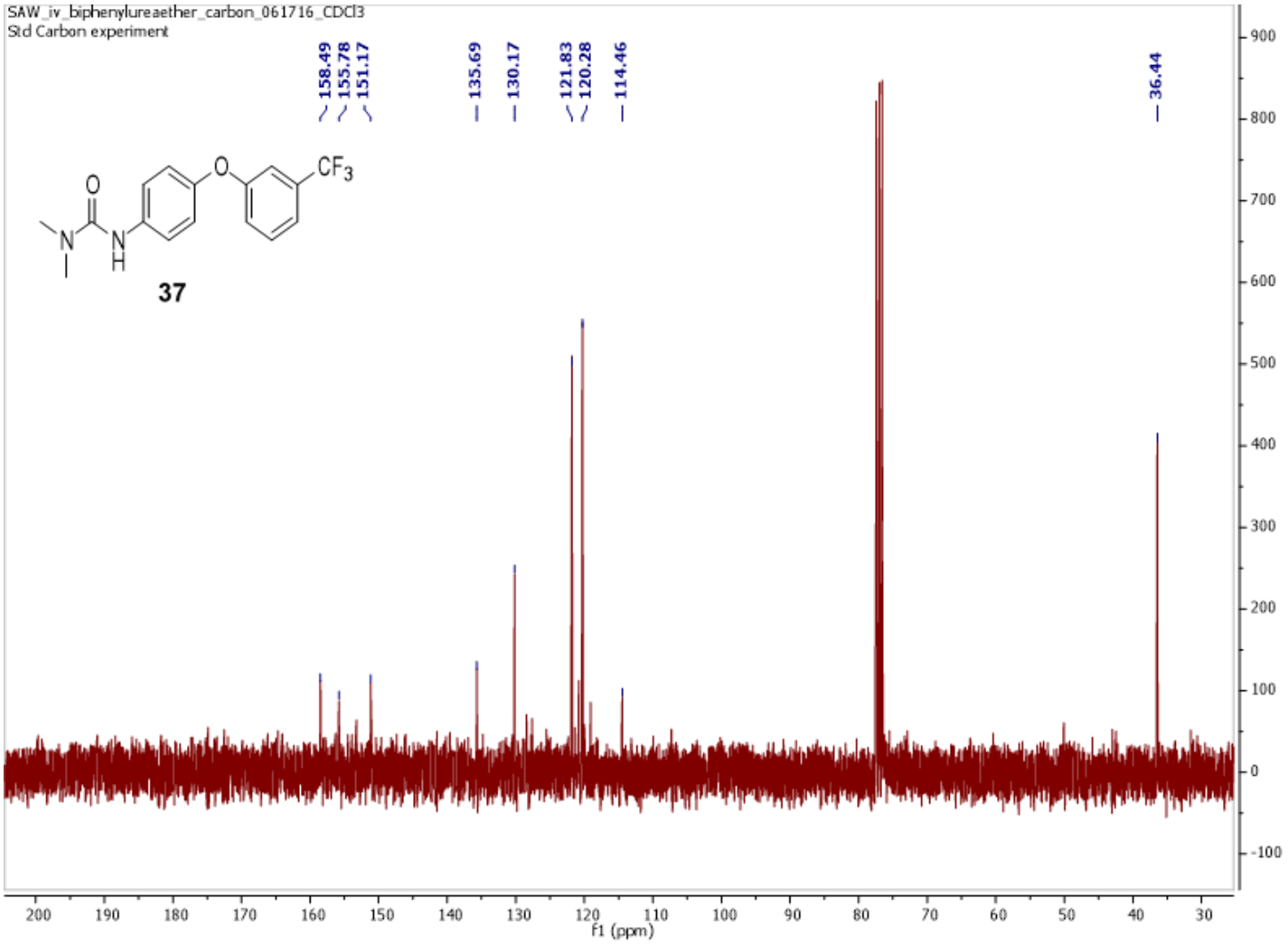
SAW_iv_biphenylureaether_carbon_061716_CDCl3
Std Carbon experiment
158.49
155.78
151.17
135.69
130.17
121.83
120.28
114.46
36.44
O
N
H
O
CF3
37
900
800
700
600
500
400
300
200
100
0
-100
200
190
180
170
160
150
140
130
120
110
100
90
80
70
60
50
40
30
f1 (ppm)

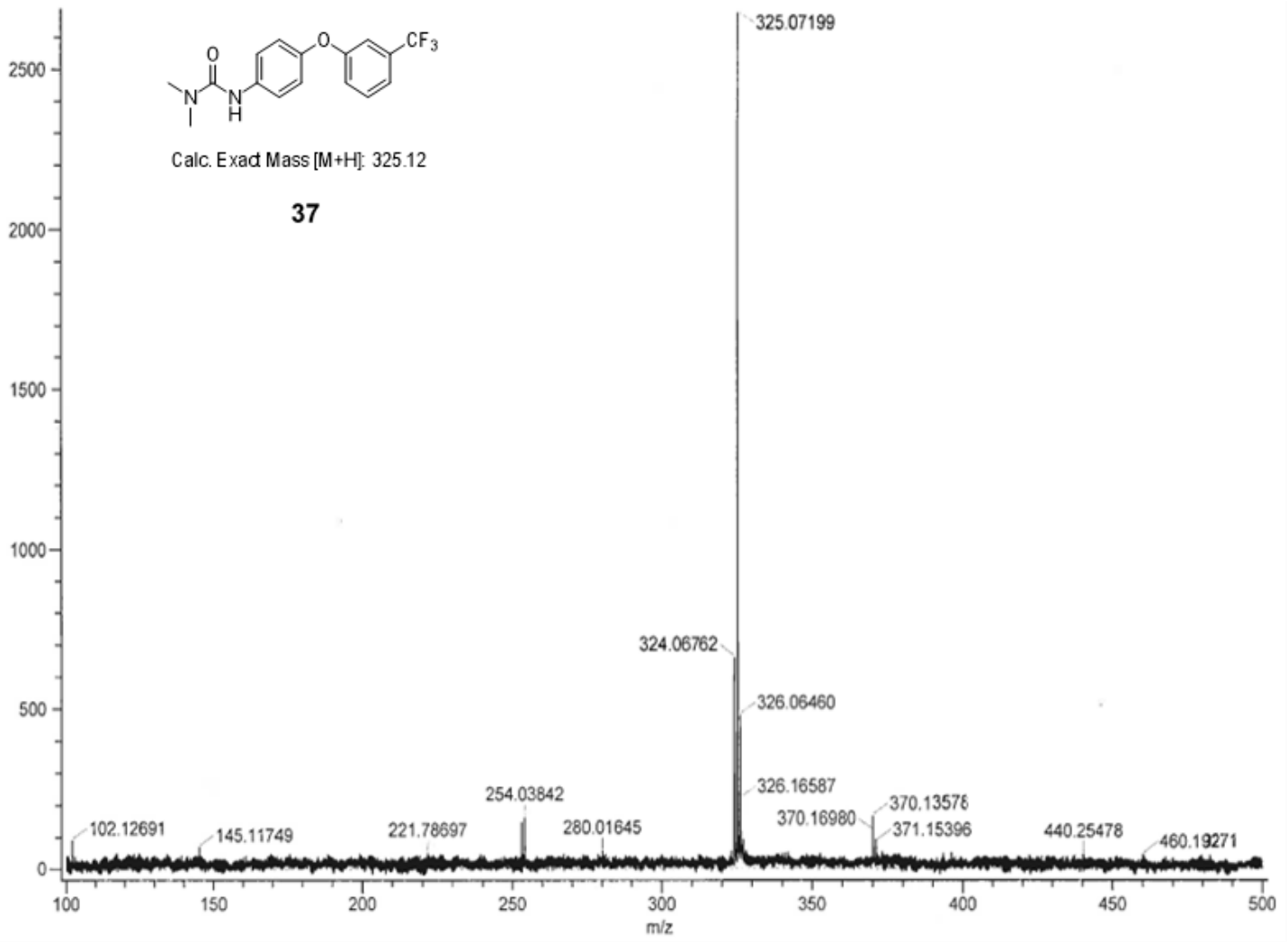
Calc. Exact Mass [M+H]: 325.12
37
325.07199
324.06762
326.06460
326.16587
254.03842
102.12691
145.11749
221.78697
280.01645
370.16980
370.13578
371.15396
440.25478
460.19271
m/z

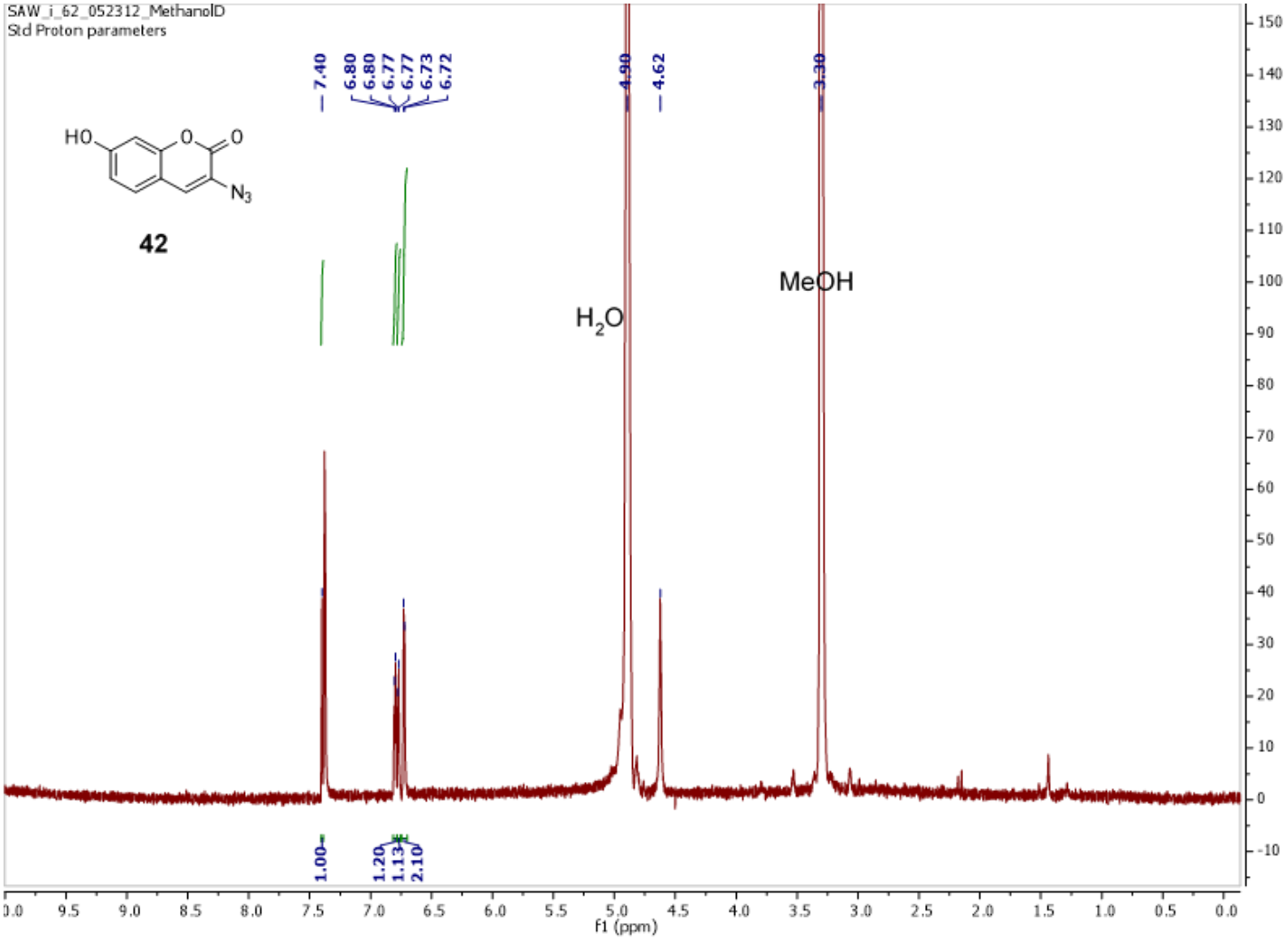
SAW_i_62_052312_MethanolD
Std Proton parameters
7.40
6.80
6.80
6.77
6.77
6.73
6.72
4.90
4.62
3.30
HO
O
O
N3
42
H2O
MeOH
1.00
1.20
1.13
2.10
f1 (ppm)

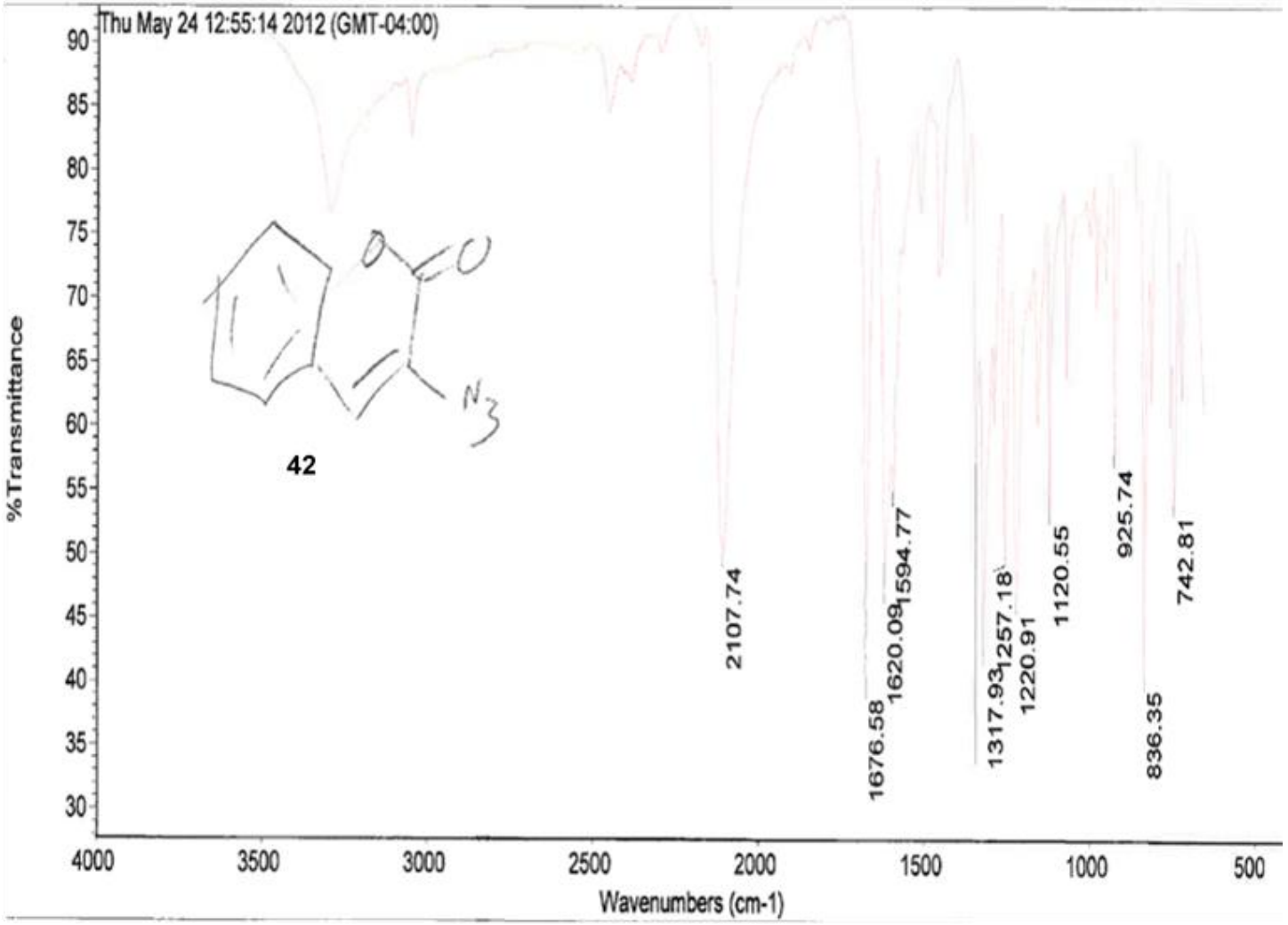
Thu May 24 12:55:14 2012 (GMT-04:00)
%Transmittance
90
85
80
75
70
65
60
55
50
45
40
35
30
4000
3500
3000
2500
2000
1500
1000
500
Wavenumbers (cm-1)
2107.74
1676.58
1620.09
1594.77
1317.93
1257.18
1220.91
1120.55
925.74
836.35
742.81
O
O
N3

42

Vita

Stuart Allen Whitehead was born on April 27th, 1989 in Libertyville, Illinois to Brian and Dana Whitehead. He moved to Essex Town, Vermont in 1998, and graduated from Essex High School in 2007. He took his curious mind back to the mid-west where he attended Purdue University in West Lafayette, IN from 2007 to 2011, graduating with a B.S. in chemistry. In the middle of his studies, he spent time abroad at the University of Canterbury in Christchurch, New Zealand during the spring 2010 semester and there he learned that toilets in southern hemisphere do not flush in the opposite direction. In fall 2011, he enrolled at the University of Tennessee, Knoxville to pursue a graduate degree in organic chemistry, and learned how to become a mature adult and grow adequate facial hair. He met his fiancée, Marissa Wilson, in Knoxville and the two will be getting married two days after he walks across the stage to earn his degree.